

The Pennsylvania State University
The Graduate School

**AN INVESTIGATION OF LIPOPOLYSACCHARIDE DEGRADATION AND THE ROLE OF LIPID
A MODIFICATIONS ON INNATE IMMUNE RESPONSE AND ANTIBIOTIC RESISTANCE**

A Dissertation in
Biochemistry, Microbiology, and Molecular Biology

by

Michael Maybin

© 2023 Michael Maybin

Submitted in Partial Fulfillment
of the Requirements
for the Degree of

Doctor of Philosophy

December 2023

The dissertation of Michael Maybin was reviewed and approved by the following:

Timothy C. Meredith
Associate Professor of Biochemistry and Molecular Biology
Dissertation Advisor
Chair of Committee

Kenneth C. Keiler
Professor of Biochemistry and Molecular Biology

Timothy Miyashiro
Associate Professor of Biochemistry and Molecular Biology

Emily Weinert
Associate Professor of Biochemistry and Molecular Biology

Darrell Cockburn
Assistant Professor of Food Science

Santhosh Girirajan
Professor of Biochemistry and Molecular Biology
Interim Head of the Department of Biochemistry and Molecular Biology

ABSTRACT

Lipopolysaccharide (LPS) is a major component of the outer membrane (OM) in Gram-negative bacteria. Due to its location in the outer leaflet of the OM LPS acts as the first line of defense for the bacterial cell. Overall, LPS provides structural stability while also facilitating several interactions between the cell and its environment. These roles include maintaining membrane permeability, providing antibiotic resistance, and modulating immune responses all of which contribute to overall bacterial survival and pathogenesis. LPS is composed of three main structural regions consisting of lipid A, the core oligosaccharide, and the O-antigen. The lipid A region of LPS is the most conserved portion of LPS that bacteria regularly modify as a response to environmental factors. Modifications altering to the acylation state or overall charge of LPS, through additions of charged groups like phosphoethanolamine (PEtN) and 4-amino-4-deoxy-L-arabinose (Ara4N), alter membrane permeability or increase resistance to cationic antimicrobial peptides (AMPs) respectively. In addition, LPS recognition by the innate immune response is facilitated by the lipid A region whereby bacterial modifications modulate LPS immunogenicity. LPS is recognized by the Toll-like receptor 4/myeloid differentiation factor-2 (TLR4/MD2) complex where the acylation state and presence of the 1 and 4'-phosphate groups on lipid A are key for immunogenicity.

This dissertation investigates the structure-activity relationship between lipid A and immune recognition, detoxification, and bacterial antibiotic resistance. Specifically, the substrate specificity of intestinal alkaline phosphatase against LPS is determined using

chemically defined LPS chemotypes and demonstrates no appreciable activity against the key 1- and 4'- lipid A phosphate groups unless acyl chains adjacent to the phosphate groups are first removed. PEtN modifications on lipid A are demonstrated to enhance TLR4/MD2 agonist activity of underacylated LPS chemotypes. A mechanism of polymyxin resistance in a sub-population of *Escherichia coli* B is elucidated whereby increased lipid A modification with Ara4N due to insertion sequence mediated genome amplifications drives phenotypic resistance. Finally, the development and evaluation of three orthogonal assays for bacterial derived LPS degradation (LPS-ase) activity is described, and their applications are discussed.

TABLE OF CONTENTS

LIST OF FIGURES	vii
LIST OF TABLES	ix
ACKNOWLEDGEMENTS	x
Chapter 1 Introduction to Lipopolysaccharide Structure, Synthesis, Modification, and Detection by Innate Immunity.....	1
Overview	2
LPS Structure	4
LPS Biosynthesis	6
Lipid A Modifications and Regulation	12
LPS Roles in Membrane Permeability and Antimicrobial Resistance	15
LPS Roles in Innate Immunity	16
Overview of Chapters in This Work	18
References.....	20
Chapter 2 Substrate Structure-Activity Relationship Reveals a Limited Lipopolysaccharide Chemotype Range for Intestinal Alkaline Phosphatase.....	35
Abstract	36
Introduction.....	37
Results	43
Discussion.....	63
Materials and Methods	72
References.....	87
Chapter 3 Insertion Sequence Mediated Tandem Chromosomal Amplification of the <i>arn</i> Operon Facilitates Polymyxin B Resistance in <i>E. coli</i> B Strains.....	107
Abstract	108
Introduction.....	109
Results	112
Discussion.....	126
Materials and Methods	129
References.....	142
Chapter 4 Development and Evaluation of Assays for Lipopolysaccharide Degradation Activity Among Gut Commensal Bacteria	153

Introduction.....	154
Results	157
Discussion.....	171
Materials and Methods	173
References.....	181
 Chapter 5 Conclusions and Future Directions.....	 188
 Overview and Discussion	 189
References.....	193

LIST OF FIGURES

Figure 1-1: Lipopolysaccharide biosynthesis.	2
Figure 1-2: Lipid A and LPS structure.	5
Figure 1-3: Overview of the Raetz pathway.	9
Figure 2-1: MS analysis of EptA-modified Re LPS.	44
Figure 2-2: Hydrolysis of phosphoanhydride linked PEtN-lipid IV _A is spontaneous and pH dependent..	45
Figure 2-3: O-Phosphorylethanolamine (O-PEtN) is a substrate for cIAP.	48
Figure 2-4: : De-O-acylated lipid A is rapidly dephosphorylated by cIAP.	50
Figure 2-5: De-O-acylated lipid A substrates are dephosphorylated by cIAP.....	51
Figure 2-6: Binding model of tetra-acylated lipid IV _A at the active site of cIAP.	53
Figure 2-7: LPS modification with PEtN by EptA induces NF-κB activity through hTLR4/MD2 signaling.	56
Figure 2-8: Pre-incubation in buffer of increasing pH reduces hTLR4 agonist activity for PEtN-modified lipid IV _A	57
Figure 2-9: Purification of individual PEtN-lipid IV _A species from <i>E. coli</i> B strain TXM844 by anion exchange chromatography.	59
Figure 2-10: MS analysis and TLR activity of purified 2-PEtN and 1-PEtN modified lipid IV _A samples..	60
Figure 2-11: ³¹ P-NMR analysis of 1-PEtN lipid IV _A	60
Figure 2-12: Simulated hTLR4/MD2 binding of 2-PEtN modified lipid IV _A	62
Figure 2-13: Docking of lipid IV _A to bacterial EcAP.....	69
Figure 3-1: Heteroresistance leads to inconsistency between MIC and frequency of resistance.....	113
Figure 3-2: SDS-PAGE analysis of LPS extracted from PMB resistant isolates.....	115

Figure 3-3: Polymyxin B resistant isolates display increased levels of Ara4N modification on lipid A.	116
Figure 3-4: 24 additional PMB resistant isolates from the Parent background display chromosomal amplification mediated increases in Ara4N modification.	117
Figure 3-5: Insertion sequence flanked chromosomal amplifications found in the PMB resistant mutants.	119
Figure 3-6: Majority of the 24 PMB resistant isolates revert to PMB sensitive phenotype in the absence of PMB.	120
Figure 3-7: C1 and C2 IS1-18 dependent chromosomal amplifications impart minimal fitness cost.	121
Figure 3-8: IS1-18 mediated chromosomal amplifications containing the <i>arn</i> operon lead to increased frequency of resistance.	122
Figure 3-9: Deletion of IS1-18 primarily alters frequency of resistance in strains lacking <i>eptA</i> but containing the <i>arn</i> operon.	123
Figure 3-10: Role of IS1 mediated chromosomal amplifications is maintained in a more wildtype E. coli B strain.	125
Figure 4-1: Diagram of luminal content translocation to the bloodstream.	155
Figure 4-2: K-12 LPS Sandwich ELISA.	158
Figure 4-3: ELISA LPS chemotype specificity.	160
Figure 4-4: Example sample set for LPS ELISA assay.	166
Figure 4-5: Summation of LPS ELISA data.	167
Figure 4-6: Time-dependent loss of ELISA signal observed for <i>L. rhamnosus</i> LMS2-1 (HM-106).	169
Figure 4-7: Radio-TLC analysis of K-12 LPS after 48-hour incubations with multiple strains.	171

LIST OF TABLES

Table 2-1 : Primers used in this study.....	73
Table 2-2 : Bacterial strains and plasmids used in this study.....	75
Table 3-1 : Polymyxin B (PMB) minimum inhibitory concentration (MIC) values.	113
Table 3-2 : Bacterial strains and plasmids.	130
Table 3-3 : Primers used in this study.....	131
Table 4-1 : Full list of strains tested via LPS ELISA.	162
Table 4-2 : Bacterial strains and plasmids.	174
Table 4-3 : Primers used in this study.....	175

ACKNOWLEDGEMENTS

It has been a long journey and I owe a thank you to many friends and family members who have helped me along the way.

First I want to thank Dr. Timothy Meredith my advisor and mentor for being a constant source of guidance and motivation. Your patience, even during difficult times, truly helped in me coming this far. Thank you.

To Dr. Gloria Komazin-Meredith thank you for always being willing to help out. Your kindness and helpfulness, especially when I first joined the lab, really helped me to adjust to the new environment.

To all my committee members, thank you for always providing useful feedback to improve my dissertation work and my professional growth.

To Krista and Kelvin, thank you both for the wonderful times in and out of lab. I could not imagine my first few years here without you both and I truly appreciate all of the help and good times!

To the current graduate students of the Meredith lab, G4, Aditi, Amena, and Rachel I cannot thank you all enough. You all have provided one of the best work environments anyone could ask for and have helped support me even when I doubted myself. I could not imagine these last few years without you all.

I also want to give a special shoutout to Aditi. LPS group!! Thank you immensely, together we have made some amazing strides on the LPS project and I cannot wait to see were you and Tim push it next.

To all the friends I made along the way at Elon, UNCG and PSU thank you. You all helped this introverted guy have some fun through the years, even if I sometimes I had to be dragged along.

Lastly I want to thank my family. Thank you for always being my rock, my guiding star, and motivator to keep pushing on. Especially to my parents, thanks for everything. I guess I have come a long way from that kindergarten kid sitting at the dining room table absolutely hating having to do homework, love you.

This work was funded in part by the National Institutes of Health (R21AI38152, R01GM127482). The findings and conclusions herein do not necessarily reflect the view of this funding agency.

Chapter 1

Introduction to Lipopolysaccharide Structure, Synthesis, Modification, and Detection by Innate Immunity

OVERVIEW

The cell envelope of Gram-negative bacteria is distinguished by its dual membranes, an inner membrane (IM) enclosing the cytoplasm and an outer membrane (OM) encapsulating the cell and shielding it from its environment. Positioned between these membranes is the periplasm, which houses a peptidoglycan cell wall that is comparatively thin compared to those found in Gram-positive bacteria (1). While the typical biological membrane consists of a phospholipid bilayer, the OM of most Gram-negative bacteria is unique in that it is highly asymmetrical. This asymmetry is due to the localization of the specialized saccharolipid lipopolysaccharide (LPS), also known as endotoxin, to the outer leaflet where it is the major component (Fig. 1-1) (1–3). In this position as the outermost component of the cell envelope, LPS of Gram-negative bacteria facilitates interactions between the cell and its environment.

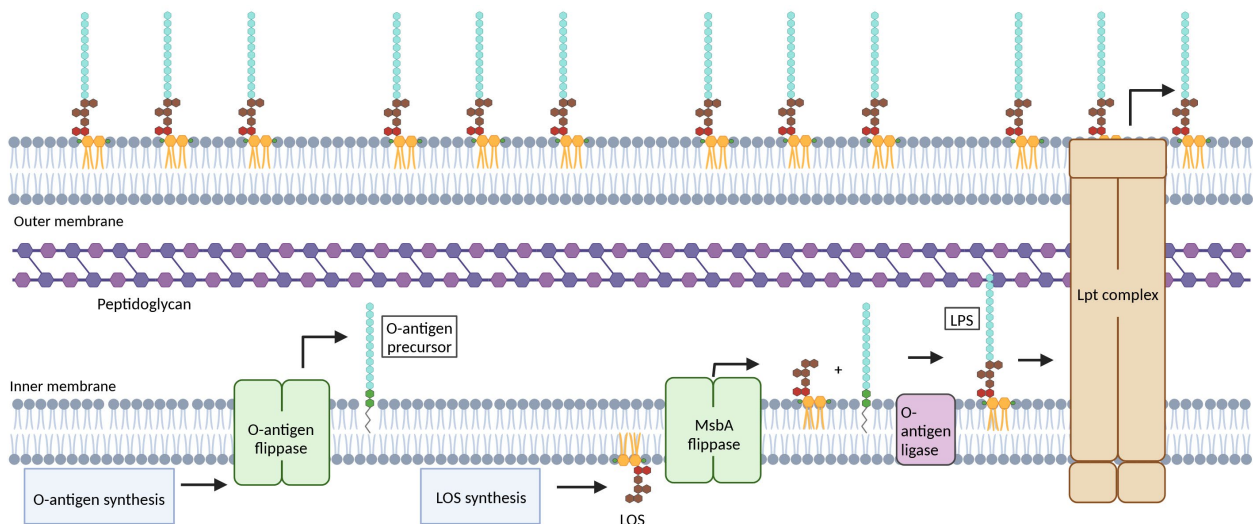


Figure 1-1: Lipopolysaccharide biosynthesis. LPS biosynthesis in *E. coli* is outlined with the synthesis of lipid A and O-antigen occurring in the IM and flipping to the periplasmic face occurring by MsbA and an O-antigen flippase respectively. The two components are ligated and then transported to the OM by the Lpt complex.

As an integral part of the OM, LPS provides structural support and thus stability to the membrane. Indeed, in most but not all Gram-negative bacteria the absence of LPS is lethal (4). The functions of LPS in bacteria extend beyond OM stability however, given its location at the bacterial cell surface it can facilitate interactions with the growth environment and is critical in many bacterial responses to the environment (5, 6). These roles include maintaining membrane permeability, providing antibiotic resistance, and modulating immune responses all of which contribute to overall bacterial survivability and pathogenesis (5, 6).

The overall structure of LPS and the presence of modifications on LPS play an integral role in modulating the innate immune response and antibiotic resistance. Therefore, this dissertation seeks to increase our understanding of LPS structure, modification, and degradation/detoxification as it relates to the recognition of LPS by the innate immune system via Toll-like receptor 4 (TLR4), and resistance to cationic antimicrobial peptides (CAMPs). Both interactions are of importance to human health where understanding how LPS modification affects CAMP resistance is of increasing importance as resistance to our antibiotics of last defense, such as polymyxins, has been on the rise (7). Additionally, LPS recognized by TLR4 leads to the release of inflammatory cytokines and an overall pro-inflammatory state. While this inflammatory state is beneficial in the context of a normal infection, a chronic low-level inflammatory state can be detrimental. In fact, such a proinflammatory state has clinical associations with several disease states including insulin resistance, atherosclerosis, obesity, and non-alcoholic fatty liver disease (8–10). Elevated levels of LPS in the blood, a state called metabolic endotoxemia (ME), results in this same detrimental inflammatory state (11, 12). LPS, while typically sequestered to the lumen of the gut can translocate to the serum when the

luminal epithelial barrier becomes more permeable, an effect of high-fat diets (13). Thus as the prevalence of high-fat diets increases, an understanding of LPS degradation/detoxification mechanisms provided by the host or by the microbiome will better prepare us to manage these chronic conditions.

In this chapter I will provide an overview of LPS structure and biosynthesis in *Escherichia coli*, primarily focusing on lipid A synthesis known as the Raetz pathway. Additionally, I will discuss modifications to the lipid A structure focusing on phosphoethanolamine (PEtN) and 4-amino-4-deoxy-L-arabinose (Ara4N) modifications and how the two-component systems PmrAB and PhoPQ regulate modification. An overview of host-bacteria interactions mediated by LPS will be provided and bacterial antibiotic resistance mechanisms facilitated by LPS will be introduced. Finally, I will discuss areas in which this dissertation work progresses our understanding of LPS and its roles in bacterial survivability and host-bacteria interactions.

LPS STRUCTURE

LPS consists of three main structural regions: lipid A, the core oligosaccharide, and the O-antigen (Fig. 1-2B). Lipid A is the hydrophobic portion of the molecule that anchors LPS into the OM, it is composed of an acylated β -1'-6-linked glucosamine disaccharide. In *E. coli*, lipid A is hexa-acylated and the glucosamines are phosphorylated at the 1 and 4' positions (Fig. 1-2A). Lipid A acylation is separated into four primary and two secondary acyl chains where two primary N-linked β -hydroxyacyl chains are attached at the 2 and 2' positions, and two primary O-linked β -hydroxyacyl chains at the 3 and 3' positions (14). The two secondary acyl chains attached to the

β -hydroxy groups of the 2' and 3' acyl chains ultimately result in an asymmetrical hexa-acylated mature lipid A (Fig. 1-2A) (14). The lipid A structure is the most highly conserved region of LPS although the number and length of acyl chains can vary based on growth conditions and bacterial species (14).

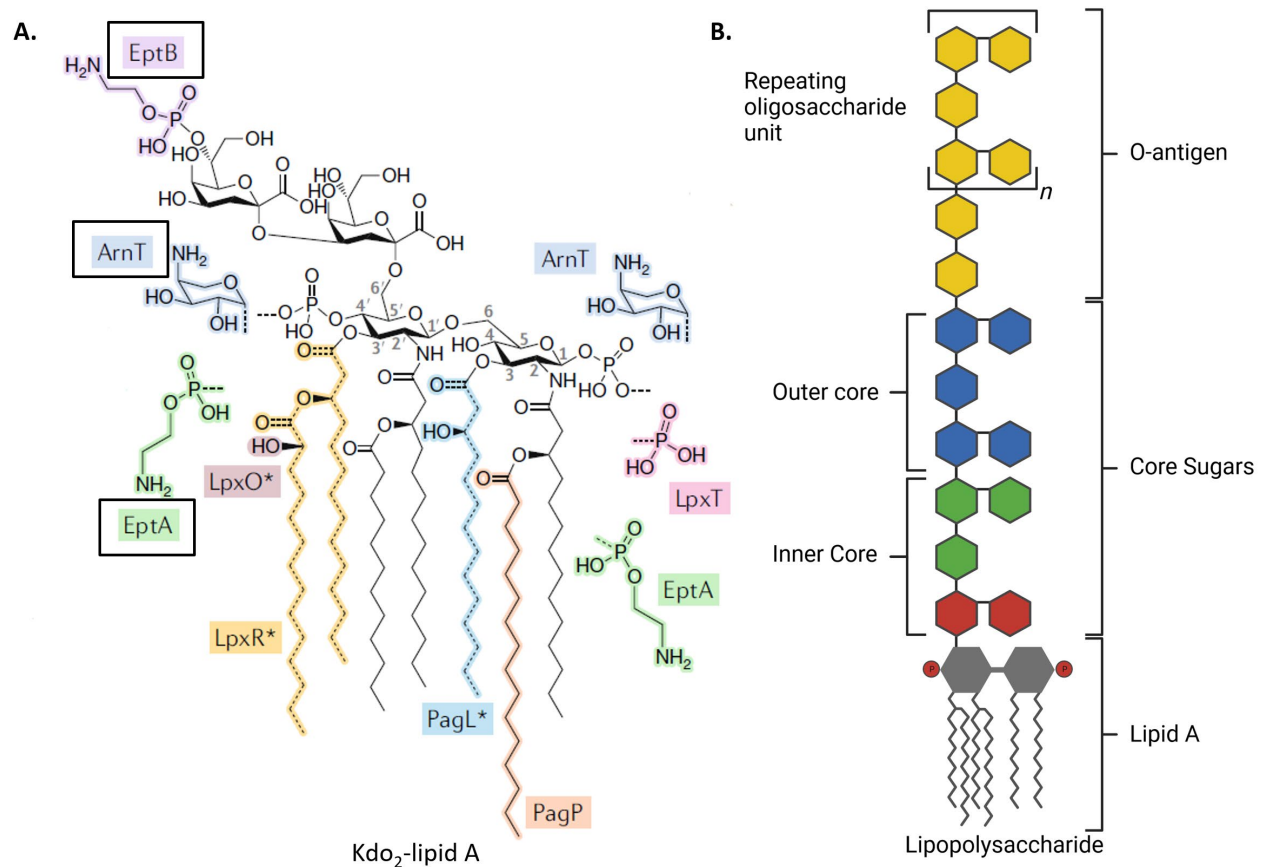


Figure 1-2: Lipid A and LPS structure. **A)** Kdo₂-Lipid A structure with modifications to the structure highlighted and color coded with responsible enzymes. Boxed enzymes are of import to this thesis work. Groups drawn with dotted lines indicate that the enzymatic activity is removal via hydrolysis. Asterisks on LpxO, LpxR, and PagL indicate that these enzymes are not found in *E. coli* K-12 but are found in *Salmonella*. Adapted from “Simpson BW, Trent MS. 2019. Pushing the envelope: LPS modifications and their consequences. *Nat Rev Microbiol* 17:403–416.” **B)** General structure of LPS with the three major regions identified.

Directly linked to the glucosamines of lipid A is the core oligosaccharide, a non-repeating oligosaccharide that typically contains 3-deoxy-D-*manno*-oct-2-ulosonic acid (Kdo), heptoses, and additional sugar residues (6, 15). The core oligosaccharides can be further divided into the inner core and the outer core, where the inner core directly attaches to lipid A and the outer core consists of the more distal sugar residues that the O-antigen attaches to. The core oligosaccharide structure is less conserved where the number of certain residues or the addition of atypical residues may be observed, for example *E. coli* and *Helicobacter pylori* have two and one Kdo residues in the core oligosaccharides respectively (5).

Of the three regions of LPS the O-antigen is the least conserved where the O-antigen itself is a polysaccharide composed of repeating oligosaccharides. The number of repeats can vary wildly even at the strain level, in fact some Gram-negative bacteria produce LPS lacking an O-antigen altogether which is referred to as lipooligosaccharide (LOS) (16, 17), as opposed to smooth LPS which includes the O-antigen (6). Many laboratory passaged strains, including *E. coli* K-12 and B strains studied in this thesis, have acquired mutations in biosynthetic genes involved in O-antigen and make LPS lacking O-antigen. This chemotype is often referred to as rough LPS.

LPS BIOSYNTHESIS

LPS biosynthesis begins with the construction of lipid A. Synthesis of this highly conserved region of LPS has been thoroughly studied in *E. coli* and is named the Raetz Pathway (Fig. 1-3) (14). Lipid A production occurs in the cytoplasm and is carried out by enzymes coded for by the *lpx* genes. *LpxA* carries out the first enzymatic activity in this pathway by catalyzing the acylation

of uridine diphosphate-N-acetylglucosamine (UDP-GlcNAc) with a fatty acid, forming UDP-3-O-acyl-GlcNAc (18). UDP-GlcNAc is a nucleotide sugar coenzyme that is commonly used in the production of glycolipids. In *E. coli*, LpxA is selective for the 14 carbon acyl chain β -hydroxymyristate carried by the acyl carrier protein (ACP), however this specificity can vary, for example in *Pseudomonas aeruginosa* a ten carbon chain is preferred (19). Importantly this first acylation step is not favorable resulting in the second reaction in the pathway being the first committed step in LPS synthesis (20). The zinc metalloenzyme LpxC catalyzes this irreversible step where it deacetylates UDP-3-O-acyl-GlcNAc forming UDP-3-O-acyl-GlcN (21). As the first committed step of the Raetz pathway LpxC is highly regulated and has become a target for LPS synthesis inhibition (22–24). A second β -hydroxymyristate is added by LpxD following deacetylation, forming UDP-2,3-diacylglucosamine, again with an acyl-ACP donor specificity (25). The pyrophosphatase LpxH subsequently cleaves UDP-2,3-diacylglucosamine releasing the UDP nucleotide carrier and 2,3-diacylglucosamine-1-phosphate also known as lipid X (26). The β -1'-6-linked glucosamine disaccharide at the center of lipid A is generated by LpxB condensing lipid X and another UDP-2,3-diacylglucosamine, formed by LpxD, ultimately releasing the second UDP carrier. Before the pathway continues this tetraacylated lipid A disaccharide is inserted into the inner leaflet of the IM where phosphate is added at the 4' position by the kinase LpxK, forming what is known as lipid IV_A (27). The next step in this pathway involves the addition of Kdo residues to the lipid IV_A precursor. This activity is performed by WaaA and as mentioned above, in *E. coli* two Kdo moieties are added however the number of Kdo moieties added can vary (5, 14). The final steps in the Raetz pathway involve the addition of the secondary acyl chains. This activity is carried out by LpxL and LpxM in a sequential manner whereby LpxM activity is more efficient

after acylation by LpxL but not dependent on it (28, 29). LpxL and LpxM add lauryl and myristoyl groups on the 2'- β -hydroxyacyl and 3'- β -hydroxyacyl groups respectively (28, 29). Just like LpxA and LpxD these acyltransferases have a specificity for acyl-ACP donors. The final product of the Raetz pathway in *E. coli* is Kdo₂-lipid A, also called Re-LPS, and is the precursor for the formation of LOS after addition of the core sugars.

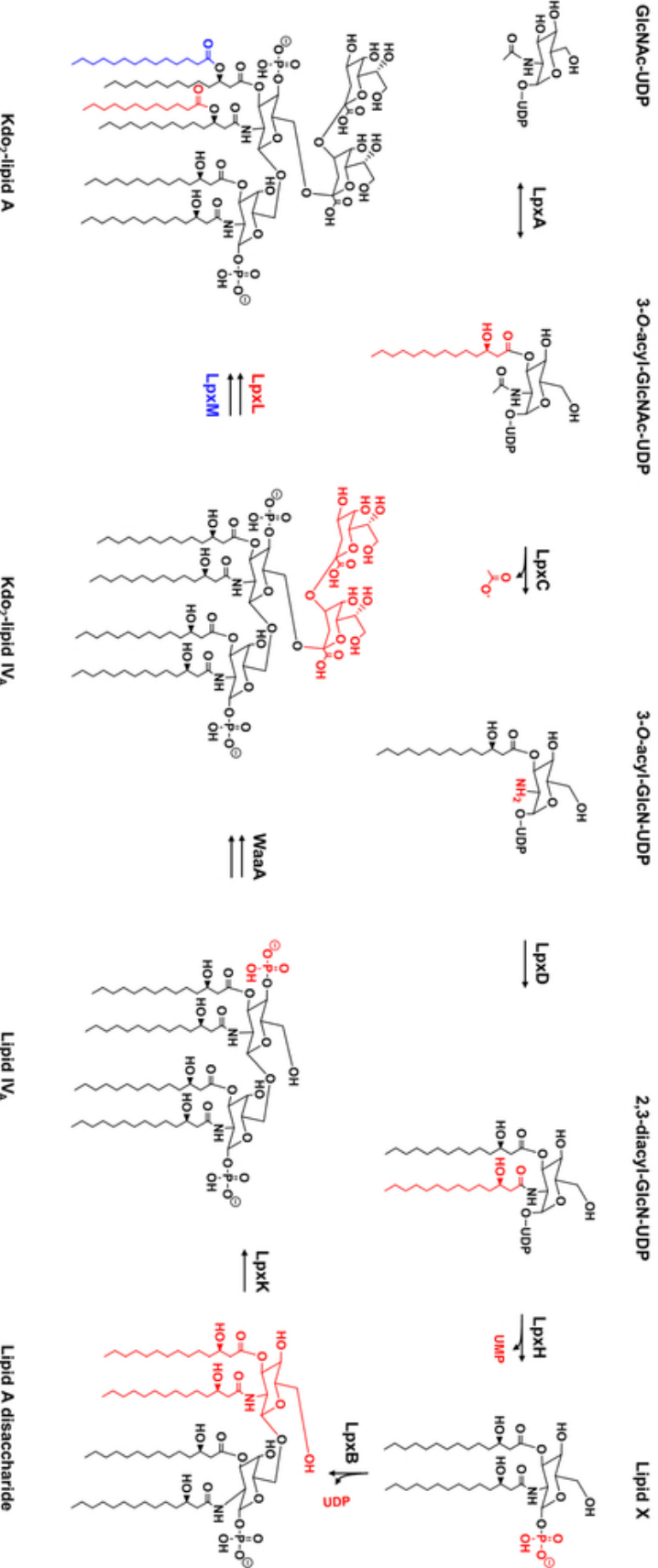


Figure 1-3: Overview of the Raetz pathway. Modifications to the preceding structure marked in red, except for the last step which is color coded in red and blue. Donor molecules are not displayed. Source: Bertani B, Ruiz N. 2018. Function and Biogenesis of Lipopolysaccharides. EcoSal Plus 8

The core oligosaccharide of LPS is synthesized in a sequential manner, starting with construction of the inner core, with the lipid A moiety anchored into the inner leaflet of the IM. While included in the Raetz pathway the first step in this process is the addition of Kdo residues onto the disaccharide backbone of lipid A, an activity catalyzed by WaaA. WaaA is one of several glycosyltransferases encoded for by the *waa* gene cluster which oversees the construction of the entire oligosaccharide core. The enzymes WaaA, WaaC, WaaF, WaaP, WaaQ, and WaaY build the inner core in a sequential manner whereby WaaC, WaaF, and WaaQ are glycosyltransferases that add L-glycero-D-manno-heptose groups and WaaP and WaaY are kinases that add phosphate groups to the heptose residues added by WaaC and WaaF respectively (15, 30, 31). The overall structure of the inner core is relatively well conserved within *E. coli* strains unlike the outer core which can vary from strain to strain resulting in various “core types”. Briefly, in *E. coli* strains with the K-12 core type the outer core synthesis is handled by WaaG, WaaO, WaaB, WaaJ, and WaaU glycosyltransferases which add glucose, galactose (WaaB), and heptose (WaaU) groups. Of note is the conservation of activity in the first step of outer core synthesis, regardless of core type in *E. coli* or *Salmonella*, there is the addition of a glucose group to the second inner core heptose group, catalyzed by WaaG (30).

Before addition of the O-antigen, in strains that do add one, the final product of core synthesis, core-lipid A, is flipped from the cytoplasmic leaflet of the IM to the periplasmic leaflet by the inner membrane flippase MsbA, a member of the ATP-binding cassette (ABC) transporter

superfamily (Fig. 1-1) (32). Once in the outer leaflet of the IM core-lipid A awaits additional modifications and/or the addition of the O-antigen. As previously mentioned, the O-antigen is highly diverse resulting in a wide-variety observed in Gram-negative species where even within *E. coli* strains over 200 different variants have been identified (33). Unlike the core oligosaccharide, the O-antigen is synthesized independently of the rest of LPS and then transferred onto the core-lipid A structure in the periplasm. O-antigen synthesis begins in the cytoplasm with sugar residues attached to the lipid carrier undecaprenol pyrophosphate (Und-PP) (34). The resultant sugar-Und-PP acts as an acceptor for additional sugar transfers (17) before ultimately being flipped to the periplasmic leaflet of the IM. O-antigen polymerization can occur either before or after the flipping action and this differs based on the pathway with which the bacterium utilizes to form the O-antigen. The three pathways include the Wzy-dependent pathway, ABC-dependent pathway, and the synthase-dependent pathway. The Wzy-dependent pathway involves the transfer of Und-PP-O-antigen subunits to the periplasmic face before polymerization onto a single Und-PP carrier (17, 35, 36). In contrast, the ABC-dependent pathway involves the complete polymerization of the O-antigen in the cytoplasm before flipping to the periplasmic face by an ABC transporter (17, 37). The final pathway is the least understood and currently is relegated to a single example found in *Salmonella enterica* serovar Borreze (rfbO:54) (38, 39). However, it is believed that the synthase (WbbF) both polymerizes and flips the O-antigen across the IM (38–40). Regardless of which pathway is utilized the O-antigen polymer is ligated to the awaiting core-lipid A by WaaL ligase (14, 41). Finally, the completed LPS molecule is transported to the OM via the LPS transport (Lpt) system. Briefly, the Lpt system is a seven-subunit protein complex that bridges the OM and IM, whereby, in an ATPase-dependent

mechanism, it transports multiple LPS molecules from subunit to subunit referred to as the “PEZ” model (Fig. 1-1) (42–45).

LIPID A MODIFICATIONS AND REGULATION

A variety of LPS structures can be observed from different bacteria solely due to variations in the LPS synthesis pathway, however bacteria will additionally alter the LPS and lipid A structure as a response to environmental factors. These modifications typically involve altering the acyl chains, phosphate groups or sugar backbone of lipid A and the core oligosaccharide. Adding to this variety is the non-stoichiometric addition of modifications, so even LPS synthesized by a single strain is not entirely uniform. Here I will introduce a few key LPS modifications and their regulation in *E. coli* and other enterobacteria (Fig. 1-2A).

Acyl chain modifications to lipid A involve addition or removal of fatty acids by enzymes in the outer membrane. These include the enzymes LpxR, PagL, and PagP where PagL is not found in *E. coli* (46–48). PagL is a lipase that removes the O-linked β -hydroxyacyl chain at position 3 of lipid A (48). Similarly, LpxR deacylates lipid A via the removal of the O-linked β -hydroxyacyl chain at position 3' of lipid A, additionally removing any secondary acyl chains bound to it. Interestingly, while homologs of *lpxR* can be found in *E. coli* strains it is relegated to pathogenic strains such as *E. coli* O157:H7 where it is regulated with virulence factors and plays a role in modulating the host immune response (49). Lastly the acyltransferase PagP alters the acylation state of lipid A via the addition of a palmitate to the hydroxy group of the N-linked β -hydroxyacyl chain at

position 2 of lipid A, producing an hepta-acylated lipid A implicated in survival in harsh environments (50–53).

In addition to variation to the acylation state of lipid A, modifications can also be utilized to change the electrostatic charge of the molecule. Charge alteration is carried out via additions to the diglucosamine backbone of lipid A, typically on the 1- and 4'- phosphates and these modifications take place in the IM before transport to the OM via the Lpt system. Of note are the enzymes LpxT, EptA, and ArnT all of which alter the charge of LPS via additions to lipid A phosphates. LpxT is a kinase that adds a second phosphate group to the 1-phosphate of lipid A and utilizes Und-PP as a substrate, overall increasing the negative charge of the lipid A (54, 55). EptA and ArnT decrease the negative charge of lipid A by addition of positively charged groups PEtN and Ara4N respectively. PEtN modification by EptA is carried out via transfer of PEtN from phosphatidylethanolamine to either the 1- or 4'- phosphate on lipid A, and this addition can occur twice resulting in a PEtN modification at both positions (56–59). In a similar fashion, PEtN modifications can be added to Kdo or the directly attached heptose sugar by the activity of EptB and EptC respectively. Meanwhile, ArnT is encoded for by a gene, *arnT*, in the *arn* operon which together converts and transfers UDP-glucose in the cytoplasm to the ArnT substrate Und-P-Ara4N in the IM, whereby ArnT then transfers the Ara4N from Und-P to lipid A (60–64).

All the above-mentioned modification systems play significant roles in the bacterial response to environmental conditions. Lipid A modification can change the electrostatic charge, hydrophobicity, and rigidity of the OM adjusting the cells to their living environment. These activities are thusly regulated by bacteria, and in the case of the aforementioned modification systems they are all regulated, directly or indirectly, by the two component systems (TCS) PhoPQ

(46, 65) and PmrAB (66, 67). These TCS systems consist of a sensor kinase (PhoQ and PmrB) that responds to extracellular signals through autophosphorylation of a histidine residue. The phosphate is subsequently transferred to a related response regulatory protein (PhoP and PmrA). The regulatory protein then turns on and off gene expression in a phosphorylation dependent manner. The PhoPQ system is primarily involved in sensing environmental stimuli such as acidic pH, low concentrations of divalent cations such as Mg^{2+} , and antimicrobial peptides (AMPs) (65, 68–73). PhoQ contains three regions spanning the IM consisting of cytoplasmic, transmembrane, and periplasmic domains. The periplasmic domain is essential for sensing divalent cations and cationic AMPs and the cytoplasmic domain senses pH changes activating PhoQ (74, 75). Once activated PhoP is phosphorylated and it upregulates transcription of *pagP* and *pagL* and indirectly regulates *eptA* and the *arn* operon via *pmrD* (76, 77). PmrD is an adapter protein that couples the PhoPQ system and the PmrAB system by binding to and protecting the phosphorylated PmrA response regulator from dephosphorylation (78). PmrB is the sensor kinase of the PmrAB system and it responds to changes in metal concentrations in the periplasm, such as Fe^{3+} , and acidic pH (67, 79, 80). Activated PmrB phosphorylates PmrA which directly upregulates the *arn operon* and *eptA* resulting in increased levels of lipid A modification and an overall increase in negative charge in the OM. In tandem with this, phosphorylated PmrA also upregulates PmrR, a small protein that inhibits the activity of LpxT thusly decreasing its contribution of negatively charged phosphate. The resulting increased positive character of the OM limits the amount of Fe^{3+} that enters the periplasm and thus tunes the PmrAB response. While PhoPQ and PmrAB are TCS utilized by many bacteria to regulate LPS modifications they are not an exhaustive list and other TCS are also

utilized. For example, the ArcAB TCS is also utilized by *Salmonella* strains where it responds to oxygen availability (81).

LPS ROLES IN MEMBRANE PERMEABILITY AND ANTIMICROBIAL RESISTANCE

For survival it is important for bacteria to be able to respond to environmental stressors and the modifications of LPS is a powerful mechanism by which Gram-negative bacteria do so. A large component to this response is alteration of the OM permeability, as LPS is a major component of the outer leaflet of the OM. The stability of the outer membrane can thus be tied to the rigidity with which LPS is packed. LPS or LOS is effective permeability barrier against small, hydrophobic molecules that would otherwise cross phospholipid bilayers including antibiotics and bile salts (82, 83). This ability is in part because of its amphipathic nature as the lipid A portion provides hydrophobic character limiting entry of hydrophilic compounds. The effectiveness of the barrier is reliant on sufficient packing of LPS, driven in part by the hydrophobic interaction of acyl chains in lipid A but also by electrostatic interactions between phosphate in the core and on lipid A. Typically cations such as Mg^{2+} act as charge bridges between the otherwise repulsive phosphate groups (82, 83). However, in the case of growth in Mg^{2+} limiting conditions these phosphates can repel each other decreasing membrane stability (84). As described above bacteria utilize the PhoPQ system to recognize this detrimental environmental condition and adjust the membrane permeability by increasing the overall positive charge of LPS via addition of positively charged Ara4N and PEtN groups by ArnT and EptA/B/C, respectively (84).

AMP resistance is strongly tied to the OM permeability in Gram-negative bacteria (85–87). While the unmodified LPS structure provides protection against a variety of antibiotics, cationic AMPs leverage the electrostatic attraction between the compound and the negatively charged LPS to interact. In the example case of polymyxins, a clinically important class of antibiotics, positively charged amino acid side chains mediate interaction with the negatively charged groups of LPS. This promotes penetration of the hydrophobic acyl portion of the peptide into the membrane. This activity disrupts the OM and subsequently allows for further interactions with lipid A in the IM, leading to cell lysis (88–90). Resistance mechanisms involving LPS center around modifications that alter the charge state of LPS. Here again we see the effectiveness of adding positively charged groups on to the lipid A structure (ArnT/EptA) as regulated by PhoPQ/PmrAB. However, in addition to these modification methods some pathogenic bacteria, such as *Helicobacter* species, will dephosphorylate the 1- and/or 4'-phosphates of lipid A via the phosphatases LpxE and LpxF respectively (91, 92). Regardless of method, modifications of the lipid A structure resulting in decreased negative charge contributes to increased polymyxin resistance.

LPS ROLES IN INNATE IMMUNITY

As LPS adorns the surface of many Gram-negative pathogens our immune systems have adapted to readily recognize it as a microbe -, or pathogen -, associated molecular pattern (MAMPs or PAMPs) and thusly responds aggressively to it (93). Host responses to LPS can indeed be so strong as to be toxic (sepsis), hence the alternative name of endotoxin for LPS. This

response is mediated by engagement of MAMPs by pattern recognition receptors (PRR) on a variety of cells, including macrophages and adipocytes, triggering the release of pro-inflammatory cytokines (13, 94). An essential PRR for LPS detection is the Toll-like receptor 4/myeloid differentiation factor-2 (TLR4/MD2) complex which has adapted to recognizing lipid A, the most highly conserved region of LPS (93, 95). Recognition begins with binding of LPS to LPS-binding protein (LBP) and cluster of differentiation 14 (CD14) and transfer to TLR4/MD2 (95, 96) whereby the hexa-acylated, bis-phosphorylated lipid A structure, like that produced by *E. coli* and *Salmonella*, is highly immunogenic (97–99). The resultant signaling cascade induced by TLR4/MD2 stimulation occurs in one of two pathways, a myeloid differentiation primary response protein 88 (MyD88) dependent pathway or an MyD88 independent pathway (TIR domain-containing adaptor inducing interferon- β (TRIF) dependent pathway) (100–102). Recruitment of MyD88 and TRAM to the TIR domain of TLR4 results in the production of pro-inflammatory cytokines such as TNF α and IL-6 via NF κ B activation (103). The TRIF dependent pathway is undertaken when the TLR4/MD2 receptor is endocytosed and the TRIF and TRAM protein adaptors are recruited intracellularly, leading to production of type I interferons and late activation of NF κ B (100). The diversity of lipid A chemotypes leads to varying ability to trigger an immune response by TLR4/MD2 (93). Many bacteria take advantage of this to evade the immune response by modifying lipid A in ways that alter the classical immunogenic structure (hexa-acylated and bis-phosphorylated). For example, pathogens such as *H. pylori* and *Yersinia pestis* will produce underacylated lipid A to facilitate immune evasion and colonization (104, 105).

OVERVIEW OF CHAPTERS IN THIS WORK

LPS structure and modifications to it have clearly been shown to play a significant role in bacterial survival and immune evasion. In particular modifications to the lipid A structure have a direct and measured impact on cationic AMP resistance and TLR4/MD2 recognition. The work described herein seeks to further advance our understanding of the interplay between lipid A modification, antibiotic resistance, and host-microbe interactions.

Chapter 2 focuses on two facets of microbe-host interactions, in the pursuit of combating ME and thus ameliorating the associated chronic disease states. Firstly, I investigate host methods of LPS detoxification. There are two mammalian host-derived enzymes proposed to detoxify LPS, acyloxyacyl hydrolase (AOAH) (106) and alkaline phosphatase, particularly intestinal alkaline phosphatase (IAP) (107–109). While AOAH detoxifies LPS via removal of the secondary acyl chains, IAP is thought to directly dephosphorylate the lipid A phosphates. The chapter evaluates the substrate specificity of IAP on more chemically defined chemotypes of LPS. In addition, we evaluate the role PEtN modifications play on TLR4/MD2 signaling.

Chapter 3 investigates polymyxin B resistance in *E. coli*, more specifically we investigate a potential mechanism of heteroresistance in *E. coli* B strains. I describe a mechanism of resistance mediated by chromosomal amplifications of the genome containing the *arn* operon. These amplified regions of the genome are found to be bookended by insertion sequence elements, and the amplification itself dependent on their presence. Ultimately the sub-population found to have the amplicons displayed increased levels of Ara4N modification and a polymyxin B (PMB) resistance phenotype.

Finally, chapter 4 describes my efforts to develop a screen for bacterial derived LPS degradation enzymes (LPS-ases) as microbe derived LPS degrading activity could also be utilized to combat ME. Additionally, even though LPS is a highly abundant, high-energy molecule there are no known bacterial derived enzymes for its recycling. Here I describe the development and utilization of an enzyme-linked immunosorbent assay, SDS-PAGE, and autoradiographic assay to screen a variety of bacterial strains for LPS-ase activity.

REFERENCES

1. Silhavy, T. J., Kahne, D., and Walker, S. (2010) The Bacterial Cell Envelope. *Cold Spring Harb Perspect Biol.* **2**, a000414–a000414
2. Bos, M. P., Robert, V., and Tommassen, J. (2007) Biogenesis of the Gram-Negative Bacterial Outer Membrane. *Annu Rev Microbiol.* **61**, 191–214
3. Kamio, Y., and Nikaido, H. (1976) Outer membrane of *Salmonella typhimurium*: accessibility of phospholipid head groups to phospholipase C and cyanogen bromide activated dextran in the external medium. *Biochemistry.* **15**, 2561–2570
4. Zhang, G., Meredith, T. C., and Kahne, D. (2013) On the essentiality of lipopolysaccharide to Gram-negative bacteria. *Curr Opin Microbiol.* **16**, 779–785
5. Simpson, B. W., and Trent, M. S. (2019) Pushing the envelope: LPS modifications and their consequences. *Nat Rev Microbiol.* **17**, 403–416
6. Bertani, B., and Ruiz, N. (2018) Function and Biogenesis of Lipopolysaccharides. *EcoSal Plus.* 10.1128/ecosalplus.ESP-0001-2018
7. Li, Z., Cao, Y., Yi, L., Liu, J.-H., and Yang, Q. (2019) Emergent Polymyxin Resistance: End of an Era? *Open Forum Infect Dis.* 10.1093/ofid/ofz368
8. Kessoku, T., Kobayashi, T., Imajo, K., Tanaka, K., Yamamoto, A., Takahashi, K., Kasai, Y., Ozaki, A., Iwaki, M., Nogami, A., Honda, Y., Ogawa, Y., Kato, S., Higurashi, T., Hosono, K., Yoneda, M., Okamoto, T., Usuda, H., Wada, K., Kobayashi, N., Saito, S., and Nakajima, A. (2021) Endotoxins and Non-Alcoholic Fatty Liver Disease. *Front Endocrinol (Lausanne).* 10.3389/fendo.2021.770986

9. Cani, P. D., Amar, J., Iglesias, M. A., Poggi, M., Knauf, C., Bastelica, D., Neyrinck, A. M., Fava, F., Tuohy, K. M., Chabo, C., Waget, A., Delmée, E., Cousin, B., Sulpice, T., Chamontin, B., Ferrières, J., Tanti, J.-F., Gibson, G. R., Casteilla, L., Delzenne, N. M., Alessi, M. C., and Burcelin, R. (2007) Metabolic endotoxemia initiates obesity and insulin resistance. *Diabetes*. **56**, 1761–72
10. Moreno-Indias, I., Cardona, F., Tinahones, F. J., and Queipo-Ortuño, M. I. (2014) Impact of the gut microbiota on the development of obesity and type 2 diabetes mellitus. *Front Microbiol.* **5**, 190
11. Fuke, N., Nagata, N., Suganuma, H., and Ota, T. (2019) Regulation of Gut Microbiota and Metabolic Endotoxemia with Dietary Factors. *Nutrients*. **11**, 2277
12. Mohammad, S., and Thiemermann, C. (2021) Role of Metabolic Endotoxemia in Systemic Inflammation and Potential Interventions. *Front Immunol.* 10.3389/fimmu.2020.594150
13. Moreira, A. P. B., Texeira, T. F. S., Ferreira, A. B., do Carmo Gouveia Peluzio, M., and de Cássia Gonçalves Alfenas, R. (2012) Influence of a high-fat diet on gut microbiota, intestinal permeability and metabolic endotoxaemia. *British Journal of Nutrition*. **108**, 801–809
14. Raetz, C. R. H., and Whitfield, C. (2002) Lipopolysaccharide Endotoxins. *Annu Rev Biochem.* **71**, 635–700
15. Whitfield, C., Kaniuk, N., and Firdich, E. (2003) Molecular insights into the assembly and diversity of the outer core oligosaccharide in lipopolysaccharides from *Escherichia coli* and *Salmonella*; *J Endotoxin Res.* **9**, 244–249
16. Wang, L., Wang, Q., and Reeves, P. R. (2010) The Variation of O Antigens in Gram-Negative Bacteria, pp. 123–152, 10.1007/978-90-481-9078-2_6

17. Kalynych, S., Morona, R., and Cygler, M. (2014) Progress in understanding the assembly process of bacterial O-antigen. *FEMS Microbiol Rev.* **38**, 1048–1065
18. Anderson, M. S., and Raetz, C. R. (1987) Biosynthesis of lipid A precursors in *Escherichia coli*. A cytoplasmic acyltransferase that converts UDP-N-acetylglucosamine to UDP-3-O-(R-3-hydroxymyristoyl)-N-acetylglucosamine. *Journal of Biological Chemistry.* **262**, 5159–5169
19. Dotson, G. D., Kaltashov, I. A., Cotter, R. J., and Raetz, C. R. H. (1998) Expression Cloning of a *Pseudomonas* Gene Encoding a Hydroxydecanoyl-Acyl Carrier Protein-Dependent UDP-GlcNAc Acyltransferase. *J Bacteriol.* **180**, 330–337
20. Anderson, M. S., Bull, H. G., Galloway, S. M., Kelly, T. M., Mohan, S., Radika, K., and Raetz, C. R. H. (1993) UDP-N-acetylglucosamine acyltransferase of *Escherichia coli*. The first step of endotoxin biosynthesis is thermodynamically unfavorable. *Journal of Biological Chemistry.* **268**, 19858–19865
21. Jackman, J. E., Raetz, C. R. H., and Fierke, C. A. (1999) UDP-3- O -(R -3-Hydroxymyristoyl)- N -acetylglucosamine Deacetylase of *Escherichia coli* Is a Zinc Metalloenzyme. *Biochemistry.* **38**, 1902–1911
22. Schäkermann, M., Langklotz, S., and Narberhaus, F. (2013) FtsH-Mediated Coordination of Lipopolysaccharide Biosynthesis in *Escherichia coli* Correlates with the Growth Rate and the Alarmone (p)ppGpp. *J Bacteriol.* **195**, 1912–1919
23. Fuhrer, F., Langklotz, S., and Narberhaus, F. (2006) The C-terminal end of LpxC is required for degradation by the FtsH protease. *Mol Microbiol.* **59**, 1025–1036
24. Bittner, L.-M., Arends, J., and Narberhaus, F. (2017) When, how and why? Regulated proteolysis by the essential FtsH protease in *Escherichia coli*. *Biol Chem.* **398**, 625–635

25. Bartling, C. M., and Raetz, C. R. H. (2008) Steady-State Kinetics and Mechanism of LpxD, the *N*-Acyltransferase of Lipid A Biosynthesis. *Biochemistry*. **47**, 5290–5302
26. Babinski, K. J., Ribeiro, A. A., and Raetz, C. R. H. (2002) The Escherichia coli Gene Encoding the UDP-2,3-diacylglucosamine Pyrophosphatase of Lipid A Biosynthesis. *Journal of Biological Chemistry*. **277**, 25937–25946
27. Garrett, T. A., Que, N. L. S., and Raetz, C. R. H. (1998) Accumulation of a Lipid A Precursor Lacking the 4'-Phosphate following Inactivation of the Escherichia coli lpxK Gene. *Journal of Biological Chemistry*. **273**, 12457–12465
28. Clementz, T., Zhou, Z., and Raetz, Christian R. H. (1997) Function of the Escherichia coli msbB Gene, a Multicopy Suppressor of htrB Knockouts, in the Acylation of Lipid A. *Journal of Biological Chemistry*. **272**, 10353–10360
29. Brozek, K. A., and Raetz, C. R. H. (1990) Biosynthesis of lipid A in Escherichia coli. Acyl carrier protein-dependent incorporation of laurate and myristate. *Journal of Biological Chemistry*. **265**, 15410–15417
30. Qian, J., Garrett, T. A., and Raetz, C. R. H. (2014) *In Vitro* Assembly of the Outer Core of the Lipopolysaccharide from *Escherichia coli* K-12 and *Salmonella typhimurium*. *Biochemistry*. **53**, 1250–1262
31. Amor, K., Heinrichs, D. E., Fridrich, E., Ziebell, K., Johnson, R. P., and Whitfield, C. (2000) Distribution of Core Oligosaccharide Types in Lipopolysaccharides from *Escherichia coli*. *Infect Immun*. **68**, 1116–1124
32. Bonifer, C., and Glaubitz, C. (2021) MsbA: an ABC transporter paradigm. *Biochem Soc Trans*. **49**, 2917–2927

33. IGUCHI, A. (2016) A complete view of the <i>Escherichia coli</i> O-antigen biosynthesis gene cluster and the development of molecular-based O-serogrouping methods. *Nippon Saikingaku Zasshi*. **71**, 209–215
34. Whitfield, C., and Trent, M. S. (2014) Biosynthesis and Export of Bacterial Lipopolysaccharides. *Annu Rev Biochem*. **83**, 99–128
35. Liu, D., Cole, R. A., and Reeves, P. R. (1996) An O-antigen processing function for Wzx (RfbX): a promising candidate for O-unit flippase. *J Bacteriol*. **178**, 2102–2107
36. Feldman, M. F., Marolda, C. L., Monteiro, M. A., Perry, M. B., Parodi, A. J., and Valvano, M. A. (1999) The Activity of a Putative Polyisoprenol-linked Sugar Translocase (Wzx) Involved in *Escherichia coli* O Antigen Assembly Is Independent of the Chemical Structure of the O Repeat. *Journal of Biological Chemistry*. **274**, 35129–35138
37. Greenfield, L. K., and Whitfield, C. (2012) Synthesis of lipopolysaccharide O-antigens by ABC transporter-dependent pathways. *Carbohydr Res*. **356**, 12–24
38. Keenleyside, W. J., and Whitfield, C. (1996) A Novel Pathway for O-Polysaccharide Biosynthesis in *Salmonella enterica* Serovar Borreze. *Journal of Biological Chemistry*. **271**, 28581–28592
39. Wear, S. S., Hunt, B. A., Clarke, B. R., and Whitfield, C. (2020) Analysis of the Topology and Active-Site Residues of WbbF, a Putative O-Polysaccharide Synthase from *Salmonella enterica* Serovar Borreze. *J Bacteriol*. 10.1128/JB.00625-19
40. Wear, S. S., Hunt, B. A., Clarke, B. R., and Whitfield, C. (2020) Analysis of the Topology and Active-Site Residues of WbbF, a Putative O-Polysaccharide Synthase from *Salmonella enterica* Serovar Borreze. *J Bacteriol*. 10.1128/JB.00625-19

41. Han, W., Wu, B., Li, L., Zhao, G., Woodward, R., Pettit, N., Cai, L., Thon, V., and Wang, P. G. (2012) Defining Function of Lipopolysaccharide O-antigen Ligase WaaL Using Chemoenzymatically Synthesized Substrates. *Journal of Biological Chemistry*. **287**, 5357–5365
42. Sperandio, P., Martorana, A. M., and Polissi, A. (2019) The Lpt ABC transporter for lipopolysaccharide export to the cell surface. *Res Microbiol*. **170**, 366–373
43. Okuda, S., Sherman, D. J., Silhavy, T. J., Ruiz, N., and Kahne, D. (2016) Lipopolysaccharide transport and assembly at the outer membrane: the PEZ model. *Nat Rev Microbiol*. **14**, 337–345
44. Sherman, D. J., Xie, R., Taylor, R. J., George, A. H., Okuda, S., Foster, P. J., Needleman, D. J., and Kahne, D. (2018) Lipopolysaccharide is transported to the cell surface by a membrane-to-membrane protein bridge. *Science (1979)*. **359**, 798–801
45. Hicks, G., and Jia, Z. (2018) Structural Basis for the Lipopolysaccharide Export Activity of the Bacterial Lipopolysaccharide Transport System. *Int J Mol Sci*. **19**, 2680
46. Guo, L., Lim, K. B., Poduje, C. M., Daniel, M., Gunn, J. S., Hackett, M., and Miller, S. I. (1998) Lipid A Acylation and Bacterial Resistance against Vertebrate Antimicrobial Peptides. *Cell*. **95**, 189–198
47. Reynolds, C. M., Ribeiro, A. A., McGrath, S. C., Cotter, R. J., Raetz, C. R. H., and Trent, M. S. (2006) An Outer Membrane Enzyme Encoded by *Salmonella typhimurium* lpxR That Removes the 3'-Acyloxyacyl Moiety of Lipid A. *Journal of Biological Chemistry*. **281**, 21974–21987
48. Trent, M. S., Pabich, W., Raetz, C. R. H., and Miller, S. I. (2001) A PhoP/PhoQ-induced Lipase (PagL) That Catalyzes 3-O-Deacylation of Lipid A Precursors in Membranes of *Salmonella typhimurium*. *Journal of Biological Chemistry*. **276**, 9083–9092

49. Ogawa, R., Yen, H., Kawasaki, K., and Tobe, T. (2018) Activation of *lpxR* gene through enterohaemorrhagic *Escherichia coli* virulence regulators mediates lipid A modification to attenuate innate immune response. *Cell Microbiol.* **20**, e12806
50. Jia, W., Zoeiby, A. El, Petruzzello, T. N., Jayabalasingham, B., Seyedirashti, S., and Bishop, R. E. (2004) Lipid Trafficking Controls Endotoxin Acylation in Outer Membranes of *Escherichia coli*. *Journal of Biological Chemistry.* **279**, 44966–44975
51. Raetz, C. R. H., Reynolds, C. M., Trent, M. S., and Bishop, R. E. (2007) Lipid A Modification Systems in Gram-Negative Bacteria. *Annu Rev Biochem.* **76**, 295–329
52. Bishop, R. E. (2005) The lipid A palmitoyltransferase PagP: molecular mechanisms and role in bacterial pathogenesis. *Mol Microbiol.* **57**, 900–912
53. Bishop, R. E., Gibbons, H. S., Guina, T., Trent, M. S., Miller, S. I., and Raetz, C. R. H. (2000) Transfer of palmitate from phospholipids to lipid A in outer membranes of Gram-negative bacteria. *EMBO J.* **19**, 5071–5080
54. Herrera, C. M., Hankins, J. V., and Trent, M. S. (2010) Activation of PmrA inhibits LpxT-dependent phosphorylation of lipid A promoting resistance to antimicrobial peptides. *Mol Microbiol.* **76**, 1444–1460
55. Touzé, T., Tran, A. X., Hankins, J. V., Mengin-Lecreux, D., and Trent, M. S. (2007) Periplasmic phosphorylation of lipid A is linked to the synthesis of undecaprenyl phosphate. *Mol Microbiol.* **67**, 264–277
56. Lee, H., Hsu, F.-F., Turk, J., and Groisman, E. A. (2004) The PmrA-Regulated *pmrC* Gene Mediates Phosphoethanolamine Modification of Lipid A and Polymyxin Resistance in *Salmonella enterica*. *J Bacteriol.* **186**, 4124–4133

57. Gibbons, H. S., Kalb, S. R., Cotter, R. J., and Raetz, C. R. H. (2004) Role of Mg²⁺ and pH in the modification of Salmonella lipid A after endocytosis by macrophage tumour cells. *Mol Microbiol.* **55**, 425–440
58. Trent, M. S., and C. R. H. Raetz (2002) Cloning of EptA, the lipid A phosphoethanolamine transferase associated with polymyxin resistance. *J Endotoxin Res*
59. Doerrler, W. T., Gibbons, H. S., and Raetz, C. R. H. (2004) MsbA-dependent Translocation of Lipids across the Inner Membrane of Escherichia coli. *Journal of Biological Chemistry.* **279**, 45102–45109
60. Breazeale, S. D., Ribeiro, A. A., and Raetz, C. R. H. (2003) Origin of Lipid A Species Modified with 4-Amino-4-deoxy-l-arabinose in Polymyxin-resistant Mutants of Escherichia coli. *Journal of Biological Chemistry.* **278**, 24731–24739
61. Breazeale, S. D., Ribeiro, A. A., McClerren, A. L., and Raetz, C. R. H. (2005) A Formyltransferase Required for Polymyxin Resistance in Escherichia coli and the Modification of Lipid A with 4-Amino-4-deoxy-l-arabinose. *Journal of Biological Chemistry.* **280**, 14154–14167
62. Breazeale, S. D., Ribeiro, A. A., and Raetz, C. R. H. (2002) Oxidative Decarboxylation of UDP-Glucuronic Acid in Extracts of Polymyxin-resistant Escherichia coli. *Journal of Biological Chemistry.* **277**, 2886–2896
63. Trent, M. S., Ribeiro, A. A., Lin, S., Cotter, R. J., and Raetz, C. R. H. (2001) An Inner Membrane Enzyme in Salmonella and Escherichia coli That Transfers 4-Amino-4-deoxy-l-arabinose to Lipid A. *Journal of Biological Chemistry.* **276**, 43122–43131

64. Trent, M. S., Ribeiro, A. A., Doerrler, W. T., Lin, S., Cotter, R. J., and Raetz, C. R. H. (2001) Accumulation of a Polyisoprene-linked Amino Sugar in Polymyxin-resistant *Salmonella typhimurium* and *Escherichia coli*. *Journal of Biological Chemistry*. **276**, 43132–43144
65. Dalebroux, Z. D., and Miller, S. I. (2014) *Salmonella* PhoPQ regulation of the outer membrane to resist innate immunity. *Curr Opin Microbiol*. **17**, 106–113
66. Gunn, J. S. (2008) The *Salmonella* PmrAB regulon: lipopolysaccharide modifications, antimicrobial peptide resistance and more. *Trends Microbiol*. **16**, 284–290
67. Chen, H. D., and Groisman, E. A. (2013) The Biology of the PmrA/PmrB Two-Component System: The Major Regulator of Lipopolysaccharide Modifications. *Annu Rev Microbiol*. **67**, 83–112
68. Kato, A., and Groisman, E. A. The PhoQ/PhoP Regulatory Network of *Salmonella enterica*. in *Bacterial Signal Transduction: Networks and Drug Targets*, pp. 7–21, Springer New York, New York, NY, 10.1007/978-0-387-78885-2_2
69. MacRitchie, D. M., Buelow, D. R., Price, N. L., and Raivio, T. L. Two-Component Signaling and Gram Negative Envelope Stress Response Systems. in *Bacterial Signal Transduction: Networks and Drug Targets*, pp. 80–110, Springer New York, New York, NY, 10.1007/978-0-387-78885-2_6
70. Prost, L. R., and Miller, S. I. (2008) The *Salmonella* PhoQ sensor: mechanisms of detection of phagosome signals. *Cell Microbiol*. **10**, 576–582
71. Véscovi, E. G., Soncini, F. C., and Groisman, E. A. (1996) Mg²⁺ as an Extracellular Signal: Environmental Regulation of *Salmonella* Virulence. *Cell*. **84**, 165–174

72. Richards, S. M., Strandberg, K. L., Conroy, M., and Gunn, J. S. (2012) Cationic antimicrobial peptides serve as activation signals for the *Salmonella* Typhimurium PhoPQ and PmrAB regulons in vitro and in vivo. *Front Cell Infect Microbiol.* 10.3389/fcimb.2012.00102
73. Yuan, J., Jin, F., Glatter, T., and Sourjik, V. (2017) Osmosensing by the bacterial PhoQ/PhoP two-component system. *Proceedings of the National Academy of Sciences.* 10.1073/pnas.1717272114
74. Bader, M. W., Sanowar, S., Daley, M. E., Schneider, A. R., Cho, U., Xu, W., Klevit, R. E., Le Moual, H., and Miller, S. I. (2005) Recognition of Antimicrobial Peptides by a Bacterial Sensor Kinase. *Cell.* **122**, 461–472
75. Choi, J., and Groisman, E. A. (2016) Acidic pH sensing in the bacterial cytoplasm is required for *Salmonella* virulence. *Mol Microbiol.* **101**, 1024–1038
76. Kox, L. F. F. (2000) A small protein that mediates the activation of a two-component system by another two-component system. *EMBO J.* **19**, 1861–1872
77. Guo, L., Lim, K. B., Gunn, J. S., Bainbridge, B., Darveau, R. P., Hackett, M., and Miller, S. I. (1997) Regulation of Lipid A Modifications by *Salmonella typhimurium* Virulence Genes *phoP-phoQ*. *Science (1979).* **276**, 250–253
78. Kato, A., and Groisman, E. A. (2004) Connecting two-component regulatory systems by a protein that protects a response regulator from dephosphorylation by its cognate sensor. *Genes Dev.* **18**, 2302–2313
79. Perez, J. C., and Groisman, E. A. (2007) Acid pH activation of the PmrA/PmrB two-component regulatory system of *Salmonella enterica*. *Mol Microbiol.* **63**, 283–293

80. Wösten, M. M. S. M., Kox, L. F. F., Chamnongpol, S., Soncini, F. C., and Groisman, E. A. (2000) A Signal Transduction System that Responds to Extracellular Iron. *Cell*. **103**, 113–125
81. Fernández, P. A., Velásquez, F., Garcias-Papayani, H., Amaya, F. A., Ortega, J., Gómez, S., Santiviago, C. A., and Álvarez, S. A. (2018) Fnr and ArcA Regulate Lipid A Hydroxylation in *Salmonella Enteritidis* by Controlling IpxO Expression in Response to Oxygen Availability. *Front Microbiol*. 10.3389/fmicb.2018.01220
82. Carpenter, T. S., Parkin, J., and Khalid, S. (2016) The Free Energy of Small Solute Permeation through the *Escherichia coli* Outer Membrane Has a Distinctly Asymmetric Profile. *J Phys Chem Lett*. **7**, 3446–3451
83. Nikaido, H. (2003) Molecular Basis of Bacterial Outer Membrane Permeability Revisited. *Microbiology and Molecular Biology Reviews*. **67**, 593–656
84. Murata, T., Tseng, W., Guina, T., Miller, S. I., and Nikaido, H. (2007) PhoPQ-Mediated Regulation Produces a More Robust Permeability Barrier in the Outer Membrane of *Salmonella enterica* Serovar Typhimurium. *J Bacteriol*. **189**, 7213–7222
85. Exner, M., Bhattacharya, S., Christiansen, B., Gebel, J., Goroncy-Bermes, P., Hartemann, P., Heeg, P., Ilshner, C., Kramer, A., Larson, E., Merkens, W., Mielke, M., Oltmanns, P., Ross, B., Rotter, M., Schmithausen, R. M., Sonntag, H.-G., and Trautmann, M. (2017) Antibiotic resistance: What is so special about multidrug-resistant Gram-negative bacteria? *GMS Hyg Infect Control*. **12**, Doc05
86. Gupta, V., and Datta, P. (2019) Next-generation strategy for treating drug resistant bacteria: Antibiotic hybrids. *Indian Journal of Medical Research*. **149**, 97

87. Miller, S. I. (2016) Antibiotic Resistance and Regulation of the Gram-Negative Bacterial Outer Membrane Barrier by Host Innate Immune Molecules. *mBio*. 10.1128/mBio.01541-16
88. Velkov, T., Thompson, P. E., Nation, R. L., and Li, J. (2010) Structure–Activity Relationships of Polymyxin Antibiotics. *J Med Chem*. **53**, 1898–1916
89. Velkov, T., Deris, Z. Z., Huang, J. X., Azad, M. A., Butler, M., Sivanesan, S., Kaminskis, L. M., Dong, Y.-D., Boyd, B., Baker, M. A., Cooper, M. A., Nation, R. L., and Li, J. (2014) Surface changes and polymyxin interactions with a resistant strain of *Klebsiella pneumoniae*. *Innate Immun*. **20**, 350–363
90. Manioglu, S., Modaresi, S. M., Ritzmann, N., Thoma, J., Overall, S. A., Harms, A., Upert, G., Luther, A., Barnes, A. B., Obrecht, D., Müller, D. J., and Hiller, S. (2022) Antibiotic polymyxin arranges lipopolysaccharide into crystalline structures to solidify the bacterial membrane. *Nat Commun*. 10.1038/s41467-022-33838-0
91. Renzi, F., Zähringer, U., Chandler, C. E., Ernst, R. K., Cornelis, G. R., and Ittig, S. J. (2016) Modification of the 1-Phosphate Group during Biosynthesis of Capnocytophaga canimorsus Lipid A. *Infect Immun*. **84**, 550–561
92. Needham, B. D., and Trent, M. S. (2013) Fortifying the barrier: the impact of lipid A remodelling on bacterial pathogenesis. *Nat Rev Microbiol*. **11**, 467–481
93. Scott, A. J., Oyler, B. L., Goodlett, D. R., and Ernst, R. K. (2017) Lipid A structural modifications in extreme conditions and identification of unique modifying enzymes to define the Toll-like receptor 4 structure-activity relationship. *Biochimica et Biophysica Acta (BBA) - Molecular and Cell Biology of Lipids*. **1862**, 1439–1450

94. Tlaskalová-Hogenová, H., Štěpánková, R., Kozáková, H., Hudcovic, T., Vannucci, L., Tučková, L., Rossmann, P., Hrnčíř, T., Kverka, M., Zákostelská, Z., Klimešová, K., Příbylová, J., Bártová, J., Sanchez, D., Fundová, P., Borovská, D., Šrůtková, D., Zídek, Z., Schwarzer, M., Drastich, P., and Funda, D. P. (2011) The role of gut microbiota (commensal bacteria) and the mucosal barrier in the pathogenesis of inflammatory and autoimmune diseases and cancer: contribution of germ-free and gnotobiotic animal models of human diseases. *Cell Mol Immunol.* **8**, 110–120
95. Sassi, N., Paul, C., Martin, A., Bettaieb, A., and Jeannin, J.-F. (2009) Lipid A-Induced Responses In Vivo, pp. 69–80, 10.1007/978-1-4419-1603-7_7
96. Simmons, D., Tan, S., Tenen, D., Nicholson-Weller, A., and Seed, B. (1989) Monocyte antigen CD14 is a phospholipid anchored membrane protein. *Blood.* **73**, 284–289
97. Maeshima, N., and Fernandez, R. C. (2013) Recognition of lipid A variants by the TLR4-MD-2 receptor complex. *Front Cell Infect Microbiol.* 10.3389/fcimb.2013.00003
98. Kong, Q., Six, D. A., Liu, Q., Gu, L., Wang, S., Alamuri, P., Raetz, C. R. H., and Curtiss, R. (2012) Phosphate Groups of Lipid A Are Essential for Salmonella enterica Serovar Typhimurium Virulence and Affect Innate and Adaptive Immunity. *Infect Immun.* **80**, 3215–3224
99. Kong, Q., Six, D. A., Liu, Q., Gu, L., Roland, K. L., Raetz, C. R. H., and Curtiss, R. (2011) Palmitoylation State Impacts Induction of Innate and Acquired Immunity by the Salmonella enterica Serovar Typhimurium *msbB* Mutant. *Infect Immun.* **79**, 5027–5038
100. Kawai, T., and Akira, S. (2011) Toll-like Receptors and Their Crosstalk with Other Innate Receptors in Infection and Immunity. *Immunity.* **34**, 637–650
101. Kagan, J. C., and Medzhitov, R. (2006) Phosphoinositide-Mediated Adaptor Recruitment Controls Toll-like Receptor Signaling. *Cell.* **125**, 943–955

102. Casella, C. R., and Mitchell, T. C. (2008) Putting endotoxin to work for us: Monophosphoryl lipid A as a safe and effective vaccine adjuvant. *Cellular and Molecular Life Sciences*. **65**, 3231–3240
103. Takeuchi, O., and Akira, S. (2010) Pattern Recognition Receptors and Inflammation. *Cell*. **140**, 805–820
104. Montminy, S. W., Khan, N., McGrath, S., Walkowicz, M. J., Sharp, F., Conlon, J. E., Fukase, K., Kusumoto, S., Sweet, C., Miyake, K., Akira, S., Cotter, R. J., Goguen, J. D., and Lien, E. (2006) Virulence factors of *Yersinia pestis* are overcome by a strong lipopolysaccharide response. *Nat Immunol*. **7**, 1066–1073
105. Cullen, T. W., Giles, D. K., Wolf, L. N., Ecobichon, C., Boneca, I. G., and Trent, M. S. (2011) *Helicobacter pylori* versus the Host: Remodeling of the Bacterial Outer Membrane Is Required for Survival in the Gastric Mucosa. *PLoS Pathog*. **7**, e1002454
106. Munford, R. S., and Hunter, J. P. (1992) Acyloxyacyl hydrolase, a leukocyte enzyme that deacylates bacterial lipopolysaccharides, has phospholipase, lysophospholipase, diacylglycerollipase, and acyltransferase activities in vitro. *J Biol Chem*. **267**, 10116–21
107. Bentala, H., Verweij, W. R., der Vlag, A. H.-V., van Loenen-Weemaes, A. M., Meijer, D. K. F., and Poelstra, K. (2002) Removal of Phosphate from Lipid A as a Strategy to Detoxify Lipopolysaccharide. *Shock*. **18**, 561–566
108. Bates, J. M., Akerlund, J., Mittge, E., and Guillemin, K. (2007) Intestinal Alkaline Phosphatase Detoxifies Lipopolysaccharide and Prevents Inflammation in Zebrafish in Response to the Gut Microbiota. *Cell Host Microbe*. **2**, 371–382

109. Koyama, I., Matsunaga, T., Harada, T., Hokari, S., and Komoda, T. (2002) Alkaline phosphatases reduce toxicity of lipopolysaccharides in vivo and in vitro through dephosphorylation. *Clin Biochem.* **35**, 455–461

Chapter 2

Substrate Structure-Activity Relationship Reveals a Limited Lipopolysaccharide Chemotype Range for Intestinal Alkaline Phosphatase

This chapter was adapted from: Komazin, G.; Maybin, M.; Woodard, R.W.; Scior, T.; Schwudke, D.; et al., Substrate Structure-Activity Relationship Reveals a Limited Lipopolysaccharide Chemotype Range For Intestinal Alkaline Phosphatase. *J Biol Chem.* **2019**, 294, 19405-19423.

Note: Strain construction performed by Gloria Komazin. All MS and NMR analyses were carried out by Nicholas Gisch and Uwe Mamat. Modeling was performed by Thomas Scior.

ABSTRACT

Lipopolysaccharide (LPS) from the Gram-negative bacterial outer membrane potently activates the human innate immune system. LPS is recognized by the Toll-like receptor 4/myeloid differentiation factor-2 (TLR4/MD2) complex, leading to the release of pro-inflammatory cytokines. Alkaline phosphatase (AP) is currently being investigated as an anti-inflammatory agent for detoxifying LPS through dephosphorylating lipid A, thus providing a potential treatment for managing both acute (sepsis) and chronic (metabolic endotoxemia) pathologies wherein aberrant TLR4/MD2 activation has been implicated. Endogenous LPS preparations are chemically heterogeneous, and little is known regarding the LPS chemotype substrate range of AP. Here, we investigated the activity of AP on a panel of structurally defined LPS chemotypes isolated from *Escherichia coli* and demonstrate that calf intestinal AP (cIAP) has only minimal activity against unmodified enteric LPS chemotypes. Inorganic phosphate was only released from a subset of LPS chemotypes harboring spontaneously labile phosphoethanolamine (PEtN) modifications connected through phosphoanhydride bonds. We demonstrate that the spontaneously hydrolyzed *O*-phosphorylethanolamine is the actual substrate for AP. We found that the 1- and 4'-lipid A phosphate groups critical in TLR4/MD2 signaling become susceptible to hydrolysis only after de-*O*-acylation of ester linked primary acyl chains on lipid A. Furthermore, PEtN modifications on lipid A specifically enhanced hTLR4 agonist activity of underacylated LPS preparations. Computational binding models are proposed to explain the limitation of AP substrate specificity imposed by the acylation state of lipid A, and the mechanism of PEtN in enhancing hTLR4/MD2 signaling.

INTRODUCTION

Low-grade systemic inflammation associated with a number of metabolic syndromes has been proposed to originate from bacterial flora (1-7). Bacterial products (microbe-associated molecular patterns, MAMPs, or pathogen-associated molecular patterns, PAMPs) from the intestinal flora are normally contained within the lumen by the intestinal epithelium layer. However, high fat diets, obesity, and inflammatory bowel diseases help increase the permeability of the intestinal mucosal barrier, allowing luminal contents to breach containment and enter the blood stream. MAMP engagement by pattern recognition receptors (PRR) on target cells triggers the release of pro-inflammatory cytokines, setting a low-grade systemic inflammatory tone (8, 9). Inflammation and oxidative stress is further accelerated by adipose tissue deposits, which can directly respond to MAMPs as well and secrete pro-inflammatory adipocytokines (10, 11). A central PRR-MAMP pair in these processes is the Gram-negative bacterial outer membrane (OM) component lipopolysaccharide (LPS or endotoxin) and the Toll-like receptor 4/myeloid differentiation factor-2 (TLR4/MD2) complex. Collectively termed metabolic endotoxemia (ME), elevated serum endotoxin levels and the ensuing aberrant TLR4/MD2 activity have been associated with the complications of metabolic diseases (6, 12). So far LPS constitutes the only known bacterial MAMP that can induce obesity as well as insulin resistance when infused subcutaneously into mice (2, 13). Thus, preventing ME through degradation and detoxification of LPS offers a potential therapeutic strategy for managing the onset, severity, and progression of ME (14).

According to the endotoxin principle, the 1- and 4'- lipid A phosphates of LPS are critical for biological activity as chemically dephosphorylated lipid A congeners weakly stimulate TLR4/MD2-directed pro-inflammatory cytokine release (15). Alkaline phosphatase (AP) has thus far received the most attention as a potential tool to detoxify LPS and attenuate inflammation through lipid A dephosphorylation (16-19). Recombinant AP is currently being examined in multiple clinical trials to treat a host of chronic (ME) or acute (sepsis) inflammatory conditions where endotoxin-induced inflammation is a suspected component of the underlying pathology (20-22). There are four AP encoding genes in humans, three of which demonstrate tissue specific expression [intestinal AP (IAP, *ALPI*), placental or embryonic AP (PLAP, *ALPP*) and germ cell AP (GCAP, *ALPPL2*)] along with a tissue nonspecific AP (TNAP, *ALPL*) isoform (23, 24). IAP, being a native defense factor within the intestinal mucosal brush border, is a particularly promising therapeutic candidate as the anti-inflammatory mechanism of IAP has been attributed in part to the direct dephosphorylation of LPS (22, 25-30). Presumably, IAP hydrolyses critical phosphates from lipid A involved in TLR4/MD2 recognition, although structural characterization of the IAP dephosphorylated LPS product has not hitherto been reported (31, 32). IAP activity to this point has instead been indirectly evaluated through the release of inorganic phosphate using variants of the molybdate malachite green assay (33), in tandem with the apparent loss of biological activity. The potential LPS chemotype substrate specificity spectrum is unknown, as is the unanswered question of which of the many phosphate groups present on LPS are actually subject to dephosphorylation by IAP.

LPS from *Escherichia coli* possesses among the highest endogenous endotoxin activity and can be non-stoichiometrically modified with a variety of moieties. Variations in LPS acylation

state, saccharide core, and phosphorylation patterns could conceivably affect IAP recognition and processing. Of note, *E. coli* converts the 1- and 4'- lipid A phosphate groups from phosphomonoesters into phosphodiester upon addition of phosphoethanolamine (PEtN) and 4-amino-4-deoxy-L-arabinose (Ara4N) residues. PEtN and Ara4N addition are governed by a complex network of alternative transcription factors, two component systems, and regulatory RNAs (34). In *Salmonella enterica*, the regulators controlling LPS remodeling with PEtN/Ara4N are in the mouse intestinal lumen environment (35). These regulatory systems could thus not only enable bacterial survival, but also block IAP-mediated LPS detoxification.

Given the complex and structurally heterogeneous nature of LPS (36, 37), previous work done in the Meredith lab sought to determine IAP substrate specificity using a panel of defined LPS chemotypes isolated from *E. coli*. A highly purified *E. coli* B LPS feedstock sample was first isolated using an extended isolation protocol that included specific steps to remove phospholipid and nucleic acid contaminants that could contribute to background phosphate release. *E. coli* B was chosen as the parent LPS strain source firstly because of a native insertion sequence element within the outer saccharide core *waaT* gene, encoding for a UDP-galactose:(glucosyl) LPS α 1,2-galactosyltransferase glycosyltransferase, that truncates the LPS to a structure of relatively low complexity (38, 39), and secondly for the high levels of endogenous PEtN and Ara4N modifications observed when this strain is grown in standard rich medium (40). Analysis by mass spectrometry confirmed a highly PEtN/Ara4N-substituted LPS, with an average total phosphate content of between 4 to 5 Pi equivalents per molecule of LPS (41). Calf intestinal alkaline phosphatase (cIAP) was initially tested with LPS preparations from wildtype *E. coli* B LPS for phosphate release using the inorganic phosphate specific malachite green assay (41). While

phosphate release was readily detected, the amount plateaued well short of the total LPS-associated phosphate input (~25 μM LPS with 100-125 μM total phosphate). Since there are multiple tissue specific AP isoforms (23, 24), a panel of commercially available APs was tested to determine if a more robust phosphate release could be realized. However, all APs (including human intestinal alkaline phosphatase, hALPI) demonstrated a plateau similar to cIAP even after a prolonged 96-hour incubation period (41). Varying reaction conditions by adding bile salts to act as detergent, bovine serum albumin, 10% whole serum, or extensive pre-sonication of LPS vesicles did not appreciably enhance the amount of phosphate released. Detection of inorganic phosphate was completely dependent on inclusion of AP. This suggested that only a fraction of the total LPS phosphate content was subject to hydrolysis, irrespective of either the AP isoform or presence of de-aggregation agents (41).

To determine which LPS phosphate group(s) was being released, the assay was repeated using a structurally defined Re LPS chemotype as substrate. Re LPS extracted from *E. coli* TXM333 lacks all sugars but Kdo (3-deoxy- α -D-manno-oct-2-ulosonic acid) from the saccharide core due to deletion of the D-sedoheptulose 7-phosphate isomerase gene *lpcA* (*gmhA*) as well as all types of PEtN/Ara4N modifications on lipid A due to deletions in the respective biosynthetic genes *eptA/arnA*. Re LPS was extensively purified as described above for wildtype, and analysis by MS confirmed a nearly homogeneous population of the Re chemotype (41). In striking contrast to wildtype LPS, no phosphate was liberated from Re chemotype when incubated under identical conditions (41). This indicated inefficient cleavage of core lipid A phosphates by APs, and that the phosphate liberated from wildtype LPS likely originates from either lipid A PEtN or saccharide core modifications attached distal to Kdo residues.

PEtN groups are added in nonstoichiometric amounts to LPS at three distinct positions by a set of related membrane-bound transferases: *i.*) EptA onto either lipid A phosphate (42), *ii.*) EptB onto KdoII (43), or *iii.*) EptC onto phosphorylated HepI (*L-glycero-D-manno-heptose*) (44). A panel of deletions in *eptA* was constructed since this transferase can add PEtN to both phosphates of lipid A. Indeed, the amount of phosphate released was closely correlated with the presence of EptA, and plasmid-borne EptA alone restored phosphate release when testing Re LPS chemotype as substrate (41). Deletion of *arnA*, which modifies lipid A phosphate groups with Ara4N (45), alone or in tandem with *eptA* had minimal influence on phosphate release.

While phosphate installed by EptA accounted for the bulk of the total released, significant amounts of phosphate (up to ~30% of the total) was still liberated from LPS chemotypes isolated from $\Delta eptA$ strain backgrounds (41). This suggested some of the detected phosphate originated from the saccharide core as well. Phosphate liberation from LPS chemotypes produced by strains harboring various combinations of *eptA/B/C* was thusly tested (41). All strains were $\Delta arnA$ to limit any variability arising from substrate competition by ArnA with EptA. Since the native promoters of each of the PEtN transferases is subject to complex regulation, constructs with constitutive promoters were used to achieve comparable high-level PEtN modification levels as assessed by MS (41). Next to $\Delta eptA$, the least amount of phosphate release was detected from LPS extracted from strains lacking EptC and WaaP, the HepI kinase that forms the *P*-HepI acceptor substrate utilized by EptC (46). Overexpression of EptC, but not EptB, enhanced phosphate release although the amount remained well below EptA. The data collectively suggested that EptA installs most of the total labile phosphate pool in *E. coli* wildtype LPS, with EptC making a minor contribution while the phosphate content added by EptB is stable to hydrolysis (41).

With the knowledge that phosphate release via AP is specifically dependent on LPS chemotypes modified with PEtN groups EptA or EptC, we sought to determine whether AP directly releases phosphate from PEtN attached to LPS. Herein I investigate the role PEtN modifications play in the observed phosphate release post incubation with cIAP, determine the minimal LPS structure wherein cIAP can hydrolyze the lipid A bound phosphate groups, and examine how PEtN modifications alter TLR4/MD2 response. In summary, we demonstrate that PEtN attached to LPS by a phosphoanhydride bond by EptA spontaneously hydrolyzes at neutral to basic pH to release free PEtN, which in turn generates the actual substrate for cIAP. The lipid A bound phosphate groups that are critical to TLR4/MD2 signaling only become susceptible to IAP activity after de-*O*-acylation of ester linked primary acyl chains on lipid A. Importantly, LPS with PEtN covalently attached to lipid A on the 1- and 4'- lipid A phosphates through phosphoanhydride bonds stimulates TLR4/MD2 signaling activity in comparison to congeners lacking PEtN. The extent of TLR4/MD2 stimulation by PEtN modifications on lipid A is enhanced with decreasing acylation states and converts the otherwise antagonist tetra-acylated lipid IV_A ligand into a weak agonist. Computational binding models are applied to explain the substrate specificity of IAP, as well as the effects of PEtN modification on lipid IV_A binding to human and murine TLR4/MD2 receptors. The apparent inability for IAP to dephosphorylate the critical lipid A backbone phosphates in fully acylated substrates suggests the physiological role of IAP in suppressing LPS induced inflammation does not involve dephosphorylation of LPS as has previously been proposed (25-30) and alternative models besides TLR4/MD2 regulation are discussed.

RESULTS

PEtN release from LPS is spontaneous

The PEtN groups attached by EptA and EptC are both connected by a phosphoanhydride bond, while EptB installs a typical phosphodiester bond at KdOII. The data thus supported one of three scenarios, wherein either: *i.*) cIAP specifically recognizes PEtN residues attached by EptA/EptC, *ii.*) cIAP only cleaves phosphoanhydride linked PEtN groups, or *iii.*) PEtN connected through a phosphoanhydride bond spontaneously hydrolyzes to free *O*-PEtN monoester that then supplies the actual substrate for cIAP. We initially suspected the third scenario, given the reactivity of high-energy phosphoanhydride bonds and the fact that the majority of characterized AP substrates are phosphomonoesters (23, 47). To test for non-enzymatic hydrolysis, Re LPS modified with phosphoanhydride linked PEtN added by EptA (from TXM343) was incubated with or without cIAP, extracted, and analyzed by MS for doubly modified, singly modified, and unmodified Re LPS (Fig. 2-1). Reactions were performed within dialysis tubing and continuously dialyzed to prevent any potential product inhibition by liberated inorganic phosphate. PEtN hydrolysis was monitored by a mass shift of $\Delta m = 123$ u, which corresponds to a single PEtN residue. While the total PEtN content clearly decreased after incubation (buffer pH=7.1, 16 hours) when compared to directly injected samples, the MS profile of mock-treated Re LPS was nearly indistinguishable from cIAP-treated samples (Fig. 2-1, middle and bottom panels).

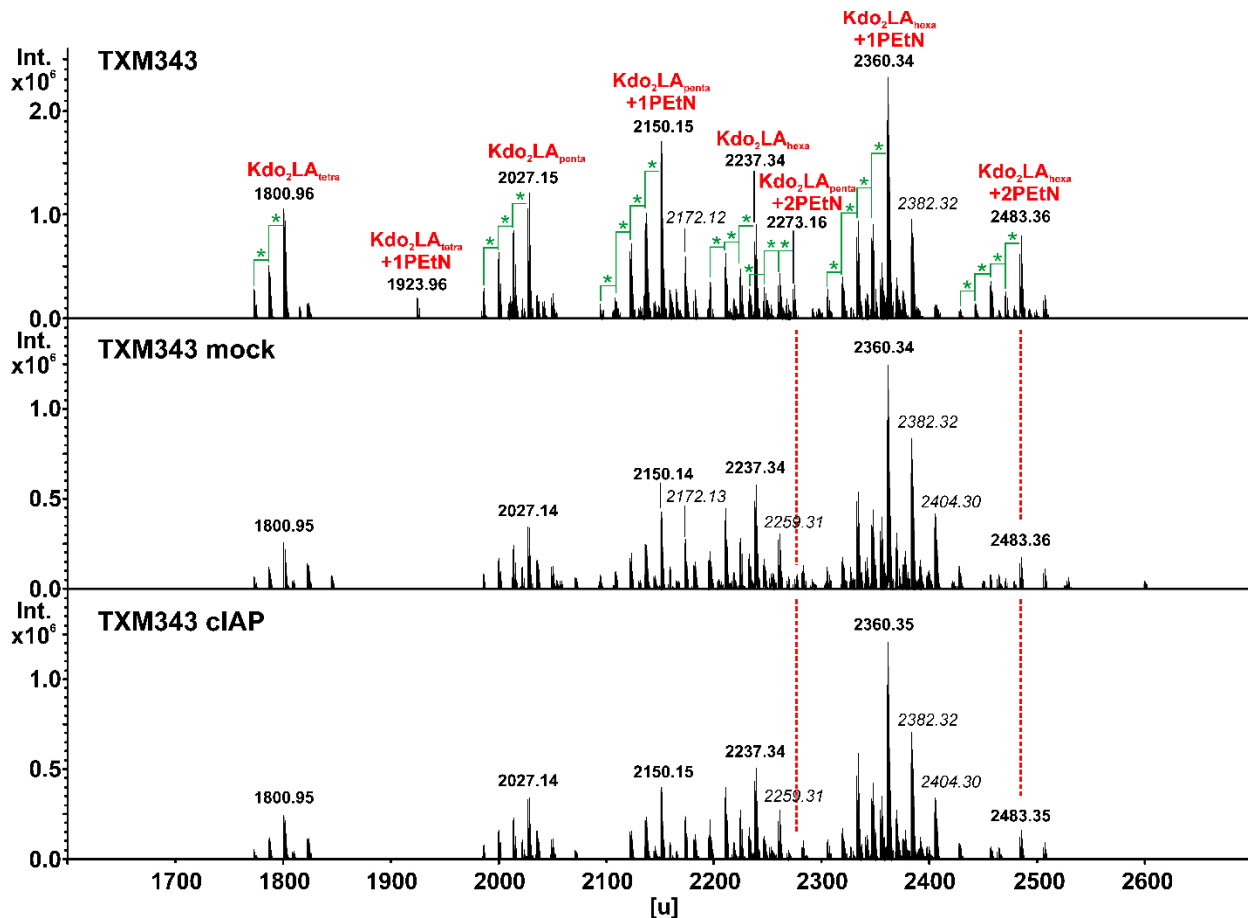


Figure 2-1: MS analysis of EptA-modified Re LPS. Re LPS was extracted from TXM343 [*lpcA::gentR eptA::catR* *arnA::kanR* (pSEVA434-*eptA*)] and analyzed by MS. Samples were either directly analyzed (top panel), or incubated for 16 hours at 37 °C in buffer [100 µg/ml substrate, 50 mM Tris-HCl (pH = 7.1), 100 mM NaCl, 1 mM MgCl₂, 20 µM ZnCl₂] alone (mock) or with cIAP (4 U/ml). Reactions were assembled within dialysis tubing and continuously dialyzed against buffer to remove potentially inhibitory inorganic phosphate product. Masses in italic type represent sodium adducts ($\Delta m = 22$ u), while those marked with a green star account for a difference of $\Delta m = 14$ u, consistent with a methylene unit (-CH₂-). Done in collaboration with Gloria Komazin and MS analysis carried out by Nicholas Gisch.

To confirm spontaneous (*i.e.* non-enzymatic) hydrolysis, we examined a second set of PEtN-modified chemotypes with a more homogenous composition since quantitative comparison of Re LPS MS peaks is complicated by multiple glycoforms within the same population. We previously had constructed a mutant *E. coli* strain that elaborates only lipid IV_A, a chemotype lacking glycosylation with uniform 3-OH-C14:0 tetra-acylation, that remains viable

due to suppressor mutations in LPS transport systems (48, 49). By introducing pEptA into this genetic background, we obtained PEtN-modified lipid IV_A substrate preparations with 2-PEtN, 1-PEtN, or unmodified lipid IV_A (Fig. 2-2A). When assayed for phosphate release, a nonlinear correlation between the amount of released inorganic phosphate and the units of cIAP added was observed well before the total amount of input PEtN-linked lipid IV_A phosphate should become rate limiting (Fig. 2-2B). This is consistent with an initial slower, non-enzymatic hydrolytic step preceding cIAP catalysis, namely the putative dephosphorylation of free PEtN.

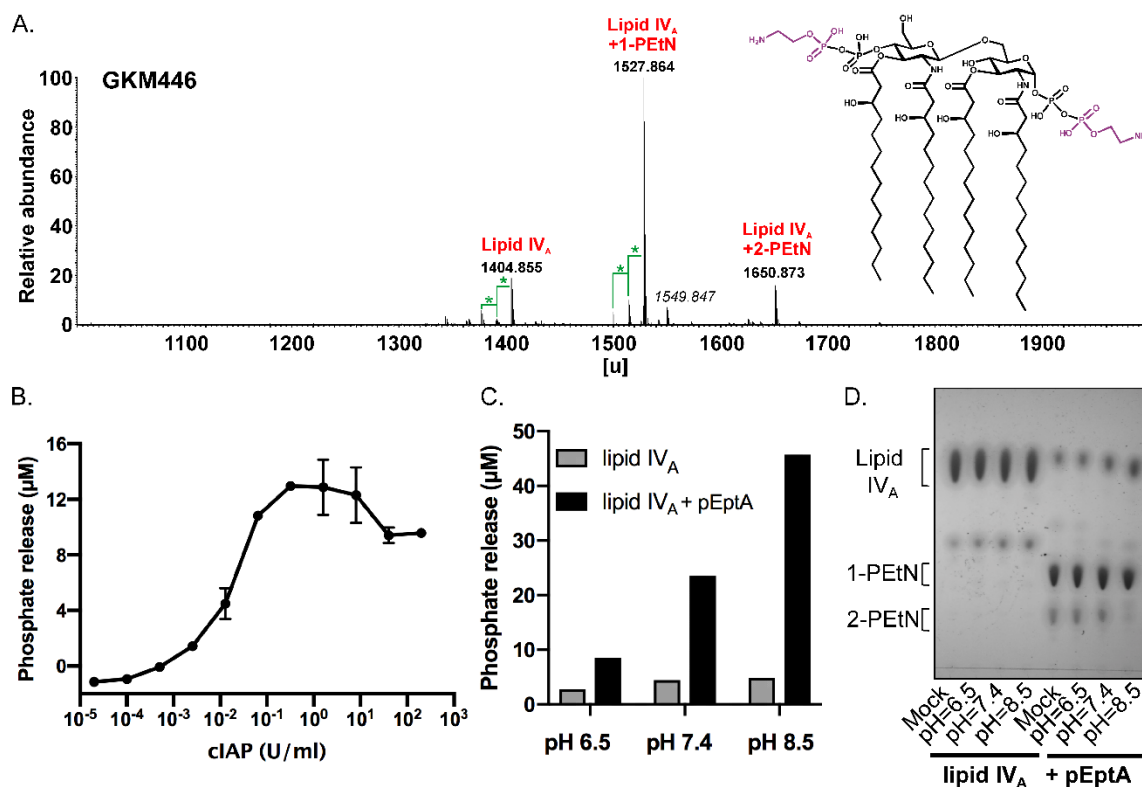


Figure 2-2: Hydrolysis of phosphoanhydride linked PEtN-lipid IV_A is spontaneous and pH dependent. (A) MS analysis in the negative anion mode of lipid IV_A isolated from GKM446 ($\Delta\text{eptA}\Delta\text{gutQ}\Delta\text{kdsD}\Delta\text{lpxL}\Delta\text{lpxM}\Delta\text{lpxP}\Delta\text{pagP}$ + pEptA). The structure of lipid IV_A modified with two PEtN residues in non-stoichiometric amounts at C1'-GlcNI and C4'-GlcNII when EptA is expressed is indicated (*purple*). Masses in italic style represent sodium adducts ($\Delta m = 22$ u), differences marked with a green star account for a difference of $\Delta m = 14$ u, consistent with a methylene unit ($-\text{CH}_2-$). (B) Phosphate release was measured as a function of increasing concentrations of cIAP after incubation for 6 hours at 37 °C [100 $\mu\text{g}/\text{ml}$ PEtN-lipid IV_A substrate, 50 mM Tris-HCl (pH =

8.25), 100 mM NaCl, 1 mM MgCl₂, 20 μM ZnCl₂] using PEtN-lipid IV_A substrate isolated from GKM446. Phosphate was measured using the malachite green assay, and data are representative of two independent experiments conducted in triplicate with the error bars showing SDs. (C) Either lipid IV_A alone (*ClearColi*[®] K-12 GKM445 Δ *eptA* Δ *gutQ* Δ *kdsD* Δ *lpxL* Δ *lpxM* Δ *lpxP* Δ *pagP*) or with PEtN added by EptA (GKM446 Δ *eptA* Δ *gutQ* Δ *kdsD* Δ *lpxL* Δ *lpxM* Δ *lpxP* Δ *pagP* + pEptA) was incubated for 48 hours at 37 °C in MOPS-Tris buffer [100 μg/ml substrate, 50 mM MOPS/50 mM Tris (adjusted to pH 6.5, 7.4, or 8.5), 100 mM NaCl, 1 mM MgCl₂, 20 μM ZnCl₂), and then treated with cIAP (10 U/ml cIAP) to release inorganic phosphate from spontaneously hydrolyzed PEtN. Phosphate was quantified using the malachite green assay. (D) Lipid IV_A species were hydrolyzed for 48 hours in MOPS-Tris buffer at the indicated pH as described in (C) except samples were isolated by extraction before separation by TLC. Total lipid was visualized by sulfuric acid charring. Done in collaboration with Gloria Komazin

Hydrolysis of phosphoanhydride-linked PEtN from LPS is pH dependent

We next tested the stability of PEtN linkages attached by EptA on lipid IV_A by incubation in buffer at defined pH (Fig. 2-2C). Liberated PEtN was indirectly quantified by adding excess cIAP at the end of the incubation period and measuring inorganic phosphate levels using the malachite green assay. The extent of phosphate released increased as the pH of the pre-incubation buffer was raised, consistent with a base-labile phosphoanhydride bond. Hydrolysis was minimal at acidic pH, an environmental condition that naturally induces *eptA* expression and lipid A modification with PEtN in *E. coli* and *Salmonella enterica* (50, 51). We repeated the incubation a second time, except samples were not treated with cIAP and the resulting lipid IV_A population was extracted and separated by TLC for visualization by sulfuric acid charring (Fig. 2-2D). Unmodified lipid IV_A was stable across the entire pH range tested, whereas the dually modified 2-PEtN lipid IV_A population disappeared with a concomitant increase in free lipid IV_A as hydrolysis incubation conditions became more basic.

We hypothesized that the released *O*-PEtN monoester is the actual substrate of cIAP. To support this theory, we directly tested *O*-PEtN as a substrate for cIAP and hALPI (Fig. 2-3A).

Typical Michaelis-Menten kinetics (K_m of $173 \pm 27 \mu\text{M}$ and V_{max} of $1.09 \pm 0.05 \mu\text{M}/\text{min}$ for cIAP and K_m of $197 \pm 56 \mu\text{M}$ and V_{max} of $1.05 \pm 0.1 \mu\text{M}/\text{min}$ for hALPI) were observed for both enzymes with *O*-PEtN as substrate. Using the crystal structure of the highly homologous rat IAP ortholog (~70% identity with cIAP across 486 non-gapped residues) as a model (52), *O*-PEtN can be readily accommodated within the substrate binding pocket in the active site (Fig. 2-3B). This is in contrast to modeling of fully acylated lipid A as the putative IAP substrate (see below). This data, in combination with the qualitative MS results using PEtN-modified Re LPS (Fig. 2-1) and the TLC analysis of lipid IV_A (Fig. 2-2), supports a two-step mechanism whereby cIAP catalyzes phosphate release from spontaneously hydrolyzed *O*-PEtN that had initially been bound to LPS in a labile phosphoanhydride linkage.

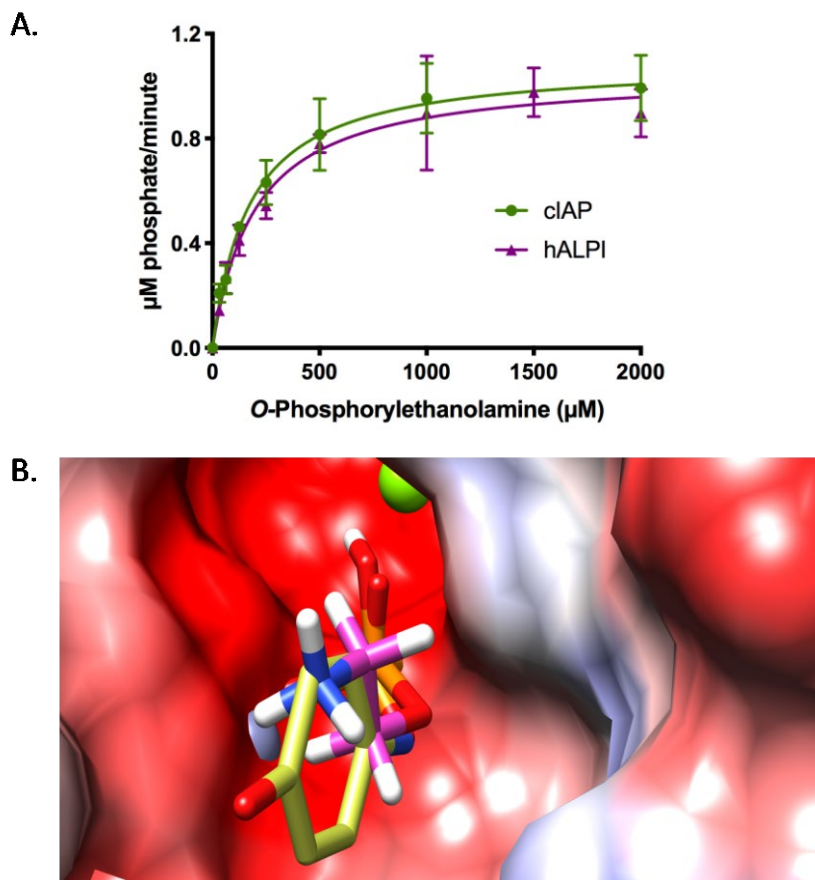


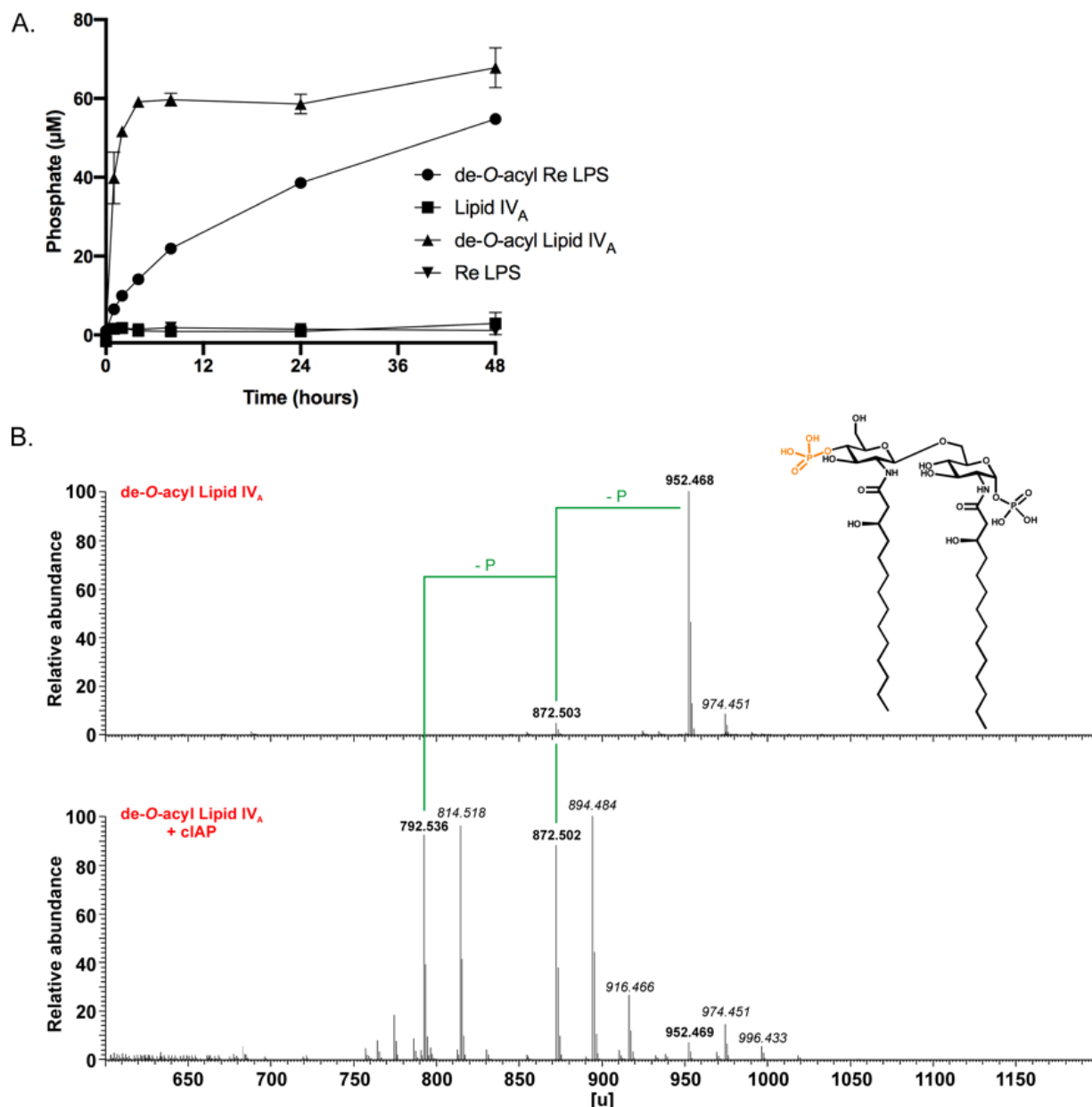
Figure 2-3. *O*-Phosphorylethanolamine (*O*-PETN) is a substrate for cIAP. (A) The rate of inorganic phosphate released by calf intestinal alkaline phosphatase (cIAP, 0.04 U/ml, *green*) or human intestinal alkaline phosphatase (hALPI, 0.17 µg/ml, *purple*) was measured as a function of *O*-PETN substrate concentration (0 to 2000 µM) using the malachite green assay. Reactions were incubated in 50 mM Tris-HCl buffer (pH 8.25), 100 mM NaCl, 1 mM MgCl₂, and 20 µM ZnCl₂ at 37 °C and stopped by adding malachite green reagent at either time 0, 5, 10, 15, 20 or 30 minutes. Data using *O*-PETN as substrate was fit using the standard Michaelis-Menten equation (K_m of 173 ± 27 µM and V_{max} of 1.09 ± 0.05 µM/min for cIAP and K_m of 197 ± 56 µM and V_{max} of 1.05 ± 0.1 µM/min for hALPI). Data are plotted as an average of at least two independent experiments conducted in duplicates with error bars showing SDs. (B) Display of *O*-PETN at a mammalian AP active site. The surface was computed for rat IAP (4KJD.pdb, 4KJG.pdb) (52). While the PETN position was computed, the phosphate and phenol fragment (a substrate analog) take their locations from observed phosphatase co-crystal structures (52). They were merged into all models as reference to validate the computed poses of equivalent mono-phosphorylated glucosamine rings of lipid A (see Fig. 2-6). Stick colors: *orange* P, *red* O, *blue* N, *yellow* C of *para*-nitro-phenol (substrate analog) and *white* H and *magenta* C atoms of PETN. Surface colors reflect positive (blue) or negative (red) partial charges from functional residue groups. More nonpolar (neutral, mostly aliphatic) zones of amino acids show fading colors while deeper blue or red colors symbolize increasing positive or negative charge densities (53). Smaller bright and dark shading imitate light reflection and shadows in space for three-dimensional impression. Two of

the three metal ions are partially visible (*grey*: Zn²⁺, *green* Mg²⁺). The locations of the cleavage sites of EcAP (5TJ3.pdb) and rat IAP (4KJD.pdb) can be brought on the same footage guided by the superposition of their phosphates and catalytic residues (not displayed).

ciAP directly releases inorganic phosphate from de-O-acylated lipid A chemotypes

The recalcitrance of all LPS chemotypes thus far tested to being directly dephosphorylated by ciAP suggested that steric interference may prevent the AP active site from engaging target lipid A phosphate monoesters. To test this hypothesis, we removed all ester linked acyl chains from lipid IV_A and Re LPS to generate di-*N*-acyl de-*O*-acyl lipid A derivatives (Fig. 2-4). De-*O*-acyl lipid A (the *N,N*-diacylated) only contains amide linked 3-OH-C14:0 acyl chains at C2 of GlcNI and C2' of GlcNII. If steric hindrance is indeed problematic, this should facilitate enzyme access to the phosphate groups, particularly at C4' of GlcNII which is now adjacent to a free hydroxyl group in comparison to the steric bulk of a 3-OH-C14:0 acyl chain in lipid IV_A. Furthermore, decreasing the acyl chain density on the lipid A backbone substrate also increases the conformational flexibility. Unlike the tetra-acylated lipid IV_A parent, de-*O*-acyl lipid A was rapidly dephosphorylated in an initial phase that was followed by an extended period of slow phosphate release (Fig. 2-4A). De-*O*-acylated Re LPS, which has two Kdo residues attached to C6' of GlcNII (Fig. 2-5A, *inset*), was likewise dephosphorylated in a biphasic manner albeit at a slower overall rate (Fig. 2-4A). MS analysis of ciAP treated products revealed the entire population had lost at least one phosphate group from both de-*O*-acyl lipid A and Re LPS substrates (Fig. 2-4B and Fig. 2-5A). NMR analysis of the residual phosphate remaining after treatment of de-*O*-acyl lipid A with ciAP indicated the majority (~77%) of the anomeric GlcNI phosphate group was retained under these conditions (Fig. 2-5B). In sum, the data is consistent with quantitative

hydrolysis of a highly cIAP susceptible phosphate group on GlcNII followed by a slower second dephosphorylation event on GlcNI that remains incomplete even after a 48-hour reaction period.



treatment with cIAP (*bottom* panel, calculated masses of 872.501 u and 792.535 u for monophosphoryl and non-phosphorylated products, respectively; recorded in positive ion mode). The highly cIAP susceptible phosphate at C4'-GlcNII is colored *orange*. Masses resulting from dephosphorylation events are indicated (P), while masses in italic style represent sodium adducts ($\Delta m = 22$ u).

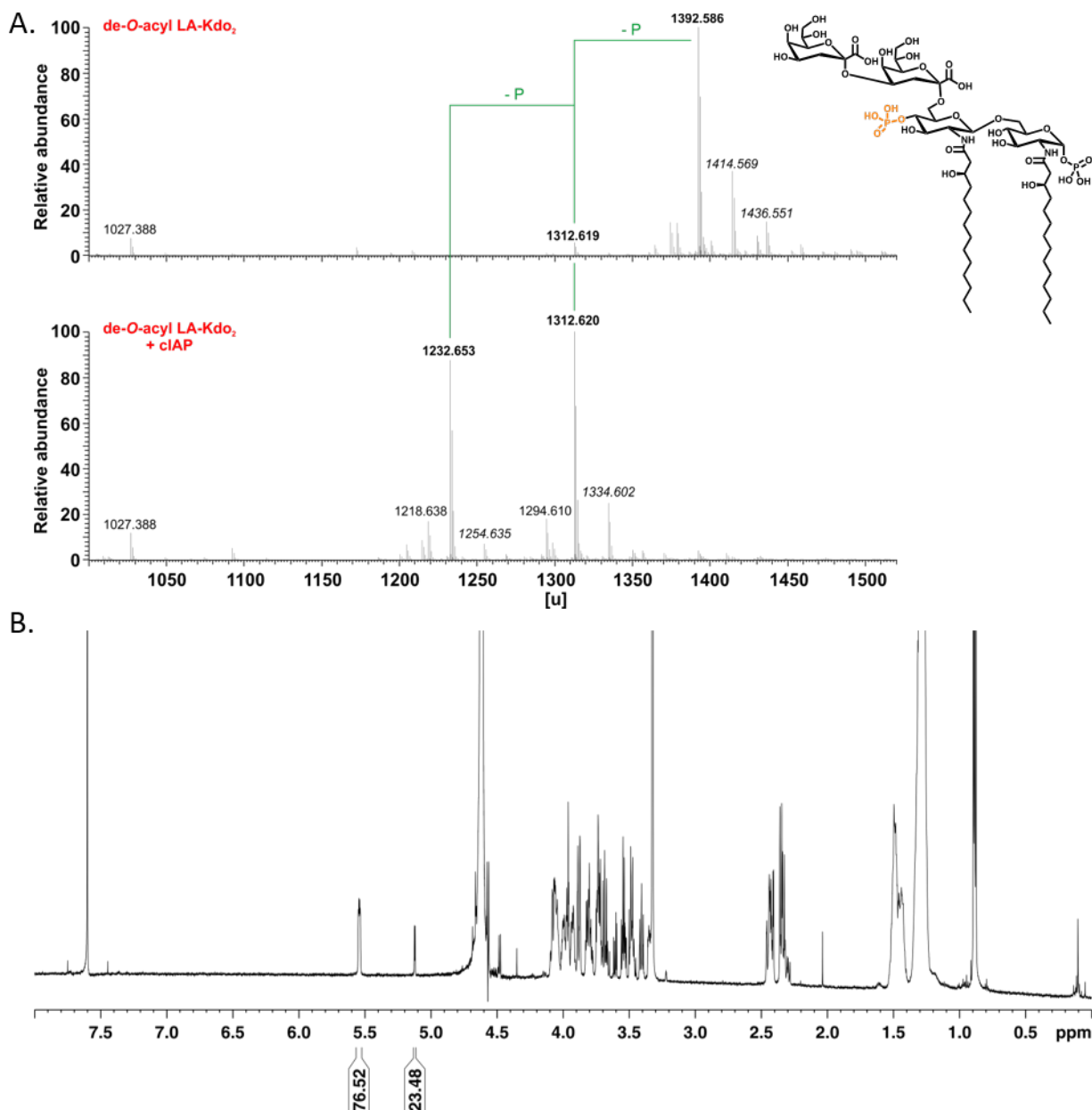


Figure 2-5: De-O-acylated lipid A substrates are dephosphorylated by cIAP. (A) MS analysis in the negative ion mode of de-O-acyl Re LPS before (*top* panel, calculated mass 1392.584 u) and after treatment with cIAP (*bottom* panel, calculated masses of 1312.618 u and 1232.651 u for monophosphoryl and non-phosphorylated products, respectively). The more cIAP-susceptible

phosphate at C4'-GlcNII is colored *orange*. Masses resulting from dephosphorylation events are indicated (P), while masses in italic style represent sodium adducts ($\Delta m = 22$ u). (B) ^1H NMR analysis of cIAP products from de-*O*-acyl lipid A that had been prepared from *ClearColi*[®] BL21 (DE3) (TXM843). Integration of the downfield β -anomeric proton signals indicates that the majority (~77%) of the monophosphoryl products retain the GlcNI phosphate ($\delta_{\text{H}} 5.54$ ppm). The *O*-1-dephosphorylated GlcNI is represented by the doublet for H1 at $\delta_{\text{H}} 5.12$ ppm. LA = lipid A.

We subsequently generated a model of the cIAP active site using the crystal structure of the highly similar rat IAP ortholog (~70% identity with cIAP across 486 non-gapped residues) as a structural template (52). Whereas de-*O*-acyl lipid A could be accommodated within the active site, lipid IV_A could not be docked successfully (Fig. 2-6A). Detrimental van der Waals contacts arise between the protein surface with the two *O*-acyl side chains at all times when the GlcNII phosphate was positioned to occupy the active site. In particular, the 3'-*O*-acyl chain on GlcNII clashed with amino acid chains flanking the active site. During simulations, the *N*-acylated side chains, however, adopted conformations that could avoid steric clashes when docked with the cIAP susceptible de-*O*-acyl lipid A GlcNII phosphate orientated in the active site. Likewise, docking of the anomeric C1-GlcNI phosphate lipid IV_A into the catalytic cleft resulted in multiple steric interferences (Fig. 2-6). The computed binding models are consistent with the non-anomeric 4'-phosphate of de-*O*-acyl lipid A being the preferred position for cIAP-mediated dephosphorylation.

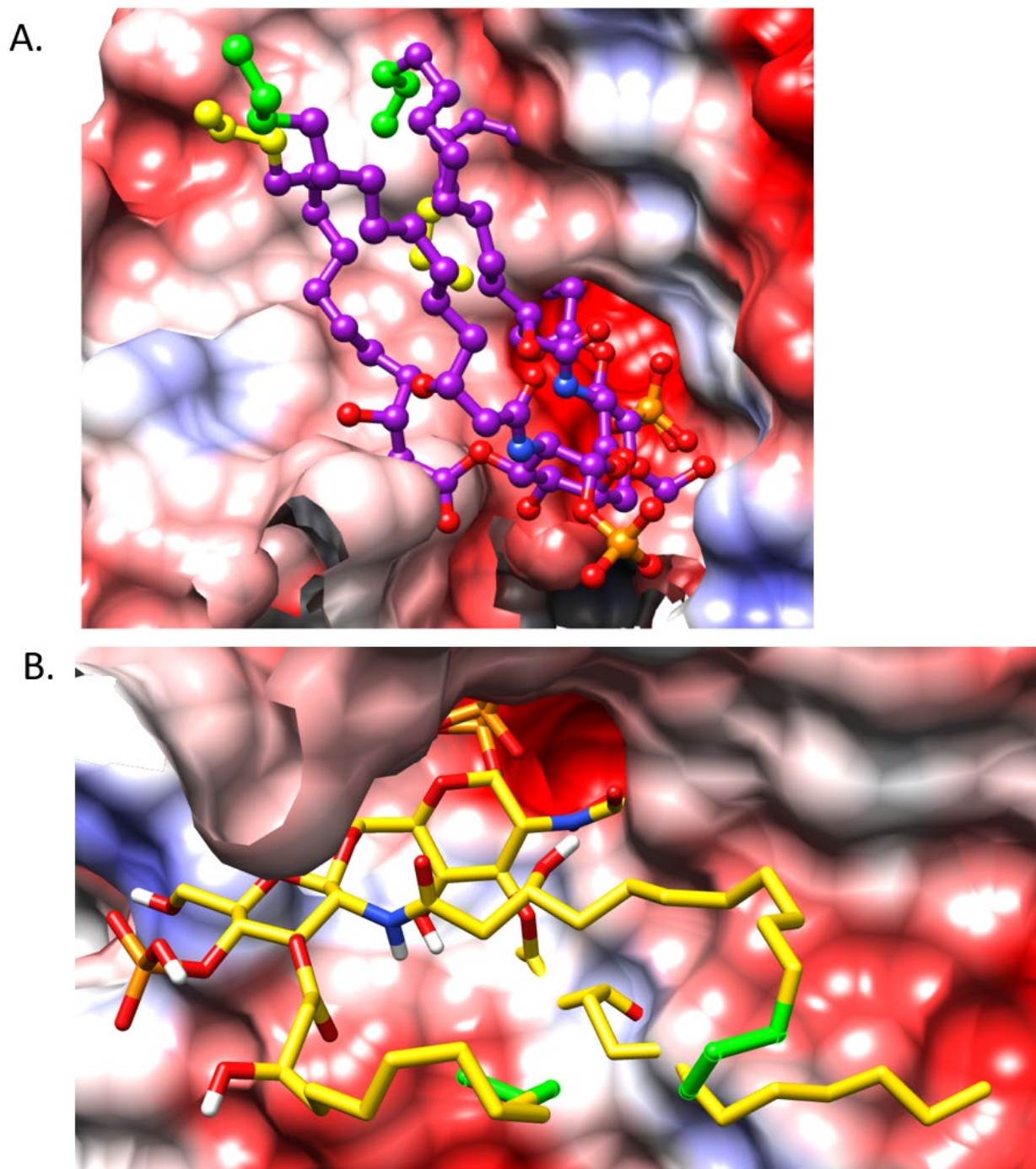


Figure 2-6: Binding model of tetra-acylated lipid IV_A at the active site of cIAP (A) Binding model of tetra-acylated lipid IV_A with the C4'-GlcNII phosphate at the active site of cIAP. The phosphorylated catalytic serine covalent intermediate (*bottom-right*, deeply buried in the cleft) is aligned with the C4'-GlcNII lipid IV_A phosphate as reference (Fig. 2-3). Proximal atoms of the two *O*-acylated side chains (with the terminal Ω , Ω -1, Ω -2 carbon atoms colored in *yellow*) permeate the protein surface. The two *N*-acylated side chains can occupy the cleft in their entirety

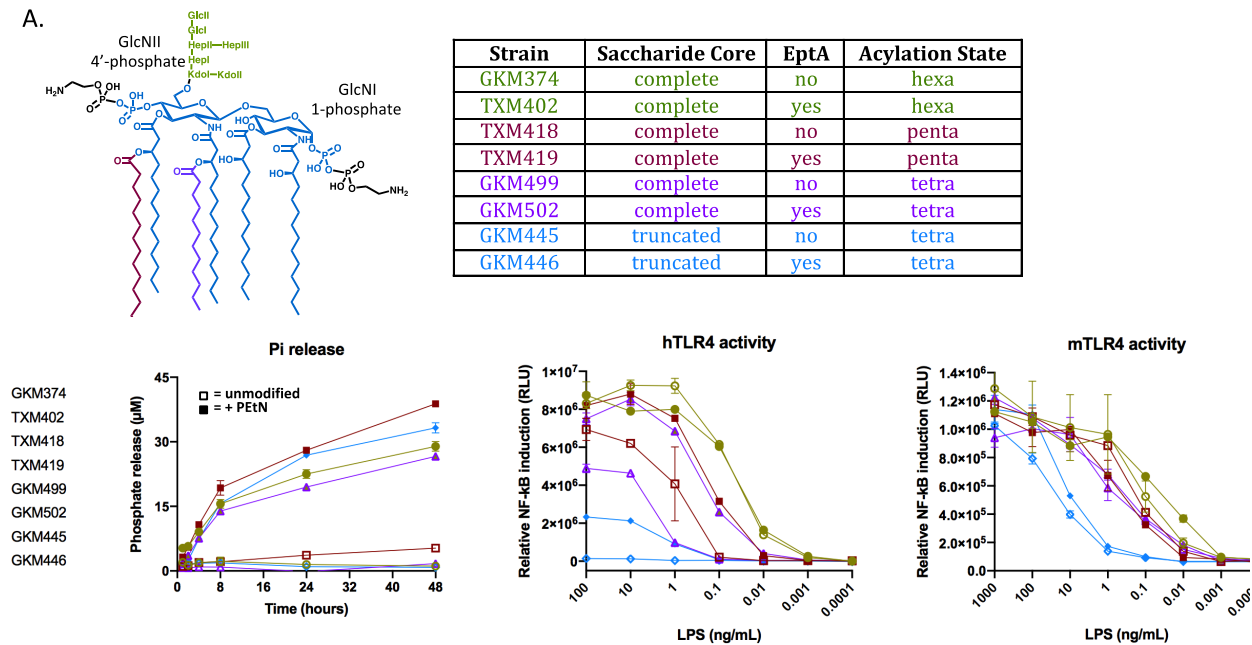
length without any steric clashes (*green caps*). The anomeric 1-phosphate group of GlcNI lies to the front (*bottom most, right*) and is only slowly cleaved in de-*O*-acyl lipid A (*N,N*-di-acylated lipid IV_A derivative, modeled in Figure 2-6). Red, blue, and white surface colors indicate negative, positive, and neutral partial charges, respectively. Hydrogen atoms are not displayed. (B) Stick model of tetra-acylated lipid IV_A with the anomeric C1-GlcNI phosphate group positioned in the cIAP catalytic cleft. The phosphorylated catalytic serine covalent intermediate is included for reference (*topmost* deeply buried in the cleft) (52). In this orientation, both acyl groups (ester and amide linked) on GlcNI of lipid IV_A will clash with the protein surface if the anomeric phosphate is appropriately positioned for cleavage. In contrast, a di-acylated derivative with only the two acyl side chains on GlcNII (terminal Ω , Ω -1, Ω -2 carbon atoms colored in *green*) could occupy the active site without steric hindrance.

PEtN modification enhances hTLR4 agonist activity of underacylated LPS chemotypes

Our data indicates a mechanistic model whereby PEtN spontaneously hydrolyzes from phosphoanhydride linkages on LPS to generate free *O*-PEtN, a monoester substrate that is processed by cIAP to liberate inorganic phosphate. This interpretation would explain the apparent dependence of cIAP for detection of free inorganic phosphate release from LPS under *in vitro* reaction conditions since the malachite green assay does not detect organic phosphate as in *O*-PEtN. Yet that alone does not account for the observed decrease in TLR4/MD2 activity after *in vitro* cIAP treatment considering the critical role lipid A phosphates at C1-GlcNI and C4'-GlcNII play during binding to TLR4/MD2 (54, 55). Our data indicates these key phosphate groups remain intact after exposure to cIAP unless primary *O*-ester acyl chains on lipid A have first been removed. Transforming lipid A into a good cIAP substrate through prior de-*O*-acylation would itself abrogate TLR4/MD2 activity, which argues against de-*O*-acyl glycoform dephosphorylation being relevant to endotoxin neutralization.

Previous studies have, however, demonstrated PEtN modifications of lipid A in *Neisseria meningitidis* (56-59) and *Campylobacter jejuni* (60) increase TLR4/MD2 signaling. Spontaneous hydrolysis of PEtN, which can only be detected by inorganic phosphate assays with added AP,

could account for the apparent decrease in biological activity. We therefore determined whether PEtN modification of *E. coli* lipid A, which has an asymmetric lipid A acyl chain distribution unlike in *N. meningitidis*, also affects TLR4/MD2 recognition in a similar fashion. We initially constructed a strain panel that synthesized lipid A glycoforms varying in acylation state and either with or without EptA-appended PEtN modifications (Fig. 2-7A). As expected, comparable amounts of inorganic phosphate were only detected in the presence of cIAP with LPS substrates that had been isolated from parent strains expressing EptA (Fig. 2-7B). We next directly compared TLR4/MD2 stimulation using a HEK293/hTLR4/MD2-CD14 whole cell NF- κ B reporter assay (Fig. 2-7C). We utilized a luciferase based reporter assay instead of the secreted embryonic AP (SEAP) HEK-Blue™ colorimetric reporter system, since the placental AP (PLAP) isoform has been reported to dephosphorylate LPS (29). While PEtN addition to hexa-acylated lipid A had minimal impact, PEtN modifications of the penta- and tetra-acylated lipid A glycoforms containing a full saccharide core enhanced TLR4 signaling by ~10-fold. Tetra-acylated lipid IV_A glycoform did not stimulate hTLR4/MD2, consistent with lipid IV_A being a known human TLR4 antagonist (61-64). Surprisingly, PEtN addition by EptA to lipid IV_A imparted low but definite agonist activity (Fig. 2-7C). Restoration of hTLR4/MD2 activity by PEtN modification of lipid IV_A was suppressed by pre-incubation in buffer in a pH-dependent manner (Fig. 2-8), as expected considering the labile nature of the lipid IV_A-PEtN phosphoanhydride bond with increasing pH (Fig. 2-2C and 2-2D). Collectively this suggests that PEtN addition to lipid IV_A can convert an LPS-like hTLR4 antagonist into a weak agonist. The contribution of PEtN to hTLR4 activity is more determinant with sub-optimal, underacylated *E. coli* LPS ligands, and is consistent with previous observations made using the *N. meningitidis* lipid A scaffold (57).



Since key amino acid differences at the TLR4/MD2/LPS interface endow species specific lipid IV_A responses (65), we repeated the assay using the same panel of LPS chemotypes but with NF-κB reporter cells expressing mouse TLR4/MD2 (Fig. 2-7D). The pattern observed with hTLR4/MD2 was not replicated with the murine receptor complex, as PEtN attachment had minimal affect on signaling for any of the tested lipid A acylation states. This demonstrates that

the enhanced signaling observed with hTLR4/MD2 is not an inherent biophysical property of PEtN modified lipid A, but rather due to species-specific ligand recognition and engagement inherent to the respective TLR4/MD2 receptor complexes.

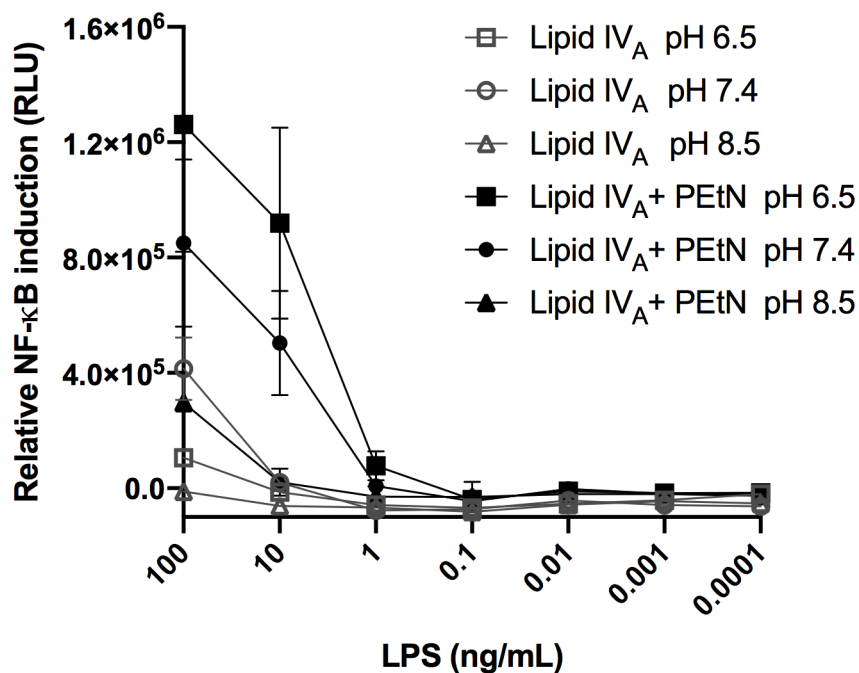


Figure 2-8: Pre-incubation in buffer of increasing pH reduces hTLR4 agonist activity for PEtN-modified lipid IV_A. Relative NF-κB induction in HEK293/hTLR4-MD2-CD14 cells stimulated with lipid IV_A [GKM445 *ClearColi*[®] K-12 (Δ eptA Δ gutQ Δ kdsD Δ lpxL Δ lpxM Δ lpxP Δ pagP)] or PEtN-modified lipid IV_A [GKM446 (Δ gutQ Δ kdsD Δ lpxL Δ lpxM Δ lpxP Δ eptA, pEptA) that had been pre-incubated for 48 hours at 37 °C in MOPS/Tris buffer at pH 6.5, 7.4, or 8.5. Data are representative of three independent experiments performed in duplicates with the error bars showing SDs.

PEtN substitution of both lipid IV_A phosphates is required for maximum hTLR4 agonism

EptA can covalently add PEtN groups via phosphoanhydride bonds to either of the two lipid A phosphate groups, at C1 of GlcNI or C4' of GlcNII. Hence we sought to determine whether both PEtN groups (2-PEtN) are required or if a single PEtN moiety (1-PEtN) is sufficient to restore hTLR4/MD2 signaling. To accomplish this, we utilized an *E. coli* B lipid IV_A PEtN producing strain

since this genetic background elaborates higher levels of PEtN modified lipid A in comparison to the K-12 strain used in the prior experiments (40). We next developed a lipid IV_A purification protocol to remove any contaminating lipoproteins and phospholipids, as well as to isolate 1-PEtN and 2-PEtN lipid IV_A species to allow for more quantitative comparisons between glycoforms. The previously established purification methods utilized for LPS chemotypes containing at least part of the saccharide core failed when applied to PEtN-lipid IV_A material extracted using the PCP method (see Experimental Procedures). We thus developed a pair of nonionic detergent aided lipase pre-treatment steps to remove phospholipids and deacylate interfering lipoproteins. Anion exchange chromatography has been successfully used by Raetz and coworkers to separate Ara4N and PEtN modified chemotypes (66, 67). We modified the solvent system to improve the ensuing chromatographic separation of PEtN-lipid IV_A species, and were able to isolate 2-PEtN and 1-PEtN lipid IV_A species in high purity (Fig. 2-9).

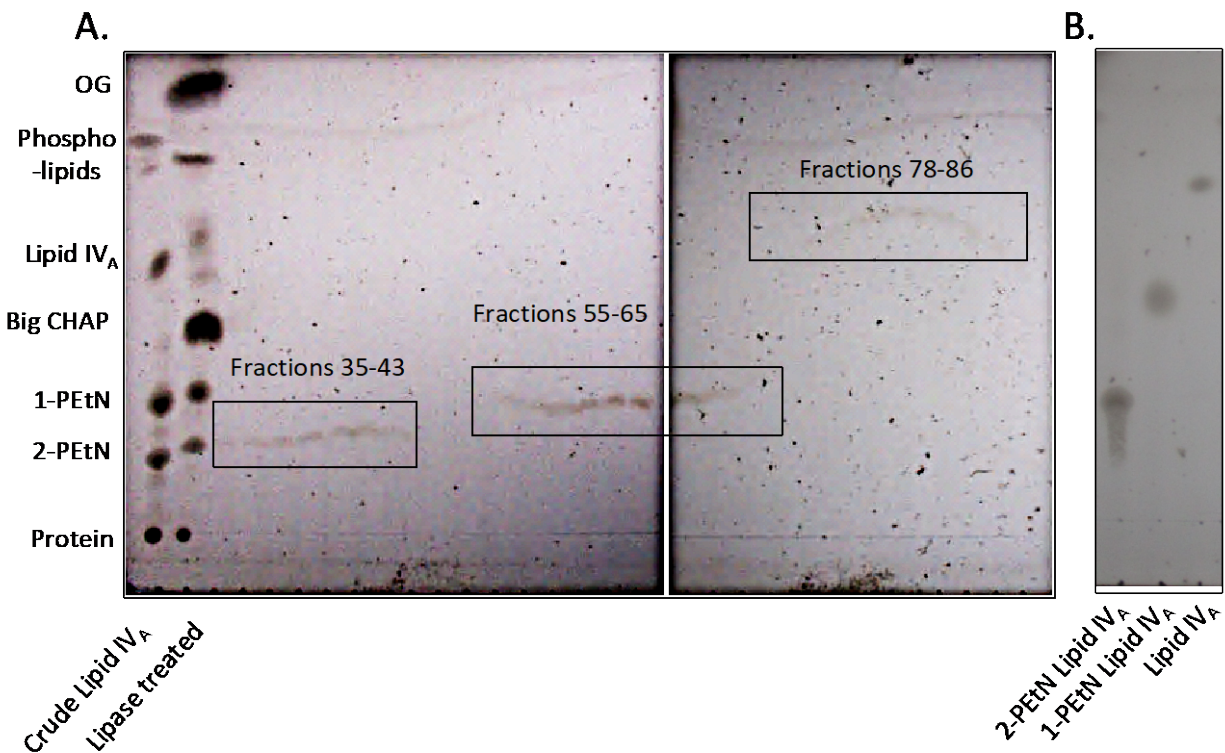
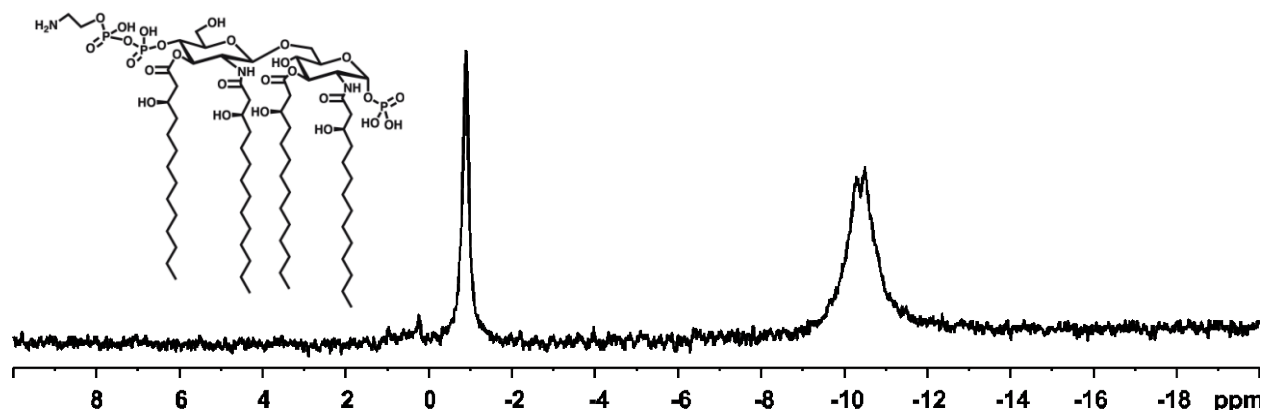
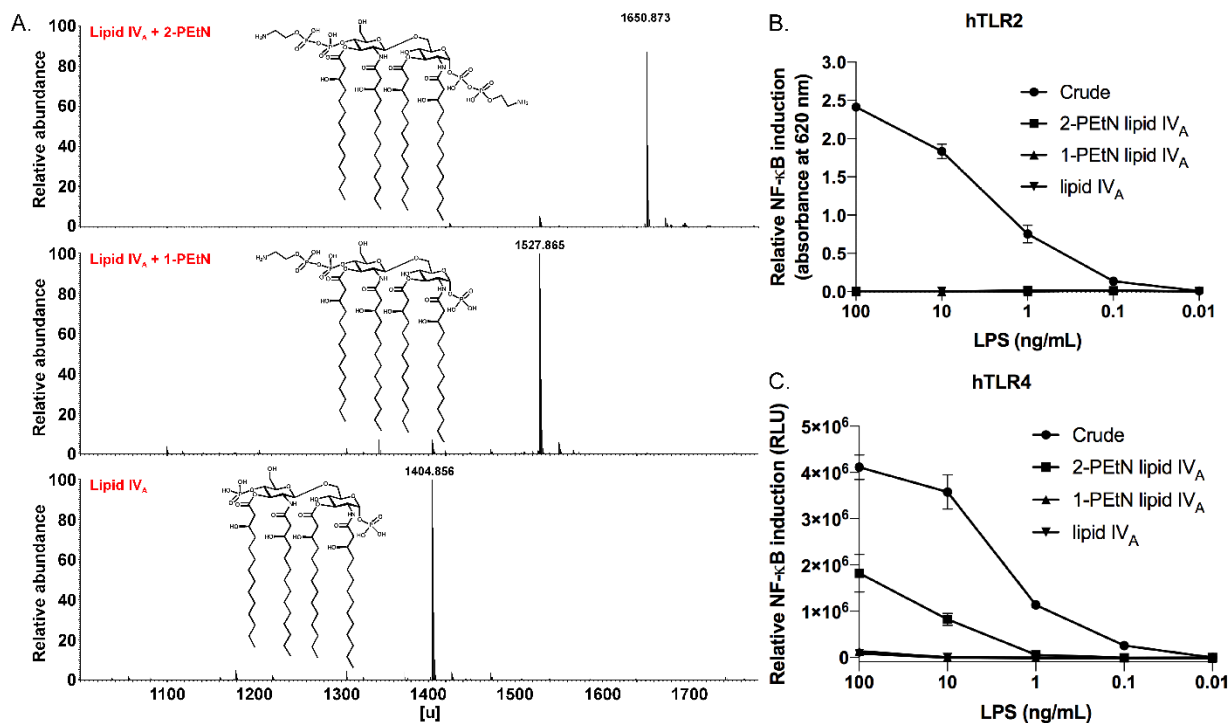


Figure 2-9: Purification of individual PEtN-lipid IV_A species from *E. coli* B strain TXM844 by anion exchange chromatography. (A) Crude PEtN-lipid IV_A isolated by PCP extraction was sequentially treated with two rounds of lipase digestion using the nonionic detergents BIG-CHAP and octyl β-D-glucopyranoside (OG). The product was loaded onto a DEAE column, and fractions screened by TLC after visualization by sulfuric acid charring. Fractions corresponding to lipid IV_A, 1-PEtN lipid IV_A (1-PEtN), and 2-PEtN lipid IV_A (2-PEtN) were pooled. (B) Pooled fractions were rechromatographed to confirm purity of isolated lipid IV_A, 1-PEtN lipid IV_A, and 2-PEtN lipid IV_A preparations.

Lipid IV_A samples modified with 2- and 1-PEtN groups were highly pure with respect to PEtN content as judged by MS analysis (Fig. 2-10A) and free of TLR2 activating lipoprotein (2-10B). In addition, ³¹P NMR analysis confirmed PEtN substitution solely at C4' of GlcNII in the purified 1-PEtN fraction (Fig. 2-11). When comparing hTLR4/MD2 stimulating activity of the purified fractions, only the 2-PEtN modified lipid IV_A demonstrated agonist activity (Fig. 2-10C). PEtN substitution at C1 of GlcNI on the lipid IV_A scaffold (with four symmetrically distributed acyl chains) is therefore critical to restoring agonistic character.



Molecular modeling suggests hTLR4/MD2 residues responsible for species specific enhanced recognition of PEtN-modified lipid A

Signaling assays with TLR4/MD2 reporter cells unveiled that while lipid IV_A is endotoxically inactive in human receptor complexes as expected, PEtN addition by EptA restores detectable activity (Figs. 2-7C and 2-10C). The relative contribution of PEtN to enhancing activity was more pronounced as the lipid A ligand became increasingly underacylated (Fig. 2-7). This trend, however, was not observed in murine receptor (mTLR4/MD2) reporter cells. MD2 is highly conserved between species, except for a few key residues (Fig. 2-12) (65). In the human receptor complex, a non-conserved cationic residue (hLys122 vs. anionic mGlu122) on the rim of MD2 interacts with the negative charge of lipid A phosphate anions and causes the ligand to be buried more deeply within the MD2 cavity in an antagonistic pose. In contrast, mGlu122 forces the ligand's phosphate groups to move away by charge repulsion into an agonist pose that is well positioned for interactions with other subunits within the complex. Given the constant space in the MD2 binding cleft, underacylated lipid A congeners become more deeply buried than fully acylated ligands in hMD2 until eventually all agonist character is lost as with tetra-acylated lipid IV_A. Our binding model suggests that as a direct consequence of PEtN substitution, ligand is prevented from sinking too deep within hMD2 and remains sufficiently exposed to form contacts with the second TLR4* subunit, triggering dimerization between the [TLR4/MD2] and [TLR4*/MD2*] ectodomains and initiating downstream signaling (Fig. 2-12). The influence of PEtN groups is thus most evident when needed, *i.e.* for binding underacylated lipid A ligands in the hTLR4/MD2 complex. This effect of PEtN substitution is more muted in mTLR4/MD2 since mGlu122 is already preventing lipid A from binding too deeply in MD2. In addition, there are

more potential favorable electrostatic interaction points between hTLR4 residues (e.g. hAsp294 and hGlu369) with the amino groups of PEtN (Fig. 2-12B), helping to bridge the space between TLR4 and TLR4*. In contrast, the murine receptor complex with mLys367 in place of hGlu369 is less favorable due to positive charge repulsion.

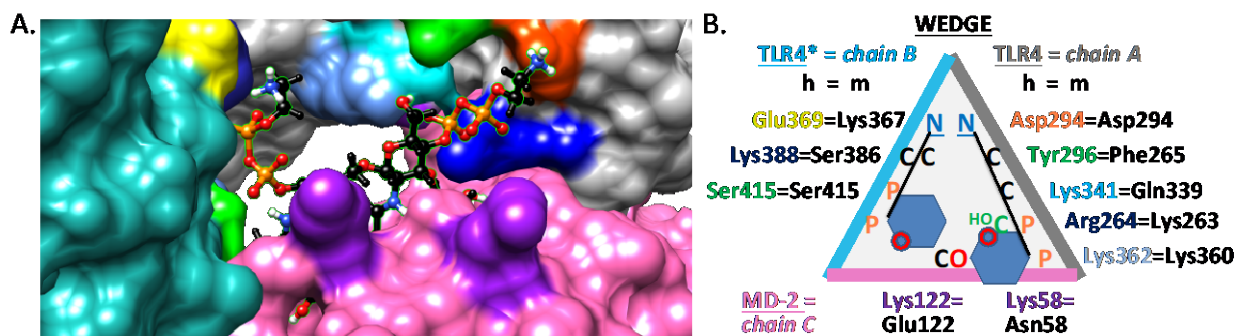


Figure 2-12: Simulated hTLR4/MD2 binding of 2-PEtN modified lipid IVA. **(A)** Computational model of hTLR4/MD2 with 2-PEtN modified lipid IVA substrate bound at the hTLR4 homodimer interface. Surface color codes are *grey* for TLR4 (A chain, right), *turquoise* for the second TLR4* subunit (B chain, left), and *pink* for MD2 (C chain, bottom). Key substrate binding determinants on each subunit chain are indicated as follows. For MD2, hLys122 and hLys58 (bottom) are indicated by two *purple* patches. Patches on TLR4* to the left highlight hGlu369 (*yellow*, equivalent to mLys367), hLys388 (*blue*, behind hGlu369), and hSer415 (*green*, below hGlu369). Highlighted mid-section patches on TLR4 are hLys362 (*powder blue*) and hLys341 (*cyan*), while top right-side patches include hTyr296 (53), hAsp294 (*orange*), and hArg264 (*blue*). Atom colors for the 2-PEtN modified lipid IV_A ligand: *black* C-H, *orange* P, *red* O, *blue* N, *white* polar H. The GlcNII ring is visible in the cleft while the GlcNI moiety is occluded by hLys122. The two cationic H₃N⁺ head groups of PEtN contact anionic hGlu369 (anomeric C1-phosphate of GlcNI) and hAsp294 (non-anomeric C4'-phosphate of GlcNII). The MD2 lipophilic cavity buries all four acyl chains of lipid IV_A. Tyr296 is positioned to contact the 6'-C-OH group or the 4'-pyrophosphate group of PEtN on GlcNII. **(B)** Binding map schematic highlighting critical residues that vary between the human (colored text to match panel 8A) and murine (black text) TLR4/MD2 receptor complex. To bind LPS-like ligands, the dimerized receptor complex provides a binding site contoured by TLR4*/MD2/TLR4. When projected onto a plane from a certain perspective, the three proteins (B/C/A chains) form a triangle (wedge). Amino acids potentially serving as favorable electrostatic contact points for the cationic amino head groups of PEtN moieties are noted, including anionic hAsp294 (TLR4) and hGlu369 (TLR4*) residues. Of note, the latter is replaced by a non-homologous lysine (mLys367) residue in the mTLR4 receptor. As in panel (A), hTyr296 (53) is interacting with the C6-OH group of GlcNII (53) or with the adjacent

pyrophosphate group (orange). The amino acid residue numbering scheme has been described (63).

DISCUSSION

The anti-inflammatory properties of IAP and APs in general have generated broad interest as potential therapeutics for treating a number of systemic and acute inflammatory conditions. Dissecting and isolating the relevant phosphorylated molecular targets involved, however, is a complicated endeavor due to the broad substrate specificity of IAP. IAP can dephosphorylate both bacterial derived MAMP/PAMPs as well as pro-inflammatory endogenous damage-associated molecular patterns (DAMPs) of host cell origin produced in response to LPS-mediated TLR4/MD2 inflammation. Flagellin, CpG DNA motifs, and extracellular nucleotides have all been proposed to be relevant IAP dephosphorylation targets (28). Flagellin and CpG motifs in bacterial DNA are MAMP/PAMP TLR ligands (69), while extracellular ATP nucleotide binds to purinergic receptors (70) and UDP to the P2Y₆ pyrimidinergic receptor (71). The anti-inflammatory mechanism of IAP is further confounded by the difficulty in separating IAP specific effects (i.e. the direct dephosphorylation of MAMP/PAMP/DAMP stimuli) from nonspecific ones resulting from general downregulation of the inflammatory tone (17).

LPS has emerged as an often cited and most likely MAMP/PAMP-related molecular target for AP, due to its potent inflammatory potential when present at low concentrations. The conclusion that IAP dephosphorylates LPS *in vitro* predominantly rests on the observation that LPS-derived inorganic phosphate is only detectable if AP is added when using either the molybdate complex or tissue histology-based assays as readouts. The corresponding LPS

preparations treated with AP have diminished capacity to induce inflammation through TLR4/MD2 stimulation, as would be expected for hydrolysis of the lipid A backbone phosphate groups since these groups are central in TLR4/MD2 recognition. Direct evidence pertaining to which phosphate groups are indeed removed by AP is lacking, however. LPS preparations can also have multiple phosphate groups on the inner saccharide core in addition to those on lipid A. In *E. coli* for instance, WaaP and WaaY heptose kinases phosphorylate HepI and HepII, respectively (46), while KdkA kinase modifies Kdo in bacteria with phosphorylated mono-Kdo residues such as *Haemophilus influenzae* (72). We thus sought to determine the origin of the inorganic phosphate released by AP. While our results are consistent with inorganic phosphate release being contingent on AP activity for structurally heterogeneous LPS preparations, we found defined substrates such as Re LPS chemotype that only have lipid A phosphate monoester groups to be completely inert to enzymatic dephosphorylation (41). In previous studies where defined LPS chemotypes were tested for AP activity, a decrease in phosphate release has also been noted. Tuin et al. recorded lower phosphate release when histology scoring rat liver sections challenged with Re LPS from *S. enterica* sv. Minnesota (73), while Pettengill et al. observed low phosphate release from *S. enterica* sv. Minnesota Re LPS and no measurable phosphate release from monophosphoryl lipid A (MPLA) substrate using recombinant TNAP (31). Re LPS lacks the Hep acceptor for the inner core PEtN transferase EptC, which we have now shown is an apparent source of cIAP-released phosphate along with the lipid A PEtN transferase EptA (41). PEtN groups are common in many Gram-negative bacteria where they are added to both lipid A and the LPS inner saccharide core to increase the net positive charge (74). The increased positive charge imparts resistance to cationic peptides and enhances outer membrane

integrity, particularly under more challenging growth environments. Both EptC and EptA enzymes add PEtN in a phosphoanhydride linkage using phosphatidylethanolamine phospholipid head groups as PEtN donors, forming a rather unique bond type in the process considering the extracellular location. While other bacterial surface phosphoanhydride bonds such as in bactoprenol glycosyl donors do exist, these are generally fleeting intermediates whose high energy character is used to drive the polymerization of peptidoglycan, O-antigen, and other cell surface polymer pathways since intracellular ATP is not directly accessible. Considering the inherent reactivity of phosphoanhydride bonds, we suspected spontaneous hydrolysis might play a role since phosphate was only released from LPS substrate containing phosphoanhydride linked PEtN groups and not from phosphodiester linked PEtN groups appended to Kdo by EptB (Fig. 2-7B) (41). Indeed, phosphodiester-linked PEtN remained stable across a wide pH range, whereas PEtN connected by phosphoanhydride bonds became labile in neutral to basic pH and was only stable under mildly acidic conditions (Fig. 2-2C and 2-2D). Intriguingly, acidic environmental conditions induce EptA (75), suggesting that phosphoanhydride linked PEtN may be hydrolytically susceptible by design so as to transiently tailor the LPS layer provided acidic conditions persist. Certain bacteria do not add phosphoanhydride linked PEtN to lipid A, but rather hydrolyze lipid A phosphate first before transferring PEtN to form phosphodiester bound PEtN (76, 77). Presumably such PEtN phosphodiesters are more stable, as observed here for phosphodiester-bound Ara4N-modified lipid A and PEtN attached by EptB (41). Apparently, cIAP is unable to directly release PEtN or phosphate from LPS, but does dephosphorylate spontaneously hydrolyzed PEtN phosphomonoesters (Figs. 2-1 and 2-2). Free *O*-PEtN is a characterized substrate

for PLAP (78), and experiments here confirm it is a good substrate for the cIAP isozyme as well (Fig. 2-3).

In this study, we used commercially purified cIAP as AP enzyme source. In the intestinal lumen, IAP is enriched within luminal vesicles secreted by enterocytes (79), a native environment which could enhance IAP catalytic activity towards LPS. When the apparent phosphate released from LPS by luminal vesicles and purified IAP was directly compared, however, activities were comparable (80). A second consideration for any *in vitro* based LPS assays is substrate presentation. Highly aggregated LPS may not be bioavailable to IAP without accessory proteins to expose the lipid A phosphate groups. In serum, lipopolysaccharide binding protein (LBP), soluble CD14 (sCD14), and albumin all have integral roles in deaggregating LPS and enhancing presentation to the TLR4/MD2 receptor complex (81, 82). Likewise, the activity of the LPS acyloxyacyl hydrolase, which cleaves secondary acyl chains on lipid A (83, 84), is stimulated up to 100-fold when substrate is presented by either sCD14 or LBP (85). Glycosylation can also influence activity in certain AP isozymes (86). However, neither deaggregation agents or native preparations of AP enzymes extracted from tissue to capture relevant post-translational modifications increased phosphate release (41). It should be noted that even with tetra-acylated lipid IV_A, which lacks secondary acyl chains and is more polar than hexa-acylated lipid A, there was no appreciable phosphate released by cIAP (Fig. 2-7). If LPS is not a relevant IAP substrate, then the bulk of the anti-inflammatory effects observed with AP would seem more likely to arise from dephosphorylation of ATP and UDP rather than through detoxification of LPS (18, 19, 87). IAP has been reported to shape the microbiota composition in a mouse IAP *Akp-3* knockout model (88) and to directly inhibit *E. coli* growth in culture (89), offering a possible indirect role

for IAP in modulating the endotoxin load present in the intestinal lumen that does not involve dephosphorylation of LPS.

Although the exact structure of LPS and lipid IV_A was unknown at the time, initial studies investigating AP activity also concluded that LPS was completely resistant to AP sourced from bacteria (90-92). However, ~50% of the total phosphate could be released from "lipid A precursor" (*i.e.* later named lipid IV_A) if first de-*O*-acylated by treatment under mild alkaline conditions (91, 92). The authors concluded that the C4'-GlcNII phosphate is recognized by AP, and that the C1-GlcNI anomeric phosphate remains intact. The resistance of C1 to hydrolysis was attributed to steric hindrance by the C2 amide linked 3-OH-C14:0 acyl chain, which unlike the 3-OH-C14:0 ester acyl chain neighboring the C4' phosphate of GlcNII, remains intact after base treatment. It was also suggested that de-*O*-acylation may decrease the aggregation state, facilitating enzyme access to substrate. Since these studies focused on an AP enzyme of bacterial origin with low sequence similarity, we replicated their study using cIAP with highly purified lipid IV_A preparations (Fig. 2-4). As reported for bacterial AP, cIAP rapidly dephosphorylates de-*O*-acylated lipid A in comparison to tetra-acylated lipid IV_A. Bacterial phosphate monoesterases (EC 3.1.3.1) such as *E. coli* alkaline phosphatase (EcAP) resemble mammalian IAP in catalytic site topology (catalytic residues, trimetallo core, Zn-binding and crown-like flap) (93, 94). Bacterial and mammalian mono-phosphoesterases with a trimetallo core (here: EcAP and rat IAP) share highly conserved amino acids for Zn²⁺ and Mg²⁺ complexation (52, 93). Computational docking of lipid IV_A ligand into the active site of mammalian IAP (Fig. 2-6A) as well as bacterial AP (Fig. 2-13A) revealed steric hindrance by neighboring 3'-OH C14:0 acyl chains that prevent positioning of the C4'-phosphate of lipid A at the active site. Likewise, the approach of the anomeric

phosphate is hindered by the amide acyl chain at C2 of GlcNI (Fig. 2-6 and Fig. 2-13B for mammalian and bacterial AP, respectively), in keeping with our experimental data for cIAP (Fig. 2-4) and data using bacterial AP (91, 92). The anomeric phosphate can be removed after de-*O*-acylation, as a small but completely dephosphorylated population is clearly observed by MS and NMR (Fig. 2-4 and Fig. 2-5). The increased conformational flexibility of the remaining *N*-acyl chains after de-*O*-acylation likely accounts for the appearance of weak phosphatase activity at C1-GlcNI. The presence of Kdo residues in de-*O*-acyl Re LPS substrate slowed but did not prevent dephosphorylation (Fig. 2-4A), indicating prior hydrolysis of the saccharide core is not necessarily required for cIAP activity.

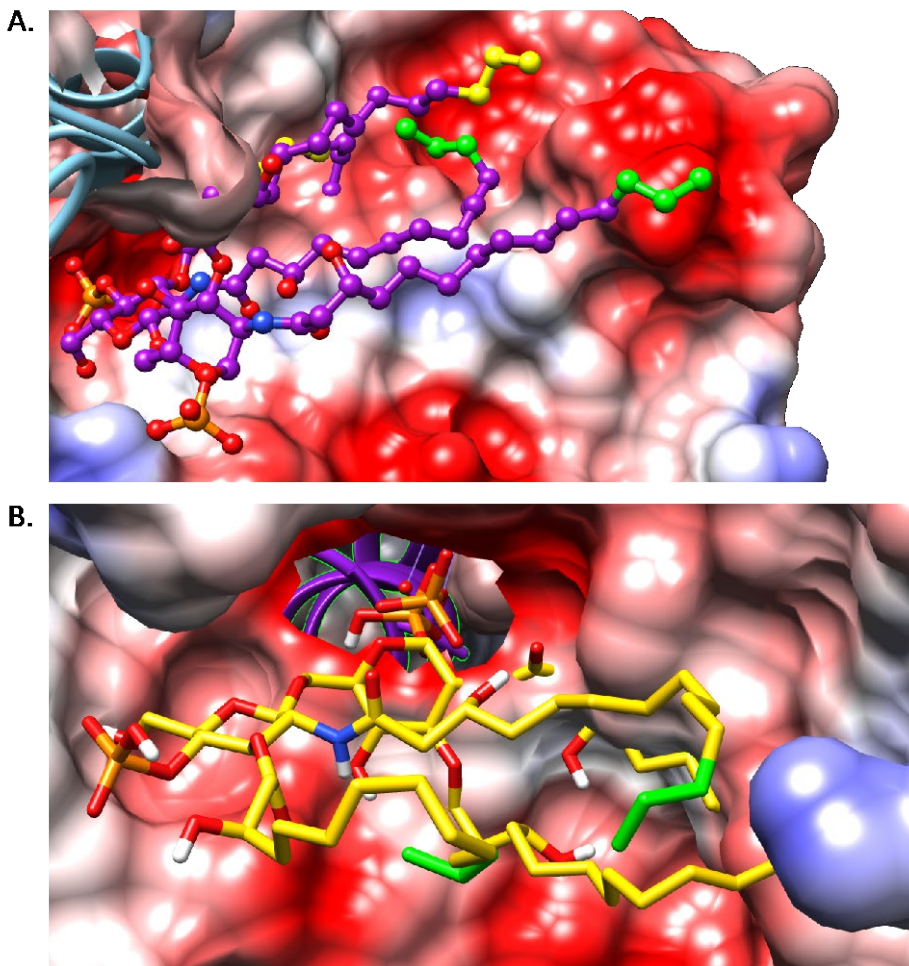


Figure 2-13: Docking of lipid IV_A to bacterial EcAP. (A) Ball and stick model of lipid IV_A with its non-anomeric C4'-GlcNII phosphate group in the bacterial catalytic cleft. The 3D model represents the EcAP crystal structure (1ALK.pdb) (93). The anomeric phosphate group is oriented outwards (foremost bottom, left). In this orientation only both *N*-acyl side chains (terminal Ω, Ω-1, Ω-2 carbon atoms colored in *green*) can be accommodated. The adjacent *O*-linked fatty acids (*bottom left* between both phosphate groups) are in steric conflict with the protein and permeating the surface so that they remain partially hidden (terminal Ω, Ω-1, Ω-2 carbon atoms colored in *yellow*). As in the cIAP model (Fig. 2-6), an *N,N*-diacylated lipid IV_A congener is predicted to be able to bind and present only its non-anomeric phosphate for cleavage. (B) Stick model of lipid IV_A with its anomeric C1-GlcNI phosphate group in the bacterial active site cleft. In order to be cleaved, the lipid IV_A phosphate must reach the position represented by the reference phosphate (center, top) to be in close proximity to catalytic serine and Zn²⁺ (grey ball in front of *purple* ribbons). This binding mode is feasible only for a di-acylated lipid IV_A derivative where one *N*-acyl and one *O*-acyl chain are attached to GlcNII (terminal Ω, Ω-1, Ω-2 carbon atoms colored green, foreground) because both chains fit into the cleft without being sterically impeded by the protein surface.

While de-*O*-acylated lipid A is rapidly dephosphorylated, the direct relevance in endotoxin detoxification is questionable given de-*O*-acylated lipid A is already a weak TLR4/MD2 agonist. However, many of the more common gut-associated bacteria (as from bacteria in the order *Bacteroidales*) remodel their lipid A to underacylated chemotypes (95, 96). Underacylated chemotypes not only have lower intrinsic endotoxin activity, but also dampen TLR4/MD2 signaling and inflammation from more potent lipid A congeners with higher acylation states as found in *Enterobacteriaceae* through competition for TLR4/MD2 receptor. It is conceivable that endogenous underacylated chemotypes from gut associated bacteria may be selectively subject to further detoxification by IAP, or that IAP may play an indirect role in lowering the endotoxin burden by processing the underacylated antagonistic lipid A population pool.

The influence of lipid A acylation state on attenuating hTLR4/MD2 activity has long been recognized. However, the importance of PEtN modification on lipid A is just beginning to be appreciated. Indeed, the structure-hTLR4/MD2 activity relationship of EptA modified lipid A is nearly as equipotent as the removal/addition of secondary acyl chains (Fig. 2-7C). The PEtN effect is not unique to *E. coli*, as the potency of other lipid A scaffolds in *N. meningitidis* (56-59) and *C. jejuni* (60) is likewise enhanced by PEtN. The influence of PEtN-modified lipid A on TLR4/MD2 signaling demonstrates marked species dependent effects, as the degree of mTLR4/MD2 stimulation was agnostic to the presence of EptA in the producing strain across all the tested lipid A acylation states (Fig. 2-7D). Of note, EptA expression in a lipid IV_A producing strain restored some hTLR4/MD2 agonist character (Fig. 2-10). This raises the possibility that detoxification by acyloxyacyl hydrolase through removal of secondary acyl chains may be less effective when PEtN

modified LPS is abundant. Our computational binding model suggests this is due to key residues specific to hTLR4/MD2 (Fig. 2-12). The weak activity of 2-PEtN lipid IV_A is particularly interesting, considering this is a lipid A-based hTLR4/MD2 agonist with inherently self-limiting biological activity as the phosphoanhydride linked PEtN groups are unstable at physiological pH (Fig. 2-2C and 2-2D). These properties suggest a potential design for engineering safe next generation adjuvants. Utilizing lipid A analogs agonists to bolster immune responses to synthetic vaccines antigens without inducing toxicity is a major challenge (57, 97-99). Chemically unstable 2-PEtN lipid IV_A type analogs will spontaneously convert over time from an agonist to antagonist under physiological conditions, offering an intriguing adjuvant strategy that warrants further investigation.

We cannot definitively rule out a direct LPS dephosphorylating activity for select AP-LPS chemotype pairs, as the *E. coli* LPS chemotypes-AP pairs studied here is a far from exhaustive list. The complement of respective intestinal AP isozymes varies widely among vertebrates, so that biological roles may be species specific. It has been proposed that the intestinal AP dephosphorylation activities have co-evolved to complement the substrates being produced by the particular resident microbiota (100). If hexa-acylated LPS is a *bona fide* substrate however, there is clearly an integral missing component from the reconstituted *in vitro* system. Regardless, the labile nature of phosphoanhydride linked PEtN modifications on LPS and the ensuing diminished TLR4/MD2 signaling precludes using phosphate release and decreased endotoxin activity as sole determinants of AP-mediated LPS detoxification. It also emphasizes the advantages of using chemically defined LPS chemotypes, given that the PEtN content will not only depend on the particular source strain, but will also vary according to both the growth media and

the extraction and purification methods. Defined chemotypes will allow more robust comparisons between studies and ultimately a better understanding of the role of AP in ameliorating LPS-induced inflammation.

MATERIALS AND METHODS

Reagents

Calf intestinal alkaline phosphatase (cIAP) was purchased from New England BioLabs. Human placenta (PLAP) and human liver alkaline phosphatase (TNAP) were ordered from Lee Biosolutions Inc., while porcine kidney alkaline phosphatase was from Sigma. Human intestinal alkaline phosphatase (ALPI) was obtained from Sino Biological. All chemicals were purchased from Sigma Millipore unless noted otherwise.

Bacterial strain construction

Gene deletions were introduced into *E. coli* strains using the λ -Red recombinase system as described (101). Targeting cassettes were obtained by PCR amplification using P1-P2 primer pairs (Table 2-1). Each primer contained a 5' 42-bp homology extension arm and a 3' 18-bp sequence specific for the indicated antibiotic selection marker of the plasmid template. For the *arnA::kanR* and *lpxM::kanR* cassettes, genomic DNA was purified from the Coli Genetic Stock Center strains CGSC#9813 and #9540 and used as a template to flank the antibiotic cassette with FRT sites for subsequent marker excision using the FLP recombinase plasmid pCP20 (102). Integration cassettes were purified and electroporated into recipient strains harboring the

arabinose-inducible λ -Red recombinase plasmid pKD46 (101). Plasmids were cured by passaging at 37°C, colonies were checked for loss of plasmid, and cassette insertion was confirmed using check primers (Table 2-1). For construction of tetra-acylated LPS strains containing a complete saccharide core (GKM499 and GKM502), plasmid pMMW52-msbA was first introduced to enhance LPS transport and improve fitness. In this background, deletion cassettes were then introduced by generalized transduction using P1*vir*. Strain genotypes are listed in Table 2-2.

Table 2-1: Primers used in this study.

Primer name	Primer Sequence ^{a,b}
GK425-ArnA::KanR-P1	GGTGACCTGCCTTACCACAAC
GK426-ArnA::KanR-P2	TCGTGATGTTTAGCCGCTTC
TM448-EptA::catR-P1	GTTGGCCGCTTTTTATATCTCTATCTGCCTGAATATTGCCTTGCGCCT ACCTGTGACGGA
TM449-EptA::catR-P2	TGTTGCGTTTGCGCCTGTTTTGCAGGCAGTTCTGGTCAACCCTTAC GCCCCGCCCTGCC
GK429-LpcA::gentR-P1	CACTGCATTTTGTCTATTACATTTATGCTGAAGGATATCCTCCTCGAA TTGACATAAGCC
GK430-LpcA::gentR-P2	TGCCGGATGCGGCGTAAACGTCTTATCCGGCCTACGCCAGACGTCG GCTTGAACGAATTG
Tm520-WaaP::gentR-P1	AGCCGTTTGCCACGTTATGGCGCGGTAAAGATCCTTTTGAGGCTCG AATTGACATAAGCC
Tm521-WaaP::gentR-P2	CGTTCTTTCCTGATTTTTGTGGCTTTTGCTTCTGCTTGCAGTCGGC TTGAACGAATTG
Tm543-EptB::gentR-P1	GATACATCAAATCGATTACACAGCAGAAGCTGAGCTTTTTGCCTCG AATTGACATAAGCC
Tm544-EptB::gentR-P2	GTTAGCCGCTGCCTCTTTTGCTGCGGGATGTGACACCAGTTTACGG CTTGAACGAATTG
Tm547-EptC::gentR-P1	GCATTCCACAGAAGTCCAGGCTAAACCTCTTTTAGCTGGAACCTCGA ATTGACATAAGCC
Tm548-EptC::gentR-P2	CTGATTACCCACCTGATCGCCATACGGCAGTGTGTCGTAATCTACGG CTTGAACGAATTG
Tm582-LpxM::kanR-P1	GATTTTTGCCTTATCCGAAACTGG
Tm583-LpxM::kanR-P2	CAGGCGAAGGCCTCCTCGCGAG
Tm658-LpxL::aprR-P1	CTACCCAAGTTCTCCACCGCACTGCTTCATCCGCGTTATTGGTCACCT AGATCCTTTTGG

Tm659-LpxL::aprR-P2	TCCGGGCGTGT TTTTAAAGCGACGGT GTA ACCACATATACTGCCGTT CTCCGCTCATGAGC
Tm748-PagP::hygR-P1	GTTTTATGGT CACAAATGAACGTGAGTAAATATGTCGCTATCCTATG ACCATGATTACGC
Tm749-PagP::hygR-P2	ACTAAACTTC ATTTGTCTCAAACTGAAAGCGCATCCAGGCACGTT GTAAAACGACGGC
GK433-ArnA-check_for	CGAGCGTGAGTTTGGTGAATCC
GK434-ArnA-check_rev	CCGATCCCAGTTACCGCTAC
GK435-EptA-check_for	AAACCCGTATCCCTTAGATGCACC
GK436-EptA-check_rev	CTCAAGGCTTTGTTCCGCCATC
GK431-LpcA-check_for	AGGTCTGACCACTTGTGATG
GK432-LpcA-check_rev	ATTATTCGGCCTACGGTTCG
Tm522-WaaP-check_for	GATAAGCAAATCGCCGATTTCCAG
Tm524-WaaP-check_rev	TGTCTTATTGATCATCTCTTGTGG
Tm545-EptB-check_for	CAGGGTGTTATCACCTGTTTGTCC
Tm546-EptB-check_rev	CCTTTTGATCGGCGAGAAAGTCAGC
Tm549-EptC-check_for	CCTTAAGGAATTGTCGTTACATTGC
Tm550-EptC-check_rev	GCATCCGGCAAATAGCGCCTGGCTG
Tm614-LpxM-check_for	CTGGCGCAGGCCAAAGAGATTGTGC
Tm615-LpxM-check_rev	GTAGAGTAAGTACGTTGCCGGATGC
Tm660-LpxL-check_for	GGTTGCGGGCGAAAAAATGCGACAATAC
Tm661-LpxL-check_rev	GGGAGATTTAATAGCGTGAAGGAACGC
Tm750-PagP-check_for	GTAGCTTTGCTATGCTAGTAGTAG
Tm751-PagP-check_rev	GTGGTACGCTTTGTCCAGTGTAAC
Tm497-EptA-for_EcoRI	gcggccgcgcaatt A TTTTGCTTTGCGAGC
Tm498-EptA-for_BamHI	cgactctagaggatc CGTCTTCAACAATCAG
Tm557-EptB-for_EcoRI	gcggccgcgcaatt CTAAGCAGGGT GTTATC
Tm558-EptB-for_BamHI	cgactctagaggatc CGGCGAGAAAGTCAGCAG
Tm559-EptC-for_EcoRI	gcggccgcgcaatt CTGTCGTTACATT CGGCG
Tm560-EptC-for_BamHI	cgactctagaggatc CGAAATAGCGCCTGGCTG

^a Bold case type denotes DNA homology arms used for chromosomal recombination.

^b Lower case type indicates homology arms used in plasmid construction.

TABLE 2-2		
Bacterial strains and plasmids used in this study		
Bacterial strain or plasmid	Relevant genotype or phenotype^a	Source or reference
<i>E. coli</i> strains		
TXM319	Wildtype BL21 (DE3); <i>E. coli</i> B F ⁻ <i>ompT hsdS_B(r_B⁻ m_B⁻) gal dcm lon</i> λ (DE3 [<i>lacI lacUV5-T7 gene 1 ind1 sam7 nin5</i>])	Lab stock
TXM322	BL21 (DE3) <i>arnA::kanR</i> ; Kan ^r	This study
GKM329	BL21 (DE3) <i>eptA::catR</i> ; Cat ^r	This study
TXM331	BL21 (DE3) <i>eptA::catR arnA::kanR</i> ; Cat ^r Kan ^r	This study
TXM333	BL21 (DE3) <i>lpcA::gentR eptA::catR arnA::kanR</i> ; Gent ^r Cat ^r Kan ^r	This study
TXM343	BL21 (DE3) <i>lpcA::gentR eptA::catR arnA::kanR</i> [pSEVA434- <i>eptA</i>]; Gent ^r Cat ^r Kan ^r Spec ^r	This study
GKM357	BL21 (DE3) <i>eptA::catR arnA::kanR waaP::gentR</i> ; Cat ^r Kan ^r Gent ^r	This study
GKM358	BL21 (DE3) <i>eptA::catR arnA::kanR waaP::gentR</i> [pSEVA434- <i>eptA</i>]; Cat ^r Kan ^r Gent ^r	This study
GKM373	BL21 (DE3) <i>eptA::catR arnA::kanR eptB::gentR</i> ; Cat ^r Kan ^r Gent ^r	This study
GKM374	BL21 (DE3) <i>eptA::catR arnA::kanR eptC::gentR</i> ; Cat ^r Kan ^r Gent ^r	This study
GKM380	BL21 (DE3) <i>eptA::catR arnA::kanR eptB::gentR</i> [pSEVA434- <i>eptC</i>]; Cat ^r Kan ^r Gent ^r Spec ^r	This study
GKM381	BL21 (DE3) <i>eptA::catR arnA::kanR eptC::gentR</i> [pSEVA434- <i>eptB</i>]; Cat ^r Kan ^r Gent ^r Spec ^r	This study
TXM402	BL21 (DE3) <i>eptA::catR arnA::kanR eptC::gentR</i> [pSEVA434- <i>eptA</i>]; Cat ^r Kan ^r Gent ^r Spec ^r	This study
TXM418	BL21 (DE3) <i>eptA::catR arnA::FRT eptC::gentR lpxM::kanR</i> ; Cat ^r Gent ^r Kan ^r	This study
TXM419	BL21 (DE3) <i>eptA::catR arnA::FRT eptC::gentR lpxM::kanR</i> [pSEVA434- <i>eptA</i>]; Cat ^r Gent ^r Kan ^r Spec ^r	This study
GKM445	<i>ClearColi</i> [®] K-12 F ⁻ , λ- <i>ΔendA ΔrecA msbA52 frr181 ΔgutQΔkdsDΔlpxLΔlpxMΔlpxPΔeptA</i>	Lucigen
GKM446	GKM445 (pSEVA434- <i>eptA</i>); Spec ^r	This study
GKM499	BL21 (DE3) <i>eptA::catR arnA::FRT eptC::gentR lpxM::kanR lpxL::aprR pagP::hygR</i> [pMMW52- <i>msbA</i>]; Cat ^r Gent ^r Kan ^r Apr ^r Hyg ^r Carb ^r	This study
GKM502	BL21 (DE3) <i>eptA::catR arnA::FRT eptC::gentR lpxM::kanR lpxL::aprR pagP::hygR</i> [pMMW52- <i>msbA</i> , pSEVA434- <i>eptA</i>]; Cat ^r Gent ^r Kan ^r Apr ^r Hyg ^r Carb ^r Spec ^r	This study

TXM843	<i>ClearColi</i> [®] BL21 (DE3) F ⁻ <i>ompT hsdSB</i> (r ^B - m ^B -) <i>gal dcm lon</i> λ (DE3 [lacI lacUV5-T7 gene 1 <i>ind1 sam7 nin5</i>]) <i>msbA148</i> Δ <i>gutQ</i> Δ <i>kdsD</i> Δ <i>lpxL</i> Δ <i>lpxM</i> Δ <i>pagP</i> Δ <i>lpxP</i> Δ <i>eptA</i>	Lucigen
TXM844	TXM843 [pSEVA434- <i>eptA</i>]; Spec ^r	This study
Plasmids		
pSEVA434	pBBR1 ori lacIq- <i>P</i> _{trc} Spec ^r	(103)
pSEVA434-<i>eptA</i>	<i>P</i> _{trc} <i>eptA</i> from <i>E. coli</i> BL21 (DE3)	This study
pSEVA434-<i>eptB</i>	<i>P</i> _{trc} <i>eptB</i> from <i>E. coli</i> BL21 (DE3)	This study
pSEVA434-<i>eptC</i>	<i>P</i> _{trc} <i>eptC</i> from <i>E. coli</i> BL21 (DE3)	This study
pMMW52-<i>msbA</i>	pMBL19 carrying a subcloned 3.5-kb insert with <i>ycal'</i> , <i>msbA</i> , and <i>lpxK</i> ; Carb ^r	(49)
pKD3	Cat ^r template	(101)
pCP20	FLP recombinase expression plasmid; Carb ^r Cat ^r	(99)
pKD46	λ -Red recombinase expression plasmid; Carb ^r	(98)
pEXG2	Gent ^r template	(104)
pSET152	Apr ^r template	(105)
pUC19-oriT-hyg	Hyg ^r template	Lab stock

^a Kan^r- kanamycin; Cat^r- chloramphenicol; Gent^r- gentamycin; Spec^r- spectinomycin; Carb^r- carbenicillin; Apr^r- apramycin; Hyg^r- hygromycin.

Plasmids expressing either *EptA*, *EptB*, or *EptC* were constructed using the InFusion Cloning kit (Clontech). PCR primer pairs (Table 2-1) were used to amplify inserts from *E. coli* BL21DE3 genomic DNA and then cloned into the vector pSEVA434 (103) that had been digested with *EcoRI/BamHI*. Plasmids were maintained with spectinomycin (50 μ g/ml) and used without induction as basal expression was sufficient for phenotypic conversion for all three constructs.

LPS purification

Bacteria were harvested from stationary phase cultures grown at 37°C in either Lysogeny Broth (10 g tryptone, 5 g yeast extract, 10 g NaCl per liter) or TB media (39) (10 g tryptone, 5 g

yeast extract, 3 g NH₄Cl, 12 g Na₂HPO₄, 6 g KH₂PO₄, 0.5 g Na₂SO₄, 7.5 g glucose per liter) supplemented with the necessary antibiotics for plasmid selection. Dried bacterial cell biomass was obtained by sequentially stirring in ethanol overnight and then two rounds of acetone (12 hours each) at 4 °C, collecting biomass between incubations by centrifugation (6,000 x *g*, 10 min, 4 °C). All LPS and lipid IV_A chemotypes were initially extracted from cell powders via the phenol/chloroform/petroleum ether (PCP) method (106). Briefly, dried biomass was resuspended in PCP solution (90% phenol/chloroform/petroleum ether in 2:5:8 v/v/v ratio) and incubated for one hour on tube rotator. Biomass was pelleted and the supernatant collected, with the extraction being repeated twice. Pooled supernatant extract was rotavaped to remove chloroform and petroleum ether, and 100 μl of 3 M sodium acetate (pH 7.0) was added to the phenol phase. Here treatment of the samples varied depending on the chemotype. For LPS samples, precipitation was carried out via dropwise addition of water. Pelleted LPS was washed once with 80% phenol and then a second time with acetone. For lipid IV_A samples, five volumes of acetone were added to precipitate lipid IV_A from the phenol phase and then the pellet was washed once with acetone.

To remove co-extracting phospholipids from LPS, samples underwent a modified chloroform/methanol wash (107). Briefly, pellets were resuspended in chloroform/methanol/3 M sodium acetate (pH 7.0) (85:15:1, v/v/v) and 2 to 3 volumes of methanol were added to precipitate LPS. Phospholipid containing supernatant was decanted and this process was repeated twice. Removal of contaminating lipoprotein was achieved via phenol/sodium deoxycholate extraction as described by Hirschfeld et al. (108). Lipid IV_A samples could not be

efficiently recovered using either the chloroform/methanol wash or the phenol/DOC extraction, hence these steps were omitted.

All chemotypes underwent ultracentrifugation to remove any malachite green reactive nucleic acid material. LPS or lipid IV_A pellets were resuspended in 3 ml of water and added to 30 ml of a Tris-saline buffer (50 mM Tris-HCl, 100 mM NaCl, 1 mM MgCl₂, pH 7.0). Samples were centrifuged at 100,000 x *g* for 4-6 hours, resulting in a translucent pellet. The resultant pellet was quickly rinsed with buffer, resuspended in water, and dialyzed (0.5-1 kDa MWCO) against three 5-l portions of water for 48 hours (24 hours for PEtN-modified chemotypes) at 4 °C. Desalted LPS chemotypes were lyophilized to a white powder, while lipid IV_A chemotypes were further purified as described below.

Inorganic phosphate release and dephosphorylated LPS product assay

LPS samples (100 µg/ml) were incubated in alkaline phosphatase buffer [50 mM Tris-HCl at the indicated pH (pH = 8.25, 7.4, or 7.1), 100 mM NaCl, 1 mM MgCl₂, 20 µM ZnCl₂] with either cIAP (4 U/ml), human liver phosphatase (0.1 U/ml), human placenta phosphatase (1 U/ml), human intestinal phosphatase (0.17 µg/ml) or porcine kidney phosphatase (1 U/ml) at 37 °C. Aliquots were taken at different time points and phosphate release was measured with the malachite green assay as described previously (33). Briefly, one volume of malachite green solution (0.1% malachite green, 14% sulfuric acid, 1.5% ammonium molybdate, and 0.18% Tween-20) was mixed with four volumes of LPS solution and the mixture was incubated at room temperature for 10 min. Absorbance was read at 630 nm on SpectraMax Plus 384 plate reader (Molecular Devices). Sodium phosphate was used for standard curve determination.

For direct assay of dephosphorylated LPS, 10-ml reactions were assembled as described above in dialysis tubing (0.5-1 kDa MWCO). Reactions were continuously dialyzed against 500 ml of buffer to remove any released inorganic phosphate. LPS products were isolated by extensive dialysis against water and lyophilized before analysis by mass spectrometry as detailed below.

Buffer composition for assays conducted at varying pH values was 50 mM 3-morpholinopropane-1-sulfonic acid (MOPS)-50 mM Tris adjusted to either pH 6.5, 7.4, or 8.5 along with 100 mM NaCl, 1 mM MgCl₂ and 20 μM ZnCl₂. In the experiments where 10 units of cIAP was added after pre-incubation in the buffer alone, samples were incubated for 30 min at 37°C to release inorganic phosphate from spontaneously hydrolyzed PEtN.

TLR4 stimulation assay

HEK293/hTLR4-MD2-CD14, HEK293/mTLR4-MD2-CD14, and parental HEK293/Null2 control cells were grown as specified by the supplier (InvivoGen). For the stimulation assay, the cells were plated at 50,000 cells per well in a white 96 well plate with clear bottom (Costar™ 3610, Corning Incorporated) in 200 μl of growth medium (DMEM, 2 mM L-glutamine, 10% heat inactivated fetal bovine serum, 50 U/ml penicillin, 50 μg/ml streptomycin, 100 μg/ml Normocin™). The pNiFty-Luc plasmid (InvivoGen) encoding five NF-κB repeated transcription factor binding sites in front of the luciferase reporter gene was mixed with transfection reagent LyoVec™ (InvivoGen) at a concentration of 1 μg of plasmid per 100 μl of LyoVec™, and after incubation at room temperature for 20 min, the mixture (10 μl per well) was added to cells in a 96 well microplate. The next day the medium was removed and replaced with 180 μl of fresh growth medium. Various LPS chemotypes were added at different concentrations in a 20-μl

volume per well. Endotoxin-free water was used as a negative control and TNF- α (200 ng/well) was used as a positive control. Pierce™ Firefly Luciferase One-Step Glow Assay Kit was used according to manufacturer's instructions with luminescence being measured after 20 hours of stimulation. All LPS and lipid IV_A preparations were confirmed to be negative for NF- κ B induction when challenging HEK293/Null2 control cells (InvivoGen) up to the highest tested LPS concentration (100 ng/ml, data not shown).

TLR2 stimulation assay

HEK-Blue™ hTLR2 cells (InvivoGen) were propagated as specified by the supplier. For the stimulation assay, the cells were plated at 25,000 cells per well in a 96 well plate in 180 μ l of growth medium (DMEM, 2mM L-glutamine, 10% heat inactivated fetal bovine serum, 50 U/ml penicillin, 50 μ g/ml streptomycin, 100 μ g/ml Normocin™). LPS was added at different concentrations in a 20 μ l per well volume. Endotoxin-free water was used as a negative control. QUANTI Blue™ (InvivoGen) reagent was used, according to manufacturer's instructions, 20 hours later to detect NF- κ B-dependent secreted embryonic alkaline phosphatase (SEAP) activity. Absorbance at 620 nm was read following incubation of the samples with QUANTI Blue™ substrate for 3 hours at 37°C.

Lipase treatment of lipid IV_A extracts

Crude lipid IV_A (with or without PEtN) was treated with lipase via two sequential incubations. Both 12-hour reactions were conducted at 45 °C in a 20 mM phosphate buffer (pH 7.0). Each reaction contained 40 mg of crude PCP extracted lipid IV_A, *Thermomyces* Lipase (TL,

Sigma), and Novozyme® 51032 (Strem Chemicals, Newburyport, MA) at respective final concentrations of 0.1 mg/ml, 90 µg/ml, and 25 µg/ml. The initial reaction included 3.4 mM BIG CHAP (SolTec Bio Science, Beverly, MA) as a nonionic detergent additive. Immediately following this reaction, lipid IV_A was recovered by conversion to a 2:2:1.8 (v/v/v) chloroform/methanol/water Bligh-Dyer biphasic mixture. Lipid IV_A was isolated from the lower organic phase by rotary evaporation, resuspended in endotoxin-free water, and then lyophilized. Recovered lipid IV_A was treated again in a second lipase reaction with 20 mM octyl-β-D-glucopyranoside as the detergent additive, and re-isolated as described above. PEtN-modified lipid IV_A was stored at -20 °C until further use.

Chromatographic purification of lipid IV_A species

Ion exchange chromatography was performed using a 5-ml HiTrap™ SP HP cation exchange column connected in tandem to a 20-ml HiPrep™ DEAE FF 16/10 anion exchange column with the ÄKTA™ Pure FPLC system. Lipase-treated PEtN lipid IV_A prepared as described above was loaded in 15 ml of a 60% *n*-propanol solution adjusted to pH 5 with acetic acid. The system was then washed with 10 ml of the same buffer, after which the cation exchange column was removed. The anion exchange column was subsequently washed with 4.5 column volumes of 60% *n*-propanol (pH 5), before elution using a linear gradient of non-pH adjusted 0 to 80 mM ammonium acetate in 60% *n*-propanol over 20 column volumes. To identify fractions containing non-volatile organic compounds, 20 µl of each fraction was spotted onto an Analtech Silica gel G TLC plate and visualized by charring using a 10% sulfuric acid-ethanol solution with heating at 160 °C for 10 min. Fractions containing organic material were further analyzed by spotting 20 µl

on an Analtec Silica gel H TLC plate, and developed using a pyridine/chloroform/formic acid/water (50:50:16:5, v/v/v/v) mobile phase before sulfuric acid charring (109). Fractions containing lipid IV_A species were pooled, rotovaped to dryness, and subjected to two rounds of lyophilization to remove residual traces of ammonium acetate. The resulting powder was kept at -20 °C until further purification by reversed-phase high performance liquid chromatography (RP-HPLC). For this, lipid IV_A samples were subjected to RP-HPLC essentially as described (110, 111), but with some modifications. A semi-preparative Kromasil C18 column (5 µm, 100 Å, 10 × 250 mm, MZ Analysentechnik, GmbH, Mainz, Germany) was used and samples [resuspended at 5 mg/ml in chloroform/methanol/0.1 M acetic acid (8:2:1, v/v/v)] were eluted using a gradient consisting of methanol/chloroform/water (57:12:31, v/v/v) containing 10 mM ammonium acetate as mobile phase A and chloroform/methanol (70.2:29.8, v/v) with 50 mM ammonium acetate as mobile phase B. The initial solvent system consisted of 2% B and was maintained for 10 min, raised from 2 to 15% B (10–20 min), kept at 15% B for 20 min, raised from 15 to 25% B (40–50 min), kept at 25% B for 20 min, and raised from 25 to 100% B (70–100 min). The solvent was held at 100% B for 20 min, followed by re-equilibration of the column to 2% B for 10 min and held there for an additional 10 min prior to the next injection. The flow rate was 2 ml/min using a splitter between the evaporative light-scattering detector equipped with a low-flow nebulizer (Sedex model 75C ELSD, S.E.D.E.R.E., France). Nitrogen (purity 99.996%) was used as gas to nebulize the post column flow stream at 3.5 bar into the detector at 50 °C setting the photomultiplier gain to 11. The detector signal was transferred to the Gilson HPLC Chemstation (Trilution LC, version 2.1, Gilson) for detection and integration of the ELSD signal.

De-O-acylation and dephosphorylation assays of lipid IV_A and Re LPS with cIAP

Lipid IV_A was dissolved (1 to 4 mg/ml) in a 1 M NaOH aqueous solution and incubated for 20 hours at room temperature. Reactions were neutralized via addition of glacial acetic acid while stirring until pH 7.0. Neutralized reactions were extensively dialyzed against water (MWCO: 500-1000 Da) and lyophilized. Re LPS was likewise de-*O*-acylated, but was recovered by precipitation from neutralized solution using five volumes of ethanol. De-*O*-acylated products were further purified via anion exchange chromatography as described above. Fractions were pooled, concentrated by rotary evaporation, and dialyzed against water (MWCO: 500-1000 Da). Samples were lyophilized and stored at -20 °C.

Large scale (30 ml) cIAP reactions (100 µg/ml de-*O*-acyl substrate, 4 U/mL cIAP, 50 mM Tris-HCl (pH = 7.4), 100 mM NaCl, 1 mM MgCl₂, 20 µM ZnCl₂) were incubated for 24 to 48 hours at 37 °C. Samples were recovered by dialysis against water (100-500 Da MWCO) followed by lyophilization.

Mass spectrometry

LPS samples were measured on a 7-tesla APEX Qe Electrospray Ionization Fourier Transform Ion Cyclotron Resonance (ESI-FT-ICR) mass spectrometer (Bruker Daltonics). Measurements were performed in negative ion mode. Samples (approximately 0.03 mg/ml) were dissolved in a water/2-propanol/trimethylamine/acetic acid mixture (50:50:0.06:0.02, v/v/v/v). Spectra were acquired in broadband acquisition mode with nano-ESI using the Triversa Nanomate (Advion, Ithaca, NY) as ion source with a spray voltage set to -1.1 kV. Collision voltage was set to 5 V. Lipid IV_A and de-*O*-acylated samples were measured on a Q Exactive Plus mass

spectrometer (Thermo Scientific, Bremen, Germany) using a Triversa Nanomate (Advion, Ithaca, NY) as ion source. For negative ion mode, samples (approximately 0.05 mg/ml) were dissolved in either chloroform/methanol/water (60:35:4.5, v/v/v) or water/propan-2-ol/7M triethylamine/acetic acid mixture (50:50:0.06:0.02, v/v/v/v) and performed with a spray voltage set to -1.1 kV. For positive ion-mode, samples were dissolved in water/propan-2-ol/30 mM ammonium acetate/acetic acid mixture (15:15:1:0.04, v/v/v/v) with a spray voltage set to +1.1 kV. Both mass spectrometers were calibrated externally with glycolipids of known structure. All mass spectra were charge deconvoluted and given mass values refer to the monoisotopic masses of the neutral molecules, if not indicated otherwise.

NMR spectroscopy

NMR spectroscopic measurement of PEtN-lipid IV_A was performed in CDCl₃/MeOH-d₄/D₂O (60:35:8, v/v/v) and de-*O*-acyl Re LPS after treatment with cIAP in CDCl₃/MeOH-d₄/D₂O (2:3:1, v/v/v) (68), respectively, at 300 K on a Bruker Avance^{III} 700 MHz (equipped with an inverse 5-mm quadruple-resonance Z-grad cryoprobe). Deuterated solvents were purchased from Deutero GmbH (Kastellaun, Germany). TMS was used as an external standard for calibration of ¹H (δ_{H} 0.0) and ¹³C (δ_{C} 0.0) NMR spectra, and 85% of phosphoric acid was used as an external standard for calibration of ³¹P NMR spectra (δ_{P} 0.0). All data were acquired and processed by using Bruker's TOPSPIN V 3.0 software. ¹H NMR assignments were confirmed by 2D ¹H,¹H COSY and total correlation spectroscopy (TOCSY) experiments. ¹³C NMR assignments were indicated by 2D ¹H,¹³C HSQC, based on the ¹H NMR assignments. Inter-residue connectivity and further evidence for ¹³C assignment were obtained from 2D ¹H,¹³C heteronuclear multiple bond

correlation and $^1\text{H},^{13}\text{C}$ HSQC-TOCSY. Connectivity of phosphate groups were assigned by 2D $^1\text{H},^{31}\text{P}$ HMQC and $^1\text{H},^{31}\text{P}$ HMQC-TOCSY.

Molecular modeling

Standard modeling tools and protocols were conducted according to published protocols (55, 65). Modeling software [Autodock 4.2 (112), Chimera 1.13.1 (53), SPDBV 4.10 (113), VEGA ZZ 3.1.2 (114)] was licensed for academic use to generate and visualize three-dimensional model structures of lipid IV_A, TLR4/MD2, and phosphatase enzymes, in addition to partial charges, electrostatic molecular surfaces or fitted active site conformers (53, 112, 115, 116). The TLR4/MD2 docking protocol first presented by Meng *et al* (55) and later adapted (65) using the hTLR4/MD2-*E. coli* LPS crystal structure [3FXI, (117)] was utilized to model LPS-like congener binding. The large number (52) of freely rotatable bonds at the 4 side chains of lipid IV_A had to be reduced and were limited to the first three chain members including the four H-O bonds as well as the two ester bonds, while excluding the two more rigid *trans*-amide bonds. To visualize the steric hindrance associated to nonbinders (no valid docking/scoring solutions found) we superimposed them onto the final docked poses of those ligand types with favorable side chain patterns for successful cavity binding – here called the binders (Fig. 2-6A). Whereas for nonbinders any of the calculated conformations under docking conditions would show detrimental van der Waals contacts, binders provide (some not all) conformational solutions for successful binding in the micromolar range. Lipid IV_A (118) and all enzymes and receptors were retrieved from PDB repository server (119) with the exception of hitherto structurally unknown cIAP that was generated by homology modeling using described methodology (120). The cIAP

target (GenBank entry code: AAA30571.1) shares more than 70% identity with rat IAP across 486 non-gapped residues, including all active sites residues. Using the experimentally determined rat IAP crystal structures (4KJD, 4KJG) (52), a cIAP homodimer structure was generated under Swiss PDB Viewer (113). Multiple sequence alignments were carried out with built-in Clustal X under Vega ZZ (114). Of note, all phosphate groups were charged and modeled as monoanionic, e.g. bearing one -OH group. In some figures hydrogen atoms were not displayed for visual simplicity (121). All model figures were generated with Chimera (53).

REFERENCES

1. Boroni Moreira, A. P., andde Cassia Goncalves Alfenas, R. (2012) The influence of endotoxemia on the molecular mechanisms of insulin resistance *Nutricion hospitalaria* **27**, 382-390 10.1590/S0212-16112012000200007
2. Cani, P. D., Amar, J., Iglesias, M. A., Poggi, M., Knauf, C., Bastelica, D. *et al.* (2007) Metabolic endotoxemia initiates obesity and insulin resistance *Diabetes* **56**, 1761-1772 10.2337/db06-1491
3. Duseja, A., andChawla, Y. K. (2014) Obesity and NAFLD: the role of bacteria and microbiota *Clinics in liver disease* **18**, 59-71 10.1016/j.cld.2013.09.002
4. Miura, K., andOhnishi, H. (2014) Role of gut microbiota and Toll-like receptors in nonalcoholic fatty liver disease *World journal of gastroenterology : WJG* **20**, 7381-7391 10.3748/wjg.v20.i23.7381
5. Moreno-Indias, I., Cardona, F., Tinahones, F. J., andQueipo-Ortuno, M. I. (2014) Impact of the gut microbiota on the development of obesity and type 2 diabetes mellitus *Frontiers in microbiology* **5**, 190 10.3389/fmicb.2014.00190
6. Neves, A. L., Coelho, J., Couto, L., Leite-Moreira, A., andRoncon-Albuquerque, R., Jr. (2013) Metabolic endotoxemia: a molecular link between obesity and cardiovascular risk *Journal of molecular endocrinology* **51**, R51-64 10.1530/JME-13-0079
7. Tilg, H., andMoschen, A. R. (2014) Microbiota and diabetes: an evolving relationship *Gut* **63**, 1513-1521 10.1136/gutjnl-2014-306928
8. Moreira, A. P., Texeira, T. F., Ferreira, A. B., Peluzio Mdo, C., andAlfenas Rde, C. (2012) Influence of a high-fat diet on gut microbiota, intestinal permeability and metabolic

- endotoxaemia *The British journal of nutrition* **108**, 801-809
10.1017/S0007114512001213
9. Tlaskalova-Hogenova, H., Stepankova, R., Kozakova, H., Hudcovic, T., Vannucci, L., Tuckova, L. *et al.* (2011) The role of gut microbiota (commensal bacteria) and the mucosal barrier in the pathogenesis of inflammatory and autoimmune diseases and cancer: contribution of germ-free and gnotobiotic animal models of human diseases *Cellular & molecular immunology* **8**, 110-120 10.1038/cmi.2010.67
 10. Bes-Houtmann, S., Roche, R., Hoareau, L., Gonthier, M. P., Festy, F., Caillens, H. *et al.* (2007) Presence of functional TLR2 and TLR4 on human adipocytes *Histochem Cell Biol* **127**, 131-137 10.1007/s00418-006-0230-1
 11. Ouchi, N., Ohashi, K., Shibata, R., and Murohara, T. (2012) Adipocytokines and obesity-linked disorders *Nagoya journal of medical science* **74**, 19-30,
<http://www.ncbi.nlm.nih.gov/pubmed/22515108>
 12. Piya, M. K., Harte, A. L., and McTernan, P. G. (2013) Metabolic endotoxaemia: is it more than just a gut feeling? *Current opinion in lipidology* **24**, 78-85
10.1097/MOL.0b013e32835b4431
 13. Fei, N., and Zhao, L. (2013) An opportunistic pathogen isolated from the gut of an obese human causes obesity in germfree mice *The ISME journal* **7**, 880-884
10.1038/ismej.2012.153
 14. Cani, P. D., and Delzenne, N. M. (2011) The gut microbiome as therapeutic target *Pharmacology & therapeutics* **130**, 202-212 10.1016/j.pharmthera.2011.01.012

15. Schromm, A. B., Brandenburg, K., Loppnow, H., Zahringer, U., Rietschel, E. T., Carroll, S. F. *et al.* (1998) The charge of endotoxin molecules influences their conformation and IL-6-inducing capacity *J Immunol* **161**, 5464-5471,
<https://www.ncbi.nlm.nih.gov/pubmed/9820522>
16. Kaliannan, K., Hamarneh, S. R., Economopoulos, K. P., Nasrin Alam, S., Moaven, O., Patel, P. *et al.* (2013) Intestinal alkaline phosphatase prevents metabolic syndrome in mice *Proceedings of the National Academy of Sciences of the United States of America* **110**, 7003-7008 10.1073/pnas.1220180110
17. Lalles, J. P. (2014) Intestinal alkaline phosphatase: novel functions and protective effects *Nutrition reviews* **72**, 82-94 10.1111/nure.12082
18. Malo, M. S., Moaven, O., Muhammad, N., Biswas, B., Alam, S. N., Economopoulos, K. P. *et al.* (2014) Intestinal alkaline phosphatase promotes gut bacterial growth by reducing the concentration of luminal nucleotide triphosphates *Am J Physiol Gastrointest Liver Physiol* **306**, G826-838 10.1152/ajpgi.00357.2013
19. Peters, E., Geraci, S., Heemskerk, S., Wilmer, M. J., Bilos, A., Kraenzlin, B. *et al.* (2015) Alkaline phosphatase protects against renal inflammation through dephosphorylation of lipopolysaccharide and adenosine triphosphate *Brit J Pharmacol* **172**, 4932-4945
10.1111/bph.13261
20. Bilski, J., Mazur-Bialy, A., Wojcik, D., Zahradnik-Bilska, J., Brzozowski, B., Magierowski, M. *et al.* (2017) The Role of Intestinal Alkaline Phosphatase in Inflammatory Disorders of Gastrointestinal Tract *Mediators Inflamm* **2017**, 9074601 10.1155/2017/9074601

21. Fawley, J., and Gourlay, D. M. (2016) Intestinal alkaline phosphatase: a summary of its role in clinical disease *J Surg Res* **202**, 225-234 10.1016/j.jss.2015.12.008
22. Kiffer-Moreira, T., Sheen, C. R., Gasque, K. C., Bolean, M., Ciancaglini, P., van Elsas, A. *et al.* (2014) Catalytic signature of a heat-stable, chimeric human alkaline phosphatase with therapeutic potential *PLoS One* **9**, e89374 10.1371/journal.pone.0089374
23. Buchet, R., Millan, J. L., and Magne, D. (2013) Multisystemic functions of alkaline phosphatases *Methods Mol Biol* **1053**, 27-51 10.1007/978-1-62703-562-0_3
24. Rader, B. A. (2017) Alkaline Phosphatase, an Unconventional Immune Protein *Front Immunol* **8**, 897 10.3389/fimmu.2017.00897
25. Koyama, I., Matsunaga, T., Harada, T., Hokari, S., and Komoda, T. (2002) Alkaline phosphatases reduce toxicity of lipopolysaccharides in vivo and in vitro through dephosphorylation *Clin Biochem* **35**, 455-461,
<https://www.ncbi.nlm.nih.gov/pubmed/12413606>
26. Poelstra, K., Bakker, W. W., Klok, P. A., Kamps, J. A., Hardonk, M. J., and Meijer, D. K. (1997) Dephosphorylation of endotoxin by alkaline phosphatase in vivo *Am J Pathol* **151**, 1163-1169, <https://www.ncbi.nlm.nih.gov/pubmed/9327750>
27. Bates, J. M., Akerlund, J., Mittge, E., and Guillemin, K. (2007) Intestinal alkaline phosphatase detoxifies lipopolysaccharide and prevents inflammation in zebrafish in response to the gut microbiota *Cell Host Microbe* **2**, 371-382
10.1016/j.chom.2007.10.010
28. Chen, K. T., Malo, M. S., Moss, A. K., Zeller, S., Johnson, P., Ebrahimi, F. *et al.* (2010) Identification of specific targets for the gut mucosal defense factor intestinal alkaline

- phosphatase *Am J Physiol Gastrointest Liver Physiol* **299**, G467-475
10.1152/ajpgi.00364.2009 10.1152/ajprenal.zh2-5986-corr.2010
29. Bentala, H., Verweij, W. R., Huizinga-Van der Vlag, A., van Loenen-Weemaes, A. M., Meijer, D. K., and Poelstra, K. (2002) Removal of phosphate from lipid A as a strategy to detoxify lipopolysaccharide *Shock* **18**, 561-566,
<https://www.ncbi.nlm.nih.gov/pubmed/12462566>
30. Goldberg, R. F., Austen, W. G., Jr., Zhang, X., Munene, G., Mostafa, G., Biswas, S. *et al.* (2008) Intestinal alkaline phosphatase is a gut mucosal defense factor maintained by enteral nutrition *Proceedings of the National Academy of Sciences of the United States of America* **105**, 3551-3556 10.1073/pnas.0712140105
31. Pettengill, M., Matute, J. D., Tresenriter, M., Hibbert, J., Burgner, D., Richmond, P. *et al.* (2017) Human alkaline phosphatase dephosphorylates microbial products and is elevated in preterm neonates with a history of late-onset sepsis *PLoS One* **12**, e0175936
10.1371/journal.pone.0175936
32. Yang, W. H., Heithoff, D. M., Aziz, P. V., Haslund-Gourley, B., Westman, J. S., Narisawa, S. *et al.* (2018) Accelerated Aging and Clearance of Host Anti-inflammatory Enzymes by Discrete Pathogens Fuels Sepsis *Cell Host Microbe* **24**, 500-513 e505
10.1016/j.chom.2018.09.011
33. Baykov, A. A., Evtushenko, O. A., and Avaeva, S. M. (1988) A malachite green procedure for orthophosphate determination and its use in alkaline phosphatase-based enzyme immunoassay *Anal Biochem* **171**, 266-270,
<https://www.ncbi.nlm.nih.gov/pubmed/3044186>

34. Klein, G., and Raina, S. (2019) Regulated Assembly of LPS, Its Structural Alterations and Cellular Response to LPS Defects *Int J Mol Sci* **20**, 10.3390/ijms20020356
35. Merighi, M., Ellermeier, C. D., Slauch, J. M., and Gunn, J. S. (2005) Resolvase-in vivo expression technology analysis of the *Salmonella enterica* serovar Typhimurium PhoP and PmrA regulons in BALB/c mice *J Bacteriol* **187**, 7407-7416 10.1128/JB.187.21.7407-7416.2005
36. Maldonado, R. F., Sa-Correia, I., and Valvano, M. A. (2016) Lipopolysaccharide modification in Gram-negative bacteria during chronic infection *FEMS Microbiol Rev* **40**, 480-493 10.1093/femsre/fuw007
37. Raetz, C. R., Reynolds, C. M., Trent, M. S., and Bishop, R. E. (2007) Lipid A modification systems in gram-negative bacteria *Annu Rev Biochem* **76**, 295-329 10.1146/annurev.biochem.76.010307.145803
38. Klein, G., Lindner, B., Brade, H., and Raina, S. (2011) Molecular basis of lipopolysaccharide heterogeneity in *Escherichia coli*: envelope stress-responsive regulators control the incorporation of glycoforms with a third 3-deoxy- α -D-mannooct-2-ulosonic acid and rhamnose *J Biol Chem* **286**, 42787-42807 10.1074/jbc.M111.291799
39. Jansson, P. E., Lindberg, A. A., Lindberg, B., and Wollin, R. (1981) Structural studies on the hexose region of the core in lipopolysaccharides from Enterobacteriaceae *Eur J Biochem* **115**, 571-577, <https://www.ncbi.nlm.nih.gov/pubmed/7016539>

40. Mamat, U., Wilke, K., Bramhill, D., Schromm, A. B., Lindner, B., Kohl, T. A. *et al.* (2015) Detoxifying *Escherichia coli* for endotoxin-free production of recombinant proteins *Microbial cell factories* **14**, 57 10.1186/s12934-015-0241-5
41. Komazin, G., Maybin, M., Woodard, R. W., Scior, T., Schwudke, D., Schombel, U. *et al.* (2019) Substrate structure-activity relationship reveals a limited lipopolysaccharide chemotype range for intestinal alkaline phosphatase *J Biol Chem* **294**, 19405-19423 10.1074/jbc.RA119.010836
42. Lee, H., Hsu, F. F., Turk, J., and Groisman, E. A. (2004) The PmrA-regulated pmrC gene mediates phosphoethanolamine modification of lipid A and polymyxin resistance in *Salmonella enterica* *J Bacteriol* **186**, 4124-4133 10.1128/JB.186.13.4124-4133.2004
43. Reynolds, C. M., Kalb, S. R., Cotter, R. J., and Raetz, C. R. (2005) A phosphoethanolamine transferase specific for the outer 3-deoxy-D-manno-octulosonic acid residue of *Escherichia coli* lipopolysaccharide. Identification of the eptB gene and Ca²⁺ hypersensitivity of an eptB deletion mutant *J Biol Chem* **280**, 21202-21211 10.1074/jbc.M500964200
44. Klein, G., Muller-Loennies, S., Lindner, B., Kobylak, N., Brade, H., and Raina, S. (2013) Molecular and structural basis of inner core lipopolysaccharide alterations in *Escherichia coli*: incorporation of glucuronic acid and phosphoethanolamine in the heptose region *J Biol Chem* **288**, 8111-8127 10.1074/jbc.M112.445981
45. Breazeale, S. D., Ribeiro, A. A., McClarren, A. L., and Raetz, C. R. (2005) A formyltransferase required for polymyxin resistance in *Escherichia coli* and the modification of lipid A with 4-Amino-4-deoxy-L-arabinose. Identification and function of

- UDP-4-deoxy-4-formamido-L-arabinose J Biol Chem **280**, 14154-14167
10.1074/jbc.M414265200
46. Yethon, J. A., Heinrichs, D. E., Monteiro, M. A., Perry, M. B., and Whitfield, C. (1998) Involvement of waaY, waaQ, and waaP in the modification of Escherichia coli lipopolysaccharide and their role in the formation of a stable outer membrane J Biol Chem **273**, 26310-26316, <https://www.ncbi.nlm.nih.gov/pubmed/9756860>
47. Millan, J. L. (2006) Alkaline Phosphatases : Structure, substrate specificity and functional relatedness to other members of a large superfamily of enzymes Purinergic Signal **2**, 335-341 10.1007/s11302-005-5435-6
48. Mamat, U., Meredith, T. C., Aggarwal, P., Kuhl, A., Kirchhoff, P., Lindner, B. *et al.* (2008) Single amino acid substitutions in either YhjD or MsbA confer viability to 3-deoxy-d-manno-oct-2-ulosonic acid-depleted Escherichia coli Mol Microbiol **67**, 633-648
10.1111/j.1365-2958.2007.06074.x
49. Meredith, T. C., Aggarwal, P., Mamat, U., Lindner, B., and Woodard, R. W. (2006) Redefining the requisite lipopolysaccharide structure in Escherichia coli ACS Chem Biol **1**, 33-42 10.1021/cb0500015
50. Perez, J. C., and Groisman, E. A. (2007) Acid pH activation of the PmrA/PmrB two-component regulatory system of Salmonella enterica Mol Microbiol **63**, 283-293
10.1111/j.1365-2958.2006.05512.x
51. Soncini, F. C., and Groisman, E. A. (1996) Two-component regulatory systems can interact to process multiple environmental signals J Bacteriol **178**, 6796-6801,
<https://www.ncbi.nlm.nih.gov/pubmed/8955299>

52. Ghosh, K., Mazumder Tagore, D., Anumula, R., Lakshmaiah, B., Kumar, P. P., Singaram, S. *et al.* (2013) Crystal structure of rat intestinal alkaline phosphatase--role of crown domain in mammalian alkaline phosphatases *J Struct Biol* **184**, 182-192
10.1016/j.jsb.2013.09.017
53. Pettersen, E. F., Goddard, T. D., Huang, C. C., Couch, G. S., Greenblatt, D. M., Meng, E. C., and Ferrin, T. E. (2004) UCSF Chimera--a visualization system for exploratory research and analysis *J Comput Chem* **25**, 1605-1612 10.1002/jcc.20084
54. Meng, J., Gong, M., Bjorkbacka, H., and Golenbock, D. T. (2011) Genome-wide expression profiling and mutagenesis studies reveal that lipopolysaccharide responsiveness appears to be absolutely dependent on TLR4 and MD-2 expression and is dependent upon intermolecular ionic interactions *J Immunol* **187**, 3683-3693 10.4049/jimmunol.1101397
55. Meng, J., Lien, E., and Golenbock, D. T. (2010) MD-2-mediated ionic interactions between lipid A and TLR4 are essential for receptor activation *J Biol Chem* **285**, 8695-8702 10.1074/jbc.M109.075127
56. John, C. M., Liu, M., Phillips, N. J., Yang, Z., Funk, C. R., Zimmerman, L. I. *et al.* (2012) Lack of lipid A pyrophosphorylation and functional lptA reduces inflammation by *Neisseria commensals* *Infect Immun* **80**, 4014-4026 10.1128/IAI.00506-12
57. Zariri, A., Pupo, E., van Riet, E., van Putten, J. P., and van der Ley, P. (2016) Modulating endotoxin activity by combinatorial bioengineering of meningococcal lipopolysaccharide *Sci Rep* **6**, 36575 10.1038/srep36575
58. Liu, M., John, C. M., and Jarvis, G. A. (2010) Phosphoryl moieties of lipid A from *Neisseria meningitidis* and *N. gonorrhoeae* lipooligosaccharides play an important role in

- activation of both MyD88- and TRIF-dependent TLR4-MD-2 signaling pathways J Immunol **185**, 6974-6984 10.4049/jimmunol.1000953
59. Packiam, M., Yedery, R. D., Begum, A. A., Carlson, R. W., Ganguly, J., Sempowski, G. D. *et al.* (2014) Phosphoethanolamine decoration of *Neisseria gonorrhoeae* lipid A plays a dual immunostimulatory and protective role during experimental genital tract infection Infect Immun **82**, 2170-2179 10.1128/IAI.01504-14
60. Cullen, T. W., O'Brien, J. P., Hendrixson, D. R., Giles, D. K., Hobb, R. I., Thompson, S. A. *et al.* (2013) EptC of *Campylobacter jejuni* mediates phenotypes involved in host interactions and virulence Infect Immun **81**, 430-440 10.1128/IAI.01046-12
61. Loppnow, H., Brade, H., Durrbaum, I., Dinarello, C. A., Kusumoto, S., Rietschel, E. T., and Flad, H. D. (1989) IL-1 induction-capacity of defined lipopolysaccharide partial structures J Immunol **142**, 3229-3238, <https://www.ncbi.nlm.nih.gov/pubmed/2651523>
62. Nogare, A. R., and Yarbrough, W. C., Jr. (1990) A comparison of the effects of intact and deacylated lipopolysaccharide on human polymorphonuclear leukocytes J Immunol **144**, 1404-1410, <https://www.ncbi.nlm.nih.gov/pubmed/2154518>
63. Pohlman, T. H., Munford, R. S., and Harlan, J. M. (1987) Deacylated lipopolysaccharide inhibits neutrophil adherence to endothelium induced by lipopolysaccharide in vitro J Exp Med **165**, 1393-1402, <https://www.ncbi.nlm.nih.gov/pubmed/3572302>
64. Wang, M. H., Flad, H. D., Feist, W., Brade, H., Kusumoto, S., Rietschel, E. T., and Ulmer, A. J. (1991) Inhibition of endotoxin-induced interleukin-6 production by synthetic lipid A partial structures in human peripheral blood mononuclear cells Infect Immun **59**, 4655-4664, <https://www.ncbi.nlm.nih.gov/pubmed/1937825>

65. Scior, T., Alexander, C., and Zaehring, U. (2013) Reviewing and identifying amino acids of human, murine, canine and equine TLR4 / MD-2 receptor complexes conferring endotoxic innate immunity activation by LPS/lipid A, or antagonistic effects by Eritoran, in contrast to species-dependent modulation by lipid IVa *Comput Struct Biotechnol J* **5**, e201302012 10.5936/csbj.201302012
66. Raetz, C. R., Purcell, S., Meyer, M. V., Qureshi, N., and Takayama, K. (1985) Isolation and characterization of eight lipid A precursors from a 3-deoxy-D-manno-octylosonic acid-deficient mutant of *Salmonella typhimurium* *J Biol Chem* **260**, 16080-16088, <https://www.ncbi.nlm.nih.gov/pubmed/3905804>
67. Strain, S. M., Armitage, I. M., Anderson, L., Takayama, K., Qureshi, N., and Raetz, C. R. (1985) Location of polar substituents and fatty acyl chains on lipid A precursors from a 3-deoxy-D-manno-octulosonic acid-deficient mutant of *Salmonella typhimurium*. Studies by ¹H, ¹³C, and ³¹P nuclear magnetic resonance *J Biol Chem* **260**, 16089-16098, <https://www.ncbi.nlm.nih.gov/pubmed/3905805>
68. Zhou, Z., Ribeiro, A. A., and Raetz, C. R. (2000) High-resolution NMR spectroscopy of lipid A molecules containing 4-amino-4-deoxy-L-arabinose and phosphoethanolamine substituents. Different attachment sites on lipid A molecules from NH₄VO₃-treated *Escherichia coli* versus *kdsA* mutants of *Salmonella typhimurium* *J Biol Chem* **275**, 13542-13551, <https://www.ncbi.nlm.nih.gov/pubmed/10788469>
69. McClure, R., and Massari, P. (2014) TLR-Dependent Human Mucosal Epithelial Cell Responses to Microbial Pathogens *Front Immunol* **5**, 386 10.3389/fimmu.2014.00386

70. Faas, M. M., Saez, T., and de Vos, P. (2017) Extracellular ATP and adenosine: The Yin and Yang in immune responses? *Mol Aspects Med* **55**, 9-19 10.1016/j.mam.2017.01.002
71. Grbic, D. M., Degagne, E., Langlois, C., Dupuis, A. A., and Gendron, F. P. (2008) Intestinal inflammation increases the expression of the P2Y6 receptor on epithelial cells and the release of CXC chemokine ligand 8 by UDP J Immunol **180**, 2659-2668, <https://www.ncbi.nlm.nih.gov/pubmed/18250478>
72. White, K. A., Lin, S., Cotter, R. J., and Raetz, C. R. (1999) A *Haemophilus influenzae* gene that encodes a membrane bound 3-deoxy-D-manno-octulosonic acid (Kdo) kinase. Possible involvement of kdo phosphorylation in bacterial virulence J Biol Chem **274**, 31391-31400, <https://www.ncbi.nlm.nih.gov/pubmed/10531340>
73. Tuin, A., Huizinga-Van der Vlag, A., van Loenen-Weemaes, A. M., Meijer, D. K., and Poelstra, K. (2006) On the role and fate of LPS-dephosphorylating activity in the rat liver Am J Physiol Gastrointest Liver Physiol **290**, G377-385 10.1152/ajpgi.00147.2005
74. Needham, B. D., and Trent, M. S. (2013) Fortifying the barrier: the impact of lipid A remodelling on bacterial pathogenesis Nature reviews Microbiology **11**, 467-481 10.1038/nrmicro3047
75. Chen, H. D., and Groisman, E. A. (2013) The biology of the PmrA/PmrB two-component system: the major regulator of lipopolysaccharide modifications Annu Rev Microbiol **67**, 83-112 10.1146/annurev-micro-092412-155751
76. Cullen, T. W., Giles, D. K., Wolf, L. N., Ecobichon, C., Boneca, I. G., and Trent, M. S. (2011) *Helicobacter pylori* versus the host: remodeling of the bacterial outer membrane is

- required for survival in the gastric mucosa PLoS Pathog **7**, e1002454
10.1371/journal.ppat.1002454
77. Renzi, F., Zahringer, U., Chandler, C. E., Ernst, R. K., Cornelis, G. R., andIttig, S. J. (2016) Modification of the 1-Phosphate Group during Biosynthesis of Capnocytophaga canimorsus Lipid A Infect Immun **84**, 550-561 10.1128/IAI.01006-15
78. Harkness, D. R. (1968) Studies on human placental alkaline phosphatase. II. Kinetic properties and studies on the apoenzyme Arch Biochem Biophys **126**, 513-523,
<https://www.ncbi.nlm.nih.gov/pubmed/4970479>
79. McConnell, R. E., Higginbotham, J. N., Shifrin, D. A., Jr., Tabb, D. L., Coffey, R. J., andTyska, M. J. (2009) The enterocyte microvillus is a vesicle-generating organelle J Cell Biol **185**, 1285-1298 10.1083/jcb.200902147
80. Shifrin, D. A., Jr., McConnell, R. E., Nambiar, R., Higginbotham, J. N., Coffey, R. J., andTyska, M. J. (2012) Enterocyte microvillus-derived vesicles detoxify bacterial products and regulate epithelial-microbial interactions Curr Biol **22**, 627-631
10.1016/j.cub.2012.02.022
81. Esparza, G. A., Teghanemt, A., Zhang, D., Gioannini, T. L., andWeiss, J. P. (2012) Endotoxin{middle dot}albumin complexes transfer endotoxin monomers to MD-2 resulting in activation of TLR4 Innate Immun **18**, 478-491 10.1177/1753425911422723
82. Gioannini, T. L., Zhang, D., Teghanemt, A., andWeiss, J. P. (2002) An essential role for albumin in the interaction of endotoxin with lipopolysaccharide-binding protein and sCD14 and resultant cell activation J Biol Chem **277**, 47818-47825
10.1074/jbc.M206404200

83. Gorelik, A., Illes, K., and Nagar, B. (2018) Crystal structure of the mammalian lipopolysaccharide detoxifier Proceedings of the National Academy of Sciences of the United States of America **115**, E896-E905 10.1073/pnas.1719834115
84. Hall, C. L., and Munford, R. S. (1983) Enzymatic deacylation of the lipid A moiety of Salmonella typhimurium lipopolysaccharides by human neutrophils Proceedings of the National Academy of Sciences of the United States of America **80**, 6671-6675, <https://www.ncbi.nlm.nih.gov/pubmed/6356132>
85. Gioannini, T. L., Teghanemt, A., Zhang, D., Prohinar, P., Levis, E. N., Munford, R. S., and Weiss, J. P. (2007) Endotoxin-binding proteins modulate the susceptibility of bacterial endotoxin to deacylation by acyloxyacyl hydrolase J Biol Chem **282**, 7877-7884 10.1074/jbc.M605031200
86. Linder, C. H., Narisawa, S., Millan, J. L., and Magnusson, P. (2009) Glycosylation differences contribute to distinct catalytic properties among bone alkaline phosphatase isoforms Bone **45**, 987-993 10.1016/j.bone.2009.07.009
87. Moss, A. K., Hamarneh, S. R., Mohamed, M. M., Ramasamy, S., Yammine, H., Patel, P. *et al.* (2013) Intestinal alkaline phosphatase inhibits the proinflammatory nucleotide uridine diphosphate Am J Physiol Gastrointest Liver Physiol **304**, G597-604 10.1152/ajpgi.00455.2012
88. Malo, M. S., Alam, S. N., Mostafa, G., Zeller, S. J., Johnson, P. V., Mohammad, N. *et al.* (2010) Intestinal alkaline phosphatase preserves the normal homeostasis of gut microbiota Gut **59**, 1476-1484 10.1136/gut.2010.211706

89. Campbell, E. L., MacManus, C. F., Kominsky, D. J., Keely, S., Glover, L. E., Bowers, B. E. *et al.* (2010) Resolvin E1-induced intestinal alkaline phosphatase promotes resolution of inflammation through LPS detoxification Proceedings of the National Academy of Sciences of the United States of America **107**, 14298-14303 10.1073/pnas.0914730107
90. Lehrer, S., and Nowotny, A. (1972) Isolation and purification of endotoxin by hydrolytic enzymes Infect Immun **6**, 928-933, <https://www.ncbi.nlm.nih.gov/pubmed/4344633>
91. Rick, P. D., Fung, L. W., Ho, C., and Osborn, M. J. (1977) Lipid A mutants of Salmonella typhimurium. Purification and characterization of a lipid A precursor produced by a mutant in 3-deoxy-D-mannooctulosonate-8-phosphate synthetase J Biol Chem **252**, 4904-4912, <https://www.ncbi.nlm.nih.gov/pubmed/17608>
92. Rosner, M. R., Tang, J., Barzilay, I., and Khorana, H. G. (1979) Structure of the lipopolysaccharide from an Escherichia coli heptose-less mutant. I. Chemical degradations and identification of products J Biol Chem **254**, 5906-5917, <https://www.ncbi.nlm.nih.gov/pubmed/221486>
93. Hulett, F. M., Kim, E. E., Bookstein, C., Kapp, N. V., Edwards, C. W., and Wyckoff, H. W. (1991) Bacillus subtilis alkaline phosphatases III and IV. Cloning, sequencing, and comparisons of deduced amino acid sequence with Escherichia coli alkaline phosphatase three-dimensional structure J Biol Chem **266**, 1077-1084, <https://www.ncbi.nlm.nih.gov/pubmed/1898729>
94. Sunden, F., AlSadhan, I., Lyubimov, A. Y., Ressler, S., Wiersma-Koch, H., Borland, J. *et al.* (2016) Mechanistic and Evolutionary Insights from Comparative Enzymology of

- Phosphomonoesterases and Phosphodiesterases across the Alkaline Phosphatase Superfamily *J Am Chem Soc* **138**, 14273-14287 10.1021/jacs.6b06186
95. d'Hennezel, E., Abubucker, S., Murphy, L. O., and Cullen, T. W. (2017) Total Lipopolysaccharide from the Human Gut Microbiome Silences Toll-Like Receptor Signaling *mSystems* **2**, 10.1128/mSystems.00046-17
96. Vatanen, T., Kostic, A. D., d'Hennezel, E., Siljander, H., Franzosa, E. A., Yassour, M. *et al.* (2016) Variation in Microbiome LPS Immunogenicity Contributes to Autoimmunity in Humans *Cell* **165**, 842-853 10.1016/j.cell.2016.04.007
97. Gregg, K. A., Harberts, E., Gardner, F. M., Pelletier, M. R., Cayatte, C., Yu, L. *et al.* (2017) Rationally Designed TLR4 Ligands for Vaccine Adjuvant Discovery *MBio* **8**, 10.1128/mBio.00492-17
98. Needham, B. D., Carroll, S. M., Giles, D. K., Georgiou, G., Whiteley, M., and Trent, M. S. (2013) Modulating the innate immune response by combinatorial engineering of endotoxin *Proceedings of the National Academy of Sciences of the United States of America* **110**, 1464-1469 10.1073/pnas.1218080110
99. Zariri, A., and van der Ley, P. (2015) Biosynthetically engineered lipopolysaccharide as vaccine adjuvant *Expert Rev Vaccines* **14**, 861-876 10.1586/14760584.2015.1026808
100. Yang, Y., Wandler, A. M., Postlethwait, J. H., and Guillemin, K. (2012) Dynamic Evolution of the LPS-Detoxifying Enzyme Intestinal Alkaline Phosphatase in Zebrafish and Other Vertebrates *Front Immunol* **3**, 314 10.3389/fimmu.2012.00314

101. Datsenko, K. A., and Wanner, B. L. (2000) One-step inactivation of chromosomal genes in *Escherichia coli* K-12 using PCR products *Proceedings of the National Academy of Sciences of the United States of America* **97**, 6640-6645 [10.1073/pnas.120163297](https://doi.org/10.1073/pnas.120163297)
102. Cherepanov, P. P., and Wackernagel, W. (1995) Gene disruption in *Escherichia coli*: TcR and KmR cassettes with the option of Flp-catalyzed excision of the antibiotic-resistance determinant *Gene* **158**, 9-14, <https://www.ncbi.nlm.nih.gov/pubmed/7789817>
103. Silva-Rocha, R., Martinez-Garcia, E., Calles, B., Chavarria, M., Arce-Rodriguez, A., de Las Heras, A. *et al.* (2013) The Standard European Vector Architecture (SEVA): a coherent platform for the analysis and deployment of complex prokaryotic phenotypes *Nucleic Acids Res* **41**, D666-675 [10.1093/nar/gks1119](https://doi.org/10.1093/nar/gks1119)
104. Rietsch, A., Vallet-Gely, I., Dove, S. L., and Mekalanos, J. J. (2005) ExsE, a secreted regulator of type III secretion genes in *Pseudomonas aeruginosa* *Proceedings of the National Academy of Sciences of the United States of America* **102**, 8006-8011 [10.1073/pnas.0503005102](https://doi.org/10.1073/pnas.0503005102)
105. Bierman, M., Logan, R., O'Brien, K., Seno, E. T., Rao, R. N., and Schonher, B. E. (1992) Plasmid cloning vectors for the conjugal transfer of DNA from *Escherichia coli* to *Streptomyces* spp *Gene* **116**, 43-49, <https://www.ncbi.nlm.nih.gov/pubmed/1628843>
106. Galanos, C., Luderitz, O., and Westphal, O. (1969) A new method for the extraction of R lipopolysaccharides *Eur J Biochem* **9**, 245-249, <https://www.ncbi.nlm.nih.gov/pubmed/5804498>
107. Strain, S. M., Fesik, S. W., and Armitage, I. M. (1983) Characterization of lipopolysaccharide from a heptoseless mutant of *Escherichia coli* by carbon 13 nuclear

- magnetic resonance J Biol Chem **258**, 2906-2910,
<https://www.ncbi.nlm.nih.gov/pubmed/6338007>
108. Hirschfeld, M., Ma, Y., Weis, J. H., Vogel, S. N., and Weis, J. J. (2000) Cutting edge: repurification of lipopolysaccharide eliminates signaling through both human and murine toll-like receptor 2 J Immunol **165**, 618-622,
<https://www.ncbi.nlm.nih.gov/pubmed/10878331>
109. Henderson, J. C., O'Brien, J. P., Brodbelt, J. S., and Trent, M. S. (2013) Isolation and chemical characterization of lipid A from gram-negative bacteria J Vis Exp e50623
10.3791/50623
110. Kutschera, A., Dawid, C., Gisch, N., Schmid, C., Raasch, L., Gerster, T. *et al.* (2019) Bacterial medium-chain 3-hydroxy fatty acid metabolites trigger immunity in Arabidopsis plants Science **364**, 178-181 10.1126/science.aau1279
111. Ranf, S., Gisch, N., Schaffer, M., Illig, T., Westphal, L., Knirel, Y. A. *et al.* (2015) A lectin S-domain receptor kinase mediates lipopolysaccharide sensing in Arabidopsis thaliana Nat Immunol **16**, 426-433 10.1038/ni.3124
112. Morris, G. M., Huey, R., Lindstrom, W., Sanner, M. F., Belew, R. K., Goodsell, D. S., and Olson, A. J. (2009) AutoDock4 and AutoDockTools4: Automated docking with selective receptor flexibility J Comput Chem **30**, 2785-2791 10.1002/jcc.21256
113. Guex, N., and Peitsch, M. C. (1997) SWISS-MODEL and the Swiss-PdbViewer: an environment for comparative protein modeling Electrophoresis **18**, 2714-2723
10.1002/elps.1150181505

114. Pedretti, A., Villa, L., and Vistoli, G. (2004) VEGA--an open platform to develop chemo-bio-informatics applications, using plug-in architecture and script programming J Comput Aided Mol Des **18**, 167-173, <https://www.ncbi.nlm.nih.gov/pubmed/15368917>
115. Morris, G. M., Goodsell, D. S., Halliday, R. S., Huey, R., Hart, W. E., Belew, R. K., and Olson, A. J. (1998) Automated docking using a Lamarckian genetic algorithm and an empirical binding free energy function Journal of Computational Chemistry **19**, 1639-1662 Doi 10.1002/(Sici)1096-987x(19981115)19:14<1639::Aid-Jcc10>3.0.Co;2-B
116. Thompson, M. A. (2004) Molecular docking using ArgusLab, an efficient shape-based search algorithm and the AScore scoring function In ACS meeting, Philadelphia, PA
117. Park, B. S., Song, D. H., Kim, H. M., Choi, B. S., Lee, H., and Lee, J. O. (2009) The structural basis of lipopolysaccharide recognition by the TLR4-MD-2 complex Nature **458**, 1191-1195 10.1038/nature07830
118. Ohto, U., Fukase, K., Miyake, K., and Satow, Y. (2007) Crystal structures of human MD-2 and its complex with antiendotoxic lipid IVa Science **316**, 1632-1634 10.1126/science.1139111
119. Berman, H. M., Westbrook, J., Feng, Z., Gilliland, G., Bhat, T. N., Weissig, H. *et al.* (2000) The Protein Data Bank Nucleic Acids Res **28**, 235-242 10.1093/nar/28.1.235
120. Scior, T., and Wahab, H. A. (2007) Structure prediction of proteins with very low homology: A comprehensive introduction and a case study on aminopeptidase In Drug Design Research Perspectives, Kaplan S, ed. Nova Science Publishers, 675-708

121. Gasteiger, J., and Marsili, M. (1981) Prediction of Proton Magnetic-Resonance Shifts - the Dependence on Hydrogen Charges Obtained by Iterative Partial Equalization of Orbital Electronegativity *Org Magn Resonance* **15**, 353-360 DOI 10.1002/mrc.1270150408

Chapter 3

Insertion Sequence Mediated Tandem Chromosomal Amplification of the *arn* Operon Facilitates Polymyxin B Resistance in *E. coli* B Strains

This chapter is adapted from the following manuscript: Michael Maybin, Aditi Ranade, Ursula Schombel, Nicholas Gisch, Uwe Mamat, and Timothy C. Meredith “IS1-mediated Chromosomal Amplification of the *arn* Operon Leads to Polymyxin B Resistance in *Escherichia coli* B Strains” (2023) mBio. Manuscript in review.

Note: Experiments were done in collaboration with Aditi Ranade who will share first authorship in the final manuscript. Mass spec analysis was performed by Nicholas Gisch and Uwe Mamat.

ABSTRACT

Globally, antimicrobial resistance (AMR) is of increasing concern, contributing to over one million bacterial infection deaths in 2019 alone. As clinical application of drugs of last resort rises, we must consider more heavily the role bacterial heteroresistance (HR) plays in defeating treatment plans. HR is defined as the existence of a phenotypically resistant sub population of bacteria, in an otherwise sensitive population, displaying a minimum inhibitory concentration (MIC) at or above 8x the normal. Polymyxin B (PMB) is one such antibiotic of last resort that has recently been re-introduced into clinical use and bacterial isolates have been shown to display HR compounding treatment considerations. PMB is effective against gram-negative bacteria whereby it interacts with lipopolysaccharide (LPS) leading to membrane disruption and ultimately cell death. Bacterial resistance to PMB is largely facilitated by masking LPS negative charge via modifications with positively charged moieties 4-amino-4-deoxy-L-arabinose (Ara4N) and phosphoethanolamine (PEtN). Herein we describe a mechanism of PMB HR in *E. coli* B strains. Frequency of resistance (FOR) experiments done at ~8x MIC demonstrated that loss of Ara4N, but not PEtN, modification led to significant decreases in FOR suggesting a role in HR. In isolated PMB resistant mutants, we determined increased levels of Ara4N modification contributed to resistance. Strikingly among these mutants amplified regions of the chromosome were observed each containing the *arn* operon (responsible for Ara4N modification). We demonstrate that these amplifications and phenotypic resistance are driven by insertion sequence (IS) elements flanking the amplicons. Lastly, we investigate the effect the amplicons have on the transcriptome, where expression levels are shown to be affected across the genome.

INTRODUCTION

Antimicrobial resistance (AMR) is of increasing global concern as a significant contributor to deaths involving bacterial infections. In 2019 alone approximately 25% of 5 million bacterial infection deaths were directly associated with AMR (1). Ongoing efforts to develop new antibiotics and increase the efficiency of our current antibiotics are important as the role of AMR is only estimated to increase in the coming decades (2). To help address this issue, the polymyxin family of lipopeptide antibiotics has recently been reintroduced into clinical use as a drug of last resort (3–6).

The polymyxin family of antibiotics were first discovered in the 1940's from natural product extracts from *Paenibacillus polymyxa* (7). Polymyxin B (PMB) and polymyxin E (colistin) are two highly active congeners initially developed for antibiotic use but challenges with pharmacodynamics and nephrotoxicity limited use to animal agriculture (8, 9). The increase in AMR infections has seen polymyxins return as an antibiotic drug class of last resort, particularly for *Enterobacteriaceae*, multi-drug resistant (MDR) *Pseudomonas aeruginosa*, and MDR *Acinetobacter baumannii* strains (10). Polymyxins are active on Gram-negative bacteria where they bind the outer membrane by interacting with lipopolysaccharide (LPS) leading to increased permeability, drug uptake, and cell death (11–13). PMB has an acylated tripeptide stem connected to a cyclic heptapeptide with several cationic charges. The positive charges of PMB displaces cations, such as Mg^{2+} and Ca^{2+} , and forms ion bridges with the negatively charged lipopolysaccharide phosphates leading to outer-membrane disruption.

LPS is an abundant molecule found in the outer leaflet of the outer membrane in gram-negative bacteria where it plays significant roles in controlling membrane permeability (14), antibiotic resistance (15), and modulating innate immune recognition (see (16) and chapter 2). LPS consists of three major sections consisting of the O-antigen, core sugars, and lipid A which is embedded into the outer membrane. The major mechanism for PMB resistance involves bacteria reducing PMB binding by masking LPS phosphates with positively charged residues such as 4-amino-4-deoxy-L-arabinose (Ara4N) and phosphoethanolamine (PEtN) (17, 18). Mutations in the two-component transcriptional regulatory systems [PmrAB (19, 20) and PhopQ (21)] impart PMB resistance through upregulation of *ara/ept* gene expression affecting Ara4N modification and PEtN modification respectively.

Heteroresistance (HR) is an additional factor to consider when utilizing polymyxins. HR refers to a resistant subpopulation, within a larger susceptible population, demonstrating phenotypic resistance at 8 times the typical minimum inhibitory concentration (MIC) (22). A report has demonstrated a high prevalence of antibiotic HR in 41 isolates from four opportunistic gram-negative pathogens (including *E. coli*) against 28 different antibiotics. HR subpopulations were found in a quarter of all strain-antibiotic combinations (though not for polymyxins), where the majority of these were linked to amplification of a drug resistance gene (23, 24). Many of these amplified segments were bounded by homologous DNA segments including insertion sequences (IS). There have been several reports over the decades of gene amplification leading to HR (25–31), however more recent studies suggest HR via gene amplification accounts for up to 10% of all treatment failures (32).

Herein we present evidence for a mechanism of PMB HR in *E. coli* B strains. We demonstrate HR in *E. coli* BL21(DE3) by population analysis profiling (PAP) and frequency of resistance (FOR). FOR is demonstrated to be 10-100 fold higher in *E. coli* B strains than K-12 strains. In the *E. coli* BL21(DE3) background we observe a significant drop in FOR at ~8x MIC in a Δ *arnA* strain compared to wildtype and no significant difference when comparing Δ *eptA* to wildtype, suggested the *arn* operon is involved in a significant mechanism of resistance. We selected for the PMB resistant sub-population and, among the collected isolates, demonstrate an increase in levels of Ara4N modification when compared to wildtype. Next generation sequencing revealed PMB resistance was not due to typical resistance mutations in regulators but rather from unstable, spontaneous amplifications of IS1 flanked regions of the genome containing the *arn* operon. Deletion of an IS1 element common among these amplifications attenuated FOR to levels similar to that observed for K-12. Interestingly this was only observed in Δ *eptA* backgrounds suggesting genomic amplification predominates as a mechanism of resistance when Ara4N is the primary lipid A modification. RNA-seq analysis demonstrated global transcriptomic changes because of chromosomal amplification, even in areas outside of the amplified region. This mechanism of resistance was also observed in the more wildtype *E. coli* B strain ATCC11303 that shares IS1 placement throughout the genome, suggesting a conserved mechanism of resistance shared throughout the lineage.

RESULTS

***E. coli* B demonstrates PMB heteroresistance that depends on the *arn* operon**

To address the HR character of *E. coli* BL21 (DE3) the phenotype was tested with a population analysis profile (PAP) (Fig. 3-1A) and frequency of resistance (FOR) calculations (Fig. 3-1B). The PAP displays the maintenance of a substantial pre-existing subpopulation of resistant cells even in PMB concentrations greater than the USCAST recommended breakpoint of 2 µg/mL for *Enterobacteriaceae* (Fig. 3-1A) (33). The presence of a resistant subpopulation also aligns with our observations of inconsistent MIC values and well skipping in the *E. coli* B background, where MIC averaged 1.4 ug/mL but ranged from 0.06 to 4 ug/mL. In contrast, for the K-12 strain *E. coli* BW25113, the MIC value was consistently 0.06 ug/mL and no well skipping was observed. It is known that B strains display higher levels of LPS modification than K-12 strains, so we probed the role Ara4N (via the *arn* operon) and PEtN (via *eptA*) modifications play. As expected, deletion of either *eptA* or *arnA* in the B strain resulted in MICs in line with the K-12 strain (Fig. 3-1B and Table 3-1). However, PMB FOR displayed a 10-fold decrease in resistance when *arnA* was deleted but not when *eptA* was deleted (Fig. 3-1B) suggesting the *arn* operon plays some role in HR. To further probe the role of the *arn* operon in PMB HR we constructed an *E. coli* B mutant lacking *eptA*, *lpxT*, and *pagP*. LpxT adds a phosphate to the 1-position of lipid A that increases negative charge while preventing further modification (34, 35), whereas PagP appends an acyl chain to form heptacylated lipid A (36). Either modification can alter susceptibility to cationic peptides by competing for lipid A substrate of ArnT (as with *lpxT*) and altering outer membrane permeability (as with *pagP*). In this strain background, referred to herein as the Parent strain, we observed

similar MIC (Fig. 3-1B and Table 3-1) and FOR (Fig. 3-1B) to the $\Delta eptA$ strain suggesting minimal contribution of LpxT and PagP to PMB resistance, and, as expected, a significant decrease in FOR is observed when *arnA* is additionally deleted.

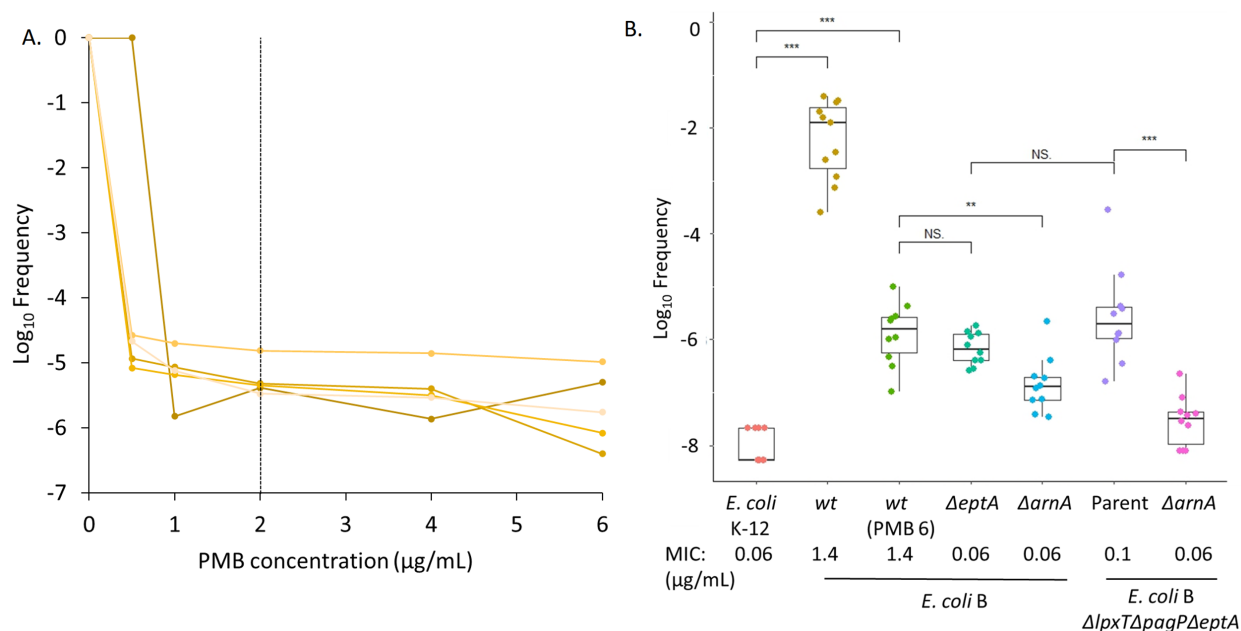


Figure 3-1: Heteroresistance leads to inconsistency between MIC and frequency of resistance. **A)** Early exponential phase cells of *E. coli* BL21 (DE3) were harvested, diluted, and plated on LBA with 0, 0.5, 1, 2, 4, and 6 µg/mL polymyxin B (PMB). Log₁₀ frequency of resistance was plotted against PMB concentration to generate the population analysis profile. Dotted line represents the USCAST breakpoint value of PMB **B)** Frequency of resistance was determined for 10 separate cultures per strain by plating dilutions of exponential growths (OD_{600nm} 0.2 to 0.7) on LBA containing 1 µg/mL PMB (6 µg/mL PMB for *wt* PMB6), then measuring the ratio of resistant CFU to total plated cells. Strain MIC values are based on the mean of three biological replicates. Significance values based on Student's t-test (**p < 0.01, ***p < 0.001, NS not significant).

Table 3-1: Polymyxin B (PMB) minimum inhibitory concentration (MIC) values

Strain	Genotype	MIC (mg/mL)*			
		REP1	REP 2	REP 3	Mean
TXM338	Wildtype BW25113; K-12 lineage	0.06	0.06	0.06	0.06
TXM319	Wildtype BL21 (DE3); B lineage	4	0.13	0.06	1.40
TXM322	BL21 (DE3) <i>arnA::kanR</i>	0.06	0.06	0.06	0.06
GKM329	BL21 (DE3) <i>eptA::catR</i>	0.06	0.06	0.06	0.06
AR1973	BL21 (DE3) <i>eptA::catR lpxT::kanR pagP::hygR</i>	0.13	0.13	0.06	0.10

(Parent)					
MM2028	BL21 (DE3) <i>eptA::catR lpxT::FRT pagP::hygR</i> <i>arnA::kanR</i>	0.06	0.06	0.06	0.06
C1	BL21 (DE3) <i>eptA::catR lpxT::kanR pagP::hygR</i>	2	2	2	2
C2	BL21 (DE3) <i>eptA::catR lpxT::kanR pagP::hygR</i>	2	2	2	2
AR2206	BL21 (DE3) <i>IS1-18::aprR</i>	2	4	4	3.33
AR2207	BL21 (DE3) <i>arnA::kanR IS1-18::aprR</i>	0.06	0.06	0.06	0.06
AR2208	BL21 (DE3) <i>eptA::catR IS1-18::aprR</i>	0.13	0.06	0.13	0.10
MM2165	BL21 (DE3) <i>eptA::catR lpxT::kanR pagP::hygR IS1-18::aprR</i>	0.13	0.06	0.06	0.08
TXM2253	BL21 (DE3) <i>eptA::catR lpxT::kanR pagP::hygR IS1-18::aprR + IS1-18 specR</i>	0.13	0.13	0.06	0.10
TXM2197	Wildtype <i>E. coli</i> (Miguela) Castellani and Chalmers ATCC11303	4	4	4	4
TXM2222	ATCC11303 <i>eptA::catR</i>	0.03	0.06	0.03	0.04
TXM2223	ATCC11303 <i>arnA::kanR</i>	0.03	0.03	0.06	0.04
MM2176	ATCC11303 <i>IS1-18::aprR</i>	4	4	4	4
TXM2233	ATCC11303 <i>eptA::catR IS1-18::aprR</i>	0.06	0.06	0.03	0.05
TXM2234	ATCC11303 <i>arnA::kanR IS1-18::aprR</i>	0.06	0.03	0.03	0.04

*Rep- biological replicate

PMB resistant *E. coli* B isolates display increased lipid A Ara4N modification

PMB resistant sub-population was isolated from the Parent strain by growth under challenge from multiple concentrations of PMB (0.03 to 0.5 $\mu\text{g}/\text{mL}$). Altogether 26 single colonies were challenged in this manner and all 26 displayed growth at the highest PMB concentration, subsequent mutant purification and MIC checks revealed resistances of 2-4 $\mu\text{g}/\text{mL}$ again at or above the USCAST breakpoint. Among the set of 26 mutants two (C1 and C2) were focused on for further characterization. We hypothesized that the PMB resistance phenotype was due to an increase in the levels of Ara4N modification. To evaluate modification levels LPS was purified from the Parent, C1, and C2 isolates grown to stationary phase in LB without PMB selective pressure. SDS-PAGE separation of extracted LPS did not reveal any changes in either the total yield or in the general banding profiles (Fig. 3-2). However, electron spray ionization mass

spectrometry (ESI-MS) of the purified LPS demonstrates a near equal amount of non-modified LPS (3420 m/z) and LPS modified with one Ara4N (3551 m/z) in the parent, while the C1 and C2 mutants display a population shift towards Ara4N (Fig. 3-3A). To confirm Ara4N was being added to the lipid A backbone, we examined exponentially growing cells by labeling LPS with ^{32}P , hydrolyzing, and freed lipid A was analyzed by thin layer chromatography (TLC) (Fig. 3-3B). The C1 and C2 mutants demonstrate clear shifts towards Ara4N-lipid A when compared to the Parent (Fig. 3-3B). This shift is also observable for the majority of the additional 24 PMB resistant mutants (Fig. 3-4).

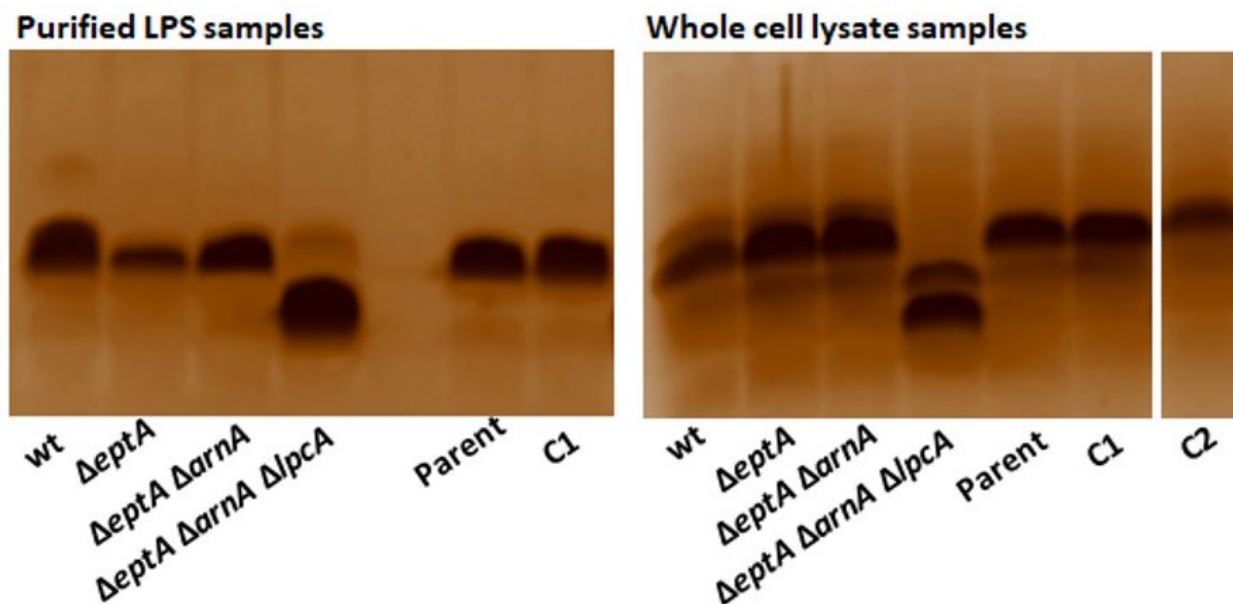


Figure 3-2: SDS-PAGE analysis of LPS extracted from PMB resistant isolates. Silver stain of purified LPS or whole cell lysates, indicated above image. *E. coli* BL21(DE3) strains are used as controls where *wt*, *ΔeptA*, and *ΔeptA ΔarnA* contain the full core but variable lipid A modification and *ΔeptA ΔarnA ΔlpcA* is a truncated (Re-LPS) chemotype without modification. *C2 whole cell lysate sample was run on the same gel as other whole cell lysate samples; intervening lanes were cropped out.

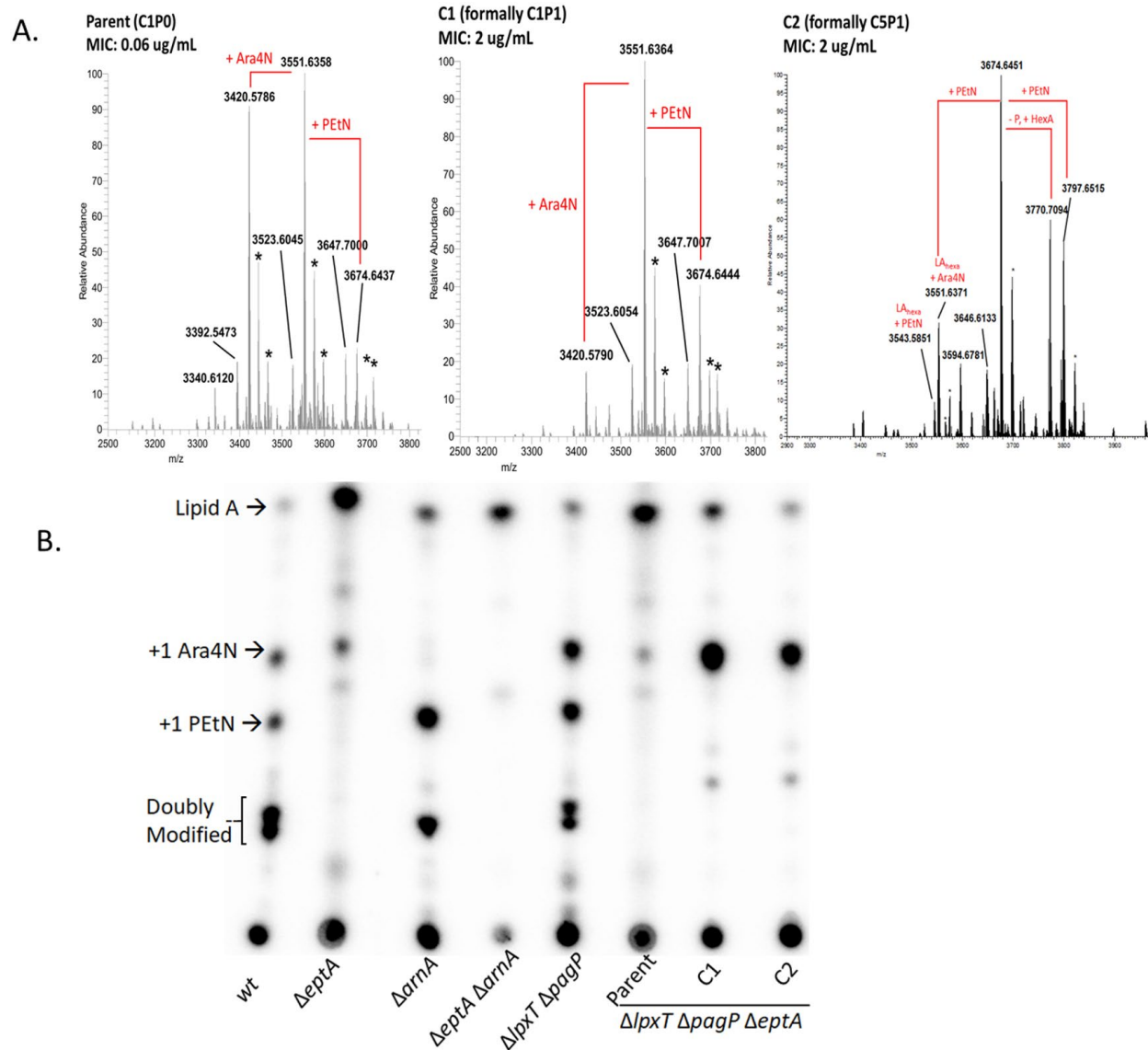


Figure 3-3: Polymyxin B resistant isolates display increased levels of Ara4N modification on lipid A. **A)** ESI-MS of LPS purified from the Parent strain, C1, and C2 isolates. Peaks with 3420 m/z represent unmodified LPS while peaks corresponding to additions to are marked in red. Asterisks indicate sodium adducts. **B)** TLC analysis of 32 P-labeled lipid A isolated from *E. coli* BL21 (DE3) *wt*, Δ eptA, Δ arnA, Δ eptA Δ arnA, Δ lpxT Δ pagP, Parent, and C1/C2 PMB resistant isolates. Signal corresponding to lipid A alone or with modification is indicated. PMB resistant isolates C1 and C2 display a marked shift to lipid A modified with Ara4N when compared to the Parent strain.

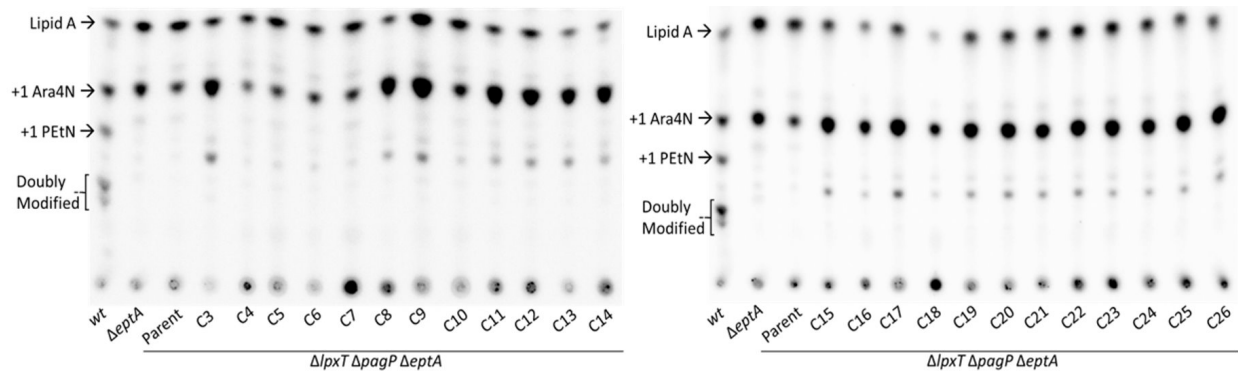


Figure 3-4: 24 additional PMB resistant isolates from the Parent background display chromosomal amplification mediated increases in Ara4N modification. **A)** TLC analysis of ^{32}P -labeled lipid A isolated from *E. coli* BL21 (DE3) *wt*, ΔeptA , Parent, and C3-C26 PMB resistant isolates. Signal corresponding to lipid A alone or with modification are indicated. The majority of samples display a shift towards Ara4N modified lipid A.

Insertion sequence (IS) flanked chromosomal amplifications containing the *arn* operon found in PMB resistant isolates

Point mutations in the two component systems governing the addition of PEtN and Ara4N, namely PmrAB and PhPQ have previously been described to confer increased resistance to PMB via increased modification (37–39). We wondered whether the resistant isolates contained similar point mutations in the *arn* specific regulatory mechanisms resulting in upregulation of Ara4N lipid A modification. We therefore used short read Illumina next generation sequencing to identify mutations in C1 and C2 (Fig. 3-5A). In both PMB resistant isolates, regions of higher relative read coverage encompassing the *arn* operon were observed, where coverage increased nearly 2- and 3-fold in C1 and C2, respectively, in comparison to the parent strain. Interestingly, amplified regions were flanked on both sides by *IS1* elements (Fig. 3-5A), a 768-bp mobile genetic element that is present in multiple copies (40). *E. coli* BL21(DE3) contains 29 copies of *IS1* (number *IS1*-1 to *IS1*-29) distributed throughout the genome (40). *IS1*-17 and *IS1*-18 flanked the C1 amplified region (~145 kb long), whereas *IS1*-16 and *IS1*-18 flanked

the C2 amplified region (~264 kb long). The three IS1 element alleles involved are nearly identical, save for a single unique bp in each. DNA amplification events bounded by repetitive stretches of DNA are thought to arise from unequal DNA exchange between sister chromosomes that results in head-to-tail duplication with an intervening third copy of the repeated element (Fig. 3-5B) (41–43). Multiplex PCR using 5 primers (two reverse primers annealing downstream of IS1-16 or IS1-17 and a forward primer annealing upstream of IS1-18 along with a primer pair to amplify the *pykA* control locus residing outside of plateau region) was thus used to confirm novel junction points (Fig. 3-5B). PCR products consistent in size with amplification events bounded by IS1-17/IS1-18 for C1 and IS1-16/IS1-18 for C2 were only observed in the C1 and C2 PMB resistant mutants, and not the parent strain (Fig. 3-5C). Sanger sequencing of the novel, hybrid IS1 junction PCR products confirmed duplication as diagrammed in Fig. 3-5B, with crossovers retaining the IS1-17 allele in C1 and the IS1-18 allele in C2. Likewise, 19 out of 24 of the other PMB resistant isolates yielded PCR products with analogous amplification boundaries to C1 or C2 (Fig. 3-5C). The remaining 5 isolates that failed to produce junction PCR products were therefore whole genome sequenced. While once again all had increased read coverage encompassing the *arn* operon, only a single boundary involved one of the above IS1 elements (Fig. 3-5D). These isolates either represent minor amplification pathways, or more likely underwent further rearrangement through recombination events which is often observed with long segments of tandemly amplified DNA (42–44). In either case, all isolates acquired PMB resistance through *arn* operon amplification mediated by flanking IS1 elements.

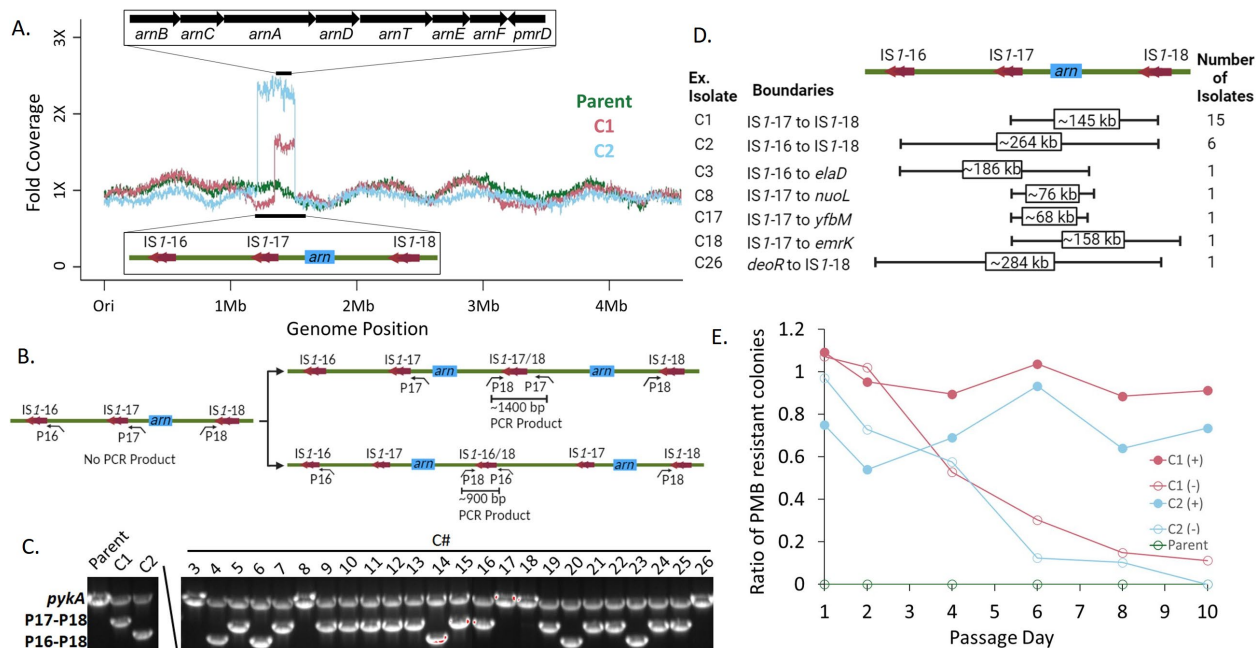


Figure 3-5: Insertion sequence flanked chromosomal amplifications found in the PMB resistant mutants. **A)** Illumina NGS read fold coverage over the genome obtained by normalizing coverage to the mean read count across the entire chromosome excluding the amplified region for C1 (pink) and C2 (light blue). Parent fold coverage (dark green) obtained by normalizing coverage to the mean read count across the entire chromosome. Amplified region of chromosomal DNA is highlighted with the flanking IS elements indicated (bottom inset). The *arn* operon and its location in the genome is indicated (top inset). **B)** Diagram of the junctions formed via tandem amplifications involving IS1-17/ IS1-18 (top) and IS1-16/ IS1-18 (bottom). Relative locations of the IS1 elements, *arn* operon, and primers used for multiplex junction PCR are indicated. **C)** Multiplex Junction PCR check for the Parent strain and the PMB resistant mutants C1-C26. Break indicates rearrangement of the gel to place Parent and C1-C2 samples first. Primers for *pykA* were used as a control for successful reactions and the product sizes of the IS1-16/IS1-18 and IS1-17/IS1-18 junctions are indicated. **D)** Diagram of the amplified regions among the 26 isolates. Boundaries of the C1 and C2 mutants are displayed as well as the boundaries of the 5 amplified regions bounded by only one IS element. **E)** IS-flanked amplifications in mutants are unstable and result in a transient polymyxin resistance phenotype. Ratio of Polymyxin B resistant colonies (PMB plate colony count: LBA plate colony count) in parent (green open circles) and mutant (pink circles, C1 and blue circles, C2) strains over 10 days of passaging in the presence (solid circles) or absence (open circles) of 1 μ g/mL polymyxin B sulfate (data representative of three independent experiments).

To determine the stability of the amplifications, we performed outcrossing experiments where the parent, C1, and C2 isolates were passaged in the presence or absence of PMB over 10 days.

Aliquots were plated daily on LB agar plates with and without PMB. In the absence of PMB, the

population of PMB susceptible cells increased, whereas mutants passaged in the presence of PMB largely retained the resistant phenotype (Fig. 3-5E). PMB resistance was also unstable to varying extents among the broader panel of 24 isolates (Fig. 3-6). The slow depletion of the PMB resistant subpopulation is consistent with a modest fitness cost for amplifying 145-kb (C1) and 264-kb (C2) genome segments flanking the *arn* operon. Indeed, growth rate defects were minimal in LB media in comparison to the parent strain (Fig. 3-7).

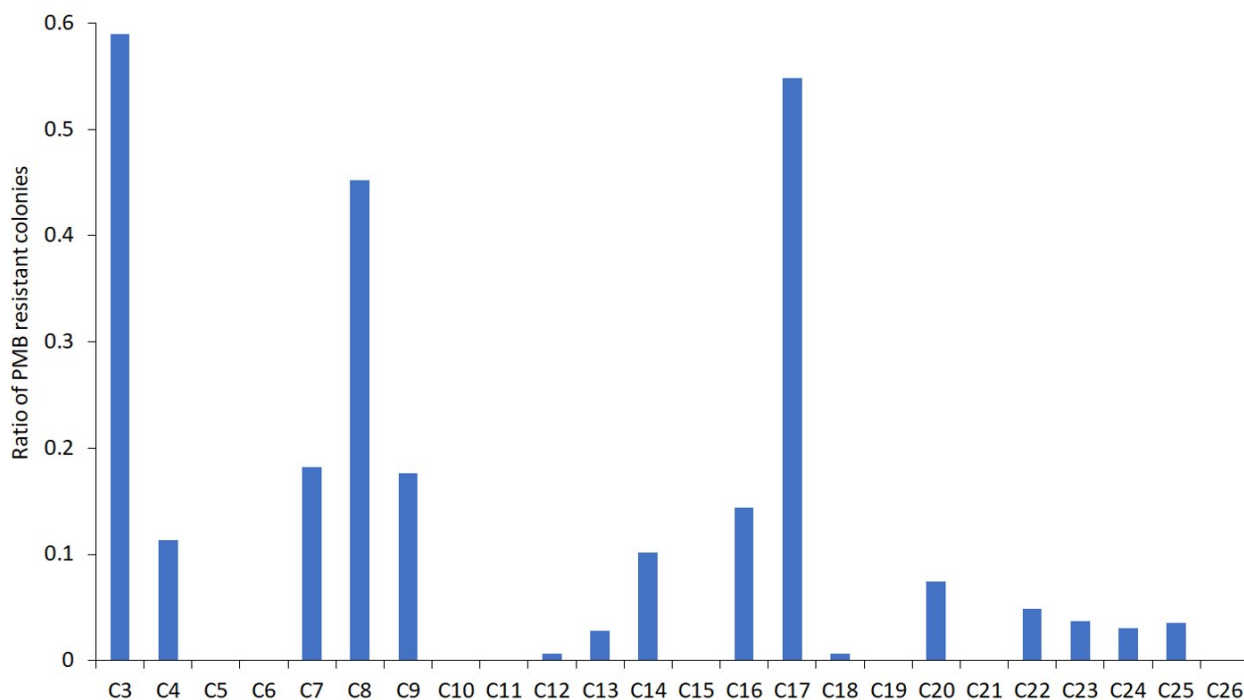


Figure 3-6: Majority of the 24 PMB resistant isolates revert to PMB sensitive phenotype in the absence of PMB. Ratio of PMB resistant colonies in the PMB resistant isolates C3-C26 on day 10 after passaging cells in the absence of PMB challenge. The majority of isolates have lost PMB resistance.

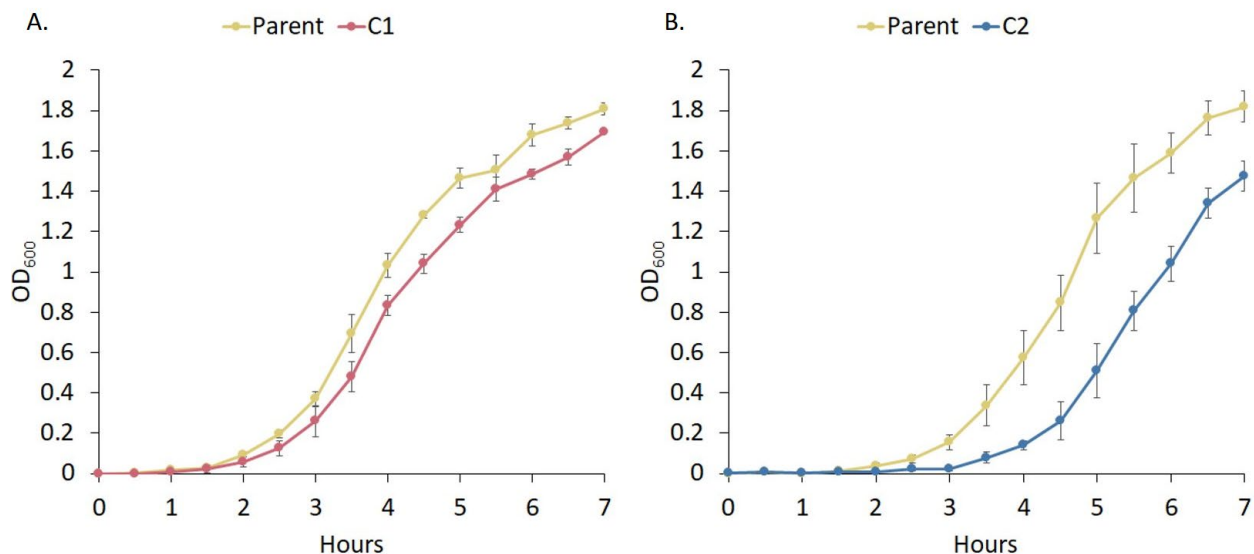


Figure 3-7: C1 and C2 *IS1-18* dependent chromosomal amplifications impart minimal fitness cost. Growth curves of the Parent strain versus C1 (panel **A**) and C2 (panel **B**) are plotted where each fit represents the average of three biological replicates with error bars indicating standard deviation. The C1 ~145 kb amplification imparts a lower fitness cost than the C2 ~264 kb amplification which displays a longer lag phase.

***IS1-18* is necessary for amplification and associated resistance**

To investigate the role of *IS1* elements on HR we constructed several $\Delta IS1-18$ strains in the *E. coli* B background ($\Delta IS1-18$, $\Delta eptA \Delta IS1-18$, $\Delta arnA \Delta IS1-18$, $\Delta lpxT \Delta pagP \Delta eptA \Delta IS1-18$) and calculated FOR as previously described. In the Parent background deletion of *IS1-18* alone decreased overall FOR by ~70-fold (Fig. 3-8A and 3-8B), FOR could be restored by reintroduction of *IS1-18* back into the same chromosomal position. Overall deletion of *IS1-18* resulted in significant decreases in FOR whenever coupled with an *eptA* deletion (Figs. 3-8A and 3-9).

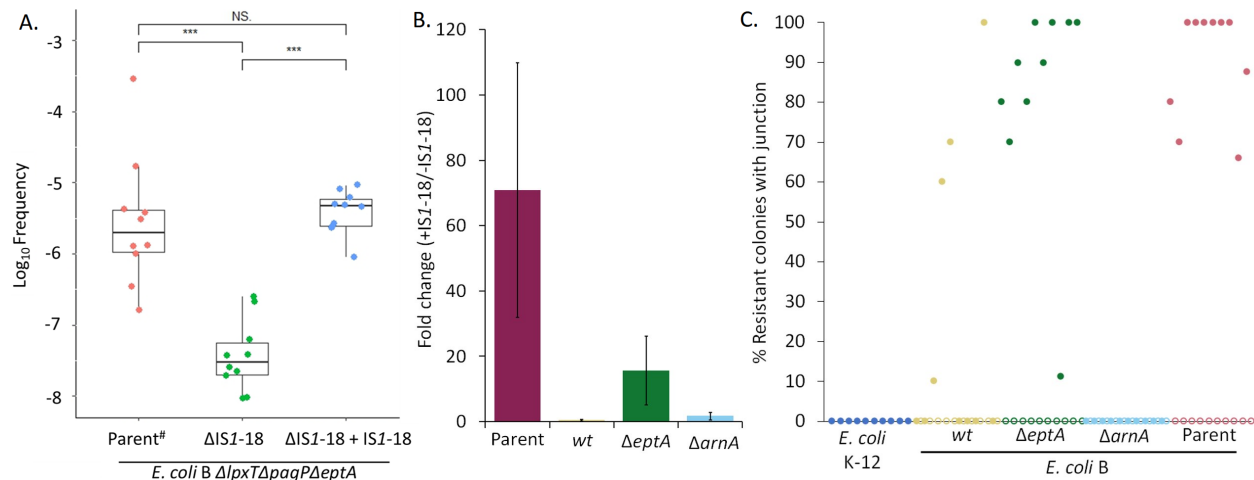


Figure 3-8: IS1-18 mediated chromosomal amplifications containing the *arn* operon lead to increased frequency of resistance. **A)** Frequency of resistance was determined for parent strain (# indicates re-plotting of previously shown data for comparison with relevant strains), parent strain lacking IS1-18, and with IS1-18 reinserted. FOR of 10 separate cultures per strain was obtained by plating dilutions of exponential growths (OD_{600nm} 0.2 to 0.7) on LBA containing 1 μg/mL PMB, then measuring the ratio of resistant CFUs to total plated cells. Significant values based on Student's t-test (***p < 0.001, NS not significant). **B)** Fold change in median FOR when deleting IS1-18 was quantified for the Parent, *E. coli* BL21 (DE3) wt, ΔeptA, and ΔarnA strains. Error bars derived from propagating median absolute deviation of values in the interquartile range. **C)** The percentage of resistant colonies containing the amplification junction was plotted for multiple strains with IS1-18 (filled circles) and with IS1-18 deleted (open circles). Up to 100 resistant colonies per strain derived from the FOR experiments were checked via multiplex PCR for the presence of the IS1-16/ IS1-18 or IS1-17/ IS1-18 amplification junctions.

Quantifying the fold change in FOR in isogenic strains with and without IS1-18 revealed no change in FOR for the wildtype and ΔarnA backgrounds but an ~15-fold higher FOR in the ΔeptA background (Fig 3-8B). The data thus far would suggest that IS1-18 plays a significant role in facilitating PMB resistance in strains that maintain a functional *arn* operon and lack the ability to modify lipid A with PEtN. To tie this phenotypic resistance with chromosomal amplification we utilized the above-mentioned multiplex junction PCR to screen resistant colonies, derived from the FOR experiments, for the presence of a tandem amplification (Fig 3-8C). In all strains lacking IS1-18 or a functioning *arn* operon (ΔarnA) the presence of amplification could not be confirmed

in any tested resistant colonies. In the wildtype background, resistance could be attributed to chromosomal amplification in roughly 30% of cases, suggesting that amplification still occurs but is one of multiple mechanisms of resistance. Hence the minimal effect on overall FOR for *eptA*⁺ strains. However, in the case of the Parent background, where resistance is almost entirely dependent on the levels of Ara4N modification, chromosomal amplification was found in approximately 90% of resistant isolates suggesting that in this background amplification is the predominant mechanism of resistance.

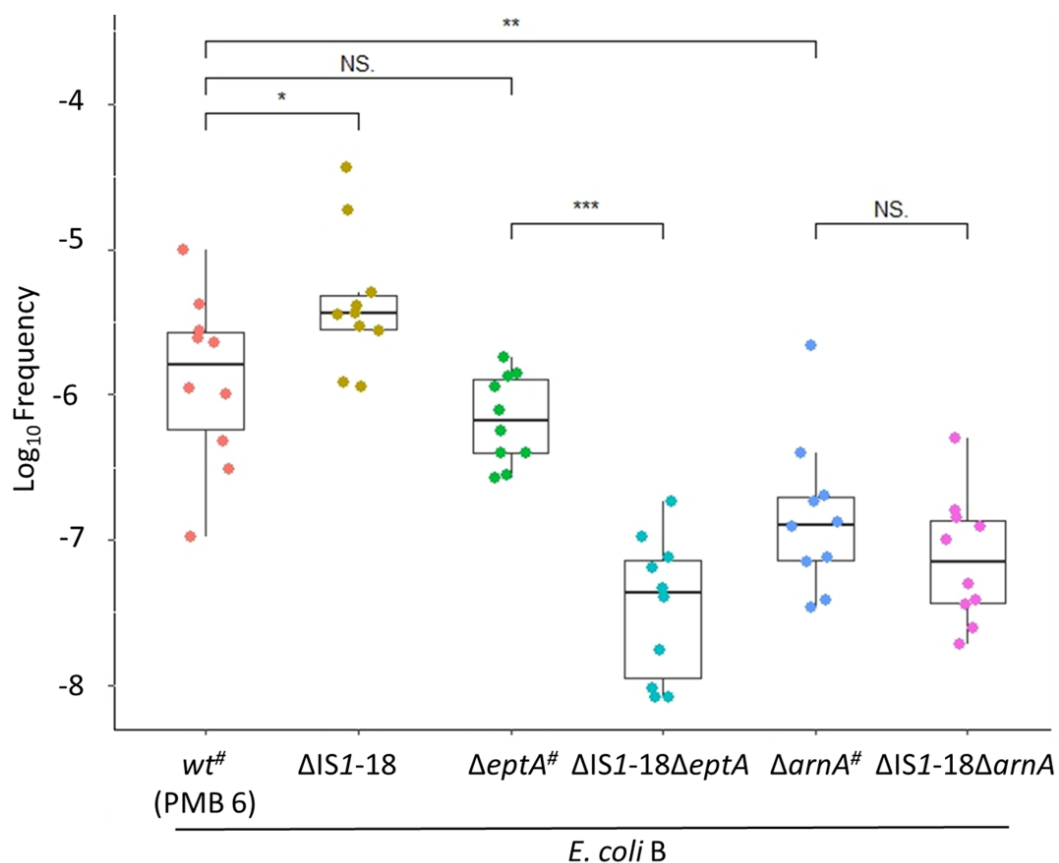


Figure 3-9: Deletion of IS1-18 primarily alters frequency of resistance in strains lacking *eptA* but containing the *arn* operon. IS1-18 was deleted in *E. coli* BL21 (DE3) *wt*, Δ *eptA*, and Δ *arnA* backgrounds and \log_{10} frequency of resistance plotted. # represents re-plotting of previously shown FOR data for comparison with relevant strains. Frequency of resistance was determined from 10 separate cultures per strain by plating dilutions of exponential growths (OD_{600nm} 0.2 to

0.7) on LBA containing 1 $\mu\text{g}/\text{mL}$ PMB (6 $\mu\text{g}/\text{mL}$ PMB for *wt* PMB 6), then measuring the ratio of resistant CFU to total plated cells. Significance values based on Student's t-test (* $p < 0.05$, ** $p < 0.01$, *** $p < 0.001$, NS not significant).

IS1 mediated PMB resistance is conserved in *E. coli* B lineages

Thus far we have evaluated the role of the *arn* operon and IS1 in driving PMB resistance in a lab strain of *E. coli* BL21(DE3). We predicted that if we would see this effect of IS1 mediated PMB resistance in other wildtype *E. coli* B lineages provided similar positioning of the IS1 elements. While IS1 elements flank the *arn* operon in *E. coli* BL21(DE3) these elements are absent in *E. coli* K-12. A search of the NCBI database revealed *E. coli* ATCC11303, another B lineage strain, shares a similar distribution of IS1 elements with BL21(DE3) (Fig. 3-10A) and most importantly contains IS1-16, IS1-17, and IS1-18 (40). PMB FOR was determined in isogenic strains of ATCC 11303 *E. coli* B strains (Fig. 3-10B). Indeed, there was a larger decrease in FOR in the ΔarnA mutant as compared to the ΔeptA mutant, supporting that ArnA is involved in HR. As observed in *E. coli* BL21(DE3) (Figs. 3-8 and 3-9), the removal of IS1-18 in the ΔeptA mutant background resulted in a ~15-fold FOR decrease but a change was not observed in the wildtype and ΔarnA backgrounds (Fig. 3-10B and 3-10C). These results point to the significance of the positioning of insertion sequence elements in the chromosome and their involvement in the chromosomal amplification driven HR phenotype.

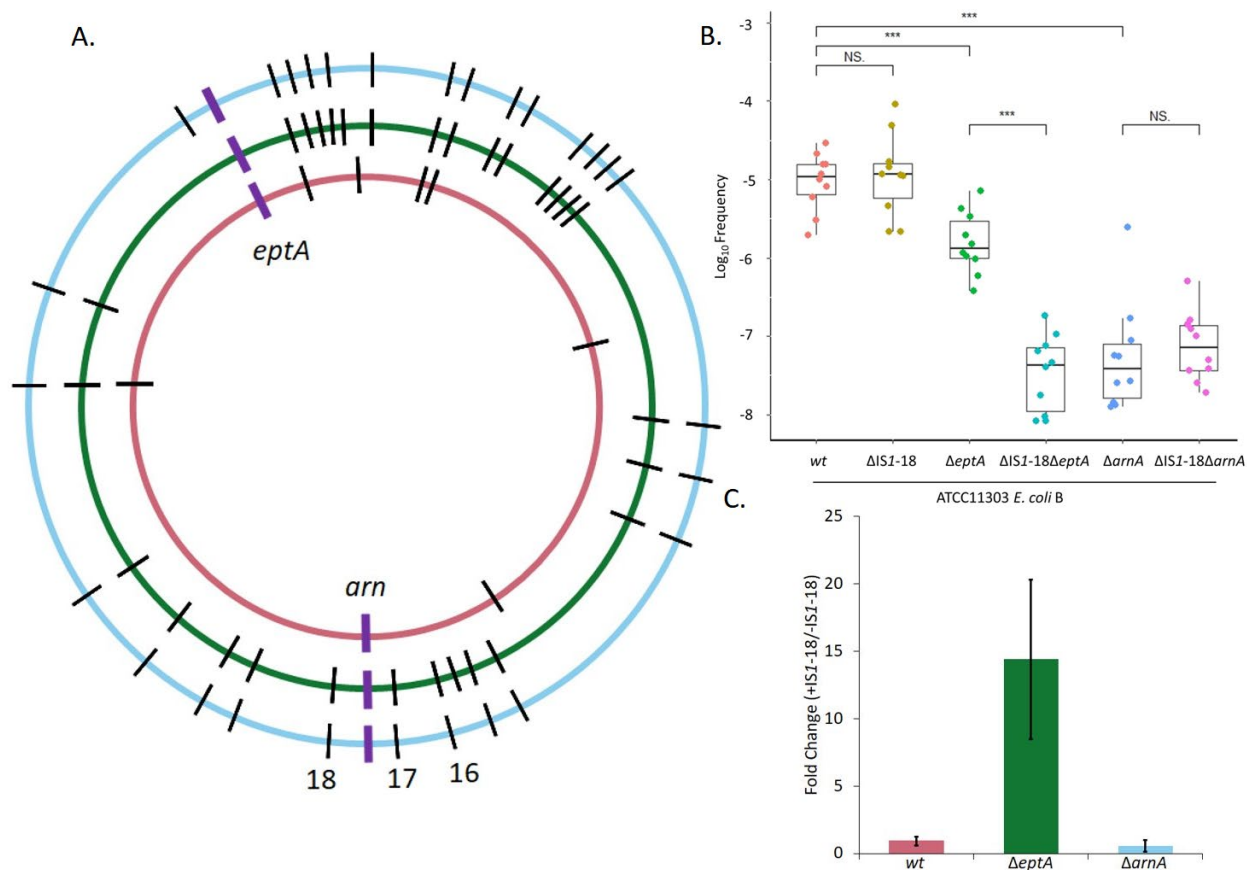


Figure 3-10: Role of IS1 mediated chromosomal amplifications is maintained in a more wildtype *E. coli* B strain. **A)** Relative positioning of IS1 elements across the genome of *E. coli* B ATCC11303 (light blue), *E. coli* BL21 (DE3) (green), and the K-12 strain *E. coli* BW25113 (pink) with 28, 29, and 7 IS1 elements respectively (black dashes). The location of *eptA* and the *arn* operon are indicated by larger purple dashes. The locations of IS1-16, IS1-17, and IS1-18 are indicated, and relative positioning shared between both *E. coli* B strains but not the K strain. **B)** In the *E. coli* B ATCC11303 background frequency of resistance was determined for *wt*, ΔeptA , and ΔarnA each with and without IS1-18. FOR was determined from 10 separate cultures per strain by plating dilutions of exponential growths ($\text{OD}_{600\text{nm}}$ 0.2 to 0.7) on LBA containing 1 $\mu\text{g}/\text{mL}$ PMB (8 $\mu\text{g}/\text{mL}$ for *wt* and $\Delta\text{IS1-18}$), then measuring the ratio of resistant CFUs to total plated cells. Significance values based on Student's t-test (***) $p < 0.001$, NS not significant) **C)** Fold change in median FOR when deleting IS1-18 was quantified for *E. coli* B ATCC11303 *wt*, ΔeptA , and ΔarnA with fold changes of approximately 1, 14, and 1 respectively. Error bars derived from propagating median absolute deviation of values in the interquartile range.

DISCUSSION

As antimicrobial resistance (AMR) concerns increase over the coming decades it is imperative that we gain a better understanding of bacterial resistance mechanisms. Of particular concern is bacterial HR, as it provides a pathway for bacteria to undermine treatment with even our drugs of last resort. Polymyxins have come back into use as a drug of last resort against AMR gram-negative bacteria including Enterobacteriaceae such as *E. coli* (3). *E. coli* BL21 (DE3), despite being a strain used to evaluate polymyxin resistance genes (45, 46), has had its polymyxin sensitivity called into question with reports claiming that *E. coli* B strains are intrinsically resistant while *E. coli* K-12 strains are sensitive (47). While many studies have investigated PMB resistance mechanisms few have probed for HR in *E. coli* B strains (48–50). Our study demonstrates that an IS1 driven chromosomal *arn* operon amplification in *E. coli* B strains facilitates PMB HR at least in part by increased Ara4N modification of lipid A.

While working with strains of *E. coli* B (16), we noticed high levels of intrinsic Ara4N modification when compared to *E. coli* K-12 despite wildtype alleles for all known regulators. As expected the MIC to PMB was also higher, albeit highly variable indicating HR, but intriguingly the FOR at ~8x their respective MICs was nearly 100 fold higher in *E. coli* B (Fig. 3-1). The FOR in *E. coli* B was unaffected by deletion of *eptA* alone or in conjunction with *lpxT* [increases negative charge by adding phosphate (51)] and PagP [decrease outer membrane permeability by adding an acyl group to LPS (52)]; in the Parent strain (Fig. 3-1). Contrastingly deletion of *arnA* resulted in a significant 10-fold drop in FOR (Fig. 3-1), suggesting that the *arn* operon plays a significant role in PMB resistance among the resistant sub-population.

This PMB resistant sub-population was found to be easily selected for from our Parent strain in a single selection step, suggesting they preexisted in cultures. While expecting to find mutations in the two component regulatory systems governing the *arn* operon, whole genome sequencing for two representative isolates (C1 and C2) revealed genomes identical to parent, except for two regions with nearly 2 and 3 times higher read counts respectively (Fig. 3-5A). Both amplified regions included the *arn* operon and were ‘bookended’ by insertion sequences (*IS1*), located either 170- (*IS1-16* in C2) or 51- (*IS1-17* in C1) kb upstream and 90-kb downstream (*IS1-18*) of the *arn* operon (Fig. 3-5B and 3-5D).

Chromosomal tandem duplications are one of the most common class of mutations and yet are hard to characterize due to their fleeting nature (53). Tandem amplifications are thought to arise from unequal DNA exchange between sister chromosomes, either through homologous recombination (in Rec⁺ hosts) or single stranded DNA exchange via cross annealing (54). In either case, a head-to-tail duplication with an intervening third copy of the repeat element results as we observed with our *IS1* junction PCR checks (Fig. 3-5B and 3-5C). Insertion sequences, a large class of small DNA elements flanked by inverted terminal repeats encoding a transposase for self-transposition (55–57), are thought to be involved in chromosomal tandem duplications in part by providing an extend stretch of homology for strand exchange. While the mechanism by which *IS1* elements promote tandem duplication is not fully understood, our data clearly show the importance of *IS1* for amplification. Deletion of *IS1-18* resulted in a 15- to 70-fold drop in FOR which could be restored by reintroducing *IS1-18* (Fig. 3-8A and 3-8B), demonstrating how *IS1* elements located hundreds of kb away can alter the PMB FOR by an order of magnitude. Furthermore, in strains lacking *arnA* the deletion of *IS1-18* had no significant effect on FOR,

highlighting that within the amplified regions the *arn* operon was the key factor leading to resistance.

Despite the large size of the amplifications the C1 and C2 *arn* operon amplified clones were relatively stable, with a resistant population surviving without PMB challenge for nearly 200 generations (Figs. 3-5E and 3-7). Analysis of the LPS structure by ³²P-lipid A radiolabeling and ESI-MS showed a bulk increase in LPS Ara4N content (Fig. 3-3), suggesting that *arn* operon duplication produces a highly modified LPS subpopulation. Different levels of Ara4N will not only impart resistance to PMB, but also to cationic antimicrobial peptides, trigger different innate immune responses, and present different outer membrane permeabilities. IS1 mediated chromosomal amplification of the *arn* operon thus could contribute to many scenarios involving bacterial survival and should thus be considered. This becomes starkly clear as we consider that the amplified regions are a strong driver of heterogeneous gene expression.

Heterogeneous gene expression levels in bacterial populations are well documented (58, 59) but the potential contribution for IS elements has so far not been explicitly investigated. When just considering *E. coli* BL21 (DE3) there are 29 IS1 elements across the genome (Fig. 3-10) resulting in multiple combinations of IS1 elements that can interact and give chromosomal amplifications with varied recombination/outcross rates and different amplification numbers all of which drives cell-to-cell variation. RNA-seq analysis of our C2 amplicon demonstrated general upregulation of genes within the amplified segment, including the *arn* operon, as well as genes/operons located outside of it being both down and upregulated [Meredith Lab (Aditi Ranade), unpublished]. In addition, volcano plots indicated changes in the glycerophospholipid

degradation (glp) pathway whereby genes, in the multiple involved operons, across the genome were upregulated [Meredith Lab (Aditi Ranade), unpublished].

Altogether, our data suggests a model where a major driver of *E. coli* B PMB HR is tandem chromosomal amplification. Whereby amplification is IS1 mediated in an incompletely understood mechanism worthy of further investigation. The sub-population with amplicons containing the *arn* operon have distinct LPS chemotypes with increased Ara4N modification resulting in PMB resistance. This study highlights the importance of considering IS element content and location along the genome when evaluating AMR.

MATERIALS AND METHODS

Bacterial strains and growth conditions

E. coli BL21(DE3) and ATCC11303 strains used in this study were grown in LB (10 g tryptone, 10 g NaCl, 5 g Yeast Extract, pH 7.0) only or in LB supplemented with appropriate antibiotics. Standard culture conditions were defined as 2-mL cultures in 14-mL Falcon snap cap culture tubes, grown at 37 °C with aeration (250 rpm). Where noted, cultures were grown in 96-well plates, 24-well plates, with or without shaking. Plasmids and strains used in this study are listed in Table 3-2.

Table 3-2: Bacterial strains and plasmids

Bacterial Strain or plasmid	Relevant Genotype/Phenotype	Source or reference
<i>E. coli</i> strains		
TXM338	Wildtype BW25113; K-12 lineage	Lab Stock
TXM319	Wildtype BL21 (DE3); B lineage	Lab Stock
TXM322	BL21 (DE3) <i>arnA::kanR</i> ; Kan ^r	(16)
GKM329	BL21 (DE3) <i>eptA::catR</i> ; Cat ^r	(16)
TXM331	BL21 (DE3) <i>eptA::catR arnA::kanR</i> ; Cat ^r Kan ^r	(16)
TXM333	BL21 (DE3) <i>eptA::catR arnA::kanR lpcA::gentR</i> ; Cat ^r Kan ^r Gent ^r	(16)
AR2206	BL21 (DE3) <i>IS1-18::aprR</i> ; Apr ^r	This study
AR2207	BL21 (DE3) <i>arnA::kanR IS1-18::aprR</i> ; Kan ^r Apr ^r	This study
AR2208	BL21 (DE3) <i>eptA::catR IS1-18::aprR</i> ; Cat ^r Apr ^r	This study
AR1972	BL21 (DE3) <i>lpxT::kanR pagP::hygR</i> ; Kan ^r Hyg ^r	This study
AR1973 (Parent)	BL21 (DE3) <i>eptA::catR lpxT::kanR pagP::hygR</i> ; Cat ^r Kan ^r Hyg ^r	This study
MM2028	BL21 (DE3) <i>eptA::catR lpxT::FRT pagP::hygR arnA::kanR</i> ; Cat ^r Kan ^r Hyg ^r	This study
MM2165	BL21 (DE3) <i>eptA::catR lpxT::kanR pagP::hygR IS1-18::aprR</i> ; Cat ^r Kan ^r Hyg ^r Apr ^r	This study
TXM2253	BL21 (DE3) <i>eptA::catR lpxT::kanR pagP::hygR IS1-18::aprR + IS1-18 specR</i> ; Cat ^r Kan ^r Hyg ^r Apr ^r Spec ^r	This study
TXM2197	Wildtype <i>E. coli</i> (Migula) Castellani and Chalmers ATCC11303	ATCC
TXM2222	ATCC11303 <i>eptA::catR</i> ; Cat ^r	This study
TXM2223	ATCC11303 <i>arnA::kanR</i> ; Kan ^r	This study
MM2176	ATCC11303 <i>IS1-18::aprR</i> ; Apr ^r	This study
TXM2233	ATCC11303 <i>eptA::catR IS1-18::aprR</i> ; Cat ^r Apr ^r	This study
TXM2234	ATCC11303 <i>arnA::kanR IS1-18::aprR</i> ; Kan ^r Apr ^r	This study
Plasmids		
pKD46	λ-Red recombinase expression plasmid; Carb ^r	(60)
pKD4	Kan ^r template	(63)
pSET152	Apr ^r template	Lab Stock
pKD3	Cat ^r template	(63)
pUC19-oriT-hyg	Hyg ^r template	Lab stock
pKFC	Vector for construction of LHA <i>IS1-18::aprR</i>	Lab stock
pCP20	FLP recombinase plasmid, Carb ^r	(63)
pCL25	Spec ^r template	Lab Stock

Kan^r- kanamycin; Cat^r- chloramphenicol; Spec^r- spectinomycin; Carb^r- carbenicillin; Apr^r- apramycin; Hyg^r- hygromycin, Gent^r- gentamicin.

Strain and plasmid construction

Gene or IS1-18 deletions along with the IS1-18 knockin back complement were constructed using the Red recombinase system (60). Gene specific P1 and P2 primers, along with the antibiotic resistance gene marker template used for selection, are listed in Table 3-3. In the case of Δ IS1-18, an apramycin (*apr*) marker was amplified by PCR (primers MM2891-2892) and flanked by DNA cassettes located up- (primers MM2896-2897) and downstream of IS1-18 (primers MM2898-2899). PCR products were assembled in the plasmid pKFC, which was then used as template for PCR amplification (primers MM2900-2901) of the integration cassette. For IS1-18 knockin to make the back complemented strain, splice overlap PCR was used to assemble the upstream DNA homology arm (primers TM3013-3018), IS1-18 (TM2983-2984), a spectinomycin resistance selection marker (TM3055-3056), and a downstream homology corresponding to the *apr* marker (TM3014-2019). All constructs were checked by PCR using primers annealing outside the integration locus for the correct size before verification by Sanger sequencing.

Table 3-3: Primers used in this study

Primer Name	Primer Sequence
IS1-18 KO	
MM2896-P1 Ins18 pKFC EcoRI	GACGGCCAGTGAATTCATGGAATAAAAATCATGCTACC
MM2897-P2 Ins18 pKFC	TCGCTTTTCCCGCTCTCATCAAATCCGTTACCG
MM2898-P3 Ins18 pKFC	AATCGCCAGGCGAAATATCAAATGAAATTAATCAAC
MM2899-P4 Ins18 pKFC HindIII	TGATTACGCCAAGCTCGGATGGTCTTACCCGGTTC
MM2891 - Ins18 aprR P1	GAGCGGGAAAAGCGAACCAACGGACTTATTTACCTGGTACGGTACCTAG ATCCTTTGG
MM 2892 - Ins18 aprR P2	TTTCGCCTGGCGATTTTGAAGTCTTTTTCAACGTTATCTCCGTTCTCCGC TCATGAGC

MM2900-Ins18::aprR pKFC for	CAATACCAGCGCTGCTTACACAGA
MM2901-Ins18::aprR pKFC rev	CGATGTCTGTGGGTAAATGGACGC
MM2927-LHA Ins18 upcheck	GCTTACCCTTTCAAATCAATCAGTG
MM2928-LHA Ins18 downcheck	GTCCAGTTACCGTTCTACGGTAGC
IS1-18 KI	
TM3018- yfdF P1	GAAGTTAATGGATTAGTACAAGAGTTC
TM3013- yfdF P2	AACCAGTTGCAAATGCGAAGATAAAACCAGG
TM2983- Ins18 KI for	CATTTGCAACTGGTTCGATCATC
TM2984-Ins18 KI rev	CCC GTT GAGCTCGTTTAC
TM3055- specIS18 for	AACGAGCTCAACGGGTTCCCCTGCTCGCGCAG
TM3056- specIS18 rev	GGTTTGCGAATCCGTGCTTGAACGAATTGTTAG
TM3014- apr P3	ACGGATTCGCAAACCGATATCACACAAACTCAGAC
TM3019- apr P4	CAGTCCAAGTGGCCCATCTTCGAG
arnA KO	
GK425-ArnA::KanR-P1	GGTGACCTGCCTTACCACAAC
GK426-ArnA::KanR-P2	TCGTGATGTTTAGCCGCTTC
GK433-ArnA-check_for	CGAGCGTGAGTTTGGTGAATCC
GK434-ArnA-check_rev	CCGATCCCAGTTACCGCTAC
eptA KO	
TM448-EptA::catR-P1	GTTGGCCGCTTTTTATATCTCTATCTGCCTGAATATTGCCTTGCGCCTACCTGTGACGGA
TM449-EptA::catR-P2	TGTTGCGTTTGC GCCTGTTTTTGCAGGCAGTTCTGGTCAACCCTTACGCCC CGCCCTGCC
GK435-EptA-check_for	AAACCCGTATCCCTTAGATGCACC
GK436-EptA_check_rev	CTCAAGGCTTTGTTCCGCCATC
lpxT KO	
MAM2381- New P1 lpxT pKD4 KanR	AGGTTGCCTGCGTTTTTTCAGTAAGATAATTAGAGAAAATATGGTAGGCTG GAGCTGCTTC
MAM2382- New P2 lpxT pKD4 KanR	GATGATGTTAATTACTGTGAGTTATTTGTTTTGGAAATGTTTTATGAATATC CTCCTTAG
MM2579- lpxT upcheck v2	CTGATTTCCAGCAGCGAAGCTGAC
MM2580- lpxT downcheck v2	GATAGATGAAAGCACGGTGCGCAT
pagP KO	
Tm748- PagP hyg P1	GTTTTATGGTCACAAATGAACGTGAGTAAATATGTCGCTATCCTATGACCA TGATTACGC
Tm749- PagP hyg P2	ACTAAAACCTTCATTTGTCTCAAACTGAAAGCGCATCCAGGCACGTTGTAA AACGACGGC
Tm750- PagP hygcheck for	GTAGCTTTGCTATGCTAGTAGTAG
Tm751- PagP hygcheck rev	GTGGTACGCTTTGTCCAGTGTAAC
Junction PCR	
TM2872- Ins17 rev (P17)	GTTGGGACTGACGTTGCCGGTAATCG

TM2873- Ins18 for (P18)	CGGAAATGATTACTTATCTCTCGGTTACTACG
TM2874- Ins16 rev (P16)	CTCTTCAGAGACTGCCACATTAGCG
TM2862- Ins18 upcheck (P18')	CACACAAACTCAGACATACGGTAACGG
AR2883 - pykA upcheck	ACGCGAAAACGACGCCATGGTGATTG
AR2884 - pykA downcheck	GCGGCGGATGAATGAAGAAGTCGAG

Population Analysis Profile (PAP)

Single colonies of wildtype *E. coli* BL21(DE3) (TXM319) were inoculated in 2 mL LB in 15 mL culture tubes. From the overnight culture, 3 mL LB was inoculated with 100 μ L of a 10^6 -fold dilution and incubated at 37 °C with shaking till cells reached early exponential phase (OD_{600nm} of 0.15-0.3). Cells were harvested by centrifugation (2 min at 5000 xg) and resuspended in an equal volume of LB with PMB (1 μ g/mL). Aliquots containing 10^7 , 10^6 , and 10^5 cells were plated on LBA (1.5% agar) with varying concentrations of PMB (0, 0.5, 1, 2, 4, 6 μ g/mL). Colony counts were obtained after an overnight incubation at 37 °C and used to calculate the FOR at the corresponding concentration of PMB.

MIC and growth curve measurements

For MIC measurements, a low CFU input was used to minimize the effect of resistant subpopulations. Single colonies of strains isolated on LBA or LBA supplemented with 0.5 μ g/mL PMB (for PMB resistant isolates) were cultured overnight under standard culture conditions in 2 mL LB or LB supplemented with 0.5 μ g/mL PMB (late stationary phase $OD_{600nm} \sim 2$). A 100 μ L aliquot of a 10^6 -fold dilution of overnight cultures in LB was mixed with 100 μ L of LB media with increasing concentrations of PMB (2-fold increments) for a final concentration of $\sim 10^3$ total CFU per well in a 96-well microplate for overnight incubation at 37 °C without shaking. The minimum

concentration of PMB with no visible growth was scored as the MIC after 18-20h of incubation. For growth curve measurements, overnight cultures of parent and mutant strains were diluted 1:1000 in 2 mL of fresh LB in 15 mL culture tubes and incubated at 37 °C with aeration by shaking (250 rpm). Growth was measured at OD_{600nm} with readings taken every 30 min.

Frequency of Resistance determination

For each strain, glycerol stocks were struck out on to LBA with required antibiotics for marker selection. Ten single colonies were used to inoculate separate LB cultures and grown overnight. The next morning, 100 µL of a 10⁶ dilution was used to inoculate a fresh 3 mL LB culture and cultures were incubated at 37 °C until an OD_{600nm} between OD_{600nm} 0.2 to 0.7. Cells were pelleted (2 min at 5000 xg) then resuspended in an equal volume of LB containing either 0.5 µg/mL or 1 µg/mL PMB (the latter was used for strains with MIC values consistently above 1 µg/mL). Each resuspension was serially 10-fold diluted, and 100 µL of each was plated on separate LB agar plates containing PMB at 4 to 8-fold higher than the MIC. The fold change is approximate as replicate MIC measurements for PMB were highly variable (See Table 3-1). The FOR was calculated based on the ratio of CFU on PMB containing plate over total CFU plated (based on LBA only plate).

Single-step derivation of independent PMB resistant isolates

To derive PMB resistant isolates, single colonies of the parent strain AR1973 (*E. coli* BL21(DE3) *eptA::catR lpxT::kanR pagP::hygR*) were used to start independent overnight cultures. Cultures were diluted into LB supplemented with increasing concentrations of PMB (final

concentration range in culture was 0.03125 µg/mL to 0.5 µg/mL) in a 24-well microplate, with a final culture volume of 3 mL at 10^6 CFU/mL to enrich the PMB HR subpopulation. The plate was incubated at 37 °C with shaking (250rpm) for 24h. Growth was observed for all cultures at the highest concentration (0.5 µg/mL). Cultures were colony purified on LBA with PMB (0.5 µg/mL) and used to make glycerol stocks. In all cases, phenotypic PMB resistance was stable provided cultures were maintained on PMB, as determined by MIC measurements (2-4 µg/mL PMB) and FOR (1 µg/mL PMB) performed as described above.

LPS Purification

Bacteria were harvested from stationary phase cultures grown at 37 °C in Lysogeny Broth (10 g tryptone, 5 g yeast extract, 10 g NaCl per liter) supplemented with necessary antibiotics. Dried biomass was gathered by stirring with ethanol overnight followed by two 12-hour rounds with acetone at 4 °C. From dried biomass LPS was extracted via the phenol chloroform petroleum ether method (61). Briefly, dried biomass was suspended in 30 mL of PCP solution (90% phenol: chloroform: petroleum ether in 2:5:8 v/v/v ratio) and incubated with flipping for 1 hour. Biomass was pelleted with centrifugation (10 minutes at 3000x g) and supernatant collected in a round bottom flask. Extraction with PCP solution was repeated twice more. Pooled extract was rotovaped for removal of chloroform. To the remaining viscous phenol phase 100 µL of 3M sodium acetate (pH 7.0) was added followed by water dropwise until LPS precipitated. LPS was pelleted via centrifugation (10 minutes at 3000x g) and the pellet washed with 80% phenol and a final wash with acetone.

From the PCP extracted LPS, coextracting phospholipids were removed by a modified chloroform methanol wash (62). Briefly, pellet was suspended in chloroform/methanol/ 3M sodium acetate (pH 7.0) (85:15:1, v/v/v ratio). LPS was precipitated via the addition of 2-3 volumes of methanol and collected by centrifugation (10 minutes at 3000x g). The wash was repeated twice more before lipoprotein contamination was removed following the phenol/sodium deoxycholate extraction as described by Hirschfeld et al (63). Briefly, LPS was resuspended in tris buffered TEA-DOC solution (0.5% sodium deoxycholate (w/v), 0.2% triethylamine (v/v), in 20 mM Tris-HCl, (pH 7.0)) An equal volume of water saturated phenol was added and mixed by inversion. Phase separation was induced by centrifugation (10 minutes at 3000x g) and upper aqueous phase containing LPS was removed. Extraction of lower phenol phase was repeated twice more and aliquots of aqueous phase pooled. Pooled aqueous phase was back extracted with fresh water saturated phenol before collection of aqueous phase and addition of 3 M sodium acetate (pH 7.0) until final concentration of 30 mM. Ethanol was added until a final concentration of 75% to precipitate LPS, sample was kept at -20 °C for 2 to 4 hours before LPS was pelleted.

Finally nucleic acid contamination was removed via ultracentrifugation. LPS pellets were resuspended in 3 mL of water and diluted with 30 mL of Tris saline buffer (50 mM Tris-HCl, 100 mM NaCl, 1 mM MgCl₂, (pH 7.0)) before centrifugation at 100,000x g for 4 hours. Supernatant was decanted and the remaining translucent pellet was suspended in miliQ water before transfer to 500-1k Da MWCO dialysis tubing. LPS was dialyzed against four 5-L portions of miliQ water at 4 °C for 48 hours. Finally LPS was lyophilized providing a fluffy white powdered LPS sample.

Mass Spectrometry

Analysis of purified LPS was performed as has been described (see (16) and Chapter 2).

³²P-labeled lipid A labeling and analysis via thin-layer chromatography (TLC)

Radio-labeled lipid A was extracted from strains via the Trent methodology (64) on a reduced scale. Overnights for each strain were prepared in LB with antibiotics as required, in the case of isolates C1 and C2 they were grown without PMB challenge and used to inoculate 7 mL of LB 1:100. Inorganic ³²P was added to 2.5 μCi/mL and cells grown for ~4 hours at 37 °C with shaking at 250 rpm. Cells were harvested by centrifugation at 2,000x g for 10 min and washed with water before resuspension in 1 mL of single phase Bligh-Dyer mixture (chloroform:methanol:water (1:2:0.8, v/v)). Suspended cells were allowed to incubate at room temperature with flipping for 15 minutes before pelleting (6,000x g for 2 minutes) and resuspension with a second aliquot of single-phase Bligh-Dyer mixture. Incubation period was repeated, LPS pelleted, and resuspended in 450 μL of 300 mM sodium acetate, pH 4.5; 1% SDS buffer by pipetting. Lipid A hydrolysis was achieved by incubating samples at 95 °C for 45 minutes. After hydrolysis samples were allowed to cool then the solution converted to a two-phase Bligh-Dyer mixture via the addition of 1 mL of chloroform:methanol (1:1, v/v) for a final chloroform:methanol:aqueous (2:2:1.8 v/v) mixture. The two-phase Bligh-Dyer was vortexed and phases separated via centrifugation, 3,000x g for ten seconds. The lower phase containing ³²P-labeled lipid A was extracted into a clean Eppendorf tube and allowed to dry overnight.

To visualize ³²P-labeled lipid A, samples were dissolved in 50 μL of 4:1 chloroform:methanol (v/v) and 5 μL spotted on a silica gel 60 TLC plate. The plate was run in a

TLC tank using a pyridine/chloroform/formic acid/water (50:50:16:5, v/v/v/v) mobile phase and allowed to air dry overnight. A storage phosphor screen [BAS-IP MS (Multipurpose Standard)] was exposed to the plastic wrapped TLC plate for ~24 hours before scanning to obtain an image.

Genome sequencing

From 1 mL of overnight cultures in LB, genomic DNA was extracted using guanidium thiocyanate as described (65). Genomic DNA was submitted to SeqCenter (Pittsburgh, PA) for Illumina next generation sequencing (1.33 million reads per sample using paired end 151 bp long short end reads). Reads were mapped to the reference genome of *E. coli* BL21(DE3) (NCBI Reference Sequence: NC_012971.2) using Geneious Prime.

Outcrossing experiment

Single colonies of parent and PMB resistant isolates were isolated on LBA or LBA supplemented with 0.5 µg/mL PMB respectively and were inoculated in 200 µL LB media either without (for parent) or with 1 µg/mL PMB in a 96-well microplate. Cultures were incubated overnight at 37 °C, without shaking. For passage 1, a 10⁵-fold dilution of overnight culture was made into 2 mL LB or LB supplemented with 0.5 µg/mL PMB in 15mL culture tubes and incubated overnight at 37 °C, with shaking (250 rpm). After 2 hr of incubation, each sample was plated on LBA and LBA containing 0.5 µg/mL PMB to verify the corresponding homogeneous susceptible (parent) or resistant PMB (C1 and C2) phenotypes. For passage 2 onwards, replicate (+/- 1 µg/ml PMB) 10⁷-fold dilutions were performed to a final 2 mL culture volume. The proportion of PMB

resistant colonies was calculated as the ratio of colony counts from LBA + 1 µg/ml PMB plates to colony counts from LBA only plates for each sample per passage per day.

Junction Multiplex PCR

Presence of the tandem chromosomal duplication was checked with a multiplex PCR. Template DNA was mixed with Thermo Scientific Phire Plant Direct PCR Master Mix and primers as follows: P18 – 5'-CGGAAATGATTACTTATCTCTCGGTTACTACG-3', P17 – 5'-GTTGGGACTGACGTTGCCGTAATCG-3', P16 – 5'-CTCTTCAGAGACTGCCACATTAGCG-3', pkyAfor – 5'-ACGCGAAAACGACGCCATGGTGATTG-3', and pykArev– 5'-GCGGCGGATGAATGAAGAAGTCGAG-3'. In $\Delta/S1$ -18 strains primer P18 was replaced with primer P18' – 5'-CACACAAACTCAGACATACGGTAACGG-3'. Template DNA was prepared via genomic DNA extraction as described above or directly from isolated single colonies as follows: colonies were resuspended in lysis buffer (10 mM Tris-HCl, 0.1 mM EDTA, 0.1% Triton X-100 (pH 8.0)), incubated for 5 min at 95 °C, then centrifuged for 10 min at 13,000x g, 0.5 uL of resultant supernatant was used as template. PCR conditions followed recommendations provided for Thermo Scientific Phire Plant Direct PCR Master Mix with an annealing temperature of 60 °C, and extension time of 40 seconds.

SDS-PAGE/Silver Stain

Whole cell lysate preparation: Whole cell lysates were prepared in the manner of Hitchcock and Brown (66) with a few modifications. Briefly bacteria were grown overnight in 2 mL lysogeny Broth with required antibiotics, c1p1 and c5p1 isolates were grown in the absence

of PMB. From the overnight growth 100 μ L was taken and cells pelleted. Pellet was solubilized in 50 μ L of lysing/loading buffer (0.5 mM EDTA, 2% SDS, 2% 2-mercaptoethanol, 0.1% bromophenol blue, 10% glycerol, 50 mM Tris (pH 7.5)). Lysates were incubated at 95 $^{\circ}$ C for 10 minutes, cooled, and proteinase K (PK) was added to a final concentration of 1 μ g/ μ L. To degrade protein lysates with PK were incubated at 60 $^{\circ}$ C for 60 minutes. Lysates were then either immediately run on SDS-PAGE gels or frozen for later use.

Purified LPS preparation: LPS from *E. coli* B strains was purified as described above. Purified LPS powder was resuspended in lysing/loading buffer to a concentration of 20 μ g/mL. Sample treatment followed that as described for whole cell lysates after pellet solubilization.

SDS-PAGE: Gels were prepared as described by Lesse et al (67), with slight modification. Briefly, two acrylamide and bisacrylamide stock solutions of 30% T, 6% C and 30% T, 2.6% C were prepared where T represents the total percentage of acrylamide and C represents the percentage of the cross-linker (bis) to the total concentration of acrylamide. The resolving gels were prepared via the addition of 30% T, 6% C stock acrylamide solution (5.44 mL), gel buffer (3 M Tris-HCl, 0.3% SDS pH 8.5)(3.3 mL), glycerol (1.3 g), and water (160 μ L). Gels were polymerized with the addition of ammonium persulfate (100 μ L 10% APS) and TEMED (10 μ L). Stacking gels were layered on top of the polymerized resolving gels and were prepared by the addition of 30% T, 2.6% C stock acrylamide solution (0.666 mL), gel buffer (3 M Tris-HCl, 0.3% SDS pH 8.5)(2 mL), and water (4 mL) before initializing polymerization via the addition of 10% APS (66 μ L) and TEMED (6.6 μ L). Final gels consisted of 16.5% T, 6% C lower resolving gel overlayed with a 3% T, 2.6% C upper stacking gel.

Either whole cell lysate sample or purified LPS samples, prepared as described above, were heated at 95 °C for 5 minutes before loading onto gels. Electrophoresis was carried out in a BioRad® Mini-PROTEAN Tetra Vertical Electrophoresis Cell with a Tris-Tricine run buffer (0.1 M Tris, 0.1 M Tricine, 0.1% SDS), and run at a constant 50 V until the dye front was at the resolving gel after which the voltage was increased to 150 V and the gel run until ~1 hour after the dye front ran off the gel.

LPS silver staining: After electrophoresis gels were washed with water and left to shake in a solution of 40% ethanol and 5% acetic acid overnight. The next morning gels were oxidized by shaking in a solution of 40% ethanol, 5% acetic acid, and 0.7% periodic acid followed by four to six 30-minute washes in water. Gels were silver stained with ammoniacal silver in the fashion of Hitchcock and Brown by a 10-minute incubation in freshly prepared staining solution (0.67% silver nitrate, 0.1 M ammonium hydroxide, and 18 mM sodium hydroxide). Stain was discarded and gel was washed four times in water, 10 minutes each. Finally, gels were soaked in developer solution (0.26 mM citric acid and 0.019% formaldehyde, pre-warmed to 37 °C) until bands were visible, typically 5-15 minutes, before quench by shaking in 1% acetic acid solution.

REFERENCES

1. Murray, C. J. L., Ikuta, K. S., Sharara, F., Swetschinski, L., Robles Aguilar, G., Gray, A., Han, C., Bisignano, C., Rao, P., Wool, E., Johnson, S. C., Browne, A. J., Chipeta, M. G., Fell, F., Hackett, S., Haines-Woodhouse, G., Kashef Hamadani, B. H., Kumaran, E. A. P., McManigal, B., Achalapong, S., Agarwal, R., Akech, S., Albertson, S., Amuasi, J., Andrews, J., Aravkin, A., Ashley, E., Babin, F.-X., Bailey, F., Baker, S., Basnyat, B., Bekker, A., Bender, R., Berkley, J. A., Bethou, A., Bielicki, J., Boonkasidecha, S., Bukosia, J., Carvalheiro, C., Castañeda-Orjuela, C., Chansamouth, V., Chaurasia, S., Chiurchiù, S., Chowdhury, F., Clotaire Donatien, R., Cook, A. J., Cooper, B., Cressey, T. R., Criollo-Mora, E., Cunningham, M., Darboe, S., Day, N. P. J., De Luca, M., Dokova, K., Dramowski, A., Dunachie, S. J., Duong Bich, T., Eckmanns, T., Eibach, D., Emami, A., Feasey, N., Fisher-Pearson, N., Forrest, K., Garcia, C., Garrett, D., Gastmeier, P., Giref, A. Z., Greer, R. C., Gupta, V., Haller, S., Haselbeck, A., Hay, S. I., Holm, M., Hopkins, S., Hsia, Y., Iregbu, K. C., Jacobs, J., Jarovsky, D., Javanmardi, F., Jenney, A. W. J., Khorana, M., Khusuwan, S., Kissoon, N., Kobeissi, E., Kostyanov, T., Krapp, F., Krumkamp, R., Kumar, A., Kyu, H. H., Lim, C., Lim, K., Limmathurotsakul, D., Loftus, M. J., Lunn, M., Ma, J., Manoharan, A., Marks, F., May, J., Mayxay, M., Mturi, N., Munera-Huertas, T., Musicha, P., Musila, L. A., Mussi-Pinhata, M. M., Naidu, R. N., Nakamura, T., Nanavati, R., Nangia, S., Newton, P., Ngoun, C., Novotney, A., Nwakanma, D., Obiero, C. W., Ochoa, T. J., Olivas-Martinez, A., Olliaro, P., Ooko, E., Ortiz-Brizuela, E., Ounchanum, P., Pak, G. D., Paredes, J. L., Peleg, A. Y., Perrone, C., Phe, T., Phommasone, K., Plakkal, N., Ponce-de-Leon, A., Raad, M., Ramdin, T., Rattanaovong,

- S., Riddell, A., Roberts, T., Robotham, J. V., Roca, A., Rosenthal, V. D., Rudd, K. E., Russell, N., Sader, H. S., Saengchan, W., Schnall, J., Scott, J. A. G., Seekaew, S., Sharland, M., Shivamallappa, M., Sifuentes-Osornio, J., Simpson, A. J., Steenkeste, N., Stewardson, A. J., Stoeva, T., Tasak, N., Thaiprakong, A., Thwaites, G., Tigoi, C., Turner, C., Turner, P., van Doorn, H. R., Velaphi, S., Vongpradith, A., Vongsouvath, M., Vu, H., Walsh, T., Walson, J. L., Waner, S., Wangrangsimakul, T., Wannapinij, P., Wozniak, T., Young Sharma, T. E. M. W., Yu, K. C., Zheng, P., Sartorius, B., Lopez, A. D., Stergachis, A., Moore, C., Dolecek, C., and Naghavi, M. (2022) Global burden of bacterial antimicrobial resistance in 2019: a systematic analysis. *The Lancet*. **399**, 629–655
2. O'Neill, J. (2014) *Antimicrobial Resistance: Tackling a crisis for the health and wealth of nations*, London, UK
 3. El-Sayed Ahmed, M. A. E.-G., Zhong, L.-L., Shen, C., Yang, Y., Doi, Y., and Tian, G.-B. (2020) Colistin and its role in the Era of antibiotic resistance: an extended review (2000–2019). *Emerg Microbes Infect.* **9**, 868–885
 4. Lenhard, J. R., Nation, R. L., and Tsuji, B. T. (2016) Synergistic combinations of polymyxins. *Int J Antimicrob Agents*. **48**, 607–613
 5. Nang, S. C., Azad, M. A. K., Velkov, T., Zhou, Q. (Tony), and Li, J. (2021) Rescuing the Last-Line Polymyxins: Achievements and Challenges. *Pharmacol Rev.* **73**, 679–728
 6. Perez, F., El Chakhtoura, N. G., Yasmin, M., and Bonomo, R. A. (2019) Polymyxins: To Combine or Not to Combine? *Antibiotics*. **8**, 38
 7. BENEDICT, R. G., and LANGLYKKE, A. F. (1947) Antibiotic activity of *Bacillus polymyxa*. *J Bacteriol.* **54**, 24

8. Andrade, F. F., Silva, D., Rodrigues, A., and Pina-Vaz, C. (2020) Colistin Update on Its Mechanism of Action and Resistance, Present and Future Challenges. *Microorganisms*. **8**, 1716
9. Hamel, M., Rolain, J.-M., and Baron, S. A. (2021) The History of Colistin Resistance Mechanisms in Bacteria: Progress and Challenges. *Microorganisms*. **9**, 442
10. Otsuka, Y. (2020) Potent Antibiotics Active against Multidrug-Resistant Gram-Negative Bacteria. *Chem Pharm Bull (Tokyo)*. **68**, 182–190
11. Velkov, T., Deris, Z. Z., Huang, J. X., Azad, M. A., Butler, M., Sivanesan, S., Kaminskas, L. M., Dong, Y.-D., Boyd, B., Baker, M. A., Cooper, M. A., Nation, R. L., and Li, J. (2014) Surface changes and polymyxin interactions with a resistant strain of *Klebsiella pneumoniae*. *Innate Immun*. **20**, 350–363
12. Velkov, T., Thompson, P. E., Nation, R. L., and Li, J. (2010) Structure–Activity Relationships of Polymyxin Antibiotics. *J Med Chem*. **53**, 1898–1916
13. Manioglu, S., Modaresi, S. M., Ritzmann, N., Thoma, J., Overall, S. A., Harms, A., Upert, G., Luther, A., Barnes, A. B., Obrecht, D., Müller, D. J., and Hiller, S. (2022) Antibiotic polymyxin arranges lipopolysaccharide into crystalline structures to solidify the bacterial membrane. *Nat Commun*. 10.1038/s41467-022-33838-0
14. Simpson, B. W., and Trent, M. S. (2019) Pushing the envelope: LPS modifications and their consequences. *Nat Rev Microbiol*. **17**, 403–416
15. Li, B., Yin, F., Zhao, X., Guo, Y., Wang, W., Wang, P., Zhu, H., Yin, Y., and Wang, X. (2019) Colistin Resistance Gene *mcr-1* Mediates Cell Permeability and Resistance to Hydrophobic Antibiotics. *Front Microbiol*. **10**, 3015

16. Komazin, G., Maybin, M., Woodard, R. W., Scior, T., Schwudke, D., Schombel, U., Gisch, N., Mamat, U., and Meredith, T. C. (2019) Substrate structure-activity relationship reveals a limited lipopolysaccharide chemotype range for intestinal alkaline phosphatase. *Journal of Biological Chemistry*. **294**, 19405–19423
17. Olaitan, A. O., Morand, S., and Rolain, J.-M. (2014) Mechanisms of polymyxin resistance: acquired and intrinsic resistance in bacteria. *Front Microbiol*. 10.3389/fmicb.2014.00643
18. Trimble, M. J., Mlynářčík, P., Kolář, M., and Hancock, R. E. W. (2016) Polymyxin: Alternative Mechanisms of Action and Resistance. *Cold Spring Harb Perspect Med*. **6**, a025288
19. Lou, Y.-C., Weng, T.-H., Li, Y.-C., Kao, Y.-F., Lin, W.-F., Peng, H.-L., Chou, S.-H., Hsiao, C.-D., and Chen, C. (2015) Structure and dynamics of polymyxin-resistance-associated response regulator PmrA in complex with promoter DNA. *Nat Commun*. **6**, 8838
20. Trent, M. S., Ribeiro, A. A., Doerrler, W. T., Lin, S., Cotter, R. J., and Raetz, C. R. H. (2001) Accumulation of a Polyisoprene-linked Amino Sugar in Polymyxin-resistant *Salmonella typhimurium* and *Escherichia coli*. *Journal of Biological Chemistry*. **276**, 43132–43144
21. Guo, L., Lim, K. B., Gunn, J. S., Bainbridge, B., Darveau, R. P., Hackett, M., and Miller, S. I. (1997) Regulation of Lipid A Modifications by *Salmonella typhimurium* Virulence Genes *phoP-phoQ*. *Science (1979)*. **276**, 250–253
22. El-Halfawy, O. M., and Valvano, M. A. (2015) Antimicrobial Heteroresistance: an Emerging Field in Need of Clarity. *Clin Microbiol Rev*. **28**, 191–207
23. Andersson, D. I., Nicoloff, H., and Hjort, K. (2019) Mechanisms and clinical relevance of bacterial heteroresistance. *Nat Rev Microbiol*. **17**, 479–496

24. Nicoloff, H., Hjort, K., Levin, B. R., and Andersson, D. I. (2019) The high prevalence of antibiotic heteroresistance in pathogenic bacteria is mainly caused by gene amplification. *Nat Microbiol.* **4**, 504–514
25. Edlund, T., and Normark, S. (1981) Recombination between short DNA homologies causes tandem duplication. *Nature.* **292**, 269–271
26. Matthews, P. R., and Stewart, P. R. (1988) Amplification of a Section of Chromosomal DNA in Methicillin-resistant *Staphylococcus aureus* following Growth in High Concentrations of Methicillin. *Microbiology (N Y).* **134**, 1455–1464
27. Nichols, B. P., and Guay, G. G. (1989) Gene amplification contributes to sulfonamide resistance in *Escherichia coli*. *Antimicrob Agents Chemother.* **33**, 2042–2048
28. Nicoloff, H., Perreten, V., and Levy, S. B. (2007) Increased Genome Instability in *Escherichia coli lon* Mutants: Relation to Emergence of Multiple-Antibiotic-Resistant (Mar) Mutants Caused by Insertion Sequence Elements and Large Tandem Genomic Amplifications. *Antimicrob Agents Chemother.* **51**, 1293–1303
29. Peterson, B. C., and Rownd, R. H. (1985) Drug resistance gene amplification of plasmid NR1 derivatives with various amounts of resistance determinant DNA. *J Bacteriol.* **161**, 1042–1048
30. Sun, S., Berg, O. G., Roth, J. R., and Andersson, D. I. (2009) Contribution of Gene Amplification to Evolution of Increased Antibiotic Resistance in *Salmonella typhimurium*. *Genetics.* **182**, 1183–1195
31. McGann, P., Courvalin, P., Snesrud, E., Clifford, R. J., Yoon, E.-J., Onmus-Leone, F., Ong, A. C., Kwak, Y. I., Grillot-Courvalin, C., Lesho, E., and Waterman, P. E. (2014) Amplification of

- Aminoglycoside Resistance Gene *aphA1* in *Acinetobacter baumannii* Results in Tobramycin Therapy Failure. *mBio*. 10.1128/mBio.00915-14
32. Band, V. I., and Weiss, D. S. (2019) Heteroresistance: A cause of unexplained antibiotic treatment failure? *PLoS Pathog.* **15**, e1007726
 33. Pogue, J. M., Jones, R. N., Bradley, J. S., Andes, D. R., Bhavnani, S. M., Drusano, G. L., Dudley, M. N., Flamm, R. K., Rodvold, K. A., and Ambrose, P. G. (2020) Polymyxin Susceptibility Testing and Interpretive Breakpoints: Recommendations from the United States Committee on Antimicrobial Susceptibility Testing (USCAST). *Antimicrob Agents Chemother.* 10.1128/AAC.01495-19
 34. Touzé, T., Tran, A. X., Hankins, J. V., Mengin-Lecreulx, D., and Trent, M. S. (2007) Periplasmic phosphorylation of lipid A is linked to the synthesis of undecaprenyl phosphate. *Mol Microbiol.* **67**, 264–277
 35. Tian, X., Manat, G., Gasiorowski, E., Auger, R., Hicham, S., Mengin-Lecreulx, D., Boneca, I. G., and Touzé, T. (2021) LpxT-Dependent Phosphorylation of Lipid A in *Escherichia coli* Increases Resistance to Deoxycholate and Enhances Gut Colonization. *Front Microbiol.* 10.3389/fmicb.2021.676596
 36. Bishop, R. E., Gibbons, H. S., Guina, T., Trent, M. S., Miller, S. I., and Raetz, C. R. H. (2000) Transfer of palmitate from phospholipids to lipid A in outer membranes of Gram-negative bacteria. *EMBO J.* **19**, 5071–5080
 37. Doijad, S. P., Gisch, N., Frantz, R., Kumbhar, B. V., Falgenhauer, J., Imirzalioglu, C., Falgenhauer, L., Mischnik, A., Rupp, J., Behnke, M., Buhl, M., Eisenbeis, S., Gastmeier, P., Gölz, H., Häcker, G. A., Käding, N., Kern, W. V., Kola, A., Kramme, E., Peter, S., Rohde, A.

- M., Seifert, H., Tacconelli, E., Vehreschild, M. J. G. T., Walker, S. V., Zweigner, J., Schwudke, D., Diaz, L. A. P., Pilarski, G., Thoma, N., Weber, A., Vavra, M., Schuster, S., Peyerl-Hoffmann, G., Hamprecht, A., Proske, S., Stelzer, Y., Wille, J., Lenke, D., Bader, B., Dinkelacker, A., Hölzl, F., Kunstle, L., and Chakraborty, T. (2023) Resolving colistin resistance and heteroresistance in *Enterobacter* species. *Nat Commun.* **14**, 140
38. Kapel, N., Caballero, J. D., and MacLean, R. C. (2022) Localized *pmrB* hypermutation drives the evolution of colistin heteroresistance. *Cell Rep.* **39**, 110929
39. McPhee, J. B., Lewenza, S., and Hancock, R. E. W. (2003) Cationic antimicrobial peptides activate a two-component regulatory system, PmrA-PmrB, that regulates resistance to polymyxin B and cationic antimicrobial peptides in *Pseudomonas aeruginosa*. *Mol Microbiol.* **50**, 205–217
40. Daegelen, P., Studier, F. W., Lenski, R. E., Cure, S., and Kim, J. F. (2009) Tracing Ancestors and Relatives of *Escherichia coli* B, and the Derivation of B Strains REL606 and BL21(DE3). *J Mol Biol.* **394**, 634–643
41. Haack, K. R., and Roth, J. R. (1995) Recombination between chromosomal IS200 elements supports frequent duplication formation in *Salmonella typhimurium*. *Genetics.* **141**, 1245–1252
42. Reams, A. B., Kofoid, E., Kugelberg, E., and Roth, J. R. (2012) Multiple Pathways of Duplication Formation with and Without Recombination (RecA) in *Salmonella enterica*. *Genetics.* **192**, 397–415
43. Reams, A. B., and Roth, J. R. (2015) Mechanisms of Gene Duplication and Amplification. *Cold Spring Harb Perspect Biol.* **7**, a016592

44. Reams, A. B., Kofoid, E., Duleba, N., and Roth, J. R. (2014) Recombination and Annealing Pathways Compete for Substrates in Making *rrn* Duplications in *Salmonella enterica*. *Genetics*. **196**, 119–135
45. Martins-Sorenson, N., Snesrud, E., Xavier, D. E., Cacci, L. C., Iavarone, A. T., McGann, P., Riley, L. W., and Moreira, B. M. (2020) A novel plasmid-encoded *mcr-4.3* gene in a colistin-resistant *Acinetobacter baumannii* clinical strain. *Journal of Antimicrobial Chemotherapy*. **75**, 60–64
46. Snyman, Y., Whitelaw, A. C., Barnes, J. M., Maloba, M. R. B., and Newton-Foot, M. (2021) Characterisation of mobile colistin resistance genes (*mcr-3* and *mcr-5*) in river and storm water in regions of the Western Cape of South Africa. *Antimicrob Resist Infect Control*. **10**, 96
47. Schumann, A., Cohn, A. R., Gaballa, A., and Wiedmann, M. (2023) *Escherichia coli* B-Strains Are Intrinsically Resistant to Colistin and Not Suitable for Characterization and Identification of *mcr* Genes. *Microbiol Spectr*. 10.1128/spectrum.00894-23
48. Juhász, E., Iván, M., Pintér, E., Pongrácz, J., and Kristóf, K. (2017) Colistin resistance among blood culture isolates at a tertiary care centre in Hungary. *J Glob Antimicrob Resist*. **11**, 167–170
49. Liao, W., Lin, J., Jia, H., Zhou, C., Zhang, Y., Lin, Y., Ye, J., Cao, J., and Zhou, T. (2020) Resistance and Heteroresistance to Colistin in *Escherichia coli* Isolates from Wenzhou, China. *Infect Drug Resist*. **Volume 13**, 3551–3561
50. Mead, A., Toutain, P.-L., Richez, P., and Pelligand, L. (2022) Quantitative Pharmacodynamic Characterization of Resistance versus Heteroresistance of Colistin in E.

- coli Using a Semimechanistic Modeling of Killing Curves. *Antimicrob Agents Chemother.* 10.1128/aac.00793-22
51. Tian, X., Manat, G., Gasiorowski, E., Auger, R., Hicham, S., Mengin-Lecreulx, D., Boneca, I. G., and Touzé, T. (2021) LpxT-Dependent Phosphorylation of Lipid A in *Escherichia coli* Increases Resistance to Deoxycholate and Enhances Gut Colonization. *Front Microbiol.* 10.3389/fmicb.2021.676596
52. Bishop, R. E., Gibbons, H. S., Guina, T., Trent, M. S., Miller, S. I., and Raetz, C. R. H. (2000) Transfer of palmitate from phospholipids to lipid A in outer membranes of Gram-negative bacteria. *EMBO J.* **19**, 5071–5080
53. Reams, A. B., and Roth, J. R. (2015) Mechanisms of Gene Duplication and Amplification. *Cold Spring Harb Perspect Biol.* **7**, a016592
54. Reams, A. B., Kofoed, E., Duleba, N., and Roth, J. R. (2014) Recombination and Annealing Pathways Compete for Substrates in Making *rrn* Duplications in *Salmonella enterica*. *Genetics.* **196**, 119–135
55. Mahillon, J., and Chandler, M. (1998) Insertion sequences. *Microbiol Mol Biol Rev.* **62**, 725–74
56. Siguier, P., Gournayre, E., and Chandler, M. (2014) Bacterial insertion sequences: their genomic impact and diversity. *FEMS Microbiol Rev.* **38**, 865–891
57. Siguier, P., Gournayre, E., Varani, A., Ton-Hoang, B., and Chandler, M. (2015) Everyman's Guide to Bacterial Insertion Sequences. *Microbiol Spectr.* 10.1128/microbiolspec.MDNA3-0030-2014

58. Davis, K. M., and Isberg, R. R. (2016) Defining heterogeneity within bacterial populations via single cell approaches. *BioEssays*. **38**, 782–790
59. Silander, O. K., Nikolic, N., Zaslaver, A., Bren, A., Kikoin, I., Alon, U., and Ackermann, M. (2012) A Genome-Wide Analysis of Promoter-Mediated Phenotypic Noise in *Escherichia coli*. *PLoS Genet*. **8**, e1002443
60. Datsenko, K. A., and Wanner, B. L. (2000) One-step inactivation of chromosomal genes in *Escherichia coli* K-12 using PCR products. *Proc Natl Acad Sci U S A*. **97**, 6640–5
61. Galanos, C., Lüderitz, O., and Westphal, O. (1969) A new method for the extraction of R lipopolysaccharides. *Eur J Biochem*. **9**, 245–9
62. Strain, S. M., Fesik, S. W., and Armitage, I. M. (1983) Characterization of lipopolysaccharide from a heptoseless mutant of *Escherichia coli* by carbon 13 nuclear magnetic resonance. *J Biol Chem*. **258**, 2906–10
63. Hirschfeld, M., Ma, Y., Weis, J. H., Vogel, S. N., and Weis, J. J. (2000) Cutting edge: repurification of lipopolysaccharide eliminates signaling through both human and murine toll-like receptor 2. *J Immunol*. **165**, 618–22
64. Henderson, J. C., O'Brien, J. P., Brodbelt, J. S., and Trent, M. S. (2013) Isolation and Chemical Characterization of Lipid A from Gram-negative Bacteria. *Journal of Visualized Experiments*. 10.3791/50623
65. Pitcher, D. G., Saunders, N. A., and Owen, R. J. (1989) Rapid extraction of bacterial genomic DNA with guanidium thiocyanate. *Lett Appl Microbiol*. **8**, 151–156

66. Hitchcock, P. J., and Brown, T. M. (1983) Morphological heterogeneity among *Salmonella* lipopolysaccharide chemotypes in silver-stained polyacrylamide gels. *J Bacteriol.* **154**, 269–277
67. Lesse, A. J., Campagnari, A. A., Bittner, W. E., and Apicella, M. A. (1990) Increased resolution of lipopolysaccharides and lipooligosaccharides utilizing tricine-sodium dodecyl sulfate-polyacrylamide gel electrophoresis. *J Immunol Methods.* **126**, 109–117

Chapter 4

Development and Evaluation of Assays for Lipopolysaccharide Degradation

Activity Among Gut Commensal Bacteria

INTRODUCTION

A number of chronic epidemic diseases such as atherosclerosis (1), non-alcoholic fatty liver disease (NAFLD) (2, 3), and type 2 diabetes mellitus (4–7) are at the forefront of public health concerns. Indeed around 6% of the world's population lives with diabetes (8), nearly 32% of adults suffer from NAFLD (9), and cardiovascular disease is the leading cause of death in the world. With obesity being an established predisposing risk factor for developing these diseases (10, 11), and the typical western high-fat/simple carbohydrate diet and sedentary lifestyle becoming more prevalent around the globe methods of managing these chronic metabolic conditions will only become more critical to lessen the burden on our healthcare system.

A common feature that accompanies metabolic diseases is a low-grade systemic inflammation (1) whereby metabolic endotoxemia (ME), a condition defined by elevated levels of lipopolysaccharide (LPS) in the blood, is a source of said inflammation that is exacerbated by high-fat diets (1, 12). As discussed in chapters 1 and 2, once in the blood LPS acts as a microbe associated molecular pattern (MAMP) and is recognized by the pattern recognition receptor (PRR) Toll-like receptor 4/myeloid differentiation factor-2 (TLR4/MD2). Recognition of LPS by the TLR4/MD2 complex results in a release of proinflammatory cytokines setting a low-grade inflammatory tone (13, 14). The role of LPS, and thus ME, in promoting metabolic disease is highlighted by its ability to induce both obesity and insulin resistance when injected subcutaneously in mice (5, 15). While LPS and other byproducts of the gut flora are normally contained within the lumen by the intestinal epithelium, high-fat diets are thought to induce structural changes to the epithelium allowing for the translocation of LPS to the bloodstream

(Fig. 4-1) (12). This hyperpermeability of the intestinal epithelium is itself a condition referred to as leaky-gut syndrome and has been demonstrated to additionally be induced by dysbiosis, an imbalance in the gut microbial community (16–21).

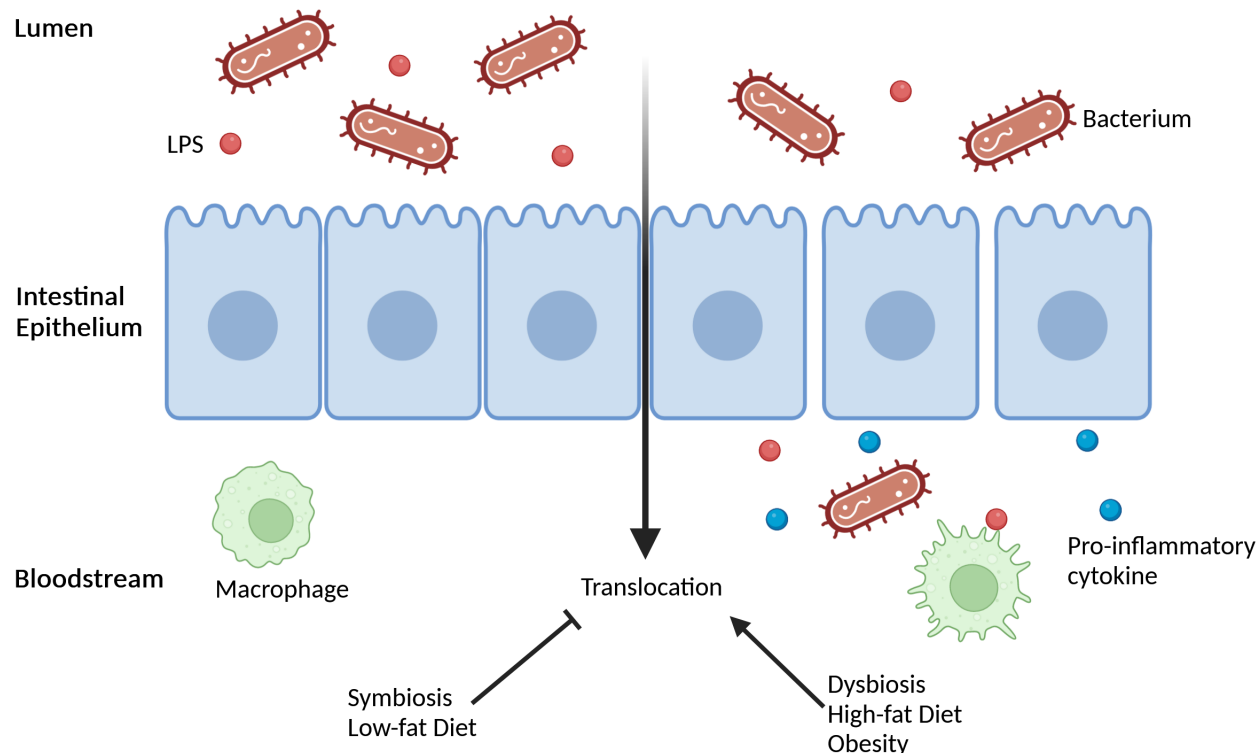


Figure 4-1: Diagram of luminal content translocation to the bloodstream. The left side represents functioning epithelial barrier action with bacteria and MAMPs sequestered to the lumen. The right side represents increased permeability of the lumen and the translocation of luminal contents across the epithelial barrier. Recognition of LPS by TLR4/MD2 expressing macrophages results in pro-inflammatory cytokine release.

Provided the link between LPS, ME, and metabolic disease one method of managing these disease states is through preventing elevated serum LPS levels (22, 23). LPS detoxification as a method of combating ME has been explored in multiple clinical trials, where exogenous intestinal alkaline phosphatase (IAP) was administered to detoxify LPS via cleavage of the 1- and 4'-

phosphates bound to lipid A (24–27). The work done in Chapter 2 demonstrates that IAP lacks the ability to detoxify immunogenic chemotypes of LPS and thus other avenues of LPS detoxification must be explored. While chapter 2 focused on the application of host derived mechanisms of detoxifying LPS, here we hypothesize that ME and the resulting inflammation can be lessened by discovering and exploiting microbiota mediated LPS degradation enzymes or “LPS-ases.” Among environmental bacteria, the most intensive effort to find LPS-ases occurred before the structure of LPS had been determined and focused on environmental bacteria (28). Interestingly, no candidate enzymes capable of extensive LPS degradation were identified in this initial study or in subsequent investigations to date (29). LPS is apparently unlike other abundant macromolecules (DNA/RNA/protein/phospholipids) that bacteria synthesize in lacking cognate degradation pathways. However, it would seem unlikely that all Gram-negative bacteria would invest so much energy into a metabolically dead-end product that all bacteria have failed to evolve mechanism to exploit. Thus, the discovery of bacteria capable of extensive LPS degradation would not only further our understanding of LPS catabolism but provide insight into potential probiotic applications for management of ME and its associated disease states.

One of the major barriers to identifying LPS-ase activity has been the lack of robust assays. Herein I describe the development and evaluation of assays for LPS-ase activity among a panel of test bacteria in a pilot screen. Three assays were developed consisting of an enzyme-linked immunosorbent assay (ELISA), a SDS-PAGE silver stain analysis, and an autoradiographic thin layer chromatography (TLC) assay. The bacterial panel consists primarily of strains representative of the four largest phyla of gut commensals (proteobacteria, actinobacteria, firmicutes, and bacteroidetes) (30). Gut commensals were chosen as they could more readily be applied as

probiotics to manage ME. For each assay test strains were grown in media supplemented with LPS purified from *Escherichia coli* BW25113 (K-12 lineage) and the three assays used to detect remaining intact LPS and or LPS degradation products. Since naturally occurring LPS is heterogenous in structure, LPS test substrate was purified and thoroughly characterized from a strain established to mainly produce a single chemotype (see Chapter 2). LPS from this strain was used as its chemotype is highly immunogenic, being hexa-acylated and bis-phosphorylated (31–33), and thus any LPS-ase activity observed would indicate selectivity for a known immunogenic chemotype.

RESULTS

LPS sandwich ELISA development

LPS can be difficult to assay given its heterogenous state, tendency to adsorb to surfaces, and propensity to aggregate. Despite these challenges we developed a sandwich-based ELISA assay using monoclonal anti-LPS antibodies (Fig. 4-2A). The system functions in a way that test strains are grown in the presence of a purified K-12 LPS and after incubation the supernatant is collected and the remaining intact LPS is detected by sandwich ELISA giving a signal. A decrease in signal compared to a no bacteria control indicated loss of LPS and potential for LPS-ase activity. A panel of commercially available LPS antibodies were initially evaluated. The antibody pair chosen for further development consisted of the monoclonal antibody mAB 26-5 (mouse), used as an immobilized capture antibody, and the secondary rAB WN1 222-5 (rabbit) antibody. This pair has the benefit of non-overlapping epitopes that can report on major changes to either lipid

A or the core region of K-12 LPS (Fig. 4-2A) (34–37). Additionally, this system provides little to no background signal when LPS, capture antibody, or secondary antibody is omitted from the sandwich (Fig. 4-2B).

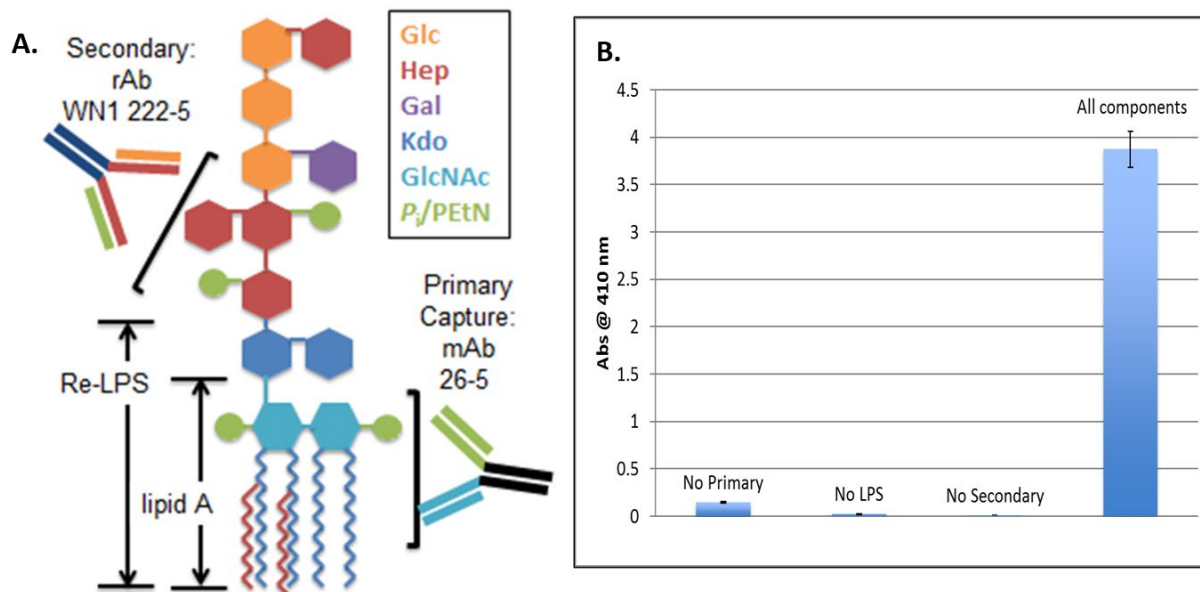


Figure 4-2: K-12 LPS Sandwich ELISA. A) Schematic of monoclonal Ab binding sites to the hexa-acylated K-12 LPS chemotype. The truncated chemotypes of RE-LPS, lipid A and lipid IV_A are indicated where lipid IV_A is the lipid A structure without the secondary acyl chains shown in red. **B)** ELISA signal is only observed when all components of the complex are present (100 ng mAb-26, 50 ng LPS, and 100 ng rAb WN1 222-5 per well). Signal was generated using anti-rabbit Ig-HRP and ABTS colorimetric substrate.

Due to the secondary antibody recognizing the core sugars of K-12 LPS, the system can discriminate between LPS chemotypes that display sufficiently different core configurations (Fig. 4-2A). Thus, any other Gram-negative bacteria tested for degradation producing their own LPS chemotypes with a differing core structure should display minimal cross reactivity. Indeed, examples include LPS from *E. coli* O111, *Pseudomonas aeruginosa*, or *Salmonella enterica* all of

which were not recognized by the sandwich ELISA (Fig. 4-3). Importantly LPS structures mimicking degradation of the core oligosaccharide were not recognized by ELISA (lipid IV_A, Re-LPS, lipid A); however chemotypes mimicking degradation products resultant from removal of secondary acyl chains or lipid A bound phosphates were still detected (Fig. 4-3). Additionally, the system was able to detect K-12 LPS alone or when added in conjunction with equal mass amounts of differing chemotypes, indicating that LPS-ase degradation products or LPS released from test strains would not interfere in detecting fed intact K-12 LPS (Fig. 4-3).

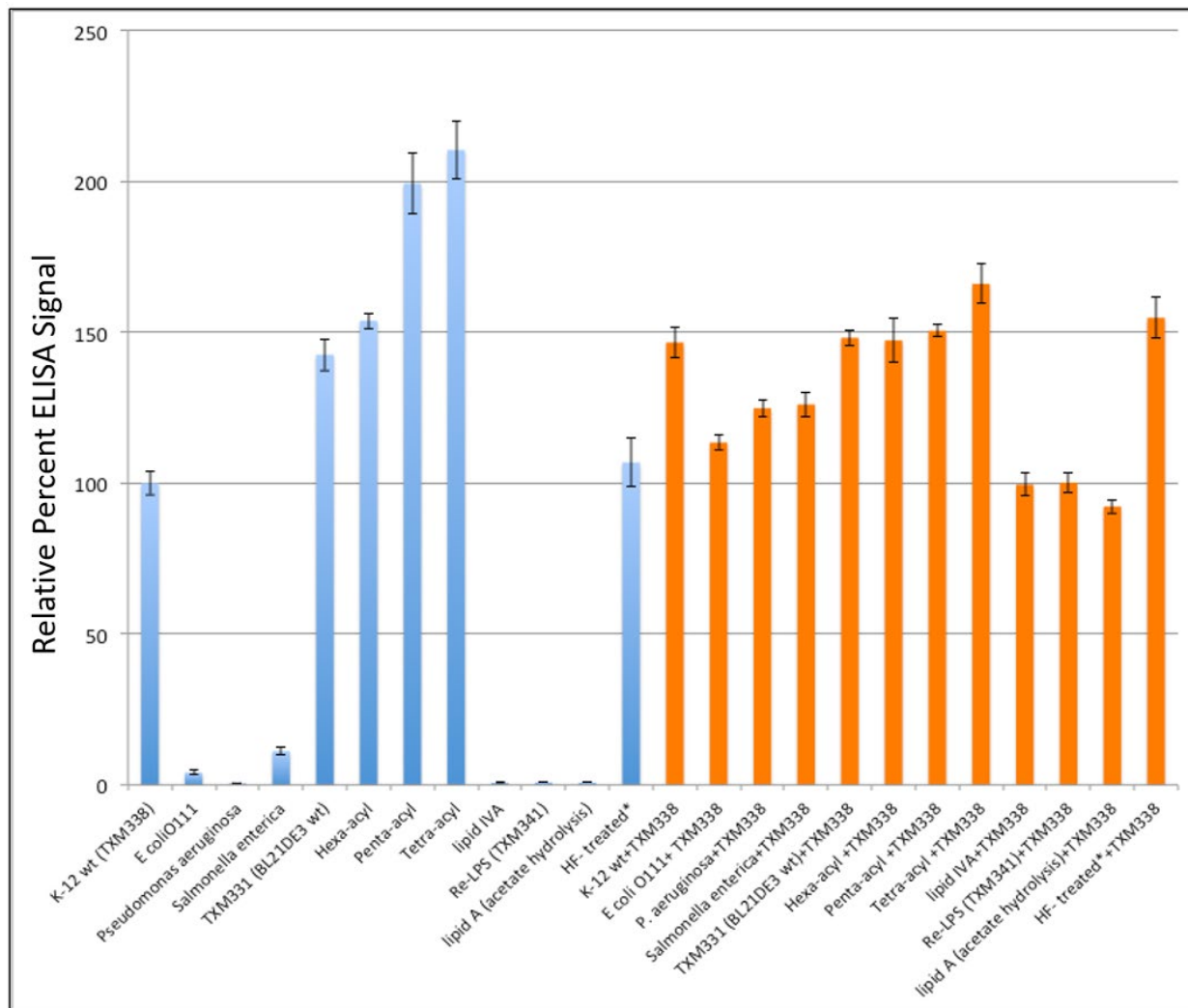


Figure 4-3: ELISA LPS chemotype specificity. Signal using purified LPS samples (50 ng/well) was normalized to K-12 LPS when added alone (*blue bars*) or with an equal mass amount K-12 LPS. No interference was observed (*orange bars*). *HF-treated: K-12 LPS treated with hydrofluoric acid (HF) for removal of lipid A phosphate groups.

Key features of the ELISA protocol that enable efficient recovery of nondegraded LPS post-culture include the addition of low levels of the detergent deoxycholate and EDTA to prevent aggregation and non-specific adsorption; disruption of LPS-protein complexes via a proteinase K treatment; and a 1:50 (v/v) dilution of the culture supernatant to minimize the amount of potentially interfering substances released during incubation with test strains. All above steps

are done before addition of the sample to mAb 26-5 coated ELISA plates and subsequent formation of the ELISA sandwich. Utilizing this system, a variety of bacterial strains (n=93) were tested in at least duplicate, and a relative percent signal for each strain, when compared to control, was gained. An example of this data can be seen in Figure 4-4, where a variety of *Bacteroides* and *Bifidobacterium* species are tested along with a few *Enterococcus faecalis* strains. Among this sub panel no strains demonstrated a greater than 50% decrease in signal and thus non were considered candidates for containing LPS-ase activity. The summation of the ELISA assay data can be found in Figure 4-5, where each point represents a bacterial strain tested. A list of strains tested can be found in Table 4-1 with sample ID's corresponding to those plotted in Figure 4-5. While most strains tested demonstrate little to no signal loss compared to control, 15 strains demonstrated a greater than 50% signal loss and were treated as candidate strains used for further investigation. Candidate strains are highlighted in green in Table 4-1.

Table 4-1: Full list of strains tested via LPS ELISA

Sample #	^A Source	Source ID	Genus	Species	Strain	^B Growth Temp	^B O ₂	^C % Rel. Signal
1	BEI	HM-1036	<i>Bacteroides</i>	<i>stercoris</i>	CC31F	37	Anaerobic	70
2	BEI	HM-1049	<i>Paenibacillus</i>	<i>barengoltzii</i>	CC33_002B	30	Aerobic	53
3	BEI	HM-1051	<i>Peptostreptococcus</i>	<i>sp.</i>	CC14N	37	Anaerobic	86
4	BEI	HM-1055	<i>Rothia</i>	<i>mucilaginoso</i>	CC87LB	37	Facultative anaerobe	39
5	BEI	HM-1056	<i>Ruminococcus</i>	<i>gnavus</i>	CC55_001C	37	Anaerobic	33
6	BEI	HM-106	<i>Lactocaseibacillus</i>	<i>rhamnosus</i>	LMS2-1	35-37	Aerobic	42
7	BEI	HM-109	<i>Corynebacterium</i>	<i>amycolatium</i>	SK46	37	Aerobic	80
8	BEI	HM-111	<i>Deinococcus</i>	<i>grandis</i>	SK125	30	Aerobic	59
9	BEI	HM-1120	<i>Bifidobacterium</i>	<i>breve</i>	JCP7499	37	Anaerobic	99
10	BEI	HM-115	<i>Neisseria</i>	<i>flavescens</i>	SK114	37	Aerobic	62
11	BEI	HM-116	<i>Rhodococcus</i>	<i>erythropolis</i>	SK121	30	Aerobic	64
12	BEI	HM-1189	<i>Bifidobacterium</i>	<i>angulatum</i>	F16_22	37	Anaerobic	90
13	BEI	HM-13	<i>Oribacterium</i>	<i>sinus</i>	F0268	37	Anaerobic	77
14	BEI	HM-147	<i>Actinomyces</i>	<i>cardiffensis</i>	F0333	37	Facultative Anaerobe	61
15	BEI	HM-154	<i>Lachnospiraceae</i>	<i>sp.</i>	2_1_58FAA	37	Anaerobic	79
16	BEI	HM-158	<i>Ralstonia</i>	<i>sp.</i>	5_2_56FAA	30	Aerobic	57
17	BEI	HM-173	<i>Clostridium</i>	<i>innocuum</i>	6_1_30	37	Anaerobic	77
18	BEI	HM-176	<i>Coprobaecillus</i>	<i>sp.</i>	8_2_54BFA A	37	Anaerobic	93
19	BEI	HM-178	<i>Eubacterium</i>	<i>sp</i>	3_1_31	37	Anaerobic	58
20	BEI	HM-179	<i>Phascolarctobacterium</i>	<i>sp</i>	3_1_syn4	37	Anaerobic	83
21	BEI	HM-20	<i>Bacteroides</i>	<i>fragilis</i>	3_1_12	37	Anaerobic	82
22	BEI	HM-200	<i>Enterococcus</i>	<i>faecalis</i>	HH22	37	Facultative anaerobe	95
23	BEI	HM-201	<i>Enterococcus</i>	<i>faecalis</i>	TX0104	37	Facultative anaerobe	88
24	BEI	HM-204	<i>Enterococcus</i>	<i>faecium</i>	TX1330	37	Facultative anaerobe	97
25	BEI	HM-209	<i>Propionibacterium</i>	<i>propionicum</i>	F0230	37	Anaerobic	89

26	BEI	HM-210	<i>Bacteroides</i>	<i>eggerthii</i>	1_2_48FAA	37	Anaerobic	81
27	BEI	HM-22	<i>Bacteroides</i>	<i>sp</i>	1_1_30	37	Anaerobic	72
28	BEI	HM-220	<i>Anaerostipes</i>	<i>sp</i>	3_2_56FAA	37	Anaerobic	61
29	BEI	HM-222	<i>Bacteroides</i>	<i>ovatus</i>	3_8_47FAA	37	Anaerobic	80
30	BEI	HM-223	<i>Klebsiella</i>	<i>sp.</i>	4_1_44FAA	35-37	Facultative anaerobe	91
31	BEI	HM-260	<i>Fusobacterium</i>	<i>nucleatum</i> <i>subsp.</i> <i>polymorphum</i>	F0401	37	Anaerobic	94
32	BEI	HM-262	<i>Streptococcus</i>	<i>mitis</i>	F0392	37	Aerobic	79
33	BEI	HM-299	<i>Citrobacter</i>	<i>freundii</i>	4_7_47CFA A	37	Facultative anaerobe	56
34	BEI	HM-30	<i>Bifidobacterium</i>	<i>sp</i>	12_1_47BFA A	37	Anaerobic	85
35	BEI	HM-300	<i>Dorea</i>	<i>formicigenerans</i>	4_6_53AFA A	37	Anaerobic	97
36	BEI	HM-304	<i>Collinsella</i>	<i>sp.</i>	4_8_47FAA	37	Anaerobic	88
37	BEI	HM-307	<i>Clostridium</i>	<i>aldenense</i>	WAL-18727	37	Anaerobic	96
38	BEI	HM-308	<i>Hungatella</i>	<i>hathewayi</i>	WAL-18680	37	Anaerobic	41
39	BEI	HM-309	<i>Clostridium</i>	<i>symbiosum</i>	WAL-14163	37	Anaerobic	77
40	BEI	HM-310	<i>Clostridium</i>	<i>perfringens</i>	WAL-14572	37	Anaerobic	49
41	BEI	HM-315	<i>Clostridium</i>	<i>citroniae</i>	WAL-17108	37	Anaerobic	57
42	BEI	HM-318	<i>Clostridium</i>	<i>bolteae</i>	WAL-14578	37	Anaerobic	78
43	BEI	HM-333	<i>Kroppenstedtia</i>	<i>eburnea</i>	8437	37	Aerobic	96
44	BEI	HM-411	<i>Bifidobacterium</i>	<i>breve</i>	EX336960VC 18	37	Anaerobic	92
45	BEI	HM-412	<i>Bifidobacterium</i>	<i>breve</i>	EX336960VC 19	37	Anaerobic	83
46	BEI	HM-473	<i>Faecalibacterium</i>	<i>prausnitzii</i>	KLE1255	37	Anaerobic	45
47	BEI	HM-480	<i>Stomatobaculum</i>	<i>longum</i>	ACC2	37	Anaerobic	66
48	BEI	HM-633	<i>Bifidobacterium</i>	<i>adolescentis</i>	L2-32	37	Anaerobic	93
49	BEI	HM-634	<i>Clostridium</i>	<i>sp.</i>	L2-50	37	Anaerobic	74
50	BEI	HM-710	<i>Bacteroides</i>	<i>fragilis</i>	CL07T12C05	37	Anaerobic	57

51	BEI	HM-717	<i>Bacteroides</i>	<i>dorei</i>	CL02T00C15	37	Anaerobic	76
52	BEI	HM-720	<i>Bacteroides</i>	<i>vulgatus</i>	CL09T03C04	37	Anaerobic	91
53	BEI	HM-725	<i>Bacteroides</i>	<i>salyersiae</i>	CL02T12C01	37	Anaerobic	91
54	BEI	HM-726	<i>Bacteroides</i>	<i>cellulosilyticus</i>	CL02T12C19	37	Anaerobic	72
55	BEI	HM-727	<i>Bacteroides</i>	<i>finnegoldii</i>	CL09T03C10	37	Anaerobic	85
56	BEI	HM-728	<i>Bacteroides</i>	<i>caccae</i>	CL03T12C61	37	Anaerobic	77
57	BEI	HM-729	<i>Parabacteroides</i>	<i>merdae</i>	CL09T00C40	37	Anaerobic	76
58	BEI	HM-730	<i>Parabacteroides</i>	<i>merdae</i>	CL03T12C32	37	Anaerobic	91
59	BEI	HM-731	<i>Parabacteroides</i>	<i>johnsonii</i>	CL02T12C29	37	Anaerobic	82
60	BEI	HM-758	<i>Fusobacterium</i>	<i>nucleatum</i>	F0419	37	anaerobic	61
61	BEI	HM-780	<i>Lachnoanaerobaculum</i>	<i>sp</i>	OBRC5-5	37	Anaerobic	97
62	BEI	HM-784	<i>Corynebacterium</i>	<i>sp</i>	HFH0082	37	Aerobic	83
63	BEI	HM-79	<i>Ruminococcaceae</i>	<i>sp.</i>	D16	37	Anaerobic	88
64	BEI	HM-81	<i>Acidaminococcus</i>	<i>sp</i>	D21	37	Anaerobic	77
65	BEI	HM-818	<i>Rothia</i>	<i>aeria</i>	F0474	37	Aerobic	64
66	BEI	HM-845	<i>Bifidobacterium</i>	<i>longum</i> subsp. <i>longum</i>	44B	37	Anaerobic	88
67	BEI	HM-846	<i>Bifidobacterium</i>	<i>longum</i> subsp. <i>longum</i>	1-6B	37	Anaerobic	73
68	BEI	HM-847	<i>Bifidobacterium</i>	<i>longum</i> subsp. <i>longum</i>	35B	37	Anaerobic	102
69	BEI	HM-848	<i>Bifidobacterium</i>	<i>longum</i> subsp. <i>longum</i>	2-2B	37	Anaerobic	99
70	BEI	HM-853	<i>Acidaminococcus</i>	<i>sp</i>	HPA0509	37	Anaerobic	87
71	BEI	HM-856	<i>Bifidobacterium</i>	<i>breve</i>	HPH0326	37	Anaerobic	88
72	BEI	HM-868	<i>Bifidobacterium</i>	<i>sp</i>	MSTE12	37	Anaerobic	86
73	BEI	HM-875	<i>Fusobacterium</i>	<i>sp.</i>	OBRC1	37	Anaerobic	79
74	BEI	HM-877	<i>Olsenella</i>	<i>uli</i>	MSTE5	37	Anaerobic	103
75	BEI	HM-882	<i>Shuttleworthia</i>	<i>sp</i>	MSX8B	37	Anaerobic	99
76	BEI	HM-97	<i>Actinomyces</i>	<i>gerencseriae</i>	F0344	37	Anaerobic	77
77	JCM	1134	<i>Lactacaseibacillus</i>	<i>casei</i>		37	Facultative anaerobe	37

78	JCM	11572	<i>Micrococcus</i>	<i>lylae</i>		30	Aerobic	74
79	JCM	1233	<i>Cronobacter</i>	<i>sakazakii</i>		37	Facultative anaerobe	31
80	JCM	1327	<i>Brevibacterium</i>	<i>linens</i>		30	Aerobic	80
81	JCM	14341	<i>Microbacterium</i>	<i>oleivorans</i>		28	Aerobic	52
82	JCM	20315	<i>Lacticaseibacillus</i>	<i>paracasei</i>		37	Facultative anaerobe	94
83	JCM	2427	<i>Staphylococcus</i>	<i>saprophyticus</i>		37	Facultative anaerobe	40
84	JCM	2512	<i>Bacillus</i>	<i>firmus</i>		30	Aerobic	34
85	JCM	2592	<i>Brevibacterium</i>	<i>epidermidis</i>		30	Facultative anaerobe	29
86	JCM	8580	<i>Enterobacter</i>	<i>cloacae</i> subsp. <i>Kobei</i>		37	Facultative anaerobe	54
87	BEI	NR-2490	<i>Paenibacillus</i>	<i>macerans</i>	NRS 888	30	Aerobic	31
88	BEI	NR-36443	<i>Lachnospiraceae</i>	<i>sp</i>	Strain 3-1	37	Anaerobic	34
89	BEI	NR-43503	<i>Peptoclostridium</i>	<i>difficile</i>	CD169	37	Anaerobic	34
90	BEI	NR-50118	<i>Sphingomonas</i>	<i>sp</i>	Ag1	30	Aerobic	46
91	BEI	NR-50119	<i>Leucobacter</i>	<i>sp</i>	Ag1	30	Aerobic	77
92	BEI	NR-681	<i>Bacillus</i>	<i>circulans</i>	Ford 26	30	Aerobic	60
93	Lab stock	TXM 333	<i>Escherichia</i>	<i>coli</i>	BL21 DE3	37	Facultative anaerobe	106

^A BEI: Strains obtained through BEI Resources, JCM: Strains obtained through the Microbe Division in RIKEN-BRC (Japanese collection of microorganisms).

^B Growth temp and O₂ indicate culture growth conditions (facultative anaerobes grown in aerobic environment).

^C % Rel. Signal indicates percentage of ELISA signal relative to control; strains that display greater than 50% signal reduction are highlighted in green.

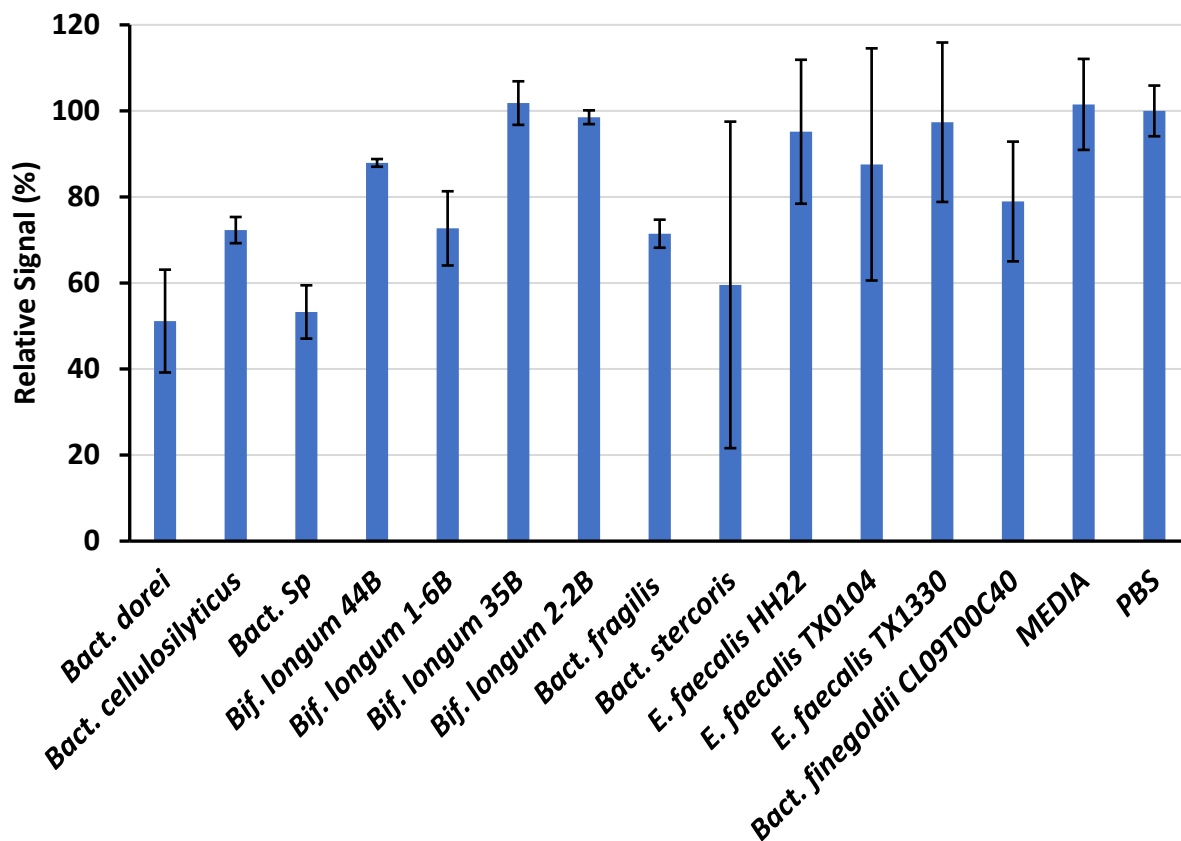


Figure 4-4: Example sample set for LPS ELISA assay. A variety of *Bacteroides* (*Bact.*), *Bifidobacterium* (*Bif.*), and *Enterococcus* strains were tested for LPS-ase activity. ELISA signal relative to phosphate buffered saline is plotted for each strain and a media only control.

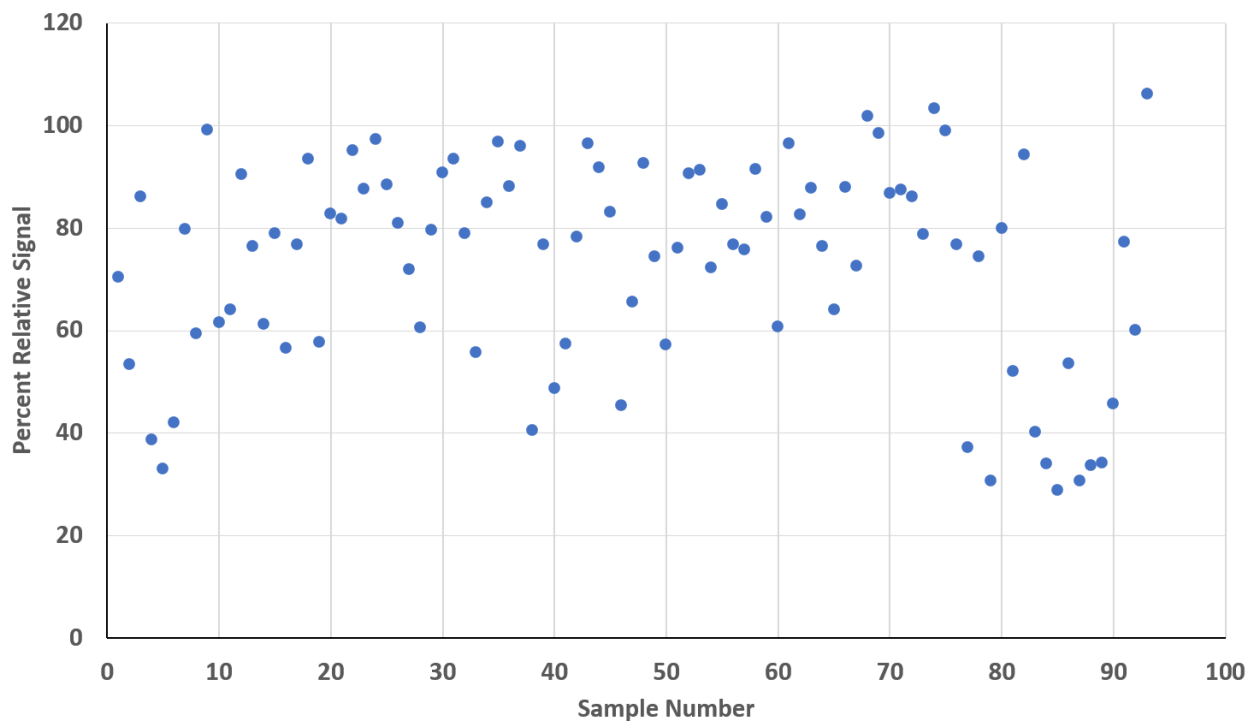


Figure 4-5: Summation of LPS ELISA data. Percent relative signal for all test strains compared to control. All strains tested were assigned a sample ID number and plotted with associated ELISA signal. Full list of strains tested with corresponding sample ID numbers can be found in Table 1.

LPS SDS-PAGE and Silver stain analysis

One candidate strain, *Lacticaseibacillus rhamnosus* LMS2-1, was chosen for further screening. Firstly the ELISA assay was repeated with extended incubation periods as we hypothesized that LPS-ase activity would display a time-dependent signal loss whereas non-specific loss of K-12 LPS would remain constant over the incubation period. Incubations were extended to 8 days (from 2 days) and supernatant was collected immediately after set-up for a 0-day sample along with a 2-, 4-, and 8-day sample collection. ELISA data suggested a time-dependent loss of signal nearly approaching signal from a LPS⁻/bacteria⁺ background control (Fig. 4-6A). This data would suggest that the LPS is being lost, a substance is being produced that interferes with ELISA detection, or LPS feedstock is adsorbed to proteins/assay containers, so we

sought to confirm this observation via additional methods. We thus utilized an SDS-PAGE/silver staining method of analyzing the test incubations for the presence of feedstock LPS. In this method the whole culture is collected, and cells lysed before proteinase K treatment. The LPS containing sample is then subjected to gel electrophoresis and LPS detected via silver stain. Benefits of this methodology is that we can avoid loss of LPS, via non-specific binding of fed K-12 LPS to the test strain, by testing the whole culture as opposed to only testing the culture supernatant as in the ELISA assay. In addition, this assay provides information about the core oligosaccharide as loss of the core sugars would result in variable electrophoretic movement. In contrast, a major downside to this methodology is the inability to test Gram-negative strains as both the feedstock LPS and LPS derived from the test strain would be detected via silver staining. In the case of *L. rhamnosus* LMS2-1 the silver stain assay from 4-day incubation samples displayed minimal if any loss of LPS compared to the media control (Fig. 4-6B) and did not align with signal loss observed in the ELISA assay. Thus far the data would suggest that *L. rhamnosus* LMS2-1 does not degrade *E. coli* K-12 LPS. However, a common con to consider for both the ELISA and silver stain assays is their poor ability to inform on changes to the lipid A structure, especially those that may contribute to detoxification of LPS, such as loss of the 1- and 4'- phosphates or deacylation (Fig. 4-3) (31–33) and thus additional assays are needed to discern lipid A degradation.

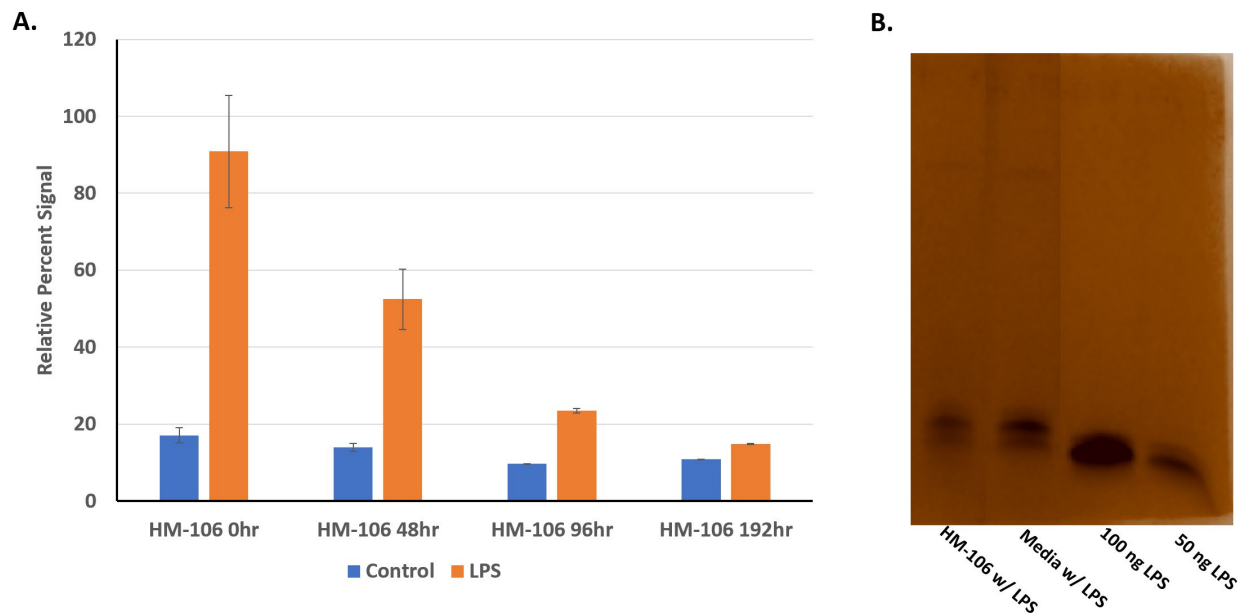


Figure 4-6: Time-dependent loss of ELISA signal observed for *L. rhamnosus* LMS2-1 (HM-106). **A)** *L. rhamnosus* LMS2-1 (HM-106) was incubated with (orange bars) or without (blue bars) K-12 LPS for 0-, 2-, 4-, and 8- days before analysis via ELISA. ELISA signal relative to a PBS control is plotted (100 ng/well LPS). **B)** *L. rhamnosus* LMS2-1 (HM-106) was incubated for 4-days with K-12 LPS before the whole culture was taken, cells lysed, electrophoresed, and LPS detected via silver stain. Samples include *L. rhamnosus* LMS2-1 (HM-106), a no bacteria control, and purified K-12 LPS (100 ng and 50 ng).

LPS autoradiographic TLC

Given the inability of the ELISA and silver stain to confidently discern changes in the lipid A region of LPS we developed an autoradiographic LPS TLC assay. This assay utilizes ^{14}C -labeled feedstock LPS purified from a strain of *E. coli* BW25113 (ΔnagB , ΔlpXT , ΔeptA , ΔarnA , ΔpagP) that I engineered to produce a single LPS chemotype that was specifically radiolabeled. This strain has NagB (glucosamine-6-phosphate deaminase) removed to allow for ^{14}C -labeling of the diglucosamine backbone of lipid A by preventing labeled glucosamine from being shunted into glycolysis (38). In addition, it produces LPS with minimal structural heterogeneity by removing

lipid A modification enzymes (see chapter 1), simplifying analysis of the assay results. As with the previous two assays K-12 LPS is fed to test strains and post-incubation presence of LPS is analyzed. In order to migrate and thus analyze by TLC, the core oligosaccharide region must first be removed from lipid A. Labeled lipid A is freed from the saccharide core via mild-acid hydrolysis before chromatography and visualization. Lipid A that has been dephosphorylated or had acyl chains removed migrate differently compared to intact lipid A, allowing for degradation products to be identified (Fig. 4-7A). Meanwhile complete degradation of lipid A due to LPS-ase activity can be readily detected as loss of the lipid A spot when compared to a no bacteria control. Unlike the silver stain assay, an advantage of the autoradiographic assay as a follow-up to the ELISA is the ability to test Gram-negative strains without interference. Using this methodology candidate strains grown under aerobic conditions, as identified by the ELISA assay (Table 4-1), were screened. None of the strains tested here, including *L. rhamnosus* LMS2-1, displayed significant loss of lipid A signal or appearance of new signals when compared to control (Fig. 4-7B).

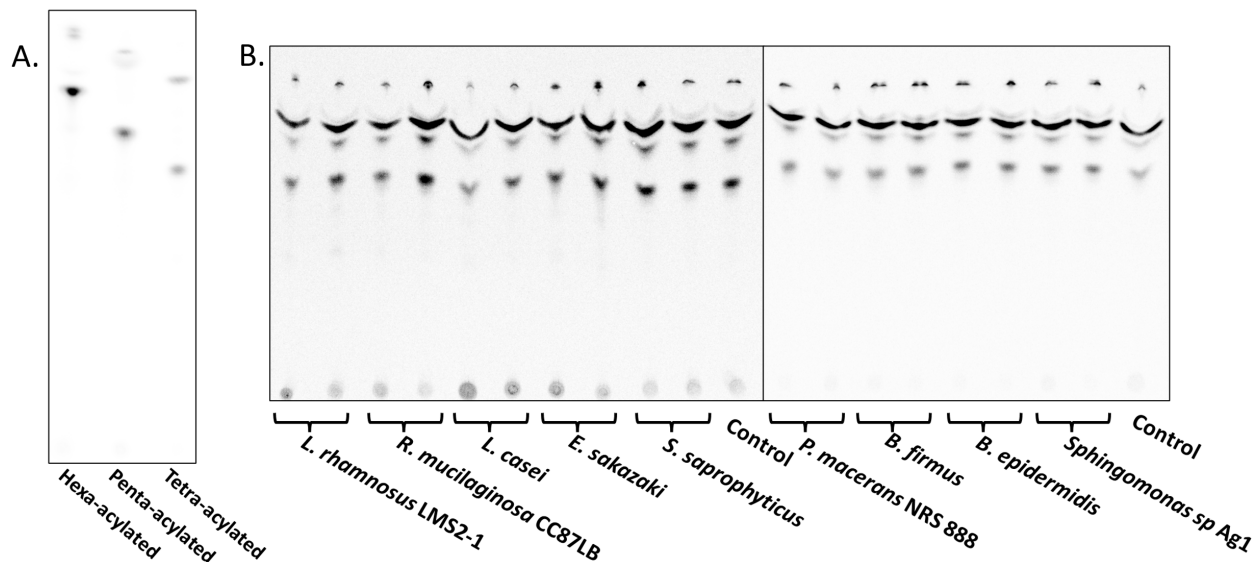


Figure 4-7: Autoradiographic TLC analysis of K-12 LPS. **A)** TLC analysis of ¹⁴C-labeled lipid A from *E. coli* BW25113 mutants producing hexa-acylated ($\Delta nagB$, $\Delta lpxT$, $\Delta deptA$, $\Delta arnA$) penta-acylated ($\Delta nagB$, $\Delta lpxT$, $\Delta deptA$, $\Delta arnA$, $\Delta pagP$ $\Delta lpxM$) and tetra-acylated ($\Delta nagB$, $\Delta lpxT$, $\Delta deptA$, $\Delta arnA$, $\Delta pagP$ $\Delta lpxM$ $\Delta lpxL$) lipid A. Samples were prepared from whole cells using the methods as described by Trent et. al (39) and in chapter 3. **B)** TLC analysis after 48-hour incubations of purified ¹⁴C-labeled K-12 LPS with multiple strains. Strains capable of growth under aerobic conditions and displaying a 50% or more decrease in ELISA signal compared to control were tested with the autoradiographic TLC assay. Control was purified labeled LPS incubated in media without bacteria.

DISCUSSION

Together the three assays described here provide a methodology by which LPS-ase activity can be screened for in a variety of bacteria. The systems work best as a whole, where the high throughput nature of the ELISA assay can report on large changes to K-12 LPS after incubation with test strains (Figs. 4-3 and 4-5) and is high throughput. The silver stain (Fig. 4-6) or autoradiographic TLC (Fig. 4-7) assays are utilized to inform on changes to the core oligosaccharide and lipid A regions of K-12 LPS respectively. However, throughput is much lower

than in the other assays. No individual assay provides all the information needed to confidently identify LPS-ase activity in a test strain. For example, a bacterium that deacylates exogenous LPS in a fashion similar to acyloxy acyl hydrolase (40) would not be discovered by the ELISA or silver stain assays but such activity would readily be observed via the autoradiographic TLC assay. It is this covering of short-comings that allows these systems to thoroughly screen for LPS-ase activity when utilized together. The lactic acid bacteria, *L. rhamnosus* LMS2-1 then provides an interesting test case and highlights the need to consider additional factors when utilizing any one assay of the screen. In particular, the time dependent decrease in ELISA signal would suggest that through some mechanism LPS was lost (Fig. 4-6A) but it was not due to degradation of either the core sugars or lipid A as determined by the silver stain and autoradiographic assays (Figs. 4-6B and 4-7). It is then possible that *L. rhamnosus* sequesters LPS in some complex formed over time that is then removed from the tested supernatant upon centrifugation. It has been reported that lactic acid bacteria produce heat shock proteins capable of binding to LPS (41), and this activity may be one such mechanism by which LPS is lost in the ELISA assay.

Ultimately, utilization of this screen will allow us for the first time to identify microbial mediated LPS degradation and elucidation of this activity will not only progress our understanding of LPS catabolism but also allow for testing of novel strategies to combat ME. Given the strong associations with ME and a variety of chronic diseases (1–7, 12), methods of attenuating or even preventing the inflammation it produces are highly sought after. For example the use of antibodies that bind and sequester cytokines is a common anti-inflammation strategy. Of note, the most widely prescribed antibody based therapeutic class (represented by Humira) adsorbs and prevents the proinflammatory signal of the cytokine TNF- α (42, 43). TNF- α is a

dominant TLR4 induced cytokine, produced upon binding with LPS (44). Immunosuppression by anti-TNF- α therapy does have side effects, however, including increasing patient susceptibility to opportunistic infections (45–47) and potential for anti-drug antibody response (48). In contrast, the use of LPS-ase activity either produced by probiotic strains or through recombinant protein technology represents an orthogonal strategy that would not have these drawbacks since it blocks an inflammatory signal at the source. The existence of LPS-ases is without question given the inherent nature of the carbon cycle, and the assays developed here thus far suggest the feasibility of finding them using our screening assays provided the right organisms are tested (see Chapter 5, Conclusions and Future Directions).

MATERIALS AND METHODS

Bacterial strains and growth conditions

All strains utilized for screening are listed in Table 4-1. Screened strains were grown in YCFA (DSMZ : *Deutsche Sammlung von Mikroorganismen und Zellkulturen*, Germany) (https://www.dsmz.de/microorganisms/medium/pdf/DSMZ_Medium1611.pdf) with growth temperature and oxygen availability as listed in Table 4-1. For all assays cultures were grown in 96-well plates without shaking. Additional strains utilized for LPS purification are listed in Table 4-2.

Table 4-2: Bacterial strains and plasmids

Bacterial Strain or plasmid	Relevant Genotype/Phenotype	Source or reference
<i>E. coli</i> strains		
TXM338	Wildtype BW25113; K-12 lineage	Lab Stock
MM1879	BW25113 <i>nagB::FRT lpxT::FRT eptA::catR arnA::kanR pagP::hygR</i> ; Cat ^r Kan ^r Hyg ^r	This Study
TXM331	BL21 (DE3) <i>eptA::catR arnA::kanR</i> ; Cat ^r Kan ^r	(49)
TXM333	BL21 (DE3) <i>eptA::catR arnA::kanR lpcA::gentR</i> ; Cat ^r Kan ^r Gent ^r	(49)
AR1776	BW25113 <i>nagB::FRT lpxT::FRT eptA::catR arnA::kanR</i> ; Cat ^r Kan ^r	Lab Stock
AR1863	BW25113 <i>nagB::FRT lpxT::FRT eptA::catR lpxM::kanR pagP::hygR</i> <i>arnA::tetR</i> ; Cat ^r Kan ^r Hyg ^r Tet ^r	Lab Stock
AR1868	BW25113 <i>nagB::FRT lpxT::FRT eptA::catR lpxM::kanR pagP::hygR</i> <i>arnA::tetR lpxL::aprR</i> [pMMW52-msbA]; Cat ^r Kan ^r Hyg ^r Tet ^r Apr ^r Carb ^r	Lab Stock
Plasmids		
pKD46	λ-Red recombinase expression plasmid; Carb ^r	(50)
pKD4	Kan ^r template	(50)
pKD3	Cat ^r template	(50)
pUC19-oriT-hyg	Hyg ^r template	Lab stock
pCP20	FLP recombinase plasmid, Carb ^r	(50)

Kan^r- kanamycin; Cat^r- chloramphenicol; Carb^r- carbenicillin; Hyg^r- hygromycin, Gent^R- gentamicin Carb^r- carbenicillin; Apr^r- apramycin; Tet^r - tetracycline.

Strain and plasmid construction

Gene deletions were constructed using the Red recombinase system (50). Gene specific P1 and P2 primers, along with antibiotic resistance gene marker template used for selection are listed in Table 4-3. All constructs were checked by PCR for the correct size, check primers listed in Table 4-3, and verified by Sanger sequencing.

Table 4-3: Primers used in this study

Primer Name	Primer Sequence
arnA KO	
GK425-ArnA::KanR-P1	GGTGACCTGCCTTACCACAAC
GK426-ArnA::KanR-P2	TCGTGATGTTTAGCCGCTTC
GK433-ArnA-check_for	CGAGCGTGAGTTTGGTGAATCC
GK434-ArnA-check_rev	CCGATCCCAGTTACCGCTAC
eptA KO	
TM448-EptA::catR-P1	GTTGGCCGCTTTTTATATCTCTATCTGCCTGAATATTGCCTGCGCCTACCT GTGACGGA
TM449-EptA::catR-P2	TGTTGCGTTTGCGCCTGTTTTGCAGGCAGTTCTGGTCAACCCTTACGCCC CGCCCTGCC
GK435-EptA-check_for	AAACCCGTATCCCTTAGATGCACC
GK436-EptA_check_rev	CTCAAGGCTTTGTTCCGCCATC
lpxT KO	
MAM2381- New P1 lpxT pKD4 KanR	AGGTTGCCTGCGTTTTTCAGTAAGATAATTAGAGAAAATATGGTAGGCTG GAGCTGCTTC
MAM2382- New P2 lpxT pKD4 KanR	GATGATGTTAATTACTGTGAGTTATTTGTTTTGGAAATGTTTTATGAATAT CCTCCTTAG
MM2579- lpxT upcheck v2	CTGATTTCCAGCAGCGAAGCTGAC
MM2580- lpxT downcheck v2	GATAGATGAAAGCACGGTGCGCAT
pagP KO	
Tm748- PagP hyg P1	GTTTTATGGTCACAAATGAACGTGAGTAAATATGTCGCTATCCTATGACCA TGATTACGC
Tm749- PagP hyg P2	ACTAAACTTCATTTGTCTCAAACTGAAAGCGCATCCAGGCACGTTGTAA AACGACGGC
Tm750- PagP hygcheck for	GTAGCTTTGCTATGCTAGTAGTAG
Tm751- PagP hygcheck rev	GTGGTACGCTTTGTCCAGTGTAAC
nagB KO	
MAM1824 – nagB catR-P1	AGACTGATCCCCCTGACTACCGCTGAACAGGTCGGCAAATGGTATGAATA TCCTCCTTAG
MAM1825 – nagB catR-P2	TCTTAAAGTCTTAACTTTAGCTCCATGGTGGAAGGTTTCATCGTAGGCTGG AGCTGCTTC
MAM1826 – nagB upcheck	GCCAACGGCTTACATTTTACTTATTG
MAM1827 – nagB downcheck	CAGGGCAGGGATAACAATTACAGACC

LPS purification

LPS was purified from *E. coli* BW25113 (K-12 lineage) as described in chapters 2 and 3.

Sandwich ELISA

Test strain incubation: Primary cultures of test strains were prepared in a 96-well plate format with 200 μL of YCFA (DSMZ) per well. An additional secondary plate was prepared with media alone and supplemented with 50 $\mu\text{g}/\text{mL}$ purified K-12 LPS but was not inoculated. Both primary and secondary plates were incubated overnight in required growth conditions for test strains (aerobic /anaerobic, 30 $^{\circ}\text{C}$ / 37 $^{\circ}\text{C}$). The next morning cultures on the primary plate were homogenized by pipetting and 10 μL used to inoculate corresponding wells on secondary plate. Primary and secondary plate layouts were designed in a manner to allow for at least two cultures of each strain in both growth conditions (with or without LPS). The secondary plate was then incubated for 48 hours before sample collection.

Sample collection: After incubation all 200 μL of the culture from each well was transferred to individual 1.7 mL Eppendorf tubes. The wells were washed with 200 μL of wash buffer (200 mM Tris-HCl, 10 mM EDTA, 0.02% sodium deoxy cholate w/v, pH 8.0) and used buffer was transferred to corresponding sample Eppendorf tubes to collect residual culture and minimize LPS loss due to adsorption to the wells. Samples were vortexed lightly before centrifugation at 4,000x g for five minutes. 300 μL of the resultant supernatant was collected and transferred to fresh Eppendorf tubes before addition of proteinase K, final concentration of 0.02 mg/mL, and incubation at 60 $^{\circ}\text{C}$ for one hour. Proteinase K was heat killed via incubation at 95 $^{\circ}\text{C}$ for 10 minutes and samples allowed to cool before freezing.

Sandwich ELISA: Immulon 4HBX plates were coated with 100 $\mu\text{L}/\text{well}$ of a 1 $\mu\text{g}/\text{mL}$ solution of monoclonal mouse Ab 26-5 (HYCULT HM6009) in 0.1 M acetate buffer (pH 5.0). The plate was

sealed with adhesive cover and stored at 4 °C overnight. The next day the plate was brought to room temperature before washing wells 3 times with 200 µL of PBS solution (LONZA, #17-516F). The final wash was aspirated and 150 µL/well of PBS casein blocking solution (ThermoFisher, #37582) was added and plate incubated for one hour at room temperature with shaking (150 rpm). Blocking solution was aspirated and wells washed five times with 200 µL/well PBS solution. After plate washing, previously prepared samples were thawed and diluted 1:50 (v/v) with PBS solution containing 1 mM EDTA. Diluted samples, 100 µL/well, were added to the ELISA plate before sealing and incubating again for two hours at room temperature with shaking (150 rpm). Unbound LPS was removed by washing twice with 200 µL/well PBS solution with 1 M NaCl and three final washes with 200 µL/well PBS solution. The second monoclonal antibody, Ab WN1 222-5 (Absolute Antibody, #AB00141-23.0) was diluted to 1 µg/mL in PBS with 1 % Ficoll400 and 0.5% polyvinylpyrrolidone (w/v) before addition to wells (100 µL/well). The plate was sealed and incubated for 2 hours. Secondary antibody was removed with 3 washes (200 µL/well) with PBS-Tween 20 (0.01% w/w), and two final washes with PBS. The secondary anti-rabbit Ig-HRP conjugate (A0545, Sigma) was diluted 1:500 (v/v) in a solution of PBS-0.1% casein before addition to wells (100 µL/well) and incubated for one hour. The plate was washed five times with PBS to remove unbound antibody before addition of 150 µL/well of ABTS detection substrate. Absorbance was read at 0-, 2.5-, 5-, 7.5-, and 10-minute intervals.

SDS-PAGE/Silver Stain

For the silver stain assay sample incubations were prepared as described above for the ELISA assay. Samples were collected by transferring 100 μ L of homogenized culture to fresh 1.7 mL Eppendorf tubes. Cells were then lysed via addition of a lysis buffer (100 mM Tris-HCl, 5 mM EDTA, and 0.01% sodium deoxycholate (w/v) final concentrations) and an enzyme master mix (285 μ g/mL lysozyme, 48 μ g/mL achromopeptidase, 0.5 U/mL mutanolysin, and 2 U/mL DNase I final concentrations) before incubation at room temperature for one hour. After cells were lysed, samples were prepared for SDS-PAGE by addition of loading buffer and proteinase K treatment in the manner of Hitchcock and Brown (51). Gel electrophoresis and silver staining were carried out as described in Chapter 3, where approximately 80 ng (24 μ L of prepared sample) of K-12 LPS was loaded assuming no degradation or non-specific loss occurred.

¹⁴C-labeled LPS purification

Overnight of the *E. coli* BW25113 Δ nagB, Δ lpxT, Δ eptA, Δ arnA, Δ pagP mutant was prepared in LB with antibiotics as required and used to inoculate 15 mL of LB 1:100. ¹⁴C-(U)-glucosamine hydrochloride (VWR# 102655-786) was added to 0.25 μ Ci/mL and cells grown for 4 hours at 37 °C with shaking at 250 rpm. Cells were harvested by centrifugation at 2,000x g for 10 minutes and washed with water before solubilization of LPS by resuspending pellet in TEA/EDTA/Doc solution (250 mM EDTA, 0.7% sodium deoxycholate (w/v) titrated with triethylamine until pH 7.5). Cells were allowed to incubate at 37 °C for 30 minutes before centrifugation at 10,000x g for five minutes. Supernatant was collected and the remaining pellet

was again incubated in TEA/EDTA/Doc solution. Centrifugation was repeated and supernatants combined and transferred to a Thermo Scientific™ Slide-A-Lyzer™ mini dialysis device (500-1k Da MWCO). The LPS containing solution was dialyzed against five 1-L portions of miliQ water at room temperature for five days. LPS was captured from the solution via addition of Bio-Rad Affi-Prep polymyxin resin (#1560010). The solution was incubated with resin for 4 hours at room temperature with flipping. Resin was pelleted by centrifugation at 10,000x g for 2 minutes and supernatant removed. Resin was washed 3 times with wash buffer (10 mM phosphate, 100 mM NaCl, pH 6.0). Finally, LPS was eluted in three rounds of incubation in elution buffer (1% sodium deoxycholate (w/v), 10 mM phosphate, pH 7) at 70 °C for 20 minutes per round. Elutes were combined and samples frozen until needed.

Autoradiographic TLC assay

Sample bacteria incubation for the autoradiographic TLC assay was carried out as described for the LPS ELISA with the exception that purified ¹⁴C-labeled LPS was used as feedstock. Post the 48-hour incubation in the 96-well plates the full sample cultures were collected and transferred to individual Eppendorf tubes. Collected samples then underwent a mild-acid hydrolysis to free labeled lipid A by addition of sodium acetate and sodium dodecyl sulfate until a final concentration of 300 mM sodium acetate, pH 4.5; 1% SDS (w/v) and incubation at 95 °C for 45 minutes. After hydrolysis samples were treated in a similar manner as described in Chapter 3, utilizing the method as described by Trent, *et al.* (39). Briefly, samples were converted to a two-phase Bligh-Dyer mixture and lipid A was collected with the lower

organic phase. Samples were allowed to dry overnight to concentrate labeled LPS before analyzing via TLC. Samples were dissolved in 10 μ L of 4:1 chloroform:methanol (v/v) and all 10 μ L spotted on a silica gel 60 TLC plate. The plate was run in a TLC tank using a pyridine/chloroform/formic acid/water (50:50:16:5, v/v/v/v) mobile phase and allowed to air dry overnight. Visualization was achieved by exposing a storage phosphor screen [BAS-IP MS (Multipurpose Standard)] to the plastic saran wrapped TLC plate for 24 hours before scanning to obtain an image.

REFERENCES

1. Neves, A. L., Coelho, J., Couto, L., Leite-Moreira, A., and Roncon-Albuquerque, R. (2013) Metabolic endotoxemia: a molecular link between obesity and cardiovascular risk. *J Mol Endocrinol.* **51**, R51–R64
2. Miura, K. (2014) Role of gut microbiota and Toll-like receptors in nonalcoholic fatty liver disease. *World J Gastroenterol.* **20**, 7381
3. Duseja, A., and Chawla, Y. K. (2014) Obesity and NAFLD. *Clin Liver Dis.* **18**, 59–71
4. Boroni Moreira, A. P., and de Cássia Gonçalves Alfenas, R. (2012) The influence of endotoxemia on the molecular mechanisms of insulin resistance. *Nutr Hosp.* **27**, 382–90
5. Cani, P. D., Amar, J., Iglesias, M. A., Poggi, M., Knauf, C., Bastelica, D., Neyrinck, A. M., Fava, F., Tuohy, K. M., Chabo, C., Waget, A., Delmée, E., Cousin, B., Sulpice, T., Chamontin, B., Ferrières, J., Tanti, J.-F., Gibson, G. R., Casteilla, L., Delzenne, N. M., Alessi, M. C., and Burcelin, R. (2007) Metabolic endotoxemia initiates obesity and insulin resistance. *Diabetes.* **56**, 1761–72
6. Moreno-Indias, I., Cardona, F., Tinahones, F. J., and Queipo-Ortuño, M. I. (2014) Impact of the gut microbiota on the development of obesity and type 2 diabetes mellitus. *Front Microbiol.* **5**, 190
7. Tilg, H., and Moschen, A. R. (2014) Microbiota and diabetes: an evolving relationship. *Gut.* **63**, 1513–21
8. Khan, M. A. B., Hashim, M. J., King, J. K., Govender, R. D., Mustafa, H., and Al Kaabi, J. (2019) Epidemiology of Type 2 Diabetes – Global Burden of Disease and Forecasted Trends. *J Epidemiol Glob Health.* **10**, 107

9. Teng, M. L., Ng, C. H., Huang, D. Q., Chan, K. E., Tan, D. J., Lim, W. H., Yang, J. D., Tan, E., and Muthiah, M. D. (2023) Global incidence and prevalence of nonalcoholic fatty liver disease. *Clin Mol Hepatol.* **29**, S32–S42
10. Frazier, T. H., DiBaise, J. K., and McClain, C. J. (2011) Gut microbiota, intestinal permeability, obesity-induced inflammation, and liver injury. *JPEN J Parenter Enteral Nutr.* **35**, 14S-20S
11. Shen, J., Obin, M. S., and Zhao, L. (2013) The gut microbiota, obesity and insulin resistance. *Mol Aspects Med.* **34**, 39–58
12. Mohammad, S., and Thiemermann, C. (2021) Role of Metabolic Endotoxemia in Systemic Inflammation and Potential Interventions. *Front Immunol.* 10.3389/fimmu.2020.594150
13. Tlaskalová-Hogenová, H., Štěpánková, R., Kozáková, H., Hudcovic, T., Vannucci, L., Tučková, L., Rossmann, P., Hrnčíř, T., Kverka, M., Zákostelská, Z., Klimešová, K., Příbylová, J., Bártová, J., Sanchez, D., Fundová, P., Borovská, D., Šrůtková, D., Zídek, Z., Schwarzer, M., Drastich, P., and Funda, D. P. (2011) The role of gut microbiota (commensal bacteria) and the mucosal barrier in the pathogenesis of inflammatory and autoimmune diseases and cancer: contribution of germ-free and gnotobiotic animal models of human diseases. *Cell Mol Immunol.* **8**, 110–120
14. Moreira, A. P. B., Texeira, T. F. S., Ferreira, A. B., do Carmo Gouveia Peluzio, M., and de Cássia Gonçalves Alfenas, R. (2012) Influence of a high-fat diet on gut microbiota, intestinal permeability and metabolic endotoxaemia. *British Journal of Nutrition.* **108**, 801–809

15. Fei, N., and Zhao, L. (2013) An opportunistic pathogen isolated from the gut of an obese human causes obesity in germfree mice. *ISME J.* **7**, 880–884
16. Kinashi, Y., and Hase, K. (2021) Partners in Leaky Gut Syndrome: Intestinal Dysbiosis and Autoimmunity. *Front Immunol.* 10.3389/fimmu.2021.673708
17. Di Tommaso, N., Gasbarrini, A., and Ponziani, F. R. (2021) Intestinal Barrier in Human Health and Disease. *Int J Environ Res Public Health.* **18**, 12836
18. Aleman, R. S., Moncada, M., and Aryana, K. J. (2023) Leaky Gut and the Ingredients That Help Treat It: A Review. *Molecules.* **28**, 619
19. Binienda, A., Twardowska, A., Makaro, A., and Salaga, M. (2020) Dietary Carbohydrates and Lipids in the Pathogenesis of Leaky Gut Syndrome: An Overview. *Int J Mol Sci.* **21**, 8368
20. Twardowska, A., Makaro, A., Binienda, A., Fichna, J., and Salaga, M. (2022) Preventing Bacterial Translocation in Patients with Leaky Gut Syndrome: Nutrition and Pharmacological Treatment Options. *Int J Mol Sci.* **23**, 3204
21. Kobayashi, T., Iwaki, M., Nakajima, A., Nogami, A., and Yoneda, M. (2022) Current Research on the Pathogenesis of NAFLD/NASH and the Gut–Liver Axis: Gut Microbiota, Dysbiosis, and Leaky-Gut Syndrome. *Int J Mol Sci.* **23**, 11689
22. Cani, P. D., and Delzenne, N. M. (2011) The gut microbiome as therapeutic target. *Pharmacol Ther.* **130**, 202–212
23. Fuke, N., Nagata, N., Suganuma, H., and Ota, T. (2019) Regulation of Gut Microbiota and Metabolic Endotoxemia with Dietary Factors. *Nutrients.* **11**, 2277

24. Pickkers, P., Snellen, F., Rogiers, P., Bakker, J., Jorens, P., Meulenbelt, J., Spapen, H., Tulleken, J. E., Lins, R., Ramael, S., Bulitta, M., and van der Hoeven, J. G. (2009) Clinical pharmacology of exogenously administered alkaline phosphatase. *Eur J Clin Pharmacol.* **65**, 393–402
25. Davidson, J. A., Urban, T. T., Tong, S., Maddux, A., Hill, G., Frank, B. S., Watson, J. D., Jagers, J., Simões, E. A. F., and Wischmeyer, P. (2019) Alkaline Phosphatase Activity and Endotoxemia After Infant Cardiothoracic Surgery. *Shock.* **51**, 328–336
26. Fawley, J., and Gourlay, D. M. (2016) Intestinal alkaline phosphatase: a summary of its role in clinical disease. *Journal of Surgical Research.* **202**, 225–234
27. Bilski, J., Mazur-Bialy, A., Wojcik, D., Zahradnik-Bilska, J., Brzozowski, B., Magierowski, M., Mach, T., Magierowska, K., and Brzozowski, T. (2017) The Role of Intestinal Alkaline Phosphatase in Inflammatory Disorders of Gastrointestinal Tract. *Mediators Inflamm.* **2017**, 1–9
28. Weinrauch, Y., Katz, S. S., Munford, R. S., Elsbach, P., and Weiss, J. (1999) Deacylation of purified lipopolysaccharides by cellular and extracellular components of a sterile rabbit peritoneal inflammatory exudate. *Infect Immun.* **67**, 3376–82
29. Rajilić-Stojanović, M., and de Vos, W. M. (2014) The first 1000 cultured species of the human gastrointestinal microbiota. *FEMS Microbiol Rev.* **38**, 996–1047
30. Maeshima, N., and Fernandez, R. C. (2013) Recognition of lipid A variants by the TLR4-MD-2 receptor complex. *Front Cell Infect Microbiol.* 10.3389/fcimb.2013.00003
31. Kong, Q., Six, D. A., Liu, Q., Gu, L., Wang, S., Alamuri, P., Raetz, C. R. H., and Curtiss, R. (2012) Phosphate Groups of Lipid A Are Essential for *Salmonella enterica* Serovar

- Typhimurium Virulence and Affect Innate and Adaptive Immunity. *Infect Immun.* **80**, 3215–3224
32. Kong, Q., Six, D. A., Liu, Q., Gu, L., Roland, K. L., Raetz, C. R. H., and Curtiss, R. (2011) Palmitoylation State Impacts Induction of Innate and Acquired Immunity by the Salmonella enterica Serovar Typhimurium *msbB* Mutant. *Infect Immun.* **79**, 5027–5038
33. Di Padova, F. E., Brade, H., Barclay, G. R., Poxton, I. R., Liehl, E., Schuetze, E., Kocher, H. P., Ramsay, G., Schreier, M. H., and McClelland, D. B. (1993) A broadly cross-protective monoclonal antibody binding to Escherichia coli and Salmonella lipopolysaccharides. *Infect Immun.* **61**, 3863–72
34. Erich, T., Schellekens, J., Bouter, A., Van Kranen, J., Brouwer, E., and Verhoef, J. (1989) Binding characteristics and cross-reactivity of three different antilipid A monoclonal antibodies. *J Immunol.* **143**, 4053–60
35. Gomery, K., Müller-Loennies, S., Brooks, C. L., Brade, L., Kosma, P., Di Padova, F., Brade, H., and Evans, S. V (2012) Antibody WN1 222-5 mimics Toll-like receptor 4 binding in the recognition of LPS. *Proc Natl Acad Sci U S A.* **109**, 20877–82
36. Müller-Loennies, S., Brade, L., MacKenzie, C. R., Di Padova, F. E., and Brade, H. (2003) Identification of a Cross-reactive Epitope Widely Present in Lipopolysaccharide from Enterobacteria and Recognized by the Cross-protective Monoclonal Antibody WN1 222-5. *Journal of Biological Chemistry.* **278**, 25618–25627
37. Vincent, F., Davies, G. J., and Brannigan, J. A. (2005) Structure and Kinetics of a Monomeric Glucosamine 6-Phosphate Deaminase. *Journal of Biological Chemistry.* **280**, 19649–19655

38. Munford, R. S., and Hunter, J. P. (1992) Acyloxyacyl hydrolase, a leukocyte enzyme that deacylates bacterial lipopolysaccharides, has phospholipase, lysophospholipase, diacylglycerollipase, and acyltransferase activities in vitro. *J Biol Chem.* **267**, 10116–21
39. Asami, K., Kondo, A., Suda, Y., Shimoyamada, M., and Kanauchi, M. (2017) Neutralization of Lipopolysaccharide by Heat Shock Protein in *Pediococcus pentosaceus* AK-23. *J Food Sci.* **82**, 1657–1663
40. Frampton, J. E. (2017) Golimumab: A Review in Inflammatory Arthritis. *BioDrugs.* **31**, 263–274
41. Sparrow, M. P. (2017) Adalimumab in ulcerative colitis - efficacy, safety and optimization in the era of treat-to target. *Expert Opin Biol Ther.* **17**, 613–621
42. Abreu, M. T. (2010) Toll-like receptor signalling in the intestinal epithelium: how bacterial recognition shapes intestinal function. *Nat Rev Immunol.* **10**, 131–44
43. Downey, C. (2016) Serious infection during etanercept, infliximab and adalimumab therapy for rheumatoid arthritis: A literature review. *Int J Rheum Dis.* **19**, 536–50
44. Ford, A. C., and Peyrin-Biroulet, L. (2013) Opportunistic infections with anti-tumor necrosis factor- α therapy in inflammatory bowel disease: meta-analysis of randomized controlled trials. *Am J Gastroenterol.* **108**, 1268–76
45. Tragiannidis, A., Kyriakidis, I., Zündorf, I., and Groll, A. H. (2017) Invasive fungal infections in pediatric patients treated with tumor necrosis alpha (TNF- α) inhibitors. *Mycoses.* **60**, 222–229

46. Pecoraro, V., De Santis, E., Melegari, A., and Trenti, T. (2017) The impact of immunogenicity of TNF α inhibitors in autoimmune inflammatory disease. A systematic review and meta-analysis. *Autoimmun Rev.* **16**, 564–575
47. Komazin, G., Maybin, M., Woodard, R. W., Scior, T., Schwudke, D., Schombel, U., Gisch, N., Mamat, U., and Meredith, T. C. (2019) Substrate structure-activity relationship reveals a limited lipopolysaccharide chemotype range for intestinal alkaline phosphatase. *Journal of Biological Chemistry.* **294**, 19405–19423
48. Datsenko, K. A., and Wanner, B. L. (2000) One-step inactivation of chromosomal genes in *Escherichia coli* K-12 using PCR products. *Proc Natl Acad Sci U S A.* **97**, 6640–5
49. Hitchcock, P. J., and Brown, T. M. (1983) Morphological heterogeneity among *Salmonella* lipopolysaccharide chemotypes in silver-stained polyacrylamide gels. *J Bacteriol.* **154**, 269–277
50. Henderson, J. C., O'Brien, J. P., Brodbelt, J. S., and Trent, M. S. (2013) Isolation and Chemical Characterization of Lipid A from Gram-negative Bacteria. *Journal of Visualized Experiments.* 10.3791/50623

Chapter 5

Conclusions and Future Directions

OVERVIEW AND DISCUSSION

Lipopolysaccharide (LPS), also commonly referred to as endotoxin, is a major component of the outer membrane (OM) of Gram-negative bacteria. It plays a variety of critical roles for the bacterium and in its interactions with its environment and hosts. These roles include structural stability of the bacterium, membrane permeability, antibiotic resistance, and immune recognition (1). Given the essentiality of said roles in bacterial physiology, pathogenicity, and interactions with the host, LPS remains a key area of research in microbiology and immunology. This dissertation investigates host-microbe interactions as well as the role modifications to lipid A, the most conserved region of LPS, play in antibiotic resistance and immune recognition.

The gut microbiome is a primary example of the importance of host-microbe interactions where mutualism between the host and microbiota is key (2). Part of maintaining this balance is the detoxification of LPS released by the microbiome (2, 3), where in the absence of such activity immunogenic chemotypes of LPS would be recognized by TLR4/MD2 and induce the release of pro-inflammatory cytokines (4). On the hosts side, one method of detoxification of LPS has been the dephosphorylation of the lipid A bound phosphate groups. The longstanding paradigm in literature holds that this activity is carried out by intestinal alkaline phosphatase (IAP) (5–9). However, the work described in (10) and chapter 2 of this dissertation refutes this. We demonstrated that IAP is not active on the immunogenically relevant chemotypes of LPS (bis-phosphorylated and hexa-acylated lipid A) but rather can only directly dephosphorylate lipid A when O-linked acyl chains on the lipid A backbone have already been removed. Dephosphorylation of an already detoxified chemotype of LPS would thus play little role in

decreasing the overall impact of LPS induced cytokine release. Further investigation revealed that the previously observed link between IAP and decreased LPS toxicity (8, 9) was due to concomitant loss of spontaneously hydrolyzed phosphoethanolamine modifications on lipid A during incubations. Indeed, PEtN modifications were observed to increase hTLR4 signaling, especially in underacylated chemotypes. We describe a model where PEtN modification on the 1 and 4'- phosphates of lipid A provide steric bulk preventing LPS from burying too far into the MD2 pocket, especially in underacylated chemotypes, and thus maintaining key interactions on the interface of MD2 and TLR4. While the data thus far supports this model future work could investigate if any sufficiently bulky modifications to the lipid A phosphates would provide similar increase to TLR4 signaling, for example 4-amino-4-deoxy-L-arabinose (Ara4N) modifications. In addition, our modeling studies have suggested key residues in human and mouse TLR4/MD2 that are important in differentiating detection of modified lipid A chemotypes. Experimental validation to test these models using point mutants is warranted.

The role of lipid A modification and antibiotic resistance was explored in chapter 3 of this dissertation. Therein we describe a mechanism of polymyxin B (PMB) heteroresistance (HR), in *Escherichia coli* B strains, dependent on insertion sequence elements. Understanding driving forces of HR is of increasing importance as HR can undermine our utilization of drugs of last resort like PMB (11, 12). Investigation of a pre-existing subpopulation of *E. coli* B cells phenotypically resistant to PMB, revealed increased Ara4N modification of lipid A. Sequencing did not reveal typical mutations in Ara4N regulators but instead demonstrated that large regions of the genome were amplified. Amplified regions were found to contain the *arn* operon (responsible for Ara4N modification) and were flanked by insertion sequence elements (*IS1*). Further investigation

revealed that the presence of the flanking IS1 elements was necessary for amplification. Altogether we demonstrate that IS elements can play a significant role in modulating gene expression and bacterial survival and highlight the importance of understanding how IS placement around the genome alters phenotypes. In the case of PMB resistance, frequencies of resistance were increased by up to 100-fold with the presence of a single IS1 element located 90-kb away. IS number and genomic location is rarely considered in genome sequencing data of phenotypically resistant clinical isolates, but this work clearly demonstrates the potential of IS content to make an outsized contribution. While the data presented herein demonstrates IS1 mediated chromosomal amplification in *E. coli* B strains, many factors of IS-mediated tandem amplification remain open for investigation. Including how amplification frequency among the population is affected by distance between IS1 elements, what genetic/environmental/stress factors control IS mediated chromosomal amplification, and to what extent this process contributes generally to single cell gene expression heterogeneity among bacterial populations.

Finally in chapter 4 of this dissertation development of a screen for LPS degrading activity (LPS-ase activity) derived from gut commensals is described. Bacterial derived LPS-ase activity is hitherto unknown and represents a gap in our understanding of LPS catabolism. The screen as described utilizes three orthologous assays (LPS sandwich ELISA, SDS-PAGE silver stain, and autoradiographic TLC) that together detect degradation of an *E. coli* K-12 LPS chemotype. Degradation of either the core oligosaccharide or lipid A structure can be determined by the combination of assays. Discovery of LPS-ase activity in any bacterium opens potential for various therapeutic strategies to degrade immunogenic LPS. Intraluminal degradation of LPS may provide particular benefits in managing metabolic endotoxemia (ME) and its associated disease

states (13–21). While the panel of bacteria used in this work is representative of the gut microbiome (22) it is by no means exhaustive, and future utilization of this screen would be benefited by expanding the panel to more diverse gut bacterium as well as including a stronger representation of environmental bacterium. Once more, utilizing different growth media (i.e. minimal media) and other deaggregating additives to help present LPS substrate for catabolism should be explored. The radiolabeling assay described here may also be used to feed heat-killed whole cells pre-labeled with LPS, which may be necessary to more closely mimic degradation conditions in complex bacterial communities. Likewise, this assay will allow investigation of complex mixtures of bacterial cultures and extracts.

REFERENCES

1. Simpson, B. W., and Trent, M. S. (2019) Pushing the envelope: LPS modifications and their consequences. *Nat Rev Microbiol.* **17**, 403–416
2. Jensen, S. K., Pærregaard, S. I., Brandum, E. P., Jørgensen, A. S., Hjortø, G. M., and Jensen, B. A. H. (2022) Rewiring host–microbe interactions and barrier function during gastrointestinal inflammation. *Gastroenterol Rep (Oxf)*. 10.1093/gastro/goac008
3. Twardowska, A., Makaro, A., Binienda, A., Fichna, J., and Salaga, M. (2022) Preventing Bacterial Translocation in Patients with Leaky Gut Syndrome: Nutrition and Pharmacological Treatment Options. *Int J Mol Sci.* **23**, 3204
4. Maeshima, N., and Fernandez, R. C. (2013) Recognition of lipid A variants by the TLR4-MD-2 receptor complex. *Front Cell Infect Microbiol.* 10.3389/fcimb.2013.00003
5. Pickkers, P., Snellen, F., Rogiers, P., Bakker, J., Jorens, P., Meulenbelt, J., Spapen, H., Tulleken, J. E., Lins, R., Ramael, S., Bulitta, M., and van der Hoeven, J. G. (2009) Clinical pharmacology of exogenously administered alkaline phosphatase. *Eur J Clin Pharmacol.* **65**, 393–402
6. Davidson, J. A., Urban, T. T., Tong, S., Maddux, A., Hill, G., Frank, B. S., Watson, J. D., Jagers, J., Simões, E. A. F., and Wischmeyer, P. (2019) Alkaline Phosphatase Activity and Endotoxemia After Infant Cardiothoracic Surgery. *Shock.* **51**, 328–336
7. Bilski, J., Mazur-Bialy, A., Wojcik, D., Zahradnik-Bilska, J., Brzozowski, B., Magierowski, M., Mach, T., Magierowska, K., and Brzozowski, T. (2017) The Role of Intestinal Alkaline

- Phosphatase in Inflammatory Disorders of Gastrointestinal Tract. *Mediators Inflamm.* **2017**, 1–9
8. Koyama, I., Matsunaga, T., Harada, T., Hokari, S., and Komoda, T. (2002) Alkaline phosphatases reduce toxicity of lipopolysaccharides in vivo and in vitro through dephosphorylation. *Clin Biochem.* **35**, 455–461
 9. Bates, J. M., Akerlund, J., Mittge, E., and Guillemin, K. (2007) Intestinal Alkaline Phosphatase Detoxifies Lipopolysaccharide and Prevents Inflammation in Zebrafish in Response to the Gut Microbiota. *Cell Host Microbe.* **2**, 371–382
 10. Komazin, G., Maybin, M., Woodard, R. W., Scior, T., Schwudke, D., Schombel, U., Gisch, N., Mamat, U., and Meredith, T. C. (2019) Substrate structure-activity relationship reveals a limited lipopolysaccharide chemotype range for intestinal alkaline phosphatase. *Journal of Biological Chemistry.* **294**, 19405–19423
 11. Band, V. I., and Weiss, D. S. (2019) Heteroresistance: A cause of unexplained antibiotic treatment failure? *PLoS Pathog.* **15**, e1007726
 12. El-Halfawy, O. M., and Valvano, M. A. (2015) Antimicrobial Heteroresistance: an Emerging Field in Need of Clarity. *Clin Microbiol Rev.* **28**, 191–207
 13. Mohammad, S., and Thiemermann, C. (2021) Role of Metabolic Endotoxemia in Systemic Inflammation and Potential Interventions. *Front Immunol.* 10.3389/fimmu.2020.594150
 14. Neves, A. L., Coelho, J., Couto, L., Leite-Moreira, A., and Roncon-Albuquerque, R. (2013) Metabolic endotoxemia: a molecular link between obesity and cardiovascular risk. *J Mol Endocrinol.* **51**, R51–R64
 15. Duseja, A., and Chawla, Y. K. (2014) Obesity and NAFLD. *Clin Liver Dis.* **18**, 59–71

16. Miura, K. (2014) Role of gut microbiota and Toll-like receptors in nonalcoholic fatty liver disease. *World J Gastroenterol.* **20**, 7381
17. Boroni Moreira, A. P., and de Cássia Gonçalves Alfenas, R. (2012) The influence of endotoxemia on the molecular mechanisms of insulin resistance. *Nutr Hosp.* **27**, 382–90
18. Cani, P. D., Amar, J., Iglesias, M. A., Poggi, M., Knauf, C., Bastelica, D., Neyrinck, A. M., Fava, F., Tuohy, K. M., Chabo, C., Waget, A., Delmée, E., Cousin, B., Sulpice, T., Chamontin, B., Ferrières, J., Tanti, J.-F., Gibson, G. R., Casteilla, L., Delzenne, N. M., Alessi, M. C., and Burcelin, R. (2007) Metabolic endotoxemia initiates obesity and insulin resistance. *Diabetes.* **56**, 1761–72
19. Moreno-Indias, I., Cardona, F., Tinahones, F. J., and Queipo-Ortuño, M. I. (2014) Impact of the gut microbiota on the development of obesity and type 2 diabetes mellitus. *Front Microbiol.* **5**, 190
20. Tilg, H., and Moschen, A. R. (2014) Microbiota and diabetes: an evolving relationship. *Gut.* **63**, 1513–21
21. Frazier, T. H., DiBaise, J. K., and McClain, C. J. (2011) Gut microbiota, intestinal permeability, obesity-induced inflammation, and liver injury. *JPEN J Parenter Enteral Nutr.* **35**, 14S-20S
22. Rajilić-Stojanović, M., and de Vos, W. M. (2014) The first 1000 cultured species of the human gastrointestinal microbiota. *FEMS Microbiol Rev.* **38**, 996–1047

Curriculum Vitae

Michael Aaron Maybin

Education:

- December 2023 Ph.D., Biochemistry, Microbiology, and Molecular Biology, The Pennsylvania State University, State College, PA
- May 2015 M.S., Biochemistry, The University of North Carolina at Greensboro, Greensboro, NC
- May 2013 B.S., Biochemistry (major) and Astronomy (minor), Elon University, Elon, NC

Honors and Awards:

- Alfred P. Sloan Minority Graduate Scholarship (2018)
Bunton-Waller Graduate Awards Program (2016)
Homer F. Braddock Fellowship and Nellie H. and Oscar L. Roberts Fellowship (2016)
The American Institute of Chemists Student Award (2015)
Phillips-Perry Black Excellence Award, Elon University (2012)

Publications:

- Gloria Komazin, **Michael Maybin**, Ronald W Woodard, Thomas Scior, Dominik Schwudke, Ursula Schombel, Nicholas Gisch, Uwe Mamat, Timothy C Meredith (2019). Substrate Structure-Activity Relationship Reveals a Limited Lipopolysaccharide Chemotype Range for Intestinal Alkaline Phosphatase. *Journal of Biological Chemistry*. 294 (50), 19405-19423
- Amena A Rizk, Gloria Komazin, **Michael Maybin**, Nushrat Hoque, Emily Weinert, Timothy C Meredith. (2023). The Extracellular Electron Transport Pathway Reduces Copper for Sensing by the CopRS Two-Component System under Anaerobic Conditions in *Listeria monocytogenes*. *J Bacteriol*. 205 (1): e00391-22
- Edward Alejandro Pierre Provencher, Molly R Ehrig, Andrew G Cecere, Shyan C Cousins, **Michael A Maybin**, Timothy C Meredith and Tim Miyashiro (2023). Inhibition of Biofilm Formation by a Lipopolysaccharide-associated Glycosyltransferase in the Bacterial Symbiont *Vibrio fischeri*. *Frontiers in Bacteriology, section Molecular Bacteriology and Microbiome*. 2:1254305
- Michael Maybin**, Aditi M Ranade, Uwe Mamat, Nicholas Gisch, Timothy C Meredith (2023) IS Mediated Tandem Chromosomal Amplification of the Arn Operon Facilitates Polymyxin B Resistance in *E. coli* B Strains. *mBIO*. 2023 (Manuscript in review)

Patents:

- Meredith, T. C., Komazin, G., **Maybin, M.A.** Lipopolysaccharide Molecules for Enhancing Immune Responses. Patent W0/2021/050778, March 18, 2021.